



University Transportation Research Center - Region 2

Final Report

Seismic Evaluation and Retrofit of Deteriorated Con- crete Bridge Components

Performing Organization: Syracuse University



June 2013

Sponsor:
Research and Innovative Technology Administration
(RITA)/USDOT

University Transportation Research Center - Region 2

The Region 2 University Transportation Research Center (UTRC) is one of ten original University Transportation Centers established in 1987 by the U.S. Congress. These Centers were established with the recognition that transportation plays a key role in the nation's economy and the quality of life of its citizens. University faculty members provide a critical link in resolving our national and regional transportation problems while training the professionals who address our transportation systems and their customers on a daily basis.

The UTRC was established in order to support research, education and the transfer of technology in the field of transportation. The theme of the Center is "Planning and Managing Regional Transportation Systems in a Changing World." Presently, under the direction of Dr. Camille Kamga, the UTRC represents USDOT Region II, including New York, New Jersey, Puerto Rico and the U.S. Virgin Islands. Functioning as a consortium of twelve major Universities throughout the region, UTRC is located at the CUNY Institute for Transportation Systems at The City College of New York, the lead institution of the consortium. The Center, through its consortium, an Agency-Industry Council and its Director and Staff, supports research, education, and technology transfer under its theme. UTRC's three main goals are:

Research

The research program objectives are (1) to develop a theme based transportation research program that is responsive to the needs of regional transportation organizations and stakeholders, and (2) to conduct that program in cooperation with the partners. The program includes both studies that are identified with research partners of projects targeted to the theme, and targeted, short-term projects. The program develops competitive proposals, which are evaluated to insure the most responsive UTRC team conducts the work. The research program is responsive to the UTRC theme: "Planning and Managing Regional Transportation Systems in a Changing World." The complex transportation system of transit and infrastructure, and the rapidly changing environment impacts the nation's largest city and metropolitan area. The New York/New Jersey Metropolitan has over 19 million people, 600,000 businesses and 9 million workers. The Region's intermodal and multimodal systems must serve all customers and stakeholders within the region and globally. Under the current grant, the new research projects and the ongoing research projects concentrate the program efforts on the categories of Transportation Systems Performance and Information Infrastructure to provide needed services to the New Jersey Department of Transportation, New York City Department of Transportation, New York Metropolitan Transportation Council, New York State Department of Transportation, and the New York State Energy and Research Development Authority and others, all while enhancing the center's theme.

Education and Workforce Development

The modern professional must combine the technical skills of engineering and planning with knowledge of economics, environmental science, management, finance, and law as well as negotiation skills, psychology and sociology. And, she/he must be computer literate, wired to the web, and knowledgeable about advances in information technology. UTRC's education and training efforts provide a multidisciplinary program of course work and experiential learning to train students and provide advanced training or retraining of practitioners to plan and manage regional transportation systems. UTRC must meet the need to educate the undergraduate and graduate student with a foundation of transportation fundamentals that allows for solving complex problems in a world much more dynamic than even a decade ago. Simultaneously, the demand for continuing education is growing – either because of professional license requirements or because the workplace demands it – and provides the opportunity to combine State of Practice education with tailored ways of delivering content.

Technology Transfer

UTRC's Technology Transfer Program goes beyond what might be considered "traditional" technology transfer activities. Its main objectives are (1) to increase the awareness and level of information concerning transportation issues facing Region 2; (2) to improve the knowledge base and approach to problem solving of the region's transportation workforce, from those operating the systems to those at the most senior level of managing the system; and by doing so, to improve the overall professional capability of the transportation workforce; (3) to stimulate discussion and debate concerning the integration of new technologies into our culture, our work and our transportation systems; (4) to provide the more traditional but extremely important job of disseminating research and project reports, studies, analysis and use of tools to the education, research and practicing community both nationally and internationally; and (5) to provide unbiased information and testimony to decision-makers concerning regional transportation issues consistent with the UTRC theme.

Project No: 49111-23-22

Project Date: June, 2013

Project Title: Seismic Evaluation and Retrofit of Deteriorated Concrete Bridge Components

Principal Investigators: Dr. Riyad Aboutaha

Co-Authors: Fares Jnaid, Sara Sotoud, and Mucip Tapan

Performing Organization: Syracuse University

Sponsors: Research and Innovative Technology Administration / USDOT

To request a hard copy of our final reports, please send us an email at utrc@utrc2.org

Mailing Address:

University Transportation Research Center
The City College of New York
Marshak Hall, Suite 910
160 Convent Avenue
New York, NY 10031
Tel: 212-650-8051
Fax: 212-650-8374
Web: www.utrc2.org

1. Report No.	2. Government Accession No. --	3. Recipient's Catalog No. --	
4. Title and Subtitle Seismic Evaluation and Retrofit of Deteriorated Concrete Bridge Components		5. Report Date June 30, 2013	
7. Author(s) Riyad Aboutaha, Fares Jnaid, Sara Sotoud, and Mucip Tapan		6. Performing Organization Code --	
9. Performing Organization Name and Address Syracuse University, Department of Civil and Environmental Engineering, 151 Link Hall, Syracuse, NY 13244, USA.		8. Performing Organization Report No. --	
12. Sponsoring Agency Name and Address Research and Innovative Technology Administration U.S. Department of Transportation 1200 New Jersey Avenue, SE Washington, DC 20590		10. Work Unit No. --	
15. Supplementary Notes		11. Contract or Grant No. 49111-23-22	
16. Abstract Corrosion of steel bars in reinforced concrete structures is a major durability problem for bridges constructed in the New York State (NYS). The heavy use of deicing salt compounds this problem. Corrosion of steel bars results in loss of steel cross section, deterioration of bond between concrete and reinforcing bars, and more important, in most cases, it results in unsymmetrical concrete section that is susceptible to shear stresses produced by torsion. Though earthquake frequency of occurrence and the expected ground accelerations in NYS is less than in western states, the potential for earthquake damage in or around NYS is still very real. Given the level of deterioration in many reinforced concrete bridges in NYS, they are considered very vulnerable to major damage during a moderate seismic event. There is an urgent need for proper guide for evaluation of deteriorated reinforced concrete bridge components that could assist structural engineers estimate the reserved strength of deteriorated bridges, and design cost-effective methods for retrofit. Proper evaluation and retrofit of existing deteriorated reinforced concrete bridges will limit the collapse of bridge during moderate seismic events in NYS and the surrounding states, and consequently save people's lives. The findings of this investigation suggest the need for seismic retrofit of deteriorated reinforced concrete bridge columns, particularly, those with corroded lap splice in the longitudinal reinforcement. The study also suggests the need for retrofit of corroded pedestal over piers and abutments, as they may cause sudden unseating of girders.		13. Type of Report and Period Covered Final Report	
17. Key Words Corrosion, bridge deterioration, seismic deficiencies, seismic retrofit, CFRP composites		14. Sponsoring Agency Code ----	
19. Security Classif. (of this report) Unclassified		18. Distribution Statement ---	
20. Security Classif. (of this page) Unclassified		21. No of Pages 34	22. Price

Disclaimer

The contents of this report reflect the views of the authors, who are responsible for the facts and the accuracy of the information presented herein. The contents do not necessarily reflect the official views or policies of the UTRC [, (other project sponsors),] or the Federal Highway Administration. This report does not constitute a standard, specification or regulation. This document is disseminated under the sponsorship of the Department of Transportation, University Transportation Centers Program, in the interest of information exchange. The U.S. Government [and other project sponsors] assume[s] no liability for the contents or use thereof.



Syracuse University
L.C. Smith College of Engineering and Computer Science
Department of Civil and Environmental Engineering

Seismic Evaluation and Retrofit of Deteriorated Concrete Bridge Components

by

Riyad S. Aboutaha, Fares Jnaid, Sara Sotoud, and Mucip Tapan

2013
Syracuse, New York

Seismic Evaluation and Retrofit of Deteriorated Concrete Bridge Components

PI: Dr. Riyad S. Aboutaha

rsabouta@syr.edu

Syracuse University

Collaborators:

Mr. Fares Jnaid,

Ms. Sara Sotoud, and

Dr. Mucip Tapan

EXECUTIVE SUMMARY

Corrosion of steel bars in reinforced concrete structures is a major durability problem for bridges constructed in the New York State (NYS). The heavy use of deicing salt compounds this problem. Corrosion of steel bars results in loss of steel cross section, deterioration of bond between concrete and reinforcing bars, and more important, in most cases, it results in unsymmetrical concrete section that is susceptible to shear stresses produced by torsion.

Though earthquake frequency of occurrence and the expected ground accelerations in NYS is less than in western states, the potential for earthquake damage in or around NYS is still very real. Given the level of deterioration in many reinforced concrete bridges in NYS, they are considered very vulnerable to major damage during a moderate seismic event.

There is an urgent need for proper guide for evaluation of deteriorated reinforced concrete bridge components that could assist structural engineers estimate the reserved strength of deteriorated bridges, and design cost-effective methods for retrofit.

Proper evaluation and retrofit of existing deteriorated reinforced concrete bridges will limit the collapse of bridge during moderate seismic events in NYS and the surrounding states, and consequently save people's lives.

The findings of this investigation suggest the need for seismic retrofit of deteriorated reinforced concrete bridge columns, particularly, those with corroded lap splice in the longitudinal reinforcement. The study also suggests the need for retrofit of corroded pedestal over piers and abutments, as they may cause sudden unseating of girders.

TABLE OF CONTENTS

1	Introduction: 1	
2	Literature Review: 3	
2.1	Corrosion:.....	Error! Bookmark not defined.
2.2	Corrosion Rates:.....	4
2.2.1	Definition:.....	4
2.2.2	Measurement:.....	6
2.3	Effect of Corrosion on Reinforcing Bars:	7
2.4	Effect of Corrosion on Material Properties:.....	8
2.5	Deterioration Stages:.....	9
3	Common Earthquake Failure Mechanisms: 10	
3.1	Introduction:.....	10
3.2	Unseating (most common):.....	10
3.3	Column Shear:.....	12
3.4	Column Flexural Capacity:	14
3.5	Inadequate Reinforcing Embedment and Laps	15
3.6	Inadequate Foundation Capacity	16
4	Unseating: 17	
4.1	Introduction:.....	17
4.2	Minimum Support Length Requirements:.....	18
4.3	Corrosion of Connections and Bearings:	20
4.3.1	Fixed bearings:.....	22
4.3.2	Expansion bearings:.....	25
4.3.3	Anchorage bolts:.....	26
4.3.3.1	Steel failure in tension:.....	28
4.3.3.2	Pullout failure in tension:	29
4.3.3.3	Concrete tensile breakout:.....	30
4.3.3.4	Concrete side-face blowout of a headed anchor in tension:	32
4.3.3.5	Bond failure of adhesive anchor in tension:.....	33
4.3.3.6	Steel failure in shear:.....	34
4.3.3.7	Concrete breakout of anchor in shear:.....	36
4.3.3.8	Concrete pryout failure of anchor in shear:.....	39
4.4	Deterioration of Seats and Caps:.....	40
4.4.1	Single column piers (Cantilevered piers):.....	41
4.4.2	Multi column piers (bents):.....	43
4.4.3	Abutments:.....	45
4.5	Deterioration of Concrete at end of Beam/Girders:	46
4.5.1	Steel reinforced girders:.....	46
4.5.2	Prestressed concrete girders:.....	49
5	Corroded RC Concrete Column: 49	
5.1	Deterioration of Reinforced Concrete Bridge Columns:.....	49
5.2	Behavior of Corroded Reinforced Concrete Columns Subjected to Lateral Loading: ..	55
5.3	Flexural Capacity:	57
5.4	Shear Capacity:	66
5.5	Lap Splices:.....	69
6	Inadequate Foundation Capacity: 74	

6.1	Introduction:	74
6.2	Spread footings:	74
6.2.1	Tilting of the footing due to a soil bearing failure:	75
6.2.2	Flexural yielding of footing reinforcement:	77
6.2.3	Concrete shear failure of footing:	79
6.2.4	Bond failure of the main column steel:	83
6.3	Pile footing:	86
6.3.1	Pile pullout:	87
6.3.2	Pile flexural and/or shear failure:	88
REFERENCES		91

List of Figures

Fig. 1:	Consequences of corrosion on structural performance (Contecvet, 2000)	3
Fig. 2:	NYS Highway Bridge Conditions	3
Fig. 3:	Averaged (P_{av}) and maximum pit depth (P_{max}) or maximum attack penetration	5
Fig. 4:	Deterioration of a structure with time (Contecvet, 2000)	5
Fig. 5:	Amount of corrosion for several environments (Val et al., 1998)	6
Fig. 6:	Residual reinforcing bar section (Contecvet, 2000)	7
Fig. 7:	Decrease of bar area for $I_{corr}=1(\mu A/cm^2)$ (Contecvet, 2000)	8
Fig. 8:	Stress-strain diagram for corroded steel reinforcement (Du et al., 2005)	8
Fig. 9:	Four stages in the corrosion deterioration of CRC bridge elements. Additional stages are possible when the deterioration is more severe (Higgins et al., 2003)	9
Fig. 10:	Hypothetical performance of a CRC structure through the four stages of deterioration (Higgins et al., 2003)	10
Fig. 11:	Collapse of the link span at Tower E9 of the San Francisco Oakland Bay Bridge due to inadequate seat lengths and anchor bolts. (Loma Prieta earthquake, 1989)	11
Fig. 12:	Hwy 5 Overcrossing, pending unseating of PS girder. (Baja California Earthquake Clearinghouse Magnitude 7.2 on April 4, 2010)	11
Fig. 13:	Showa Bridge collapse in 1964 Niigata earthquake (Moehle, 2000)	12
Fig. 14:	Shear failure of columns during the 1971 San Fernando earthquake (Moehle et al., 2000)	13
Fig. 15:	Shear failure of a column of Shinkansen bridge. 2004, Japan	13
Fig. 16:	Diagonal shear crack in lightly reinforced concrete pier of the Wu Shu bridge in Taichung (Chi Chi earthquake, 1999) (Buckle)	13
Fig. 17:	Shear failures at the base of piers due to inadequate shear reinforcement (Hyogoken–Nanbu (Kobe, Japan) earthquake, 1995, Bruneau 1998)	14
Fig. 18:	San Fernando Road Overhead damage due to insufficient flexural ductility in the 1971 San Fernando earthquake (Moehle et al., 2000)	14
Fig. 19:	Hanshin Expressway, Pier 46, damage in the 1995 Hyogo-Ken Nanbu earthquake due to insufficient flexural ductility (Moehle et al., 2000)	14
Fig. 20:	Flexural failure due to lack of confinement at bottom of reinforced concrete piers (Hyogoken–Nanbu (Kobe, Japan) earthquake, 1995, Bruneau 1998)	15
Fig. 21:	Higashi-Nada Viaduct collapse due to lap splice failure in the 1995 Hyogo-Ken Nanbu	15
Fig. 22:	Anchorage failure in column/footing joint (FEMA 451, 2006)	16

Fig. 23: Pull out of reinforcement (Saad et al. 2010).....	16
Fig. 24: Different types of foundation failure (Saad et al. 2010).....	17
Fig. 25: Collapse due to liquefaction (Saad et al. 2010).....	17
Fig. 26: Support Length, N, AASHTO.....	18
Fig. 27: Typical fixed and expansion bearings (Lindquist 2008).....	20
Fig. 28: Bridge bearing.....	21
Fig. 29: Anchor bolt corrosion inside the bearing, beneath the washer (Lindquist 2008).....	22
Fig. 30: Rocking/force distribution mechanism in fixed bearings on concrete pedestals along longitudinal direction (Ghosh and Padgett 2010).....	23
Fig. 31: Spalling and delamination of concrete due to corrosion in anchor bolts.....	25
Fig. 32: Force distribution mechanism through the anchor bolt when the keeper plate strikes the rocker.....	26
Fig. 33: Steel failure in tension (ACI 318-11).....	28
Fig. 34: Reduction in bolt cross-sectional area due to corrosion.....	29
Fig. 35: Pullout failure in tension (ACI 318-11).....	30
Fig. 36: Concrete tensile breakout (ACI 318-11).....	30
Fig. 37: calculations of A_{Nco} , A_{Nc} for single anchors and group of anchors (ACI 318-11).....	32
Fig. 38: Concrete side-face blowout and concrete splitting in tension (ACI 318-11).....	33
Fig. 39: Bond failure of adhesive anchor in tension (ACI 318-11).....	34
Fig. 40: Steel failure preceded by concrete spall (ACI 318-11).....	36
Fig. 41: Concrete breakout in shear (ACI 318-11).....	37
Fig. 42: corrosion in edge reinforcement to prevent Concrete breakout of anchor in shear.....	39
Fig. 43: Concrete pryout for anchors far from a free edge.....	40
Fig. 44: Fracture of Bearing Seat (FHWA Bridge Maintenance, Rossow).....	41
Fig. 45: Reinforcement of a single column pier cap.....	41
Fig. 46: Crack pattern and concrete delamination due to corrosion.....	42
Fig. 47: Deterioration in concrete due to corrosion of steel reinforcement.....	42
Fig. 48: Deterioration in concrete increase the risk of unseating during an earthquake.....	43
Fig. 49: Reinforcement of multi column pier cap.....	44
Fig. 50: Spalling and delamination of concrete pier cap (Bridge Inspection Manual 2010).....	44
Fig. 51: Severe Concrete Spalling on Bent Cap (BIRM, Rossow).....	45
Fig. 52: Deterioration of bridge abutment increase the risk of span unseating.....	45
Fig. 53: Typical fixed steel bearing at an abutment (note seat cracking at the edge and corrosion of its reinforcements) (Padgett et al. 2006).....	46
Fig. 54: Moderate Damage: Spalled concrete (WSDOT).....	47
Fig. 55: Deterioration of bridge girder increase the risk of span unseating during an earthquake.....	48
Fig. 56: Deterioration of a concrete bridge pier due to corrosion of reinforcing steel bars (Aboutaha, 2004).....	50
Fig. 57: Deterioration of concrete bridge pier columns due to corrosion of rebars (Aboutaha, 2004).....	50
Fig. 58: Close-up of corroded column longitudinal and transverse rebars.....	51
Fig. 59: Effect of corrosion of reinforcing steel bars on the surrounding concrete (Aboutaha, 2004).....	51
Fig. 60: Corrosion damaged rectangular concrete columns (Aboutaha, 2004).....	52
Fig. 61: Corroded longitudinal and transverse rebars for circular columns (Aboutaha, 2004).....	53

Fig. 62: Corrosion damaged circular concrete columns. Notice that the main cracks are parallel to the columns' main reinforcing steel bars (Aboutaha, 2004).....	53
Fig. 63: Deteriorated concrete bridge pier due to corrosion of rebars (Aboutaha, 2004).....	54
Fig. 64: Corrosion damage of tall concrete bridge pier columns (Aboutaha, 2004)	54
Fig. 65: Load–deformation curves (influence of rebar corrosion) (RC-COR-1: 1 st corrosion level, RC-COR-2: 2 nd corrosion level, RC-COR-3: 3 rd corrosion level) (Lee et al., 2003)	55
Fig. 66: Lateral load-displacement curve (Ma et al., 2012).....	56
Fig. 67: Push-over analysis of corroded bridge (Asri and Ou, 2011).....	57
Fig. 68: Calculations of stress and strains for a given section and strain distribution.....	60
Fig. 69: Strain distributions corresponding to points on interaction diagram (Tapan and Aboutaha, 2008).....	61
Fig. 70: Deterioration cases included in the analysis (Tapan and Aboutaha, 2011).....	61
Fig. 71: Interaction diagram for pre-defined deterioration stages, where deterioration is on the compression side of the column section	62
Fig. 72: Interaction diagram for pre-defined deterioration stages, where deterioration is on the tension side of side of the column section	63
Fig. 73: Interaction diagram for pre-defined deterioration stages, where deterioration is on the left side of the column section	63
Fig. 74: Interaction diagram for pre-defined deterioration stages, where deterioration is on all sides of the column section.....	64
Fig. 75: Interaction diagram for pre-defined deterioration stages, where deterioration is on the compression and left side of the column section	65
Fig. 76: Interaction diagram for pre-defined deterioration stages, where deterioration is on the tension and left side of the column section.....	65
Fig. 77: Plan view of concrete cracking in beam web due to corrosion for three different stirrup spacing; (a) 8-in, (b) 10-in, and (c) 12-in (Higgins et al., 2003)	67
Fig. 78: Effective depth of unsymmetrical section.....	67
Fig. 79: Information for calculating transverse and longitudinal indexes w_t and w_L : (a) membrane element; (b) beam cross section under shear, bending, and axial load; and (c) unsymmetrically reinforced sections.	68
Fig. 80: Normalized shear strength curves (Rahal, 2000)	69
Fig. 81: Conceptual model for damage due to corrosion in column specimens (Aquino and Hawkins, 2007).....	71
Fig. 82: Crack-damage pattern after corrosion and before cyclic load test. (Aquino and Hawkins, 2007).....	71
Fig. 83: Stress ratio of corroded bar to non-corroded bar.....	73
Fig. 84: Modes of failure for spread footings (FHWA).....	75
Fig. 85: Delamination of concrete leading to decrease the length of footing.....	77
Fig. 86: Reinforcement of footing in longitudinal and transversal directions	79
Fig. 87: Effective anchorage length of longitudinal reinforcement (FHWA 2006)	85
Fig. 88: Different types of foundation failure (Saad et al. 2010).....	87
Fig. 89: stirrup area within the region of D (pile diameter).....	91

List of Tables

Table 1: Corrosion intensities for several corrosive environments (Dhir et al., 1994)..... 6
Table 2: Percentage N by SDC and Acceleration Coefficient, A_s 19
Table 3: Strength reduction in different deterioration stages..... 66
Table 4: Stress ratio of corroded bar to non-corroded bar 73

Seismic Evaluation and Retrofit of Deteriorated Concrete Bridge Components

1 Introduction:

Corrosion of steel bars in reinforced concrete structures is a major durability problem for bridges constructed in the New York State (NYS). The heavy use of deicing salt compounds this problem. Corrosion of steel bars results in loss of steel cross section, deterioration of bond between concrete and reinforcing bars, and more important, in most cases, it results in unsymmetrical concrete section that is susceptible to shear failure.

Though earthquake frequency of occurrence and the expected ground accelerations in NYS is less than in western states, the potential for earthquake damage in or around NYS is still very real. Given the level of deterioration in many reinforced concrete bridges in NYS, they are considered very vulnerable to major damage during a moderate seismic event.

There is an urgent need for proper detailed guide for analysis of deteriorated reinforced concrete bridge components that could assist structural engineers estimate the reserved strength of deteriorated bridges, and design cost-effective methods for retrofit. Proper evaluation and retrofit of existing deteriorated reinforced concrete bridges will limited the collapse of bridge during moderate seismic events in NYS and the surrounding states, and consequently save people's lives.

Fig. 1 shows the USGS National Seismic Hazard Map of the United States. According to this map, the USGS identifies NYS as a region of "low-to-moderate" seismic hazard (2008). The graphic of NYS in Fig. 2 illustrates the peak ground accelerations (PGA) that have a 2% probability of being exceeded in 50 years. According to this map, the NYC and Adirondack regions are more likely to get an earthquake than the center part of the state. These figures illustrate the fact that the possibility of an earthquake is not solely a west coast concern. Though the frequency of occurrence and the expected ground accelerations may be less, the potential for earthquake damage in or around NYS is still very real, (O'Connor, 2010). Given the level of deterioration in many reinforced concrete bridges in NYS, they considered very vulnerable to major damage during a moderate seismic event.

Although the earthquake hazard is rated "low-to-moderate," the risk in NYS can be high because of the potential consequences. Although mild earthquakes occur regularly in and near NYS, and frequently go undetected, a moderate or strong one has the potential to disrupt operation of the highway system, cause injury, and result in major property damage. For instance, a highly developed area like the NYC metropolitan region has many vital structures that carry a large amount of traffic. Considerable damage to any of these structures has potential to severely disrupt traffic and impede recovery from an earthquake. Recognition of this risk is the motivation behind this proposed research project.

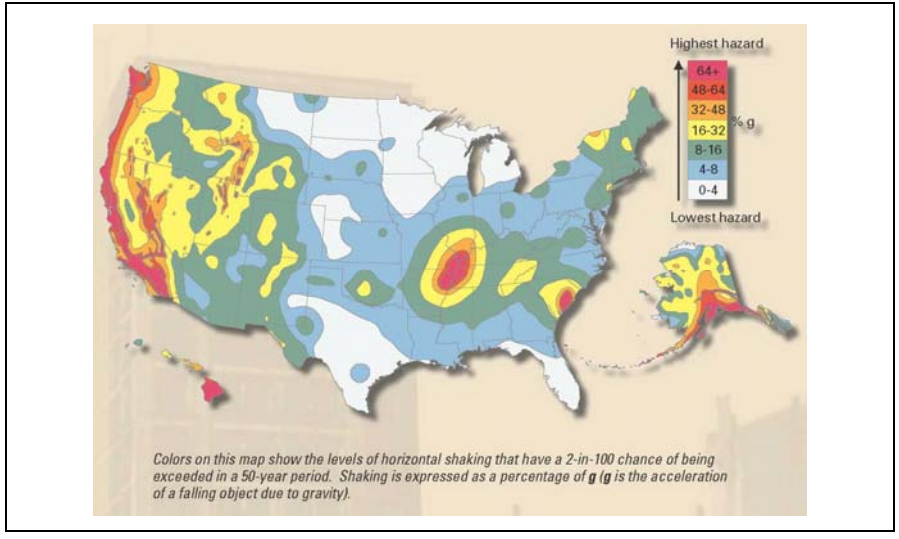


Fig. 1 United States Seismic Hazard Map (USGS) (<http://www.usgs.gov>)

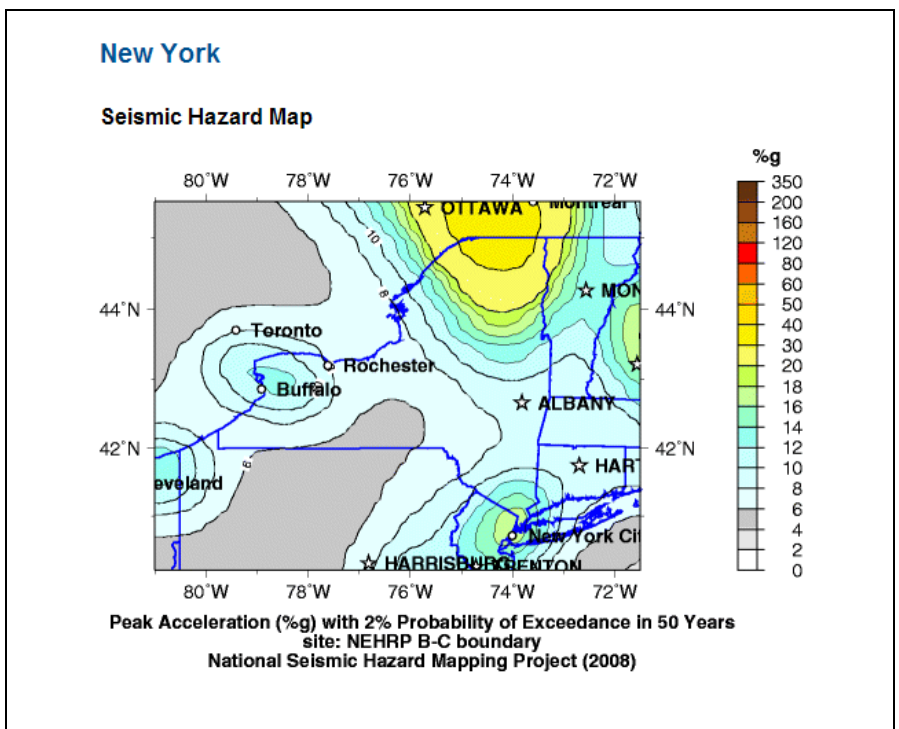


Fig. 2 New York State's Seismic Hazard (USGS) (http://earthquake.usgs.gov/regional/states/new_york/hazards.php)

The San Fernando earthquake showed that bridges built prior to 1970s are vulnerable to damage due to ground motion. Many of the interstate bridges in the USA were constructed before 1971, and therefore incorporate deficiencies that must be identified and retrofitted to avoid severe damage or collapse (Endeshaw, 2008). Moreover, a considerable number of the above bridges and some of the bridges built after 1971 are deteriorated. The deterioration of concrete bridges in the State of New York is preliminary due to the use of deicing salt causing corrosion of steel bars, which in turn results in loss of concrete cross section, reinforcing steel area, ductility, symmetry, and bond between steel and concrete. Fig. 3 shows the consequences of corrosion on structural performance (Contecvet, 2000).

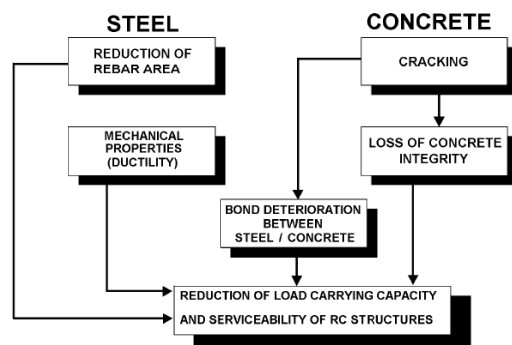


Fig. 3: Consequences of corrosion on structural performance (Contecvet, 2000)

2 Literature Review:

There are 17,000 highway bridges in the State of New York, of which 44 percent owned by the State Department of Transportation (NYSDOT), 50 percent owned by municipalities, and the rest owned by state and local authorities. According to the data submitted to the Federal Highway Administration (FHWA) in April 2008, 12 percent of the state bridges are considered, under the broad federal standards, structurally deficient and 25 percent are classified as functionally obsolete, as shown in Fig. 4. These terms are used to classify the bridges that do not meet current FHWA standards. However, the above classifications do not mean that these bridges are unsafe to use, they actually mean that these bridges require rehabilitation or retrofit in order to restore their original conditions or improve their performance (NYSDOT).

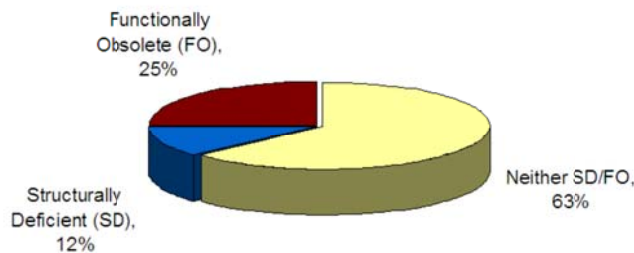


Fig. 4: NYS Highway Bridge Conditions

Bridges are considered “structurally deficient,” according to the FHWA, if significant load carrying elements are found to be in poor or worse condition due to deterioration and/or damage, the bridge has inadequate load capacity, or repeated bridge flooding causes traffic delays. The fact that a bridge is "structurally deficient" does not imply that it is unsafe or likely to collapse. A "structurally deficient" bridge, when left open to traffic, typically requires significant maintenance and repair to remain in service and eventual rehabilitation or replacement to address deficiencies. In order to remain in service, structurally deficient bridges are often posted with weight limits (NYSDOT).

“Functionally obsolete” refers to a bridge’s inability to meet current standards for managing the volume of traffic it carries, not its structural integrity. For example, a bridge may be functionally obsolete if it has narrow lanes, no shoulders, or low clearances (NYSDOT).

The New York State requires all highway bridges to be inspected at least every two years, moreover, it is one of the few states in the USA that requires bridge inspectors headed by licensed professional engineers who have undergone specific training. These inspectors must assess all individual parts of each bridge, evaluate, assign a condition score, and document the condition of up to 47 structural elements, including rating 25 components of each span of a bridge, in addition to general components common to all bridges. The rating scale usually ranges from 1 to 7, with a rating of 5 and greater considered as good condition, and a rating of 7 considered as new condition (NYSDOT).

2.1 Corrosion Rates:

2.1.1 Definition:

The corrosion rate of a metal is defined as the metal loss per unit of surface and time

$$CR = \frac{\text{metal loss}}{\text{surface} \cdot \text{time}}$$

Units:

The units of the above equation can be expressed in (g/cm².year) but are usually presented using one of the two following methods:

- 1) In μm/year or mm/year, as attack penetration depth, either localized or uniform, that can be computed from the metal mass loss through the metal density which allows P_x to be calculated in μm or mm. Fig. 5 (Contecvet, 2000).



Fig. 5: Averaged (P_{av}) and maximum pit depth (P_{max}) or maximum attack penetration (Contecvet, 2000)

2) In $\mu A/cm^2$, using Faraday's Law:

$$\frac{I \cdot t}{F} = \frac{Dw}{Wm/Z}$$

Where:

I = electrical current in Amperes

t = time in seconds

F = Faraday's constant (96500 coulombs)

Dw = mass or weight loss in grams

Wm = molecular weight of the metal

Z = valence exchanged

Faraday's law converts mass units in electrical units. However, the equivalence between the two methods of expressing the corrosion rate is as follows:

$$1\mu A/cm^2 \Leftrightarrow 11.6\mu m/year \text{ (Contecvet, 2000).}$$

This research study will consider different corrosion amounts to represent the effect of different corrosion rates for different types of environments. These corrosion amounts can be converted to deterioration time for given corrosion rates. Fig. 6, however, shows the relationship between deterioration of a reinforced concrete structure and time.

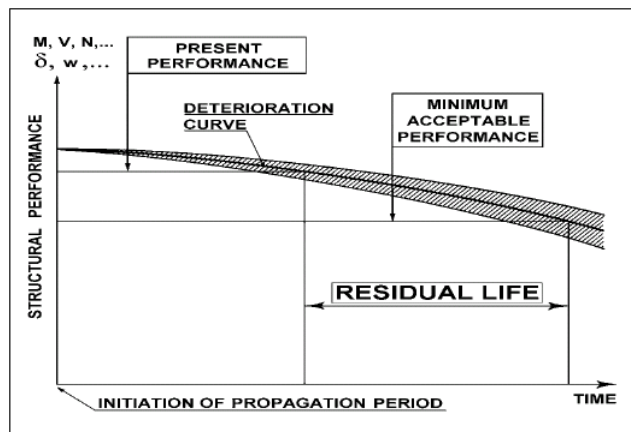


Fig. 6: Deterioration of a structure with time (Contecvet, 2000).

Moreover, Fig. 7 shows the amount of corrosion for several corrosive environments for a number 9 bar Val et al. (1998), these corrosive environments are low, moderate, and high. On the other hand, Dhir et al. (1994) suggested the different corrosion rates based on the condition of the environment, as shown in Table 1.

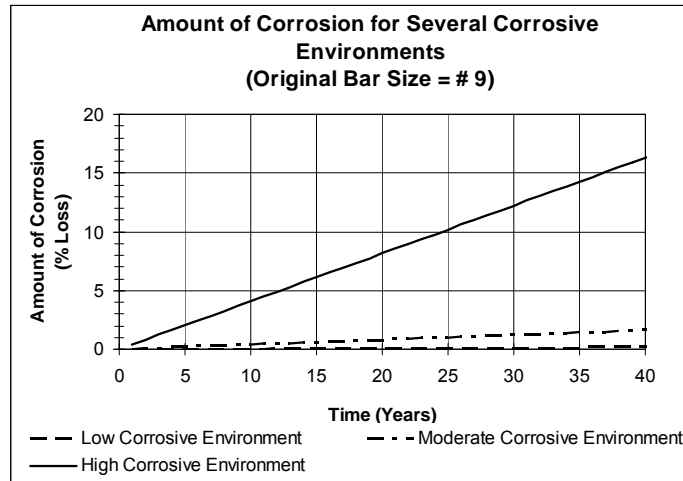


Fig. 7: Amount of corrosion for several environments (Val et al., 1998).

Table 1: Corrosion intensities for several corrosive environments (Dhir et al., 1994).

Type of Corrosive Environment	Corrosion Intensities ($\mu A/cm^2$)
Low	0.1
Moderate	1
High	10

2.1.2 Measurement:

The amount of metal which goes into oxides by unit of reinforcement, surface, and time is usually given by the measurement of the corrosion current I_{corr}^{rep} . While the cracking of the concrete cover and the loss in bond between steel and concrete are due to the amount of oxides produced, the load-carrying capacity is a result of the decrease in the steel cross-section area. Thus, the corrosion rate is considered to be an indication of the rate of decrease of the load-carrying capacity of the structure (Contecvet, 2000).

There are many electrochemical and non-destructive methods to measure the corrosion rate of reinforcing steel in existing structures. Some of methods for assessing corrosion of reinforcing steel on existing structures are:

1. Open circuit potential (OCP) measurements
2. Surface potential (SP) measurements
3. Concrete resistivity measurement
4. Linear polarization resistance (LPR) measurement
5. Tafel extrapolation
6. Galvanostatic pulse transient method
7. Electrochemical impedance spectroscopy (EIS)
8. Harmonic analysis
9. Noise Analysis
10. Embeddable corrosion monitoring sensor and
11. Cover thickness measurements
12. Ultrasonic pulse velocity technique
13. X-ray, Gamma radiography measurement
14. Infrared thermograph Electrochemical
15. Visual inspection (Song et al., 2007)

2.2 Effect of Corrosion on Reinforcing Bars:

The influence of Corrosion of reinforcing on the cross section differs widely based on the characteristics of the aggressive agent. The homogeneous attack penetration occurs in carbonated concrete, while the localized attack produced by chlorides is known as pitting, which produces a major section decrease as shown in Fig. 8. After obtaining the depth of the attack penetration, the residual bar diameter can be computed by means of the following expression:

$$\phi_t = \phi_0 - \alpha P_x \quad \text{Eq. 1}$$

Where α is the coefficient that depends on the type of attack. When homogeneous corrosion occurs, α is equal to 2. However, when localized corrosion occurs, α may reach values up to 10. A conservative value of the residual section at pits can be also predicted by the above expression (Contecvet, 2000).

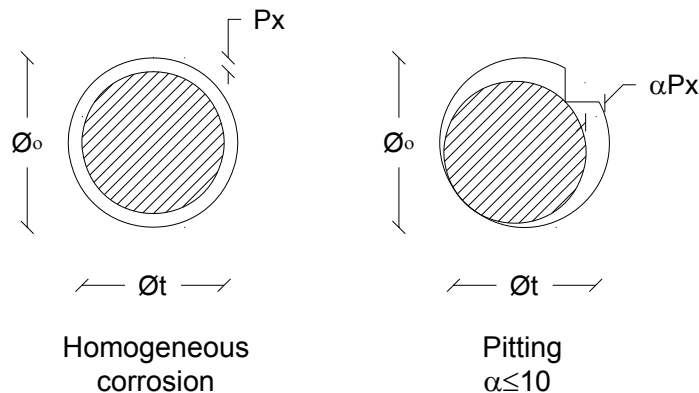


Fig. 8: Residual reinforcing bar section (Contecvet, 2000).

Moreover, Fig. 9 shows that homogeneous corrosion is negligible in terms of section reduction for high diameter bars, whereas pitting corrosion in small diameter bars has a relevant effect.

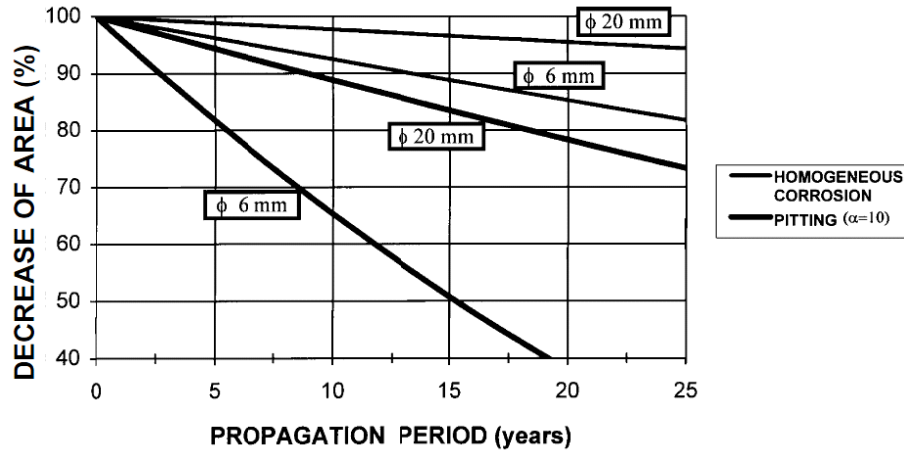


Fig. 9: Decrease of bar area for $I_{corr}=1(\mu A/cm^2)$ (Contecvet, 2000).

2.3 Effect of Corrosion on Material Properties:

When corrosion attacks, it does not considerably affect the strength ratio, hardening, strain, and the modulus of elasticity of corroded reinforcement. This is because corrosion removes iron ions only from the bar surface and does not change the nature and composition of the remaining steel reinforcement. This means that the corrosion does not significantly change the stress-strain diagram of steel. In other words, corroded reinforcement has a stress-strain diagram which is similar to that of non-corroded steel with a definite yield plateau as shown in Fig. 10 (Du et al., 2005).

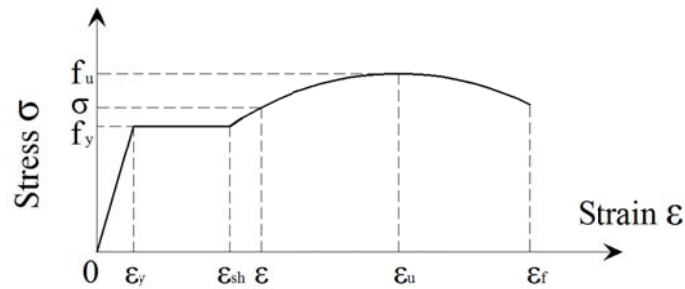


Fig. 10: Stress-strain diagram for corroded steel reinforcement (Du et al., 2005)

Moreover, Du et al. 2005 proposed empirical equations to calculate the residual cross-section and yield strength of corroded steel bars as follows:

$$f = (1 - 0.005 \cdot Q_{corr}) \cdot f_y \quad \text{Eq. 2}$$

Where:

f = yield strength of corroded bars

f_y = yield strength of non-corroded bars

Q_{corr} = amount of corrosion of reinforcement (%)

$$A_s = A_{so} \cdot (1 - 0.01 \cdot Q_{corr}) \quad \text{Eq. 3}$$

Where:

A_s = average cross-sectional area of corroded reinforcement

A_{so} = initial cross-sectional area of non-corroded reinforcement

And the amount of corrosion of reinforcement (%) can be computed as:

$$Q_{corr} = 0.046 \cdot \frac{I_{corr}}{d} \cdot t \quad \text{Eq. 4}$$

Where:

I_{corr} = corrosion rate of reinforcement in the real structure ($\mu\text{A}/\text{cm}^2$)

d = diameter of non-corroded reinforcement (mm)

t = time elapsed since the initiation of corrosion (years)

2.4 Deterioration Stages:

Fig. 11 shows the four damage stages that the inspection of usually focuses on (Higgins et al., 2003). In the first stage (Stage I), the chloride is placed on the structure surface and spreads to the depth of the reinforcing steel to start corrosion. The second stage (Stage II) is the period during which corrosion diffuses, causing surface manifestations of corrosion such as cracking of the concrete and rust staining of the structure. Stage III usually starts when the reinforcing steel becomes more accessible to the corrosive environment causing structural deterioration (cracking and delamination), and corrosion continues at a faster rate allowing more loss of steel cross-section. Stage IV is linked by spalling of the concrete allowing a full exposure of the reinforcing steel to the corrosive environment (Higgins et al., 2003). More extreme damage stages would include loss of bond between the reinforcing steel and the core concrete, diagonal cracking of the core concrete, and failure of the structural steel (Higgins et al., 2003). After performing a study on the Alesia Bay Bridge (Oregon), Tinnea and Feuer (1985) suggested that in stages III and IV reinforcing steel corrosion rates may be similar (Higgins et al., 2003).

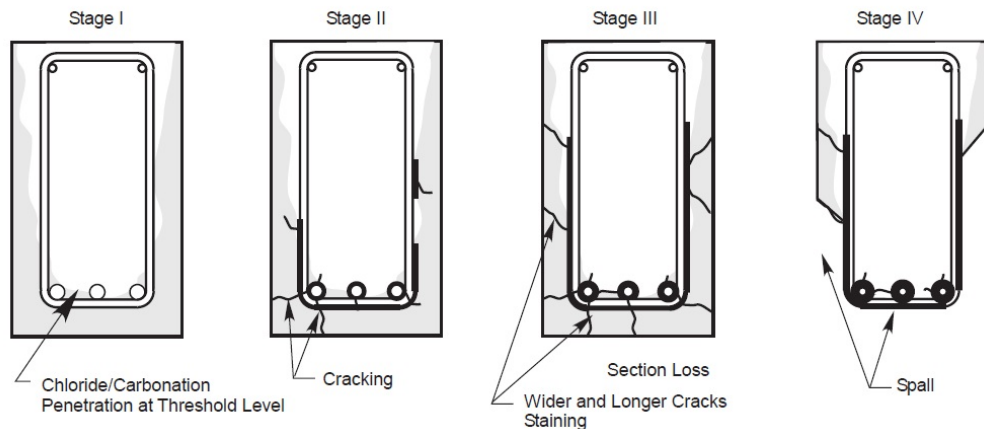


Fig. 11: Four stages in the corrosion deterioration of CRC bridge elements. Additional stages are possible when the deterioration is more severe (Higgins et al., 2003).

Fig. 12 shows the progress of a hypothetical CRC bridge through the first four damage stages as a function of structure performance. Stage I is reasonably well understood and can be quantified for well characterized concretes using Fick’s law of diffusion. However, structure environment interactions that affect this analysis, involving salt deposition, precipitation washing, and cyclic wetting and drying effects over a variety of structure microclimates, are much less well understood (Higgins et al., 2003).

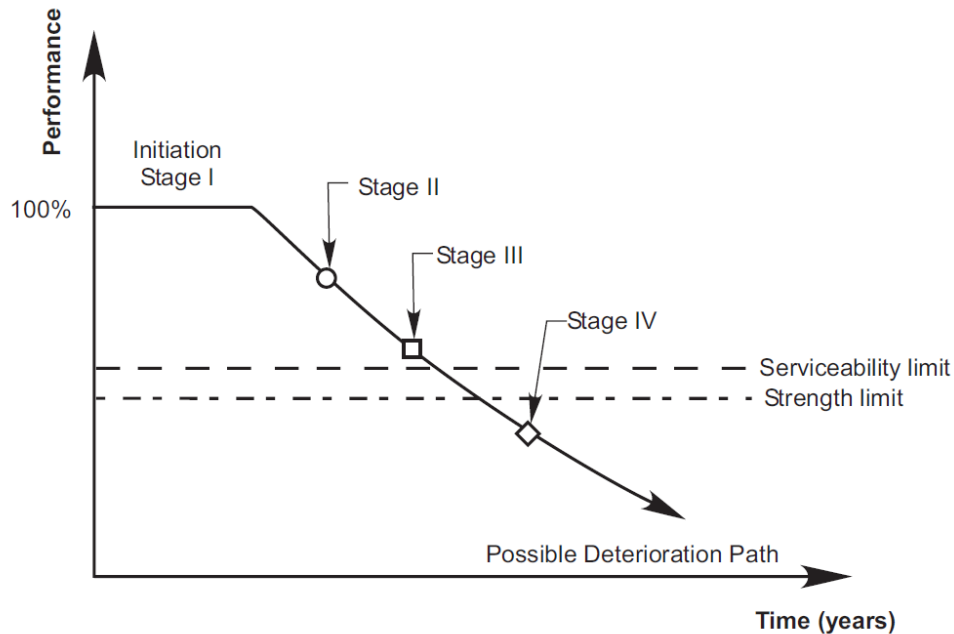


Fig. 12: Hypothetical performance of a CRC structure through the four stages of deterioration (Higgins et al., 2003).

3 Common Earthquake Failure Mechanisms:

3.1 Introduction:

The Federal Highway Administration FHWA considers the following bridge components to be more vulnerable to seismic damage than others:

- Connections, bearings, and seats (support lengths).
- Piers, columns and foundations.
- Abutments.
- Soils.

Moreover, FHWA considers connections, bearings and inadequate seat length to be the most common reason for bridge collapse, and the least costly to fix.

Saad et al., 2010, address the following most common earthquake failure mechanisms.

3.2 Unseating (most common):

This failure occurs in the superstructure and it is usually a result of the large displacements encountered during an earthquake and it is the most common failure mechanism (Saad et al. 2010). The unseating and collapse of bridge spans is due to excessive longitudinal movement at

in-span hinges, supports, or expansion joints. Span Collapse of bridges from around the world during past earthquakes has shown the vulnerability of bridges to this mode of collapse (Brunsdon et al. 2000, Kawashima et al. 1996). Bridges have collapsed due to unseating in many earthquakes such as the Niigata earthquake in 1964 (Japan), San Fernando Earthquake in 1971, Loma Prieta earthquake in 1989, Northridge earthquake in 1994, Kobe earthquake in 1995 (Japan), Chi-Chi earthquake in 1999 (Taiwan), and Kocaeli Earthquake in 199 (Turkey) (Padgett et al. 2008).



Fig. 13: Collapse of the link span at Tower E9 of the San Francisco Oakland Bay Bridge due to inadequate seat lengths and anchor bolts. (Loma Prieta earthquake, 1989)



Fig. 14: Hwy 5 Overcrossing, pending unseating of PS girder. (Baja California Earthquake Clearinghouse Magnitude 7.2 on April 4, 2010)



Fig. 15: Showa Bridge collapse in 1964 Niigata earthquake (Moehle, 2000)

Unseating of a span usually occurs due an earthquake as a result of inadequate support length. When the relative horizontal displacement at the deck exceeds the support at the intermediate hinge or abutment, the girder can deck can unseat and collapse (DesRoches et al. 2001). This is because many bridges are designed according to older seismic codes and do not provide adequate seat width. Even though that many of older bridges have been retrofitted using hinge restrainers, some bridges during the 1989 Loma Prieta earthquake experienced several cases of hinge restrainer failures (Saiidi et al. 1993). Moreover, the 1994 Northridge earthquake caused many bridges that have been retrofitted with restrainers to collapse due to unseating (Moehle 1995). However, deterioration of the concrete bridge pier caps can lead to a shortening in the support length which, in turn, leads to a catastrophic collapse of the bridge span. Also, concrete deterioration and spalling due to corrosion of steel reinforcement at the end of girders can result in unseating of bridge deck. Corrosion in bearing systems or existing retrofitting systems can also be a real concern regarding unseating. Corrosion in superstructure elements that leads to unseating during an earthquake will be discussed in detail in the following chapters.

3.3 Column Shear:

Shear failure has been a common mode of failure of RC bridge columns in many earthquakes. Inadequate transverse reinforcement, especially those with large spacing, cause this type of failure. Shear failure happens at relatively low structural displacements; it may occur even before yielding of longitudinal reinforcement. In general, inelastic loading cycles decrease shear capacity of columns alternatively which results in shear failure after flexural yielding (Moehle et

al., 2000). Shear load capacity of columns might decrease by corrosion faster than flexural load capacity, because transverse reinforcement has less concrete cover than longitudinal one, which may start to corrode first (Webster, 2000). Shear capacity of corroded RC column is discussed further in Chapter 7.



Fig. 16: Shear failure of columns during the 1971 San Fernando earthquake (Moehle et al., 2000)



Fig. 17: Shear failure of a column of Shinkansen bridge. 2004, Japan, (Moehle et al., 2000).



Fig. 18: Diagonal shear crack in lightly reinforced concrete pier of the Wu Shu bridge in Taichung (Chi Chi earthquake, 1999) (Buckle)



Fig. 19: Shear failures at the base of piers due to inadequate shear reinforcement (Hyogoken–Nanbu (Kobe, Japan) earthquake, 1995, Bruneau 1998)

3.4 Column Flexural Capacity:

For an ideal designed concrete column subjected to lateral load, mode of failure is flexural. However, even if most of the inelastic action is flexural, insufficient flexural ductility, usually due to little confinement, may lead a column not be able to maintain the imposed flexural deformations (Moehle et al., 2000). Fig. 20 to Fig. 22 are examples of failure of columns due to inadequate flexural capacity. Flexural capacity of corroded column decreases due to deteriorated concrete cross-section and reduced steel bar area. Furthermore, corrosion of transverse reinforcement reduces the modulus of elasticity of steel bar and as a result, the confinement rate decreases. There fore, corroded RC column may not be able to develop the full flexural capacity. Flexural capacity of corroded RC column is discussed further in Chapter 7.



Fig. 20: San Fernando Road Overhead damage due to insufficient flexural ductility in the 1971 San Fernando earthquake (Moehle et al., 2000)



Fig. 21: Hanshin Expressway, Pier 46, damage in the 1995 Hyogo-Ken Nanbu earthquake due to insufficient flexural ductility (Moehle et al., 2000)



Fig. 22: Flexural failure due to lack of confinement at bottom of reinforced concrete piers (Hyogoken–Nanbu (Kobe, Japan) earthquake, 1995, Bruneau 1998)

3.5 Inadequate Reinforcing Embedment and Laps

Lap splice failure of RC bridge columns may occur due to short length or poor confinement. Location of splices is often above a footing, where there is a potential plastic hinge region with high flexural demand. The splices may not be able to develop the flexural capacity of the column because of poor detailing and they may be more vulnerable to shear failure (Moehle et al., 2000). Furthermore, high longitudinal ratio, large bar size, high yield strength of longitudinal reinforcement, small spacing between vertical bars and inadequate concrete cover increase vulnerability of lap splices (Prestley et al., 1996). Lap splice failure occurs because of loss of bond; since corrosion decrease bond between steel bars and concrete significantly, it may facilitate this type of failure. Lap splice failure of corroded RC column is discussed further in Chapter 7.



Fig. 23: Higashi-Nada Viaduct collapse due to lap splice failure in the 1995 Hyogo-Ken Nanbu

Insufficient anchorage of the longitudinal reinforcement at the top of a column at the connection with the bent cap or at the bottom of a column at the connection with the foundation, may result in RC bridge column failure (Moehle et al., 2000). In order to ensure ductile frame behavior, anchorage failure must be prevented. Fig. 23 shows an anchorage failure of a bridge column (1971, San Fernando earthquake).



Fig. 24: Anchorage failure in column/footing joint (FEMA 451, 2006)

Anchorage is extremely important to assure adequate post yield response. Requirements for rebar anchorage (such as 135 degree hooks) are intended to maintain the integrity of the design. If all required detailing is provided for anchored bar, deterioration of steel, concrete or both in worse case lead the bars to pull out during earthquake. It means that, if corrosion level is too high that pull out occurs, anchored bars can be considered as straight bars and evaluate like spliced bars.



Fig. 25: Pull out of reinforcement (Saad et al. 2010).

3.6 Inadequate Foundation Capacity

The strength and stiffness of the foundation system of a bridge (abutments/piers, footings, and piles) usually control the bridge behavior during seismic events (FHWA). It is generally difficult to inspect the deterioration of the foundation of a bridge. This is because such an activity requires excavation above and around the footing and piles in order to visually inspect their integrity. However, tilting of a pier, sloughing of the fill around a footing, and flexural cracking

of the column could be signs that bridge foundations are deteriorated or that there is a risk of foundation failure during an earthquake.

O’Conner 2010 suggested that the mode of failure is dependent on the type of soil as well as the detail of foundation.

The different types of foundation failure will be discussed in detail in the coming chapters.

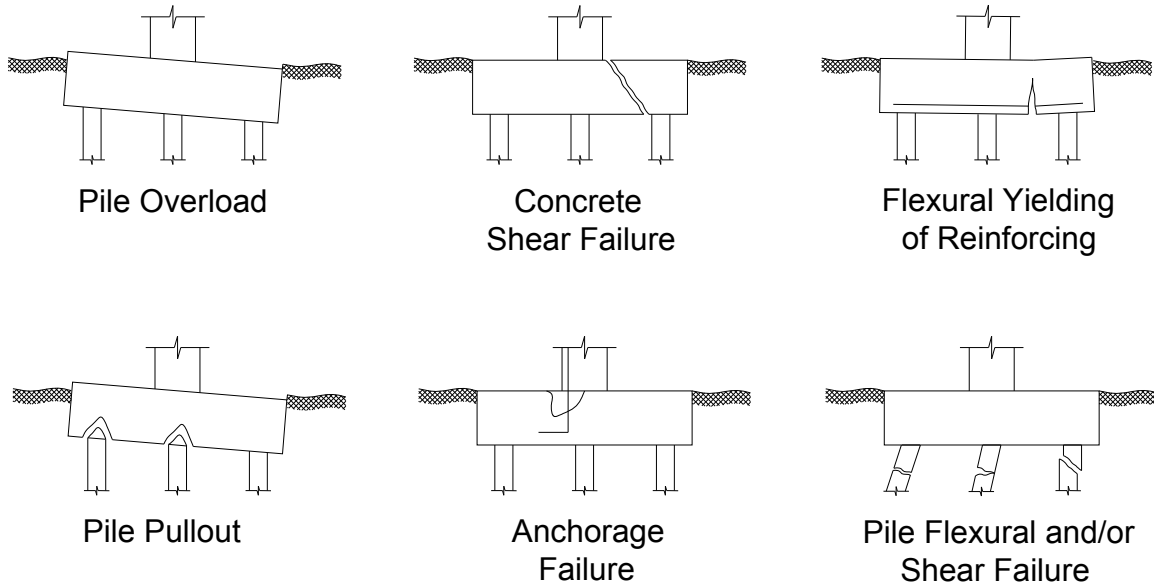


Fig. 26: Different types of foundation failure (Saad et al. 2010)



Fig. 27: Collapse due to liquefaction (Saad et al. 2010)

4 Unseating:

4.1 Introduction:

Unseating is the most common earthquake failure mechanism. This mode of failure occurs during an earthquake as a result of inadequate support length. Moreover, the Federal Highway

Administration (FHWA) considers connections, bearings and inadequate seat length to be the most common reason for bridge collapse, and the least costly to fix. The presence of corrosion increases the risk of span collapse during seismic events. High levels of corrosion in bridge seats and girders cause concrete to crack and spall which results in decreasing the support length or the length of the girder seated on the support. In addition, corrosion of steel bearings and anchor bolts decreases their strength to resist horizontal movements which can result in a catastrophic collapse of the bridge span.

4.2 Minimum Support Length Requirements:

During the San Fernando Earthquake, 1971, Most of the bridges collapsed due to the loss of supports at bearing seats and/or expansion joints, which called unseating. Unseating is the most common reason that causes failure of bridge super structure due to seismic loadings. Unseating usually occurs at movement joints due to large inelastic displacements (Itani and Liao, 2003). However, under Bridge Seat Extension, NYSDOT LRFD Bridge Design Specifications 2011 states that “The bridge seat width shall satisfy the Minimum Support Length requirements given under AASHTO 4.7.4.4 Minimum Support Length Requirements. This requirement is applicable for support lengths considering the skew effect, parallel as well as normal to the span length. When these requirements are not met, shear blocks or restrainers as given in the current version of FHWA's "Seismic Retrofitting Manual for Highway Structures: Part 1 – Bridges" shall be provided to prevent the superstructure from falling off the bridge seat”. AASHTO requires a minimum support length that needs to be provided for girders supported on an abutment, bent cap, pier wall, or a hinge seat within a span as shown in Fig. 28.

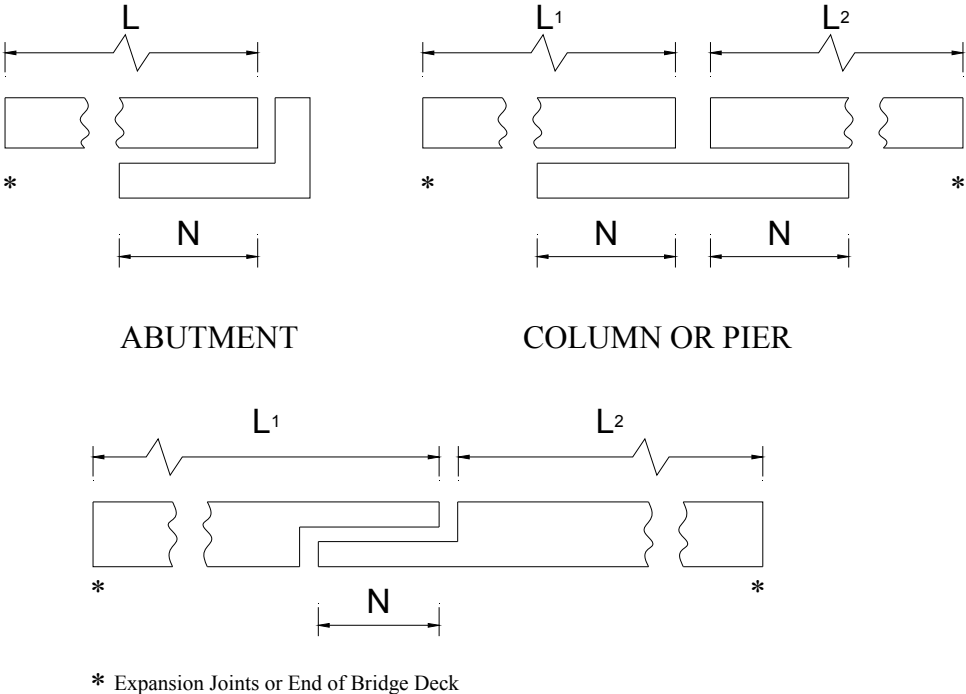


Fig. 28: Support Length, N, AASHTO

AASHTO Guide Specifications for LRFD Seismic Bridge Design states that in Seismic Design Categories SDC A, B, and C, support length at expansion bearings without shock transmission units (STUs) or dampers shall be considered to either accommodate the greater of the maximum calculated displacement, except for bridges in SDC A, or a percentage of the empirical support length, N , specified by

Error! Reference source not found..

The percentage of N , applicable to each SDC, shall be as specified in Table 2.

Where:

N = minimum support length measured normal to the centerline of bearing (in.)

L = length of bridge deck to the adjacent expansion joint, or to the end of the bridge deck; for hinges within a span, L shall be the sum of the distances to either side of the hinge; for single-span bridges, L equals the length of the bridge deck

H = for abutments, average height of columns supporting the bridge deck from the abutment to the next expansion joint (ft)

for columns and/or piers, column, or pier height (ft)

for hinges within a span, average height of the adjacent two columns or piers (ft) 0.0 for single-span bridges (ft)

S = angle of skew of support measured from a line normal to span ($^{\circ}$)

Table 2: Percentage N by SDC and Acceleration Coefficient, A_s

SDC	Acceleration Coefficient, A_s	Percentage N
A	<0.05	≥ 75
A	≥ 0.05	100
B	All applicable	150
C	All applicable	150

Minimum support length provisions provided above are equivalent to the AASHTO LRFD Bridge Design Specifications Article 4.7.4.4.

Support lengths are equal to the length of the overlap between the girder and the seat as shown in Fig. 28. The minimum values for N given in the above equation include an arbitrary allowance for cover concrete at the end of the girder and face of the seat. If above average cover is used at these locations, N should be increased accordingly (AASHTO Guide Specifications for LRFD Seismic Bridge Design).

For bridges in SDC D, hinge seat or support length, N , shall be available to accommodate the relative longitudinal earthquake displacement demand at the supports or at the hinge within a span between two frames and shall be determined as:

$$N = (4 + 1.65\Delta_{eq})(1+0.000125S^2) \quad \text{Eq. 5}$$

Where:

Δ_{eq} : seismic displacement demand of the long period frame on one side of the expansion joint (in.). The elastic displacement demand shall be modified according to the AASHTO Guide Specifications for LRFD Seismic Bridge Design Articles 4.3.2 and 4.3.3.

S = angle of skew of support measured from a line normal to span ($^{\circ}$)

The skew effect multiplier, $(1+0.000125S^2)$, may be set equal to 1 when the global model of the superstructure is modeled to include the full width and the skew effects on the displacement demands at the outer face of the superstructure (AASHTO Guide Specifications for LRFD Seismic Bridge Design).

The minimum support length required by the AASHTO Guide Specifications for LRFD Seismic Bridge Design must be provided and deteriorated bridge component that might cause an unseating mode of failure must be retrofitted. However, corrosion of steel and deterioration of concrete in the following bridge elements can cause the bridge to collapse due to unseating.

- Corrosion of connections, bearings, and seats
- Deterioration of seats and caps
- Deterioration of concrete at end of beam/girder
-

4.3 Corrosion of Connections and Bearings:

A bridge bearing is a superstructure device that provides an interface between the superstructure and the substructure. They are used to transmit loads from the superstructure (beams and girders) to the substructure (bents, abutments and piers), while facilitating translation and/or rotation.

There are many types of bearings but they are generally classified as expansion or fixed as shown in Fig. 29. Expansion bearings are designed to allow horizontal movement as the beam/girder expands, contracts, or moves. They are designed to slide, rock, roll, or deflect along with the beam/girder's motion. Fixed bearings are designed to allow rotation caused by the loads on the superstructure, they do not allow horizontal movements. Note that expansion bearings also allow rotation.



Fig. 29: Typical fixed and expansion bearings (Lindquist 2008)

According to the Bridge Inspector's Reference Manual (BIRM), a bearing consists of four basic elements as follows:

- **Sole Plate:** The sole plate is a steel plate attached to the bottom of girders or beams or imbedded into the bottom flange of a prestressed concrete girder. In cases of concrete beams, girders, or slabs, the bottom surface can also work as a sole plate.
- **Masonry Plate:** The masonry plate is a steel plate attached to the bearing seat of an abutment or pier. The main function of a masonry plate is to distribute vertical loads from the bearing to the abutment or pier.
- **Bearing or Bearing Surface:** The main purpose of the bearing surface is to transmit loads from the sole plate to the masonry plate.
- **Anchorage:** The anchorage is the anchor bolts that connect the masonry plate to the abutment or girder. Their main function is to prevent the horizontal movement of the masonry plate. As shown in Fig. 30.

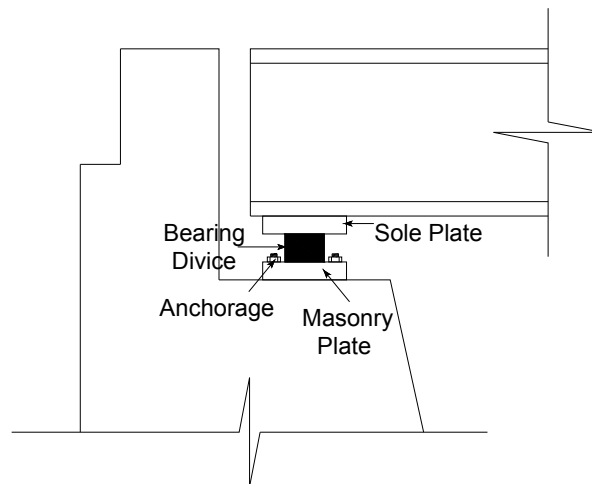


Fig. 30: Bridge bearing

In severe environments, bridge components such as Reinforced concrete columns and steel bridge bearings are subjected to chloride induced corrosion which is considered a potential form of environmental degradation (Enright and Frangopol 1998, Stewart and Rosowsky 1998, Montemor et al. 2002, Hoeke et al. 2009, Ghosh and Padgett 2010). With age, this corrosion causes deterioration of bridges in several ways, such as spalling of concrete, buildup of debris leading to corrosion of steel bearings, and corrosion of steel reinforced concrete members (Ghosh and Padgett 2010). Bridge bearings are subjected to corrosion because of the leaking of chloride-laden water at deck joints (Silano and Brinckerhoff 1993). The corrosion debris accumulation will increase bearing coefficient of friction, also corrosion of anchor bolts and keeper plates will result in a failure of the bridge bearing system (Ghosh and Padgett 2010). However, a failure in the bridge bearing system does not necessarily mean a total collapse of a span, in fact, this is a relatively rare event. For example, the toppling or failure of individual bearings will not necessarily lead to collapse if the bearing seats are wide enough to catch the superstructure (FHWA 2006).

Corrosion of bearing systems usually results in frozen or locked bearings due to excessive corrosion products, such as dirt, and debris, this may potentially restrict translational and rotational movement as a result of increased coefficient of friction (Silano and Brinckerhoff 1993). In addition, corrosion in keeper plates (bearing surface) and in anchor bolts. This could result in shift in performance during an earthquake bolts (Ghosh and Padgett 2010). The most critical parts in the corroded bearing system are the bearing anchor bolts, in fact, they are considered to be a “weak link” in the force transmission system from the superstructure to the substructure during ground motion (Mander et al. 1996). Moreover, according to the studies conducted by Rashidi and Saadeghvaziri (1997) and Mander et al. (1996), the critical stiffness of a steel bearing assembly is the stiffness of the anchor bolts connected to the concrete base. These bolts are used in both fixed and expansion bearing systems. This will be discussed in detail. Fig. 31 shows a corroded anchor bolt.



Fig. 31: Anchor bolt corrosion inside the bearing, beneath the washer (Lindquist 2008)

4.3.1 Fixed bearings:

As mentioned above, fixed bearing restrict horizontal movements, however, when corrosion starts, it decreases the ultimate lateral strength of the bearing. Fig. 32 shows the arrangement and distribution of forces for a typical fixed bearing along the longitudinal direction (Ghosh and Padgett 2010).

The ultimate lateral strength for the fixed bearing in the longitudinal direction can be calculated using the free-body diagram and the equilibrium equations (Ghosh and Padgett 2010). This strength will decrease over time with the presence of corrosion.

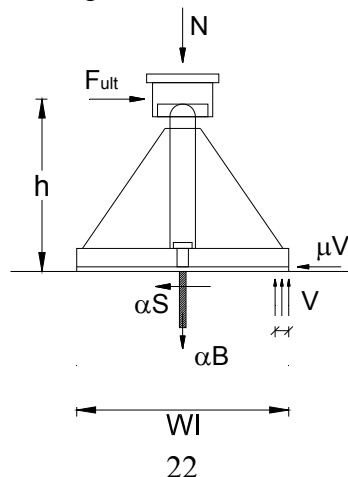


Fig. 32: Rocking/force distribution mechanism in fixed bearings on concrete pedestals along longitudinal direction (Ghosh and Padgett 2010)

From the equilibrium of the horizontal forces, the ultimate lateral strength in the longitudinal direction can be calculated as (Ghosh and Padgett 2010):

$$F_{ult} = \alpha S + \mu V \quad \text{Eq. 6}$$

The compression force on the concrete pedestal can be calculated from the equilibrium of forces in the vertical direction:

$$V = N + \alpha B \quad \text{Eq. 7}$$

And by taking the equilibrium of moments about the center of the concrete pedestal, it can be written that:

$$F_{ult} h = V \left(\frac{w_l - a}{2} \right) \quad \text{Eq. 8}$$

Where:

F_{ult} = ultimate lateral strength of the bearing in the longitudinal direction

α = number of anchor bolts

S = shear force on one anchor bolt

μ = coefficient of friction between masonry plate and bedding material

V = compression force on the concrete pedestal due to rocking

N = axial load on the bearing

B = bond strength of the swedged anchor bolt in the concrete pedestal

h = height of the bearing from the concrete pedestal to the sole plate-rocker interface

w_l = width of masonry plate in the longitudinal direction

a = depth of pedestal concrete stress block and is equal to

$$a = \frac{V}{0.85 f'_c w_t} \quad \text{Eq. 9}$$

Where:

f'_c = concrete compressive strength

w_t = width of masonry plate in the transverse direction (Ghosh and Padgett 2010)

However, the bond strength of the anchor bolt can be calculated as (Mander et al. 1996):

$$B = b_u (\pi d_b) l_d \quad \text{Eq. 10}$$

Where:

B = bond strength of the anchor bolt

$b_u = k b_a$ = bond stress that is assumed to act uniformly on the anchor bolt surface with diameter d_b over the embedment length l_d

d_b = diameter of anchor bolt

l_d = embedment length

b_a = average bond stress over the length of the anchor bolt

k = modification or judgment factor often imposed to account for reduced bearing capacity of the anchor bolts and adverse effects of cyclic loading

Using the above equations, the ultimate lateral strength of the bearing in the longitudinal direction can be expressed as (Ghosh and Padgett 2010):

$$\frac{F_{ult}}{N} = \frac{0.5w_l}{h} \left[\left(1 + \frac{\alpha B}{N}\right) - \frac{N}{0.85f'_c w_l w_t} \left(1 + \frac{\alpha B}{N}\right)^2 \right] \quad \text{Eq. 11}$$

Corrosion reduces the cross-sectional area of the anchorage bolts. In addition, it decreases the bond strength between anchors and concrete. This will reduce the bolts resistance to shear force transmitted through the bearing masonry plate. $\frac{F_{ult}}{N} = \frac{0.5w_l}{h} \left[\left(1 + \frac{\alpha B}{N}\right) - \frac{N}{0.85f'_c w_l w_t} \left(1 + \frac{\alpha B}{N}\right)^2 \right]$

Eq. 11 shows that the ultimate strength of the bearing is related to the bond strength, diameter of the anchorage bolt, and width of the masonry plate in both directions. Therefore, corrosion of the anchorage bolts or of the masonry plate will decrease the ultimate lateral strength of the bearing system increasing the risk of a fixed bearing failure, which, in turn, will lead to unseating collapse of the bridge.

Also, this will reduce the bond strength of the anchor bolts. Moreover, the extra stress caused by the corroded anchor bolts cause deterioration in the surrounding concrete. Spalling and delamination of concrete will reduce the seat length required by AASHTO as shown in Fig. 33, which in turn will increase the risk of span collapse due to unseating when the bridge undergoes seismic loads. Also, the reduction in the cross-sectional area of the bolts due to corrosion will lead to reduction in the ultimate lateral strength in the deteriorated bearing, which can cause a failure of the bearing system. This will allow the span to move horizontally and may cause a total collapse of the span if the support length is less than required.

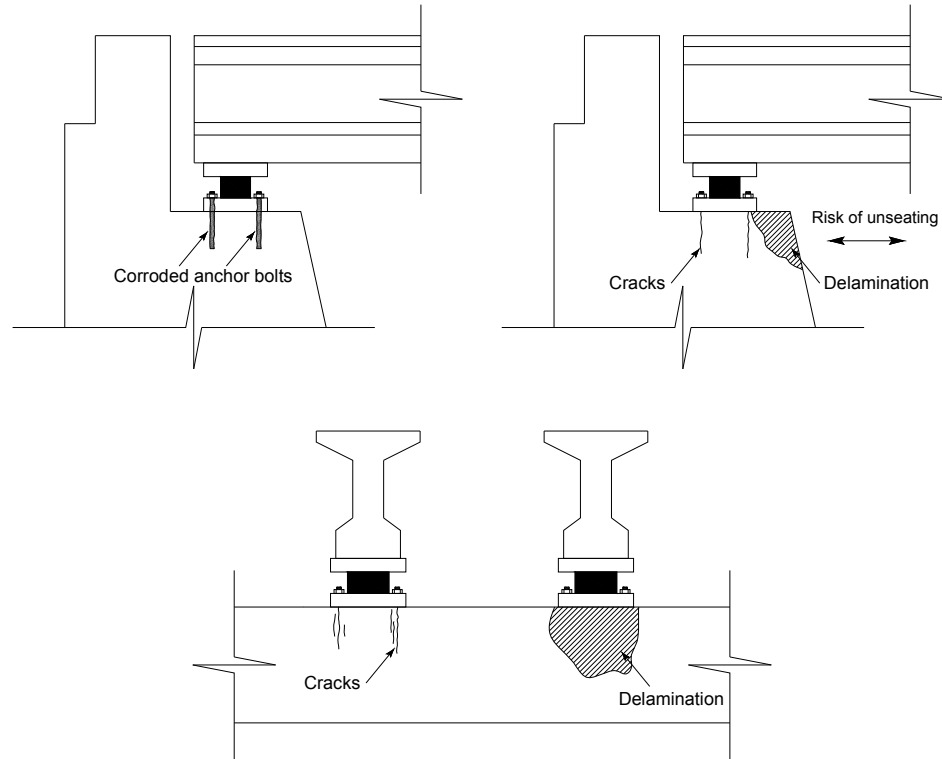


Fig. 33: Spalling and delamination of concrete due to corrosion in anchor bolts

Also, corrosion of anchor bolts will decrease the cross-section of the bolts, which in turn will decrease the shear strength of the anchor bolts, and the bolts will fail and no longer be able to transmit loads from the bearing to the seat. This will allow the bridge girder to undergo large horizontal displacements that exceeds the design limits because the fixed bearing will not be able to restrict horizontal movements. This will also increase the risk of span collapse due to unseating. Modes of failure of anchorage bolts will be discussed later.

4.3.2 Expansion bearings:

Expansion bearings, also called rocker bearings, allow motion in the longitudinal direction. This motion is mainly rocking. The ultimate lateral strength of expansion bearings is reliant on the rocking friction coefficient of the bearing (Ghosh and Padgett 2010). This coefficient of rocking friction varies from 0.04 for clean well worn rocker bearings to 0.12 for severely corroded bearings which takes into account the locking effect (Mander et al. 1996). When the horizontal frictional force exceeds the frictional resistance of the interface between the sole plate and the rocker, the sole plate slides on the rocker until the rocker bearing strikes the keeper plate provided to prevent excess transverse motion. If additional horizontal load is applied, the keeper plate bends significantly and fails by tearing of the fillet weld securing the plate (Mander et al. 1996, Ghosh and Padgett 2010). Fig. 34 shows the free body-body diagram for this case. The rocker strikes the keeper plate with a force P , this force gets transmitted through the anchor bolts in the form of shear forces S_1 and S_2 .

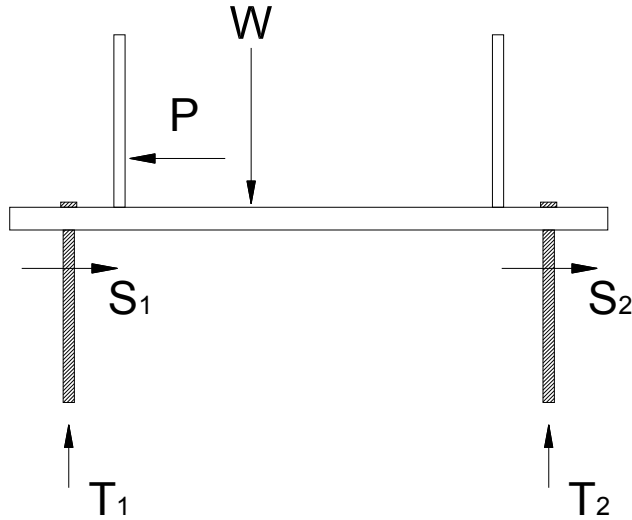


Fig. 34: Force distribution mechanism through the anchor bolt when the keeper plate strikes the rocker.

In the absence of corrosion in the anchor bolts, anchor bolts with 25 mm cross-section diameter size provide shear strength which is sufficient enough to transmit the forces. In this case the failure of the bearing is controlled solely by the tearing of the keeper plate. On the other hand, when the bolts are corroded, the cross section area of the bolts decrease, this will also decrease the shear strength of the bolts will be no longer able to transmit the forces when the rocker hits the keeper plate (Ghosh and Padgett 2010).

When the anchor bolts are not subjected to corrosion, as mentioned above, the keeper plate will determine the failure of the bearing assembly. If the keeper plate is subjected to corrosion, the failure is most likely will going to be governed by the tearing of the keeper plate. Komp 1987 suggested an empirical model to calculate the average corrosion penetration to the steel keeper plate as follows:

$$y(t) = Pt^Q \quad \text{Eq. 12}$$

Where:

$Y(t)$ = average corrosion penetration in micrometers

t = time in years

P and Q = parameters determined from regression analysis of field experimental data and usually are determined based on field tests.

4.3.3 Anchorage bolts:

Anchorage bolts transfer loads from the bearing system to the pier/abutment cap. Therefore, any reduction in their capacity that causes failure can result in unseating of the bridge superstructure. Anchorage bolts are subjected to shear and tensile forces during an earthquake. The tensile and shear forces are due to the horizontal force and bending moment transferred from the bearing. AASHTO states that “connections shall resist the least favorable combination of loads at the strength limit state and shall be installed wherever deemed necessary to prevent separation”. This is because separation can cause a severe movement of the bridge span which leads to unseating

during seismic events. AASHTO also requires the girders to be securely anchored to the substructure, and recommends the usage of cast in substructure concrete anchors when possible, (Article 14.8.3.1). This is because this type of anchors is more capable of resisting pullout than post installed anchors. In addition, it is recommended that anchor bolts are swaged or threaded to secure an adequate grip upon the material used to embed them in the holes (Article 14.8.3.1). However, shear in the fastener as well as bearing upon the connected material usually resist the load in bolted bearing-type connections, also, some uncertain amount of friction between the faying surfaces. Either shear failure of the connectors, tear out of the connected material, or unacceptable ovalization of the holes will control the final failure. Final failure load is independent of the clamping force provided by the bolts (Kulak et al., 1987), (AASHTO Article 6.13.2.1).

AASHTO Article 6.13.2.10 requires the nominal tensile resistance of a bolt, T_n , independent of any initial tightening force to be taken as:

$$T_n = 0.76A_bF_{ub} \quad \text{Eq. 13}$$

where:

A_b = area of bolt corresponding to the nominal diameter (in.²)

F_{ub} = specified minimum tensile strength of the bolt specified in Article 6.4.3 (ksi)

From the equation above, it can be seen that the nominal tensile resistance of a bolt is controlled by the area of the bolt and the specified minimum tensile strength. Corrosion decrease the area of the bolt as well as the tensile strength as discussed in the previous chapter, this in turn decreases the nominal tensile resistance of the bolt. However, since shear failure will most likely control the failure of a bolt during an earthquake. Tensile failure of bolts is not very critical.

The nominal shear resistance of an ASTM F1554 or an ASTM A307 Grade C anchor bolt at the strength limit state, according to AASHTO Article 6.13.2.12, shall be taken as:

Where threads are included in the shear plane:

$$R_n = 0.48A_bF_{ub}N_s \quad \text{Eq. 14}$$

where:

A_b = area of bolt corresponding to the nominal diameter (in.²)

F_{ub} = specified minimum tensile strength of the bolt specified in Article 6.4.3 (ksi)

N_s = number of shear planes per anchor bolt

Corrosion, as mentioned above, decrease the area of the bolt as well as the tensile strength leading to a decrease in nominal shear resistance of a bolt, increasing the risk of shear failure in the bolt, which will lead to unseating of the bridge span during ground motion.

AASHTO Article C6.13.2.12 indicates that for global design of anchorages to concrete, refer to Building Code Requirements for Structural Concrete (ACI 318-05), Appendix D. However, the latest version of ACI 318-11 requirements will be discussed in the following paragraphs.

ACI 318-11 Appendix D is used to design cast-in-place anchors, in addition, it provides some provisions for designing post-installed anchors, but it does not applicable for designing adhesive anchors. The manufacturer should provide some criteria for designing post-installed anchors and adhesive anchors (Summers 2009). ACI 318-11 discusses the potential modes of failure of anchors due to tensile loading.

4.3.3.1 Steel failure in tension:

ACI 318-11 recommends using the nominal strength of anchors in tension as a function of f_{uta} rather than f_{ya} because the large majority of anchor materials do not exhibit a well-defined yield point.

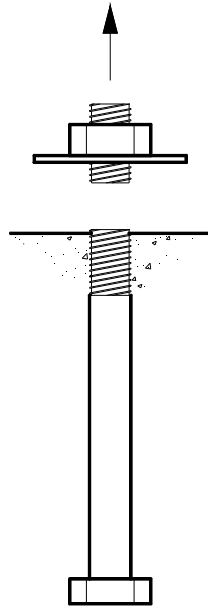


Fig. 35: Steel failure in tension (ACI 318-11)

ACI 318-11 requires the nominal strength of a single anchor or group of anchors in tension not to exceed:

$$N_{sa} = nA_{se,N}f_{uta} \quad \text{Eq. 15}$$

where:

n = number of anchors in the group

$$f_{uta} \leq \begin{cases} 1.9f_{ya} \\ 125,000 \text{ psi} \end{cases}$$

$A_{se,N}$ = effective cross-sectional area of an anchor in tension (in.²)

For threaded bolts, ANSI/ASME B1.1^{D.1} defines A_{se} as:

$$A_{se,N} = \frac{\pi}{4} \left(d_a - \frac{0.9743}{n_t} \right)^2 \quad \text{Eq. 16}$$

where:

d_a = outside diameter of anchor or shaft diameter of headed stud, headed bolt, or hooked bolt (in.)

n_t = number of threads per in.

As discussed earlier, corrosion decreases the cross-sectional area of steel, in addition, it decreases the yield strength Eqs.2, 3. This decreases the nominal strength of anchors in tension, which causes a steel failure in tension as shown in Fig. 36.

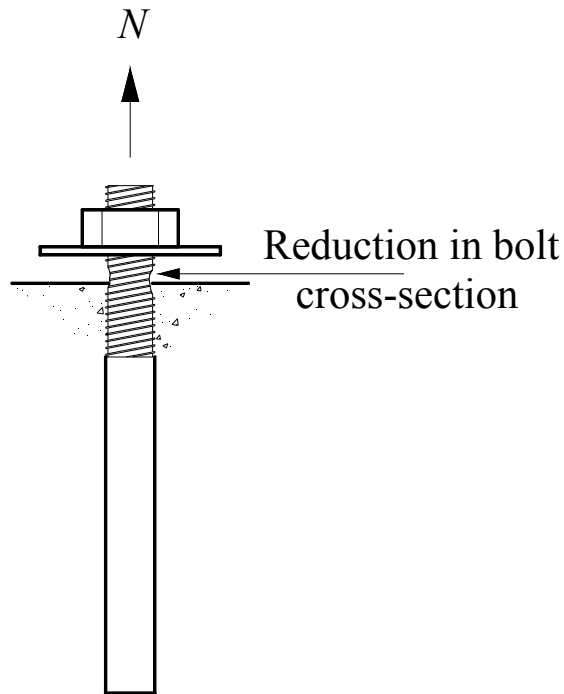


Fig. 36: Reduction in bolt cross-sectional area due to corrosion

4.3.3.2 Pullout failure in tension:

This mode of failure usually occurs when the bolt is subjected to tensile force and the steel strength is larger than the pullout strength. Pullout happens due to localized failure of concrete at the head of the anchor (Summers 2009).

ACI 318-11 Appendix D requires pullout strength of a single anchor in tension, N_{pn} , not to exceed:

$$N_{pn} = \Psi_{c,p} p N_p \quad \text{Eq. 17}$$

where:

N_p = characteristic tensile pullout or pull-through capacity of an anchor (5% fractile of test results), lb (N)

$\Psi_{c,p} = 1.4$, for an anchor located in a region of a concrete member where analysis indicates no cracking at service load levels

$\Psi_{c,p} = 1$, for an anchor located in a region of a concrete member where analysis indicates cracking at service load levels

If corrosion is advanced, it can result in severe concrete cracking, therefore, it is suggested that the value of $\Psi_{c,p}$ can be taken lower than 1.

Therefore, cracking of concrete resulting from corrosion of bolts decreases the pullout strength of an anchor. This increases the risk of a pullout failure of anchor Fig. 37.

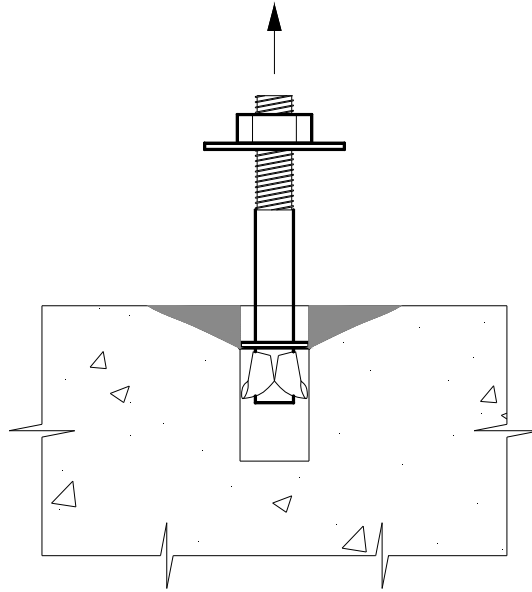


Fig. 37: Pullout failure in tension (ACI 318-11)

4.3.3.3 Concrete tensile breakout:

Concrete tensile breakout usually occurs when there are cracks in concrete, which allows the anchor to breakout along a failure plane of 35° , Fig. 38.

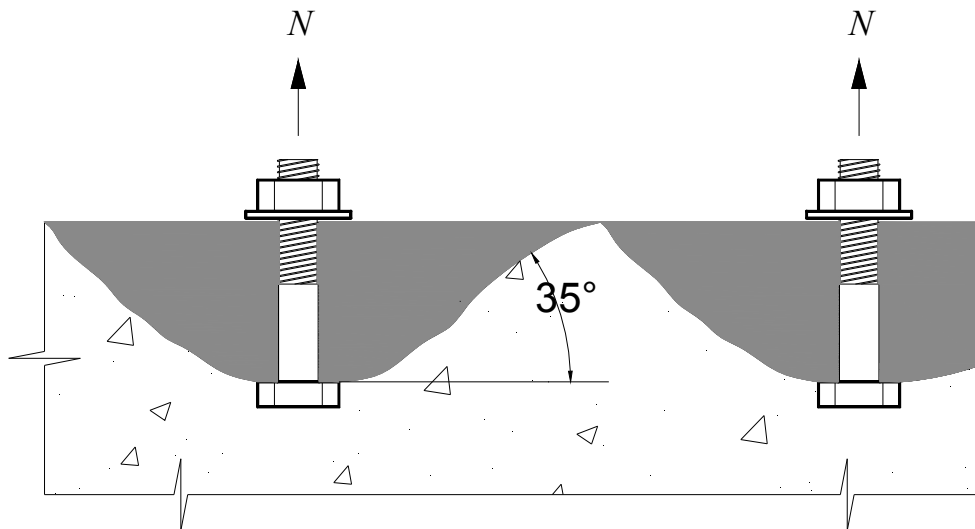


Fig. 38: Concrete tensile breakout (ACI 318-11)

ACI 318-11 requires the nominal concrete breakout strength, N_{cb} or N_{cbg} , of a single anchor or groups of anchors in tension not to exceed:

- (a) for a single anchor:

$$N_{cb} = \frac{A_{Nc}}{A_{Nco}} \Psi_{ed,N} \Psi_{c,N} \Psi_{cp,N} N_b \quad \text{Eq. 18}$$

(b) for group of anchors:

$$N_{cbg} = \frac{A_{Nc}}{A_{Nco}} \Psi_{ec,N} \Psi_{ed,N} \Psi_{c,N} \Psi_{cp,N} N_b \quad \text{Eq. 19}$$

where:

A_{Nc} = projected concrete failure area of a single anchor or group of anchors that shall be approximated as the base of the rectilinear geometrical figure that results from projecting the failure surface outward $1.5h_{ef}$ from the centerline of the anchor, or in the case of a group of anchors. A_{Nc} shall not exceed nA_{Nco} , where n is the number of tensioned anchors in the group. A_{Nco} is the projected concrete failure area of a single anchor with an edge distance equal to or greater than $1.5h_{ef}$.

$$A_{Nco} = 9h_{ef}^2 \quad \text{Eq. 20}$$

where:

h_{ef} = effective embedment depth, measured from the concrete surface to the deepest point at which the anchor tension load is transferred to the concrete, in. (mm)

In cases of severe corrosion, when concrete spalls or delaminates, this mode of failure can be very critical causing the anchor of the bearing to pullout from the pier cap or bridge seat, which in turn leads to unseating of bridge span during an earthquake.

For a detailed description of the above set of equations, refer to the Appendix “D” of the ACI Building Code Requirements for Structural Concrete (ACI 318-11).

However, ACI 318-11 requires the basic concrete breakout strength of a single anchor in tension in cracked concrete, N_b , not to exceed:

$$N_b = k_c \lambda_a \sqrt{f'_c} h_{ef}^{1.5} \quad \text{Eq. 21}$$

where:

$K_c = 24$ for cast-in anchors

$K_c = 17$ for post-installed anchors

λ_a = modification factor reflecting the reduced mechanical properties of lightweight concrete in certain concrete anchorage applications

f'_c = concrete compressive strength

h_{ef} = effective embedment depth, measured from the concrete surface to the deepest point at which the anchor tension load is transferred to the concrete, in. (mm)

Alternatively, for cast-in headed studs and headed bolts with $11 \text{ in.} \leq h_{ef} \leq 25 \text{ in.}$, N_b shall not exceed

$$N_b = 16\lambda_a \sqrt{f'_c} h_{ef}^{5/3} \quad \text{Eq. 22}$$

Note that ACI 318-11 suggests the following:

$\Psi_{c,N} = 1.4$, for cast-in anchors located in a region of a concrete member where analysis indicates no cracking at service load levels

$\Psi_{c,N} = 1.25$, for post-installed anchors located in a region of a concrete member where analysis indicates no cracking at service load levels

$\Psi_c N = 1$, for both cast-in and post-installed anchors located in a region of a concrete member where analysis indicates cracking at service load levels

Since corrosion causes more serious cracks than service loads, it is recommended to take lower values for $\Psi_c N$ when concrete is severely cracked.

In addition, if corrosion causes the concrete surrounding bolts to spall or delaminate, it can result in decreasing the effective embedment depth, h_{ef} . This will decrease the concrete strength to resist breakout and increase the vulnerability of bolt to this mode of failure.

If concrete cracks were fine and near the surface, the risk of bond failure is higher of concrete breakout failure. However, in cases of deep wide cracks either of the above modes of failure can be critical.

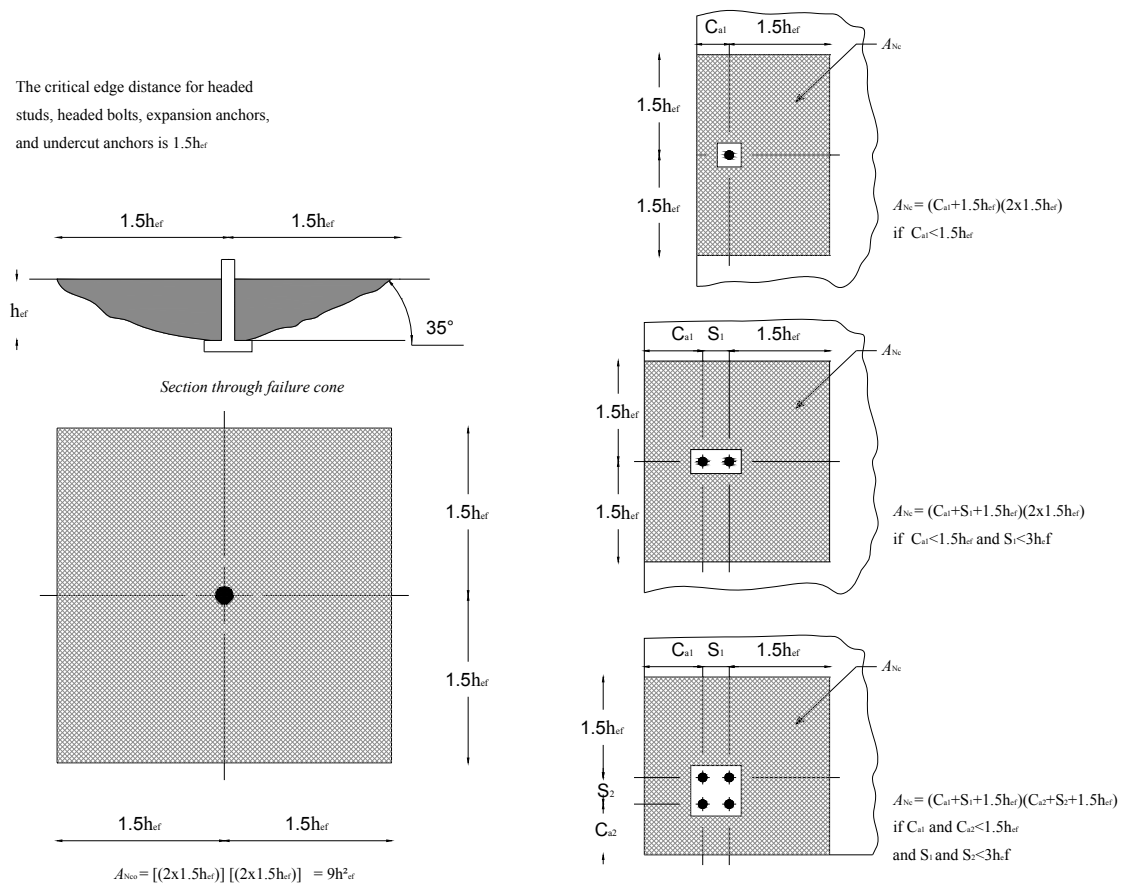


Fig. 39: calculations of A_{NCO} , A_{Nc} for single anchors and group of anchors (ACI 318-11)

4.3.3.4 Concrete side-face blowout of a headed anchor in tension:

This mode of failure will occur when the side cover is inadequate, as it will cause concrete to break to the side of the anchor bolt because of the tensile forces. This usually happens when anchors are embedded deep in the concrete and are placed near the edge of the seat. Concrete side-face blowout can be prevented by adequate reinforcement and embedment length. This is because the tensile forces will be transferred through the bolts and into the reinforcement

(summers 2009). In addition, it is important to install anchors at adequate distances from the edge of the seat (Fig. 40).

ACI 318-11 requires the nominal side-face blowout strength for a single headed anchor with deep embedment close to an edge ($h_{ef} > 2.5 c_{a1}$), N_{sb} , not to exceed

$$N_{sb} = (160c_{a1}\sqrt{A_{brg}})\lambda_a\sqrt{f'_c} \quad \text{Eq. 23}$$

where:

A_{brg} = net bearing area of the head of stud, anchor bolt, or headed deformed bar (in.²)

For multiple headed anchors with deep embedment close to an edge ($h_{ef} > 2.5 c_{a1}$) and anchor spacing less than $6c_{a1}$, the nominal strength of those anchors susceptible to a side-face blow-out failure N_{sbg} shall not exceed

$$N_{sbg} = \left(1 + \frac{s}{6c_{a1}}\right) N_{sb} \quad \text{Eq. 24}$$

where:

s = distance between the outer anchors along the edge

Corrosion decreases the net bearing area of the head of stud, in addition deterioration of concrete near the edge of pier cap or abutment seat due to corrosion of anchors or of reinforcing steel reduces the distance from the center of the bolt to the edge, c_{a1} . This will decrease the nominal side-face blowout strength for anchors.

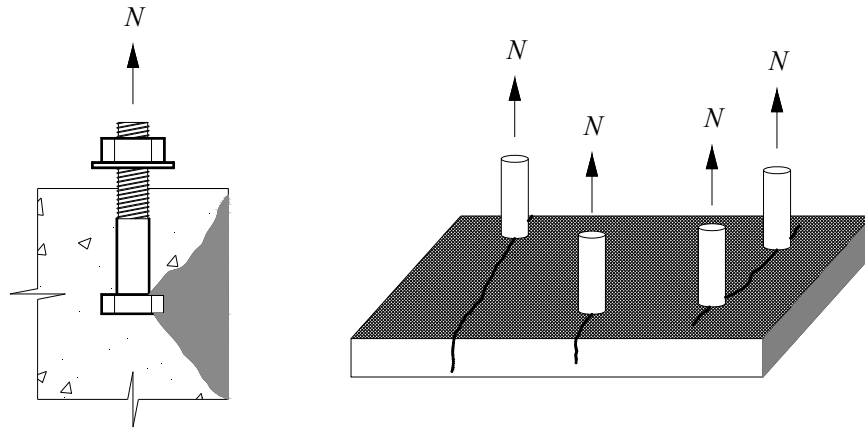


Fig. 40: Concrete side-face blowout and concrete splitting in tension (ACI 318-11)

4.3.3.5 Bond failure of adhesive anchor in tension:

Corrosion of anchors will deteriorate the bond between anchors and surrounding concrete, this will increase the risk of bond failure during seismic activities. In post-installed anchors, corrosion of anchors leads to deterioration of anchor threads, which reduces the bond between anchors and surrounding concrete significantly. This increases the risk of bond failure (Fig. 41). ACI 318-11 Appendix D, D.5.5.2 requires the basic bond strength of a single adhesive anchor in tension in cracked concrete, N_{ba} , not to exceed

$$N_{ba} = \lambda_a \tau_{cr} \pi d_a h_{ef} \quad \text{Eq. 25}$$

where:

τ_{cr} = characteristic bond stress and shall be taken as the 5 percent fractile of results of tests performed and evaluated according to ACI 355.4.

d_a = outside diameter of anchor or shaft diameter of headed stud, headed bolt, or hooked bolt (in.)

Sever corrosion of anchor bolts will cause the outside diameter of the bolt to decrease. The reduction of diameter will decrease the bond strength.

Where analysis indicates cracking at service load levels, adhesive anchors shall be qualified for use in cracked concrete in accordance with ACI 355.4.

For adhesive anchors located in a region of a concrete member where analysis indicates no cracking at service load levels, τ_{uncr} , shall be permitted to be used in place of τ_{cr} and shall be taken as the 5 percent fractile of results of tests performed and evaluated according to ACI 355.4.

For further information about the above mode of failures, refer to Building Code Requirements for Structural Concrete (ACI 318-11), Appendix D.

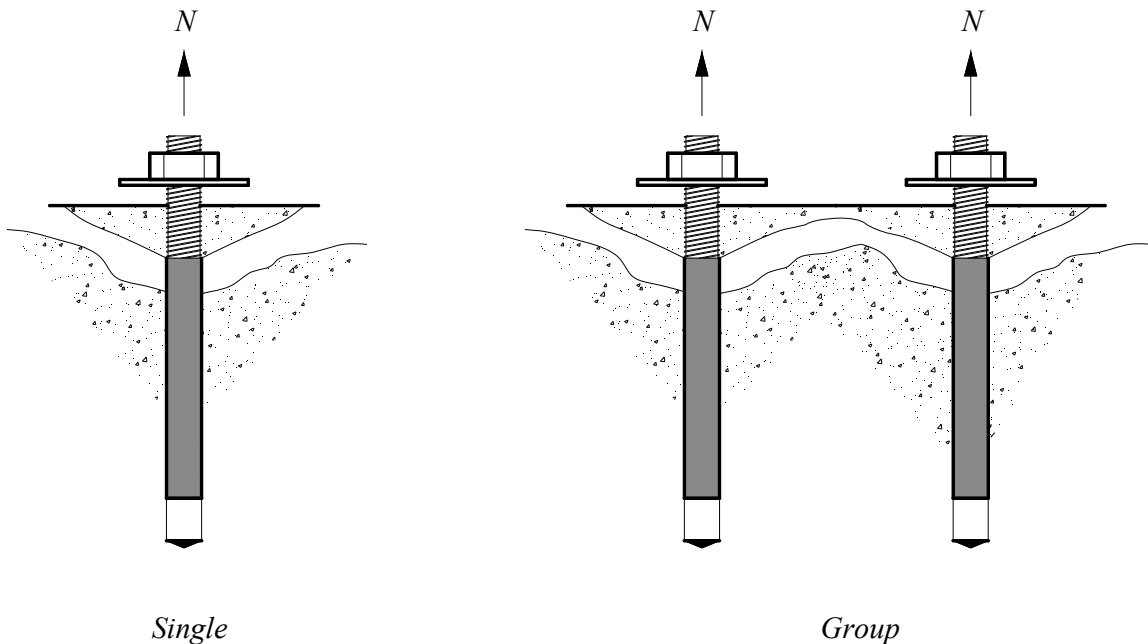


Fig. 41: Bond failure of adhesive anchor in tension (ACI 318-11)

For further information refer to Building Code Requirements for Structural Concrete (ACI 318-11), Appendix D.

4.3.3.6 Steel failure in shear:

Shear failure is more critical than tensile failure in bridge bearing bolts during an earthquake. This is because of the horizontal seismic loads that are transferred from the superstructure to the substructure through bearing assemblies and anchor bolts. Steel failure in shear happens when the shear force transferred to the anchor bolt exceeds the capacity of the bolt in shear. This mode of failure is associated with concrete crushing around the bolt as shown in Fig. 42.

ACI 318-11 states that the nominal strength of an anchor in shear as governed by steel, V_{sa} , shall be evaluated by calculations based on the properties of the anchor material and the physical

dimensions of the anchor. While corrosion does not significantly change the material properties, it does change the physical dimensions of the anchor.

ACI 318-11 requires the nominal strength of an anchor in shear, V_{sa} , not exceed (a) through (c):

(a) For cast-in headed stud anchor:

$$V_{sa} = A_{se,v} f_{uta} \quad \text{Eq. 26}$$

where:

$A_{se,v}$ = effective cross-sectional area of an anchor in shear, in.²

$$f_{uta} \leq \begin{cases} 1.9f_{ya} \\ 125,000 \text{ psi} \end{cases}$$

(b) For cast-in headed bolt and hooked bolt anchors and for post-installed anchors where sleeves do not extend through the shear plane

$$V_{sa} = 0.6A_{se,v} f_{uta} \quad \text{Eq. 27}$$

(c) For post-installed anchors where sleeves extend through the shear plane, V_{sa} shall be based on the results of tests performed and evaluated according to ACI 355.2. Alternatively, $V_{sa} = 0.6A_{se,v} f_{uta}$ Eq. 27 shall be permitted to be used.

For post-installed anchors having a reduced cross-sectional area anywhere along the anchor length, the effective cross-sectional area of the anchor should be provided by the manufacturer. For threaded rods and headed bolts, ANSI/ASME B1.1D.1 defines $A_{se,v}$ as

$$A_{se,v} = \frac{\pi}{4} \left(d_a - \frac{0.9743}{n_t} \right)^2 \quad \text{Eq. 28}$$

where:

$A_{se,v}$ = effective cross-sectional area of anchor in shear (in.²)

d_a = outside diameter of anchor or shaft diameter of headed stud, headed bolt, or hooked bolt (in.)

n_t = number of threads per in.

Note that corrosion of anchors will decrease the effective cross-sectional area of the anchors as well as yield strength of steel. Thus, it does reduce the nominal strength of an anchor in shear.

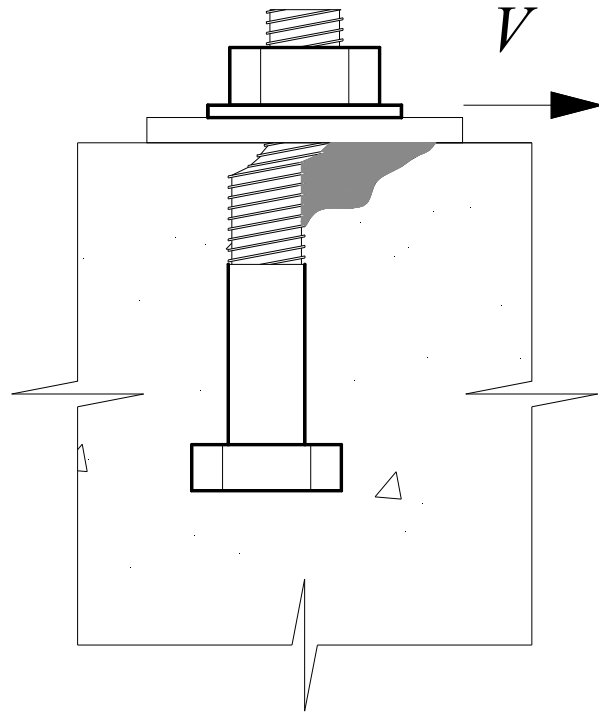


Fig. 42: Steel failure preceded by concrete spall (ACI 318-11)

4.3.3.7 Concrete breakout of anchor in shear:

This mode of failure occur when the anchor is close to the edge of the abutment seat or pier cap (Fig. 43), however, this mode of failure can be prevented by adding adequate hairpin anchor reinforcement.

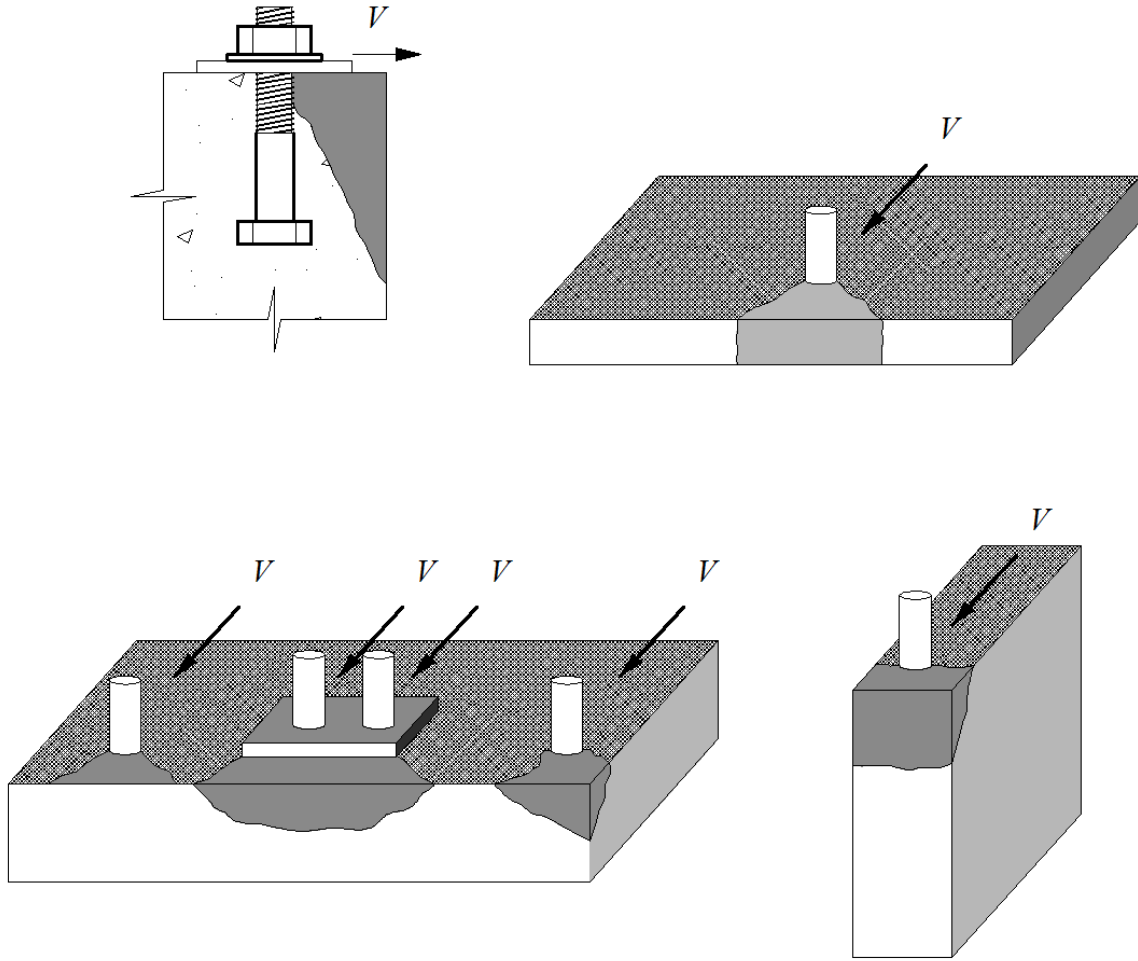


Fig. 43: Concrete breakout in shear (ACI 318-11)

ACI 318-11 requires the nominal concrete breakout strength in shear, V_{cb} of a single anchor or V_{cbg} of a group of anchors, not to exceed:

(a) For shear force perpendicular to the edge on a single anchor

$$V_{cb} = \frac{A_{vc}}{A_{vco}} \Psi_{ed,v} \Psi_{c,v} \Psi_{h,v} V_b \quad \text{Eq. 29}$$

(b) For shear force perpendicular to the edge on a group of anchors

$$V_{cbg} = \frac{A_{vc}}{A_{vco}} \Psi_{ec,v} \Psi_{ed,v} \Psi_{c,v} \Psi_{h,v} V_b \quad \text{Eq. 30}$$

(c) For shear force parallel to an edge, V_{eb} or V_{ebg} shall be permitted to be twice the value of the shear force determined from the two equations above, with the shear force assumed to act perpendicular to the edge and with $\Psi_{ed,v}$ taken equal to 1.0.

(d) For anchors located at a corner, the limiting nominal concrete breakout strength shall be determined for each edge, and the minimum value shall be used.

where:

A_{Vc} = projected area of the failure surface on the side of the concrete member at its edge for a single anchor or a group of anchors.

A_{Vco} = projected area for a single anchor in a deep member with a distance from edges equal or greater than $1.5c_{a1}$ in the direction perpendicular to the shear force.

Calculations of A_{Vc} , A_{Vco} , and the other parameter in the above equations can be conducted from ACI 318-11 Appendix D.

However, ACI 318-11 states that the basic concrete breakout strength in shear of a single anchor in cracked concrete, V_b , shall be the smaller of (a) and (b):

(a)

$$V_b = \left(7 \left(\frac{l_e}{d_a} \right)^{0.2} \sqrt{d_a} \right) \lambda_a \sqrt{f'_c} (c_{a1})^{1.5} \quad \text{Eq. 31}$$

where:

l_e = load-bearing length of the anchor for shear, and is equal to

$l_e = h_{ef}$ for anchors with a constant stiffness over the full length of embedded section, such as headed studs and post-installed anchors with one tubular shell over full length of the embedment depth

$l_e = 2d_a$ for torque-controlled expansion anchors with a distance sleeve separated from expansion sleeve

and

$l_e \leq 8d_a$ in all cases.

(b)

$$V_b = 9\lambda_a \sqrt{f'_c} (c_{a1})^{1.5} \quad \text{Eq. 32}$$

For cast-in headed studs, headed bolts, or hooked bolts that are continuously welded to steel attachments having a minimum thickness equal to the greater of 3/8 in. and half of the anchor diameter, the basic concrete breakout strength in shear of a single anchor in cracked concrete, V_b , shall be the smaller of (a) and (b):

(a)

$$V_b = \left(8 \left(\frac{l_e}{d_a} \right)^{0.2} \sqrt{d_a} \right) \lambda_a \sqrt{f'_c} (c_{a1})^{1.5} \quad \text{Eq. 33}$$

(b)

$$V_b = 9\lambda_a \sqrt{f'_c} (c_{a1})^{1.5} \quad \text{Eq. 34}$$

where l_e is the same as above.

Usually bridge seats and pier caps are provided with edge reinforcement in order to prevent this mode of failure (Fig. 44).

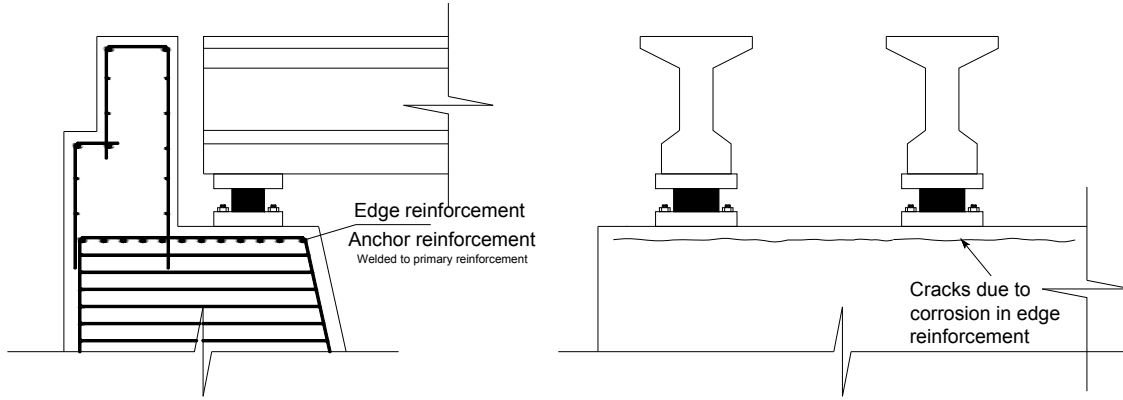


Fig. 44: corrosion in edge reinforcement to prevent Concrete breakout of anchor in shear

Corrosion of anchor bolt reduces its diameter size leading to reduction in concrete breakout strength in shear. If the corrosion is severe, it can cause the surrounding concrete to spall and delaminate which also increase the risk of this mode of failure.

In addition, corrosion in edge reinforcement can destroy the connection to the main reinforcement, moreover, it has higher risk of causing the edge concrete to spall because it is closer to the edge. Spalling of edge concrete increases the risk of the concrete to breakout in shear dramatically.

4.3.3.8 Concrete pryout failure of anchor in shear:

This mode of failure occurs when the anchor bolts are relatively far from the bridge seat edge or the pier cap edge. It is usually associated with large shear forces.

ACI 318-11 requires the nominal pryout strength, V_{cp} for a single anchor or V_{cpg} for a group of anchors, shall not exceed:

- (a) For a single anchor

$$V_{cp} = k_{cp} N_{cp} \quad \text{Eq. 35}$$

For cast-in, expansion, and undercut anchors, N_{cp} shall be taken as N_{cb} determined from $N_{cb} = \frac{A_{Nc}}{A_{Nco}} \Psi_{ed,N} \Psi_{c,N} \Psi_{cp,N} N_b$ Eq. 18 and for adhesive anchors, N_{cp} shall be the

lesser of N_{cb} determined from $N_{cb} = \frac{A_{Nc}}{A_{Nco}} \Psi_{ed,N} \Psi_{c,N} \Psi_{cp,N} N_b$ Eq. 18 and the nominal bond strength in tension, N_a of a single adhesive anchor determined from (ACI 318-11 Eq. D-18)

- (b) For a group of anchors

$$V_{cpg} = k_{cp} N_{cpg} \quad \text{Eq. 36}$$

For cast-in, expansion, and undercut anchors, N_{cpg} shall be taken as N_{cbg} determined from

$N_{cbg} = \frac{A_{Nc}}{A_{Nco}} \Psi_{ec,N} \Psi_{ed,N} \Psi_{c,N} \Psi_{cp,N} N_b$ Eq. 19 and for adhesive anchors, N_{cpg} shall

be the lesser of N_{cbg} determined from $N_{cbg} = \frac{A_{Nc}}{A_{Nco}} \Psi_{ec,N} \Psi_{ed,N} \Psi_{c,N} \Psi_{cp,N} N_b$ Eq. 19

and the nominal bond strength in tension, N_{ag} of a group of adhesive anchors determined from (ACI 318-11 Eq. D-19)

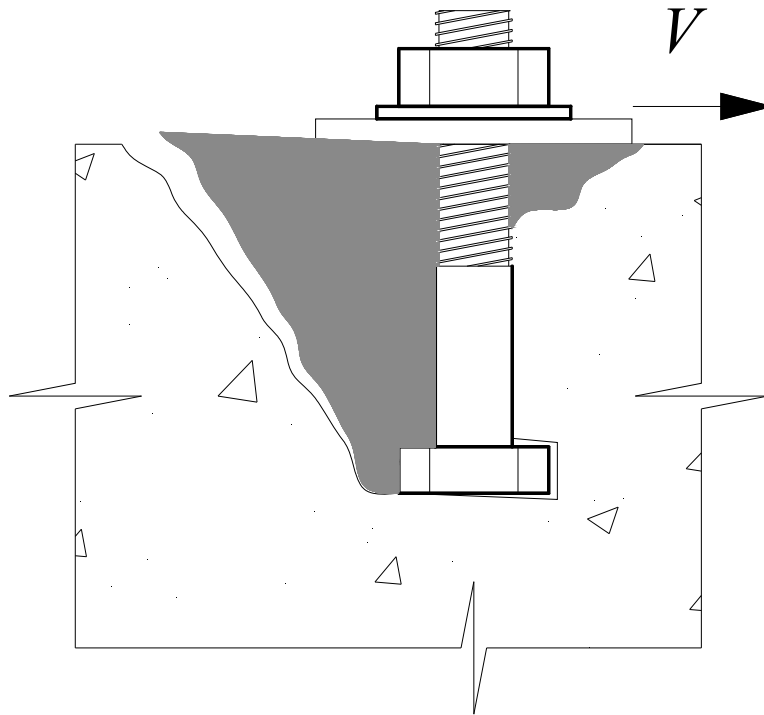


Fig. 45: Concrete pryout for anchors far from a free edge

4.4 Deterioration of Seats and Caps:

Pier cap or abutment cap provides the base or the seat the carry the bearing assembly on which the superstructure rest. A decent number of bridges have open joints over the abutments and piers. Some bridges have drainage troughs, these troughs are usually placed below the open joints. The main reason of these troughs is to intercept the runoff and debris that falls through the deck expansion joints. They discharge the debris beyond the substructure units into the stream or onto the ground below. However, these debris and runoff, which usually contain deicing chemicals, can be accumulated on the top of the pier or abutment caps if the bridge does not have a drainage troughs, leading to corrosion and deterioration in the substructure caps and bearings. The same problem can happen even in bridges with drainage troughs because of clogging and run-over (FHWA Bridge Maintenance, Rossow).

The debris and runoff mentioned above on the substructure caps hold water and deicing chemicals for long periods. These deicing chemicals cause corrosion of bearing systems. Moreover, the penetration of these chemicals into concrete results in corrosion in reinforcing steel which causes delamination and spalling in concrete cover (FHWA Bridge Maintenance, Rossow). Fig. 46 shows a corroded pier cap.

Corrosion causes the bearing system to be frozen, this causes additional stress in the substructure cap, resulting in spalling and damages to the bearing system. Also, the corrosion of the anchorage bolts of the bearing system causes the surrounding concrete to crack, which in turn

causes spalling of concrete (FHWA Bridge Maintenance, Rossow). Moreover, the presence of debris in the joints may prevent the deck from expanding and the span from moving during an earthquake.



Fig. 46: Fracture of Bearing Seat (FHWA Bridge Maintenance, Rossow)

4.4.1 Single column piers (Cantilevered piers):

Single column pier is a pier consisting of one column that carries the pier cap, it is usually used in small or pedestrian bridges. The term “pier” usually refers to a single column pier while piers with more than one column are called “bents”. In the case of single column pier, the top fibers of the pier cap will be in tension as both outer sides of the cap work as cantilevers. This means that the main tension reinforcement will be in the top part of the cap as shown in Fig. 47. Having a larger diameter and therefore a smaller concrete cover, the main reinforcement at the top of the cap is exposed to corrosion penetration at higher rates than other reinforcement. Also, the upper part of the cap is directly exposed to the water and deicing salt falling through the joints because it is located directly under deck expansion joints. This makes the top of the pier cap more vulnerable to corrosion.

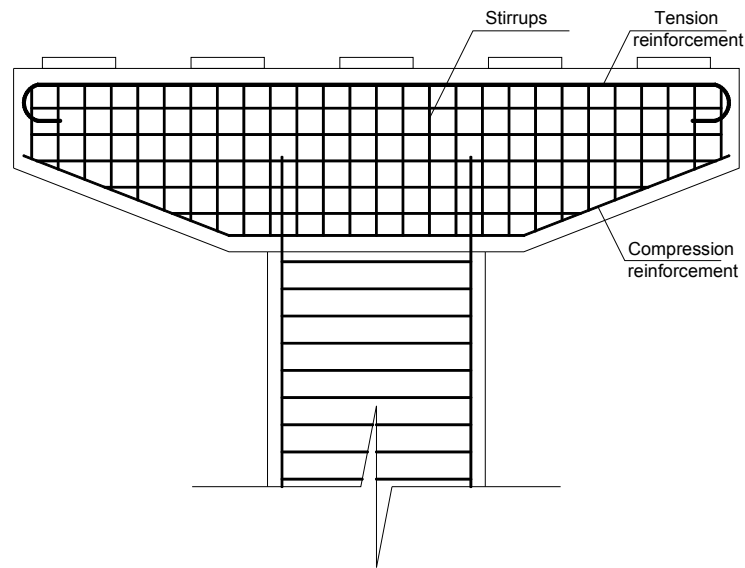


Fig. 47: Reinforcement of a single column pier cap

Corrosion of flexural and shear reinforcement will cause a decrease in the steel cross-sectional area which will lead to a decrease in the flexural and shear capacity, also, the bond between steel and surrounding concrete will decrease. Moreover, corrosion of flexural and shear reinforcement will eventually lead to cracking, spalling and delamination of concrete cover on the top and the sides of the pier cap. “A horizontal crack along the face of the pier cap, 75 to 100 mm (3 to 4 inches) from the top, normally indicates that the top mat of rebars has expanded because of corrosion and has forced up (delaminated) the concrete” (FHWA Bridge Maintenance, Rossow). Fig. 48, Fig. 49 show the crack pattern and the deterioration in concrete due to corrosion of steel reinforcement.

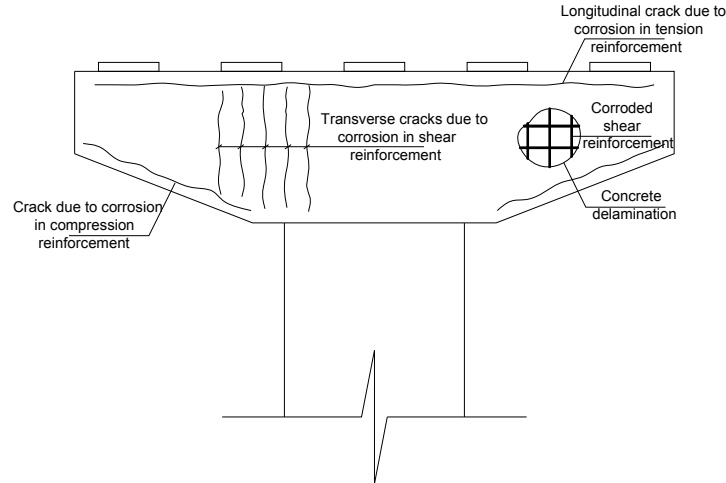


Fig. 48: Crack pattern and concrete delamination due to corrosion

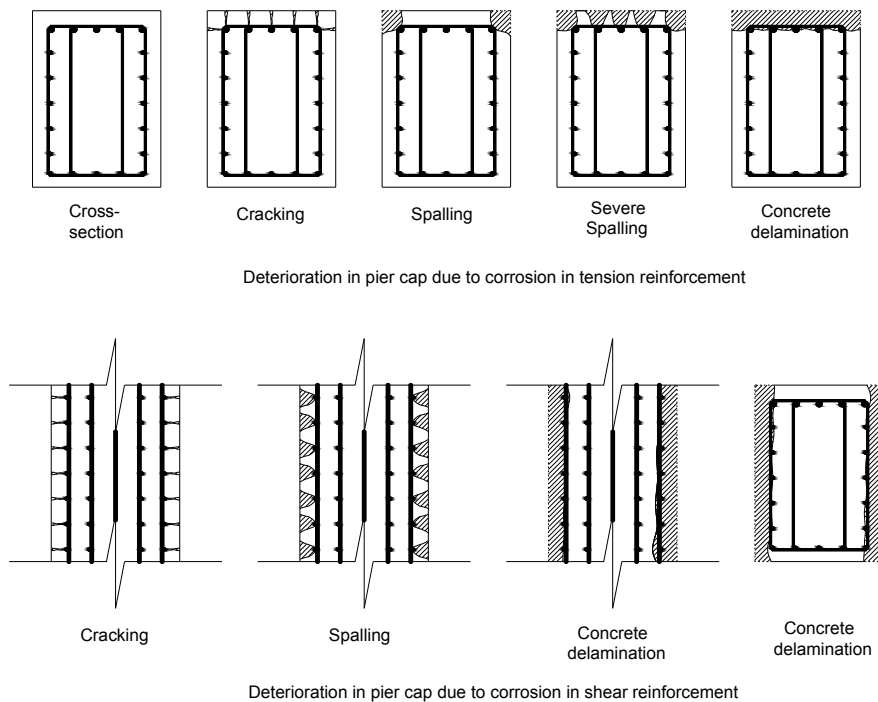


Fig. 49: Deterioration in concrete due to corrosion of steel reinforcement

Delamination of concrete will decrease the minimum support length discussed above and which is required by AASHTO, which in turn, will increase the risk of span collapse during an earthquake due to unseating as shown in Fig. 50. However, when concrete starts to crack, spall, and delaminate due to the extra stress caused by corroded reinforcing steel, it will increase the access of water and deicing salt to the non-corroded steel and will accelerate the corrosion process in the corroded bars. This will exacerbate the situation leading to an increase in delamination of seat concrete and a higher risk of unseating.

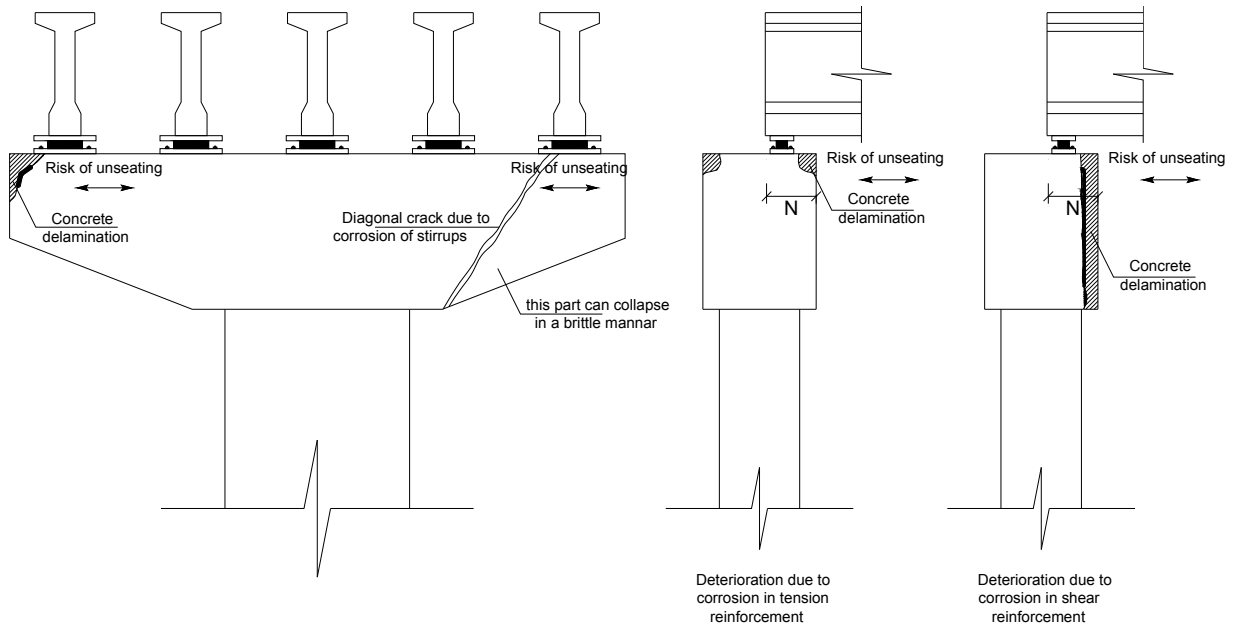


Fig. 50: Deterioration in concrete increase the risk of unseating during an earthquake

4.4.2 Multi column piers (bents):

Multi column pier is a pier consisting of more than one column carrying the pier cap. The difference between single column piers and multi column piers is that in the case of single column piers the primary tension reinforcement is at the top of the pier cap in all section, meanwhile in the multi column piers the primary reinforcement in the span between columns is at the bottom of the cross-section as shown in Fig. 51. This means that in the span between columns, the cap is less subjected to corrosion because the compression reinforcement at the top usually has a smaller diameter and a larger concrete cover than the tension reinforcement.

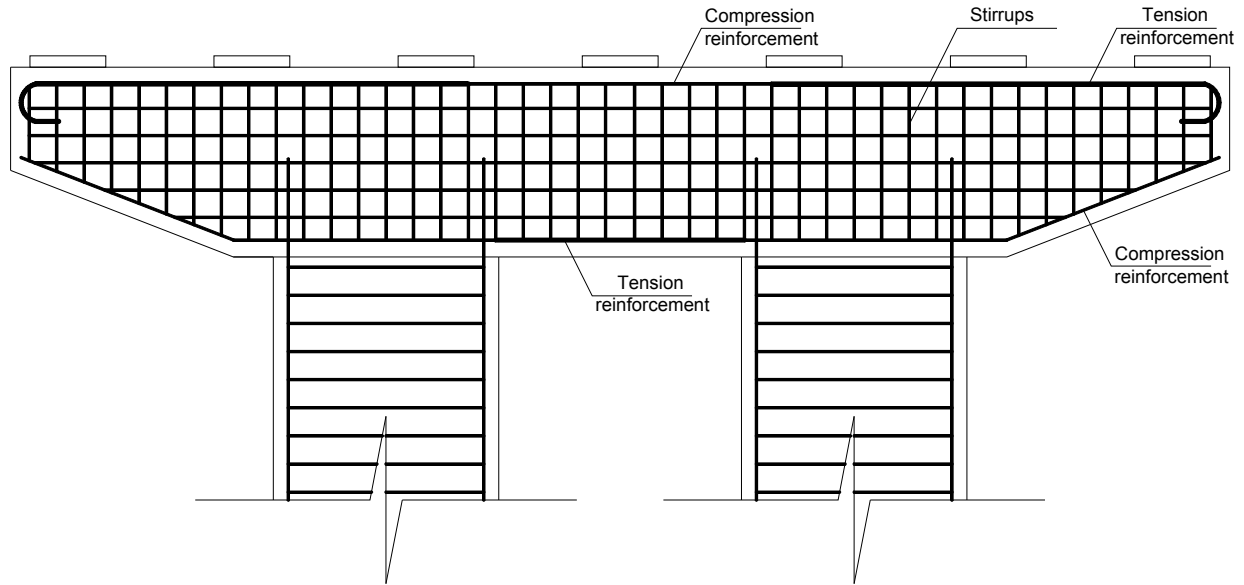


Fig. 51: Reinforcement of multi column pier cap

However, except for the location of the tension and compression reinforcement which plays a role regarding the time at which corrosion starts and the acceleration of steel corrosion and concrete deterioration, the multi column piers are subjected to the same corrosion problems as the single column piers. Fig. 52, Fig. 53 show spalling and delamination of concrete pier caps.



Fig. 52: Spalling and delamination of concrete pier cap (Bridge Inspection Manual 2010)



Fig. 53: Severe Concrete Spalling on Bent Cap (BIRM, Rossow)

4.4.3 Abutments:

The abutments are the end bents of the bridge, support the extreme ends of the bridge and confine the approach embankment, allowing the embankment to be built up to grade with the planned bridge deck (Bridge Construction Overview). Even though that most of bridge abutments consist of a footing, wall, bridge seat, wing, and mudwall, some abutments have columns that carry the cap or the seat instead of wall. However, when the abutment is designed with a wall, the steel reinforcement will be in compression in the seat cap. Corrosion of longitudinal and transverse steel reinforcement of abutment seating leads to cracking and spalling of concrete, which in turn leads to unseating of bridge span during earthquake as shown in Fig. 54.

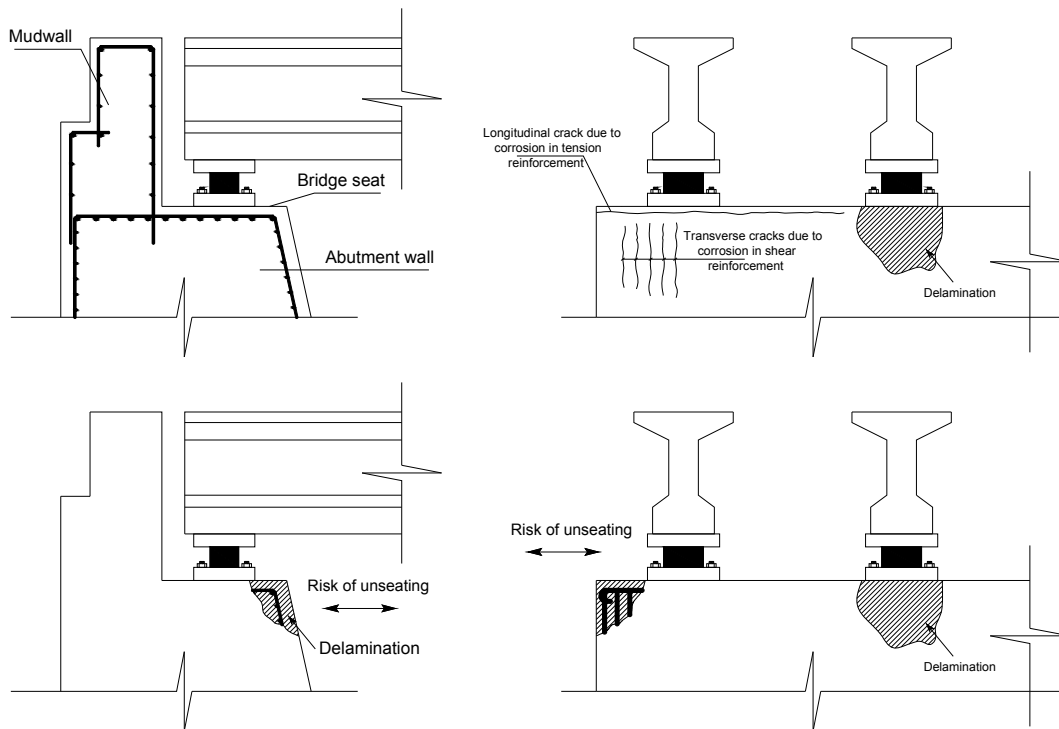


Fig. 54: Deterioration of bridge abutment increase the risk of span unseating

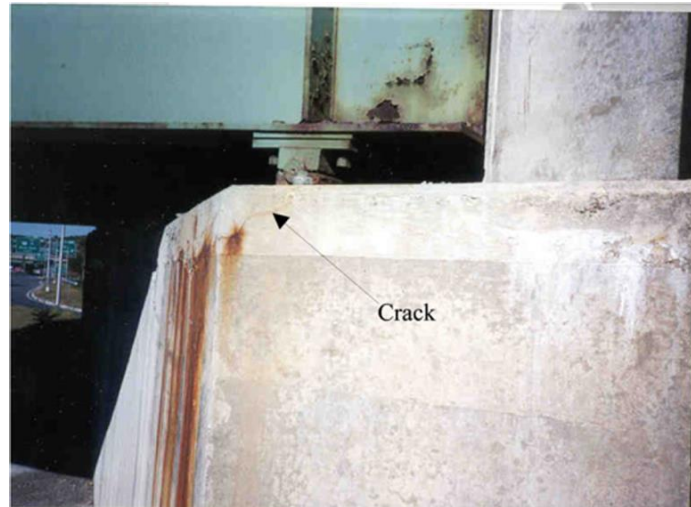


Fig. 55: Typical fixed steel bearing at an abutment (note seat cracking at the edge and corrosion of its reinforcements) (Padgett et al. 2006)

4.5 Deterioration of Concrete at end of Beam/Girders:

4.5.1 Steel reinforced girders:

A girder is “a horizontal structural member supporting vertical loads by resisting bending. The ends of girders are supported by the piers or abutments that they rest on. A girder is a large beam, sometimes made of multiple metal plates that are riveted or welded together. It is sometimes called a beam or stringer” (O’Connor 2010).

Unseating of the girders in the longitudinal or transverse directions may be the only implication of seismic event if the superstructure is isolated from the substructure through pin or roller supports (NCHRP 2004). In other words, simple span bridges are subjected to unseating during ground motion meanwhile continuous bridges the risk of unseating is reduced. This because all the horizontal forces are transmitted at the fixed ends to the piers or abutments, this makes the pier and abutments more subjected to damage during an earthquake.

Even though most of the concrete girder bridges are constructed using prestressed concrete girders, there is a decent amount of girder bridges which are designed using steel reinforced concrete girders. In both cases, corrosion of steel reinforcement, tendons, and tendon anchorage can lead to serious problems including causing total collapse of the bridge span during ground motion.

The end of the girder rests on the abutment seat or pier cap. This is usually under the expansion joints. If the bridge does not have drainage troughs or the drainage troughs are clogged, the debris and runoff that fall through the deck expansion joints, containing deicing salt, can cause corrosion to the ends of girders. In addition, the vehicles passing through the chloride-laden water beneath the bridge, cause the deicing salt to become airborne generating a fine mist that cause the bottom of bridge girders to corrode (Enright and Frangopol 1998).

An evidence of corrosion of the steel reinforcing bars imbedded in concrete is the visible rust staining on the surface of the concrete, especially in wet conditions. However, when corrosion is advanced cracks along the reinforcement bars will be seen. These cracks are initially small with widths smaller than 0.2 mm, the widths of cracks will increase with time leading to concrete spalling and delamination as shown in Fig. 56. When concrete spalls at the end of bridge girder, the length of the girder resting on the support becomes shorter, leading to higher risk of unseating. Therefore, the main problem related to corrosion of bridge girder is the spalling of concrete at the ends of the girder. In other words, corrosion of reinforcing bars in the midspan of the girder will not cause a total span collapse during seismic events even though that it will reduce the capacity of the girder.



Fig. 56: Moderate Damage: Spalled concrete (WSDOT)

Since spalling of concrete at the end of girder is critical in determining the length of the girder seated on the support, the case of unseating, it is important to estimate the time for cracks to start forming in concrete, also, it is extremely important to compute the time for concrete to start spalling due to corrosion of reinforcing bars.

Morinaga 1989 suggested empirical equations to compute the time to cracking. It is suggested that cracking of concrete will start when there is a certain amount of corrosion products forming on steel reinforcing bars. This amount is calculated as:

$$Q_{cr} = 0.602d \left(1 + \frac{2c}{d}\right)^{0.85} \quad \text{Eq. 37}$$

Where:

Q_{cr} = critical mass of corrosion products (10^{-4} g/cm²)

c = cover to the reinforcement (mm)

d = diameter of reinforcing bars (mm)

After calculating the critical mass of corrosion products, time for cracking to first occur can be calculated as follows:

$$t_{cr} = \frac{Q_{cr}}{i_{cor}} \quad \text{Eq. 38}$$

Where:

t_{cr} = time for cracking to take place (days)

Q_{cr} = critical mass of corrosion products (10^{-4} g/cm²)

i_{cor} = corrosion rate in gram per day

However, corrosion rate can be measured or estimated bases on existing data.

Kamal, Salma, and El-Abiary (1992) proposed an equation to calculate the time from beginning of corrosion until the concrete cover falls:

$$t_s = \frac{0.08(c-5)}{D.C_r} \quad \text{Eq. 39}$$

Where:

t_s = time from beginning of corrosion until the concrete cover falls

C = concrete cover thickness

D = steel bar diameter

C_r = corrosion rate units (mm/year)

The above equations show that time for concrete to crack, as well as to spall, is a function of corrosion rate, concrete cover, and bar diameter.

At the presence of corrosion, concrete starts cracking, spalling, and delaminating. When concrete at the end of the girder delaminates, the length of the girder seated on the abutment seat decreases. This increases the risk of unseating collapse during an earthquake as shown in Fig. 57.

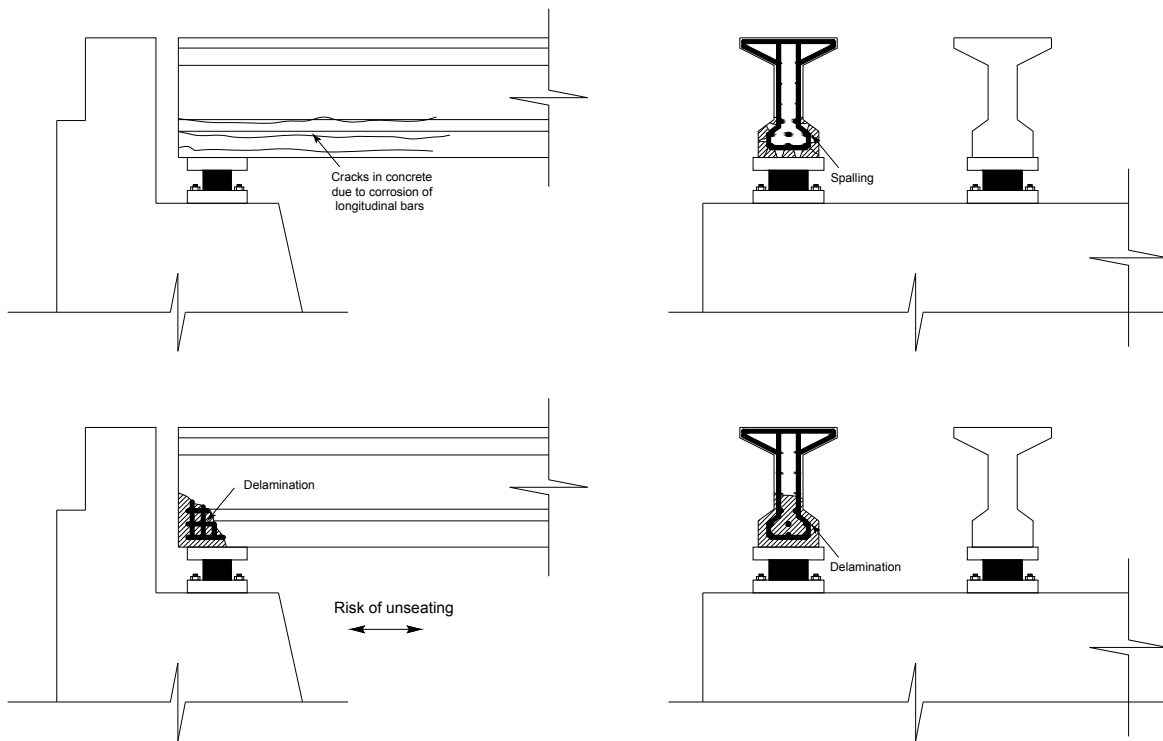


Fig. 57: Deterioration of bridge girder increase the risk of span unseating during an earthquake

4.5.2 Prestressed concrete girders:

In prestressed girders, the strands have been pretensioned, this tension is transferred to concrete as compression. This compression in the concrete will keep the girder from going into tension under loading.

Prestressed concrete girders are similar to conventionally reinforced concrete girders in that spalling and delamination of concrete at the end of girders increases the risk of span collapse during ground motion due to unseating. However, in prestressed girders, oxidation of the reinforcing steel may not produce corrosion that is enough to crack concrete (Hover, 1995). However, the loss of prestressing anchorage due to corrosion leads to loss of unbounded tendons (OECD 1989, Beal and Chamberlin 1982), this will decrease the prestressing force and will allow corrosion products to crack concrete.

Corrosion of strands, cracking and deterioration in prestressed concrete girders are more critical than conventionally reinforced concrete girders. This is because of the relatively thinner sections that prestressed concrete has. Being squeezed together due to the high tension in the tendons, a loss of concrete may cause the remaining part of the section to crush and fail. On the one hand, if a tendon breaks due to corrosion, it will only cause a minor damage. On the other hand, many tendons snapping can cause a sudden failure of the bridge (FHWA Bridge Maintenance, Rossow).

However, in prestressed concrete girders, all flexural cracks or shear cracks are considered major cracks regardless the width or the size of the crack, and must receive immediate repair (O'Connor 2010).

As mentioned above, corrosion of tendon anchorage can also lead to spalling and delamination of concrete at the end section of the girder leading to a higher risk of span collapse due to unseating during a seismic event.

5 . Corroded RC Concrete Column:

Corrosion of reinforcing steel bars is the primary durability problem that causes degradation of reinforced concrete structures located in aggressive environments (Aquino et al., 2007; Ma et al., 2012). If the rate of corrosion is high, it may reduce load-carrying capacity of reinforced concrete members, cause bond deterioration, reduce anchorage of steel bars, and decrease the confinement by transverse reinforcement (Ma et al., 2012). Recent strong earthquakes have shown that the primary cause of collapse in many existing older structures is column failure. Corrosion of reinforcement in columns makes the situation even worse. Estimation of failure mechanism of corroded column subjected to seismic load is more complicated and may vary based on corrosion rate or location of corrosion.

5.1 Deterioration of Reinforced Concrete Bridge Columns:

This section presents few common case studies of existing concrete bridge columns in the State of New York deteriorated by corrosion of reinforcing steel bars in concrete. Depending on the level of corrosion, deterioration may lead to a structural deficiency and limit the level of safety against failure (Aboutaha, 2004). Fig. 58 shows concrete bridge pier damaged by corrosion. As shown in the figure, cracks formed as a result of rebar corrosion. These cracks typically extend parallel to the rebars along its corroded length.

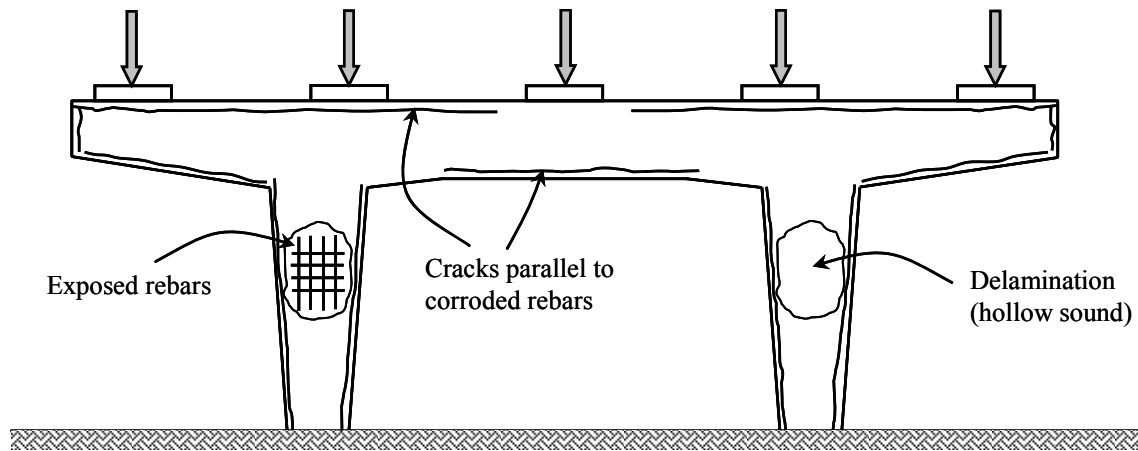


Fig. 58: Deterioration of a concrete bridge pier due to corrosion of reinforcing steel bars (Aboutaha, 2004)

When several bars corrode at one location, corroded rebars produce a splitting crack in the plane of the rebars. In its initial stage, it results in delamination, which can be easily detected by hammering. At advanced corrosion state, the concrete cover spalls off leaving rebars exposed to the external environment, as shown on the left pier column in Fig. 59 and Fig. 60 which show a view of corrosion damage on the columns, and beams.

In some advanced corrosion cases, rebar corrosion is so severe and it significantly decreases the size of the rebar, as shown in Fig. 60. In addition to loss of cross section, rebar corrosion destroys the bond between the rebar and the surrounding concrete, which results in significant decrease in the ability of the rebar to transfer forces.



Fig. 59: Deterioration of concrete bridge pier columns due to corrosion of rebars (Aboutaha, 2004).



Fig. 60: Close-up of corroded column longitudinal and transverse rebar (Aboutaha, 2004).

Fig. 61 shows the effect of rebar corrosion on the surrounding concrete. When a rebar corrodes, its volume increases by a factor of 8 to 12 times the original volume of the rebar (Aboutaha, 2004). As a result, it produces very large radial stresses on the concrete. When the internal radial stresses exceed the tensile strength of concrete, cracks form between the corroded rebar and the closest exterior surface, as shown in Fig. 61.

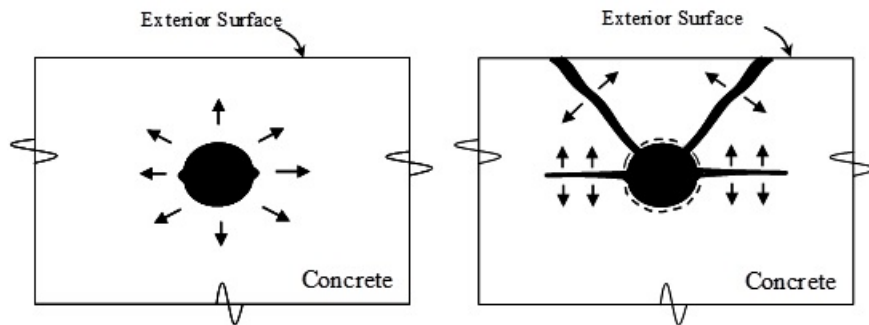
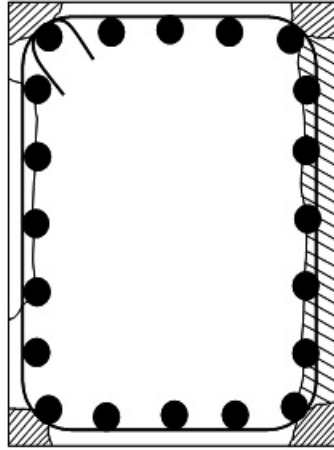


Fig. 61: Effect of corrosion of reinforcing steel bars on the surrounding concrete (Aboutaha, 2004).

Fig. 62 through Fig. 64 show examples of corrosion damaged pier columns. Fig. 62 shows photo of a rectangular column damaged by corrosion. On the east elevation, the concrete cover is still intact but delaminated and severely cracked; while on the west elevation, exposed rebar can be seen due to spalling of the concrete cover. Delaminated zones, which reflects a hollow sound when hammered upon, means that the reinforcing steel bars are corroded and their volume expanded, producing stresses larger than the tensile strength of concrete. Therefore, delaminated zones should be treated as an advanced corrosion state.



(a) Rectangular column section.



(b) West side



(c) East side



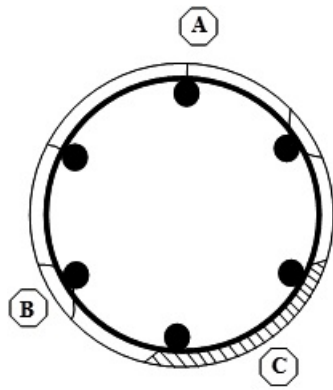
(d) North-West side

Fig. 62: Corrosion damaged rectangular concrete columns (Aboutaha, 2004).

Fig. 64(a) shows the type of corrosion-induced crack on circular column. At “A” a single crack may appear at the face of the column near a main longitudinal rebar, at “B” two cracks may form in the vicinity of a longitudinal rebar, while at “C”, an advanced state of corrosion, the concrete cover may spall off exposing the column rebars, as shown in Fig. 63.



Fig. 63: Corroded longitudinal and transverse rebar for circular columns (Aboutaha, 2004).



(a) Circular column section.



(b) New corrosion cracks, no sign of rust stain, yet.



(c) These two photos show corrosion induced cracking in circular concrete columns.

Fig. 64: Corrosion damaged circular concrete columns. Notice that the main cracks are parallel to the columns' main reinforcing steel bars (Aboutaha, 2004).

If corrosion process was allowed to continue for many years, it would completely destroy the steel reinforcing bars. For axially loaded short columns, where the effective buckling length is fairly short, loss of some of the steel cross section is not as critical as for long columns. In long columns, depending on the amount of axial load, steel bars are designed to resist both tension as well as compression. Major loss of tension steel bars would limit the bending resistance of the column (Tapan, 2008).

Loss of transverse reinforcement, as shown in Fig. 65, leaves the column section unconfined. In addition, loss of bond between the corroded bars and the surrounding concrete, as shown in Fig. 66 (b) dramatically decreases the axial load carrying capacity of the column to a plain concrete column.

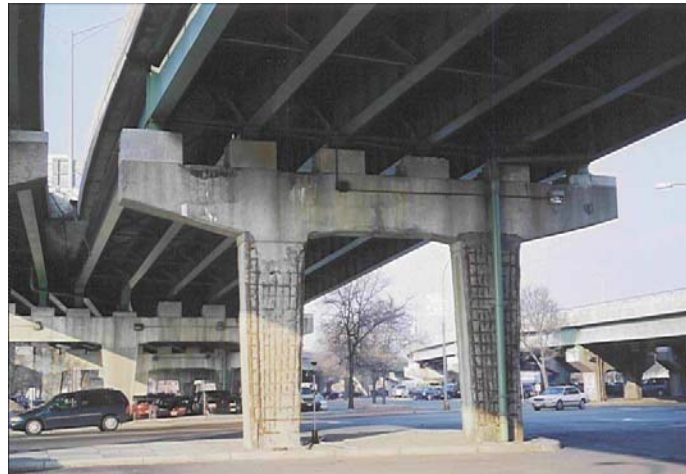


Fig. 65: Deteriorated concrete bridge pier due to corrosion of rebars (Aboutaha, 2004).



Fig. 66: Corrosion damage of tall concrete bridge pier columns (Aboutaha, 2004)

5.2 Behavior of Corroded Reinforced Concrete Columns Subjected to Lateral Loading:

The effect of corrosion on structural behavior of RC columns subjected to earthquake loading has been studied by few researchers. Lee et al. (2003) experimentally investigated structural behavior of six rectangular RC columns with cross-section of 300 mm x 300 mm and height of 1100mm. Each column was reinforced with twelve D16 longitudinal bars and D10 hoops with spacing of 80mm. Electrochemical corrosion method was used to produce different levels of corrosion in hoops. The specimens were subjected to constant axial load and cyclic loading. It was found that corrosion caused decrease in mechanical properties of rebars and spalling of concrete cover which results reduction in confining effect of reinforcement. Mode of failure for corroded specimens was shear failing which was caused by buckling of longitudinal reinforcement and failure of hoops.

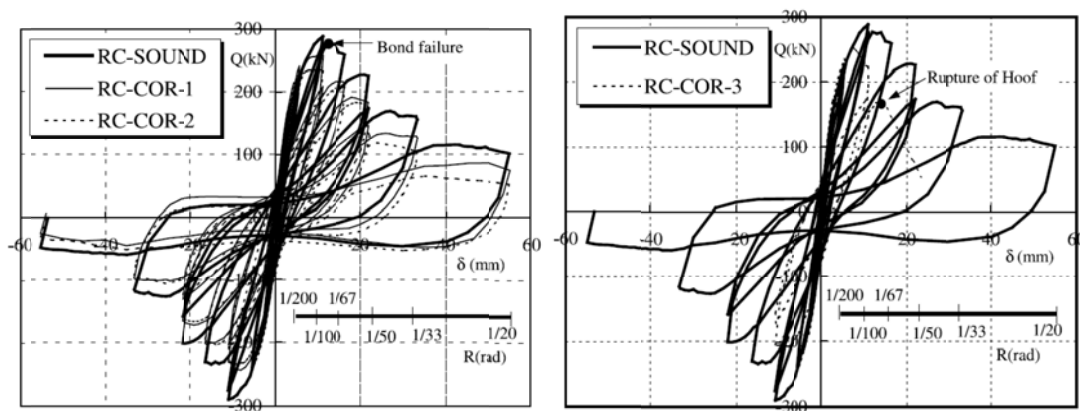


Fig. 67: Load–deformation curves (influence of rebar corrosion) (RC-COR-1: 1st corrosion level, RC-COR-2: 2nd corrosion level, RC-COR-3: 3rd corrosion level) (Lee et al., 2003)

Aquino et al. (2007) tested six circular RC columns, 500 mm in diameter and 2400 mm in height, reinforced with 12#8 longitudinal bars and #3 hoops spaced at 200 mm. External current method was used to induce corrosion in the specimens. During the test, reversed cyclic load was applied to columns and the results showed that ductility and load bearing capacity of columns reduce due to bond deterioration caused by corrosion. Same observed failure mechanism was rupture of deteriorated hoops and buckling of longitudinal bars, which resulted in shear failure of corroded specimen.

Li et al. (2009) conducted combined lateral cyclic and constant axial loading test on fourteen RC columns to investigate the effect of combined CFRP and steel jacket retrofitting system on corroded RC columns. The specimens had cross-section of 200 mm x 200 mm and clear height of 1500 mm; and reinforced with 4Φ14 mm longitudinal bars and Φ8 mm@100 mm lateral hoops. Applying lateral cyclic load at mid-span of corroded columns, they found that by increasing the lateral load, longitudinal cracks due to corrosion developed and followed by flexural cracks. Finally, complete spalling of concrete cover due to debonding between concrete cover and core caused the failure of corroded columns.

Ma et al. (2012) carried out cyclic loading tests on thirteen circular RC columns subjected to

different rates of corrosion and axial compressive loads. Circular columns with diameter of 260 mm and length of 1000 mm, having 6Φ16 mm longitudinal bars and Φ8 mm spiral with pitch of 100 mm, have been corroded using external current method. With a constant axial load, reversed cyclic lateral loading applied to the columns. They found that high corrosion levels and high axial loads lead the column to fail in brittle way and cause reduction in stiffness, ductility, energy dissipation as well as poor hysteric response. For a typical load-displacement curve of a column subjected to axial and lateral load (Fig. 68), they determined yield load of column, F_y , and corresponding displacement, Δ_y , based on assumption of equal areas for hatched region of OAB and BCY . They considered ultimate load of column, F_u , equal to 85% of maximum lateral load.

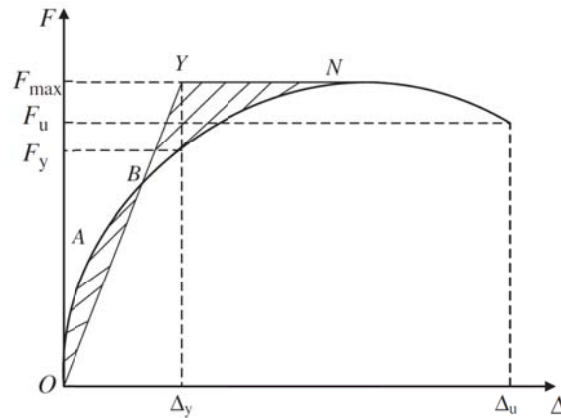


Fig. 68: Lateral load-displacement curve (Ma et al., 2012)

and F_u , yield and ultimate loads of corroded column can be expressed separately in terms of F_y and Δ_y , yield and ultimate load of non-corroded column and α , corrosion rate, based on regression of test data:

$$\text{Eq. 40}$$

$$\text{Eq. 41}$$

Where; α is the average corrosion level, in terms of $\frac{W_0 - W_f}{W_0}$, the initial weight of steel before corrosion and W_f , the final weight of steel after corrosion.

$$\text{Eq. 42}$$

Asri and Ou (2011) modeled corroded columns of a bridge using software SAP2000. She considered deterioration of material due to corrosion and carried out a push-over analysis. The following results show that base shear reduces significantly by increase in corrosion rate.

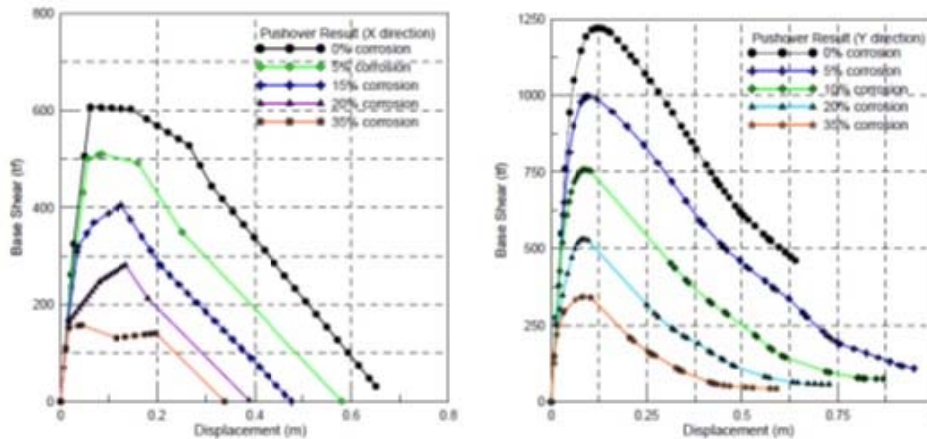
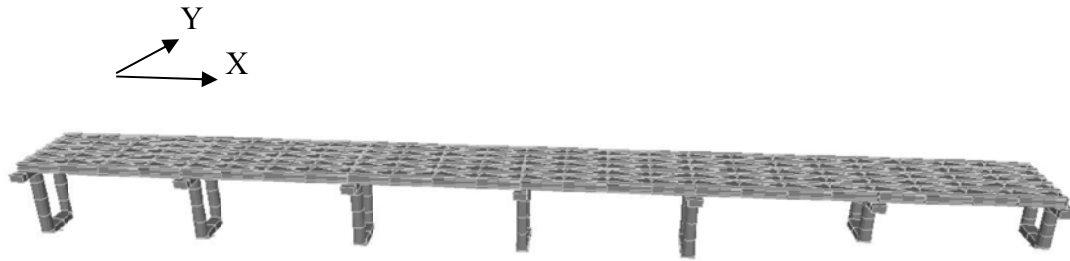


Fig. 69: Push-over analysis of corroded bridge (Asri and Ou, 2011)

5.3 Flexural Capacity:

As mentioned before, for an ideal designed concrete column subjected to lateral load, mode of failure is flexural. Flexural capacity of corroded columns subjected to axial and lateral load, which produces large bending moment, can be predicted by developing moment-axial load (M-P) interaction diagrams. An analytical model developed by Tapan (2008) is used to determine the P-M interaction diagram of deteriorated columns using the damaged geometry and material properties of deteriorated concrete and reinforcement.

Reinforcements subjected to corrosion attack suffer loss of strength and loss of ductility, thus the original strength of the reinforcement cannot be used for predicting the strength of deteriorated steel reinforcement. The empirical formula developed by Du et al. (2005) to evaluate residual capacity of corroded reinforcing bars was adopted in the analytical model presented in this paper. Their test results agreed reasonably well with those obtained under natural corrosion conditions. Therefore, the empirical equations proposed by Du et al. (2005) to assess the residual strength of corroded reinforcement embedded in concrete is used to calculate the residual capacity of corroded reinforcement (Tapan and Aboutaha, 2011).

$$f = (1 - 0.005 \cdot Q_{corr}) \cdot f_y \quad \text{Eq. 43}$$

Where; f and f_y are yield strengths of corroded and non-corroded reinforcement, respectively. Average cross-sectional area of corroded reinforcement, A_s , the amount of corrosion, Q_{corr} , were

estimated as;

$$A_s = A_{s0} \cdot (1 - 0.01 \cdot Q_{corr}) \quad \text{Eq. 44}$$

$$Q_{corr} = 0.046 \cdot \frac{I_{corr}}{d} \cdot t \quad \text{Eq. 45}$$

Where; A_{s0} is the initial cross-sectional area of non-corroded reinforcement, and Q_{corr} is the amount of corrosion of reinforcement (%), d is the diameter of non-corroded reinforcement, I_{corr} is the corrosion rate of reinforcement in real structure ($\mu A/cm$), and t is the time elapsed since the initiation of corrosion (years).

Axial load carrying capacity of a column decreases with reduction in cross-sectional area of reinforcement. If the length of corroded reinforcement exceeds a critical length, it may buckle before yielding. Stirrup corrosion as well as cracking of concrete cover increases the rate of reduction in load carrying capacity of RC columns since both result in longer unsupported longitudinal reinforcement length; which leads to premature buckling of longitudinal reinforcement. In the model, the flexural buckling strength of compression members subjected to axial compression through the centroidal axis is given by Eqs. (5)–(8). These equations were used to calculate critical buckling stress for corroded exposed reinforced bars.

$$P_n = A_g \cdot f_{cr} \quad \text{Eq. 46}$$

$$f_{cr} = (0.658^{\lambda_c^2}) \cdot f_y \quad \text{for } \lambda_c \leq 1.5 \quad \text{Eq. 47}$$

$$f_{cr} = \left(\frac{0.877}{\lambda_c^2} \right) f_y \quad \text{for } \lambda_c > 1.5 \quad \text{Eq. 48}$$

where;

$$\lambda_c = \frac{K \cdot L}{r \cdot \pi} \cdot \sqrt{\frac{f_y}{E}} \quad \text{Eq. 49}$$

A_g = Gross area of member, in².

f_y = Specified minimum yield stress, ksi.

E = Modulus of elasticity, ksi.

K = Effective Length factor

L = Laterally un-braced length of member, in.

r = Governing radius of gyration about the axis of buckling, in.

Thickness of concrete cover, tensile strength of cover concrete, reinforcement size, volume expansion of corrosion by rust and amount of rust product accommodated within the pores of the surrounding concrete without inducing fracture stresses in the concrete are important parameters control the amount of corrosion that cause cracking of the concrete cover surrounding a reinforcing bar. Cracking of the cover is assumed to occur instantaneously when the maximum hoop stress (because of internal pressure) equals to the tensile strength of concrete. Although in

reality, cracked concrete has some amount of residual strength (i.e. there are three cracking stages, initial, penetration and ultimate cracking), it is assumed that ultimate cracking occurred just after the maximum hoop stress equals to the tensile strength of concrete. It was found that “concrete cover to longitudinal reinforcement diameter” ratio plays an important role in the load carrying capacity of deteriorated reinforced concrete columns. The amount of corrosion to cause cover cracking is calculated as 2.25% for cover to longitudinal reinforcement diameter ratio equals to 1 ($C/D = 1$), and 5.25% for $C/D = 2.5$ (Tapan and Aboutaha, 2011).

For conventional reinforced concrete members, strains and stress changes can be determined in any typical section along the span using equilibrium equations, stress–strain relations, and strain compatibility. Such an analysis assumes that perfect bond exists between reinforcement and concrete, and implies that the strain change under load in the reinforcement is equal to the strain change in the concrete at the level of reinforcement.

Non-uniform reinforcement corrosion along the height and cross-section of a bridge column leads to partial or complete loss of bond between corroded steel bars and the surrounding concrete. The deterioration of the ribs of the deformed bars causes a significant reduction of the interlocking forces between the ribs of the bars and the surrounding concrete keys. As a result, it deteriorates the primary mechanism of the bond strength between deformed bars and concrete, and hence, the bond strength decreases significantly (Wang and Liu, 2004). Results from a study by Cairns and Millard (1999), indicate that it is bond which suffers the most rapid degradation as a result of corrosion, and which therefore has a serious potential to reduce structural safety. Therefore, conventional strain compatibility does not apply as is in computing stresses in corroded reinforcement (i.e. the strain changes along the corroded reinforcement length (exposed reinforcement length is averaged)), and conventional method based on strain compatibility cannot be used without any modification to determine actual capacity of deteriorated reinforced concrete members. To account for reinforcement corrosion and loss of bond while developing the interaction diagrams for different deterioration cases, the average change in the adjacent concrete over the exposed reinforcement length is calculated and the strain in deteriorated (unbonded) reinforcement is calculated as shown in

Fig. 70 using the equation below:

$$\varepsilon_{c,ave} = \varepsilon_s = \frac{\Delta L}{L} = \int_0^L \frac{\Delta \varepsilon_c}{L} dx \quad \text{Eq. 50}$$

where ε_s is the strain in deteriorated reinforcement; $\varepsilon_{c,ave}$ the average strain in deteriorated reinforcement; L the exposed (unsupported) length of the corroded reinforcement; and ε_c is the strain in concrete.

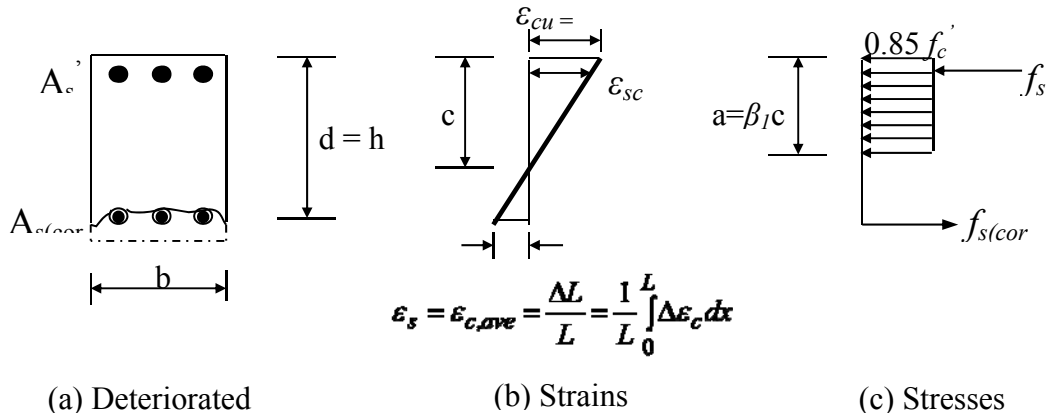


Fig. 70: Calculations of stress and strains for a given section and strain distribution

Fig. 71 illustrates a series of strain distributions and the resulting points on interaction diagram. Strain distribution at point A represents pure axial compression. Point B corresponds to crushing at one face and zero tension at the other. Since the tensile strength of concrete is ignored in the calculations, this represents the onset of cracking of the bottom face of the section. All points lower than this in the interaction diagram represent cases in which the section is partially cracked. Point C corresponds to a strain distribution with a maximum compression strain of 0.003 on one side of the section and a tensile strain of ϵ_y , the yielding strain of the reinforcement, at the level of the tension steel. This represents a balanced failure in which crushing of the concrete and yielding of the tension steel develop simultaneously. Point C, the farthest right point on the interaction diagram represents the change from compression failures for higher loads and tension failures for lower loads. At Point D the reinforcement has been strained to several times the yield strain before the concrete reaches its crushing strain. This implies ductile behavior. In contrast, for the strain distribution B, the column fails as soon as the maximum compressive strain reaches 0.003. Since the tension steel has not yielded, there are no large deformations prior to failure and this column fails in a brittle manner (Tapan and Aboutaha, 2008).

The level of load carrying capacity for any deterioration stage can be determined using several different approaches. The first approach is to find the load reduction by drawing eccentricity lines while the second one is to calculate load reduction looking through several axial loads. The procedure for the first approach starts with defining the eccentricity line using the relation M_u/P_u . Once the eccentricity line is defined, the strength reduction can be calculated for each deterioration stage. Those results can then be used to calculate load carrying capacity of the bridge columns. Second approach is based on referencing several axial loads. Although most of the columns are designed to resist small eccentricities, during a seismic activity they will experience large moments. Therefore, this approach will have much beneficial usage for evaluating load carrying capacity reduction of deteriorated reinforced concrete columns in seismic zones.

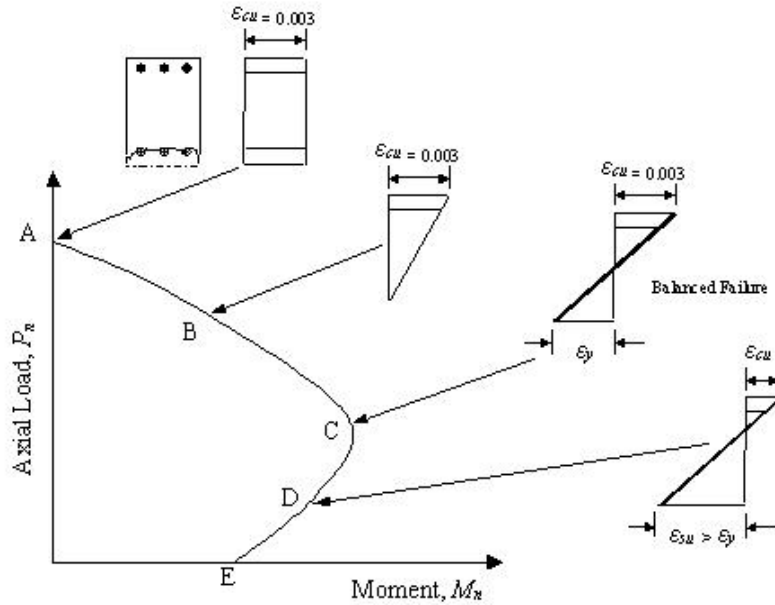


Fig. 71: Strain distributions corresponding to points on interaction diagram (Tapan and Aboutaha, 2008)

Using this methodology, Tapan and Aboutaha (2008) investigated residual structural capacity of reinforced concrete columns for several deterioration cases for the column shown in Fig. 72. As corrosion of reinforcement directly affects cover cracking; location of the corroded bars affects the load carrying capacity. The effect of corrosion and location of the corroded region on load carrying capacity is separately investigated for each deterioration stage and the results are discussed in detail. The P–M interaction diagrams for all six deterioration cases indicate that there is significant reduction in load carrying capacity beyond third deterioration stage (amount of corrosion = “2.25–10%” depending on the “As” ratio).

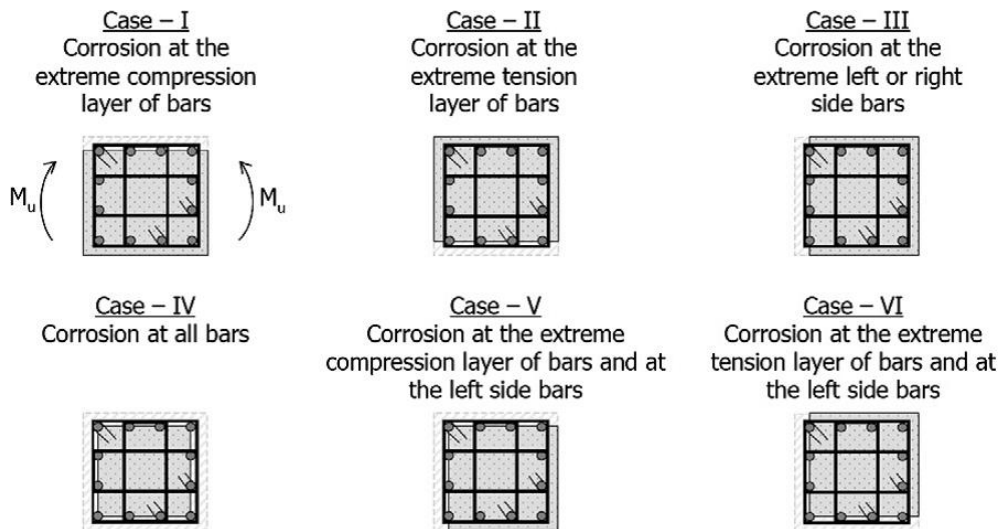


Fig. 72: Deterioration cases included in the analysis (Tapan and Aboutaha, 2011)

For the Case I, where it is assumed that corrosion takes place at the extreme layer of compression bars, the effect of reinforcement corrosion is less beyond fourth deterioration stage (amount of corrosion >10%). Axial and flexural capacities of the columns decrease, as the amount of corrosion increases. The reduction in axial and flexural capacities under balanced condition was found to be more than the reduction in compression or tension controlled regions. That is because; under balanced condition the neutral axis is fixed (because of pre-defined strain levels at concrete and reinforcement). Therefore, as the amount of corrosion increases, the forces at compression reinforcements decreases resulting in less axial load, as well as shifting of plastic centroid towards to the tension side resulting in less moment arm and finally less moment capacity.

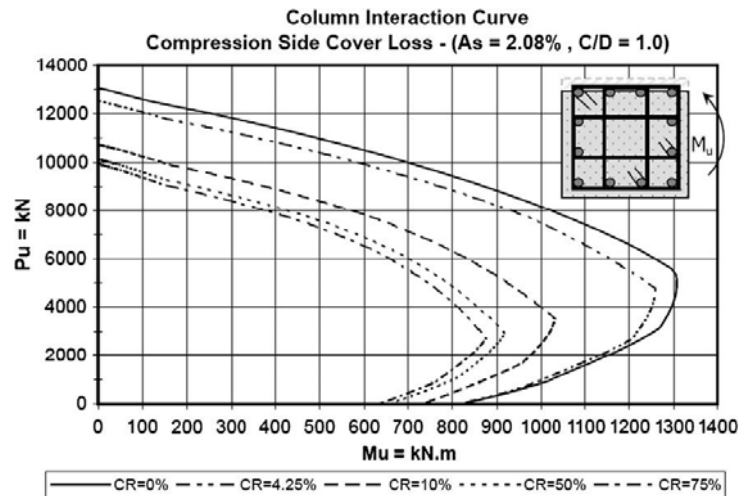


Fig. 73: Interaction diagram for pre-defined deterioration stages, where deterioration is on the compression side of the column section.

For the Case II, where it is assumed that corrosion takes place at the extreme layer of tension bars, the reduction in axial load carrying capacity under pure compression is the same as for Case I. As the corrosion amount increases, the reduction in load carrying capacity under balanced condition and pure moment is significantly higher than Case I. In addition, as corrosion amount increases, the plastic centroid of the section moves towards to the compression side to balance the reduction in bottom reinforcement bars. Since, the axial force P_n is computed by summing the individual forces in the concrete and steel, and the moment M_n is computed by summing the moments of these forces about the plastic centroid of the section, the reduction is higher for higher corrosion levels. The results indicate significant decrease under balanced and pure moment condition as corrosion amount increases. And in general, the results indicate that corrosion in tension reinforcement causes more strength reduction than corrosion of reinforcement in compression or left/right side reinforcement for high corrosion amounts (i.e. amount of corrosion $\geq 50\%$).

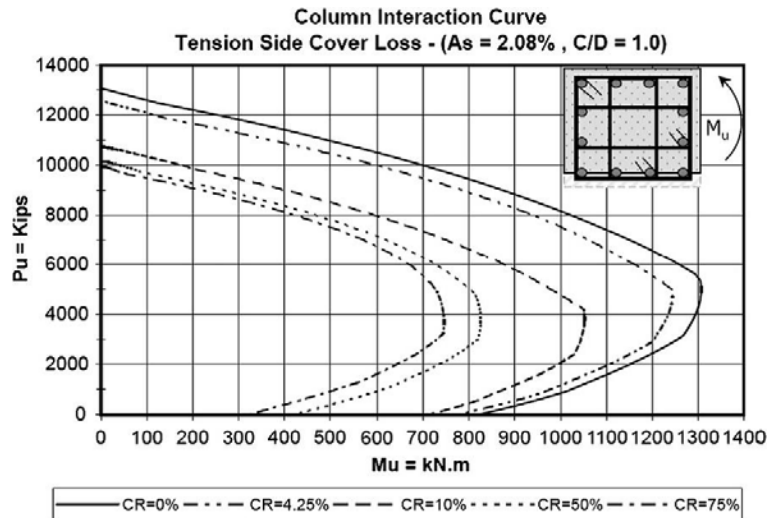


Fig. 74: Interaction diagram for pre-defined deterioration stages, where deterioration is on the tension side of side of the column section.

For the Case III, where it is assumed that corrosion takes place at the extreme left/right side layer of bars, the reduction in axial load carrying capacity under pure compression is almost the same as those of Cases I and II. Since the column is a square column and the concrete loss and reinforcement loss is the same for a given corrosion amount, the reduction in pure axial load carrying capacity is equal for Cases I, II and III. Unlike Cases I and II, reinforcement corrosion has lower load carrying capacity reduction beyond fourth deterioration stage for this case. The reduction decreases as “cover to longitudinal reinforcement diameter” ratio increases. Like the other two cases, the reduction in axial and flexural capacity under balanced condition is higher than the reduction under compression or tension controlled region. Although in Case III, the plastic centroid coincides with the centroid of the section for any corrosion amount.

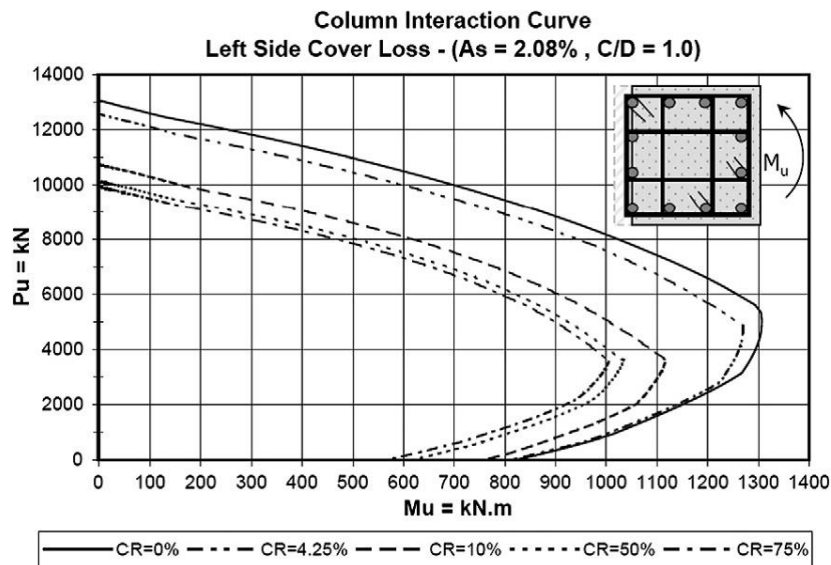


Fig. 75: Interaction diagram for pre-defined deterioration stages, where deterioration is on the left side of the column section

As the amount of corrosion increases, the forces at compression and tension reinforcements decrease resulting in less axial load and moment capacity. On other hand, because of symmetry about the bending axis ($x-x$), the reduction under balanced and pure moment is relatively lower than Cases I and II. The reduction in pure moment capacity for Case III is smaller than Case I for corrosion amounts lower or equal to 10%. As corrosion amount increases beyond 10%, the reduction in pure moment capacity for Case III increases resulting in larger flexural capacity reductions than in Case I. For all corrosion levels the reduction in pure moment capacity for Case III is less than Case II.

For the Case IV, where all bars are assumed to be corroded, there is significant load carrying capacity reduction, much more than all other cases investigated. Reinforcement corrosion beyond third deterioration stage (i.e. amount of corrosion = “2.25–10%” depending on the “ A_s ” ratio) has relatively more reduction effect on load carrying capacity. This is true due to the fact that as corrosion amount increases there will be significant reduction in reinforcement ratio leading to larger load carrying capacity reductions than other deterioration cases.

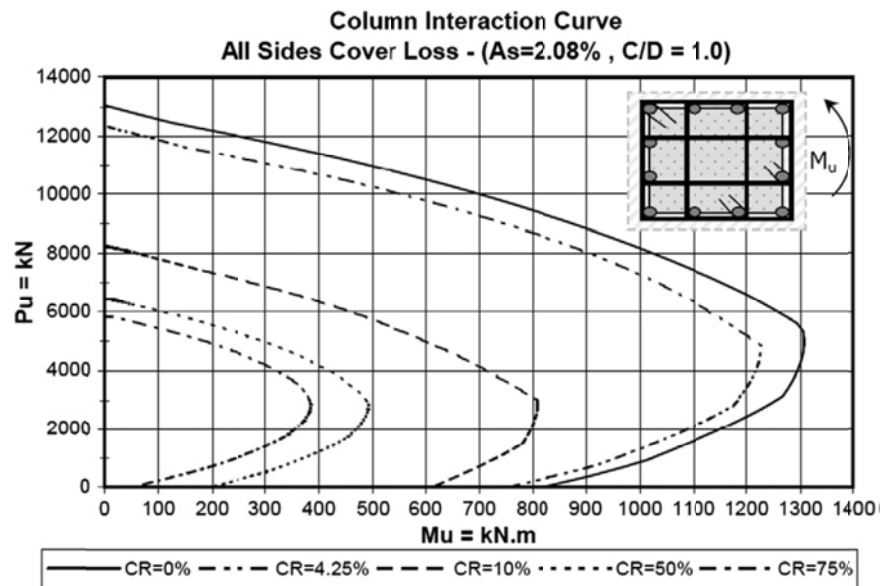


Fig. 76: Interaction diagram for pre-defined deterioration stages, where deterioration is on all sides of the column section

For the Cases V and VI, the section becomes unsymmetrical about both axes. Since all pier columns are designed against their strong axis; interaction diagrams for moment about the strong axis may be used for strength evaluation purposes (to calculate the percentage of the design load that can safely be carried). For the Case V, where it is assumed that there is corrosion at extreme compression layer of bars and left/right side bars, the reduction in axial and flexural load carrying capacity is almost equal to Case VI, where it is assumed that there is corrosion at extreme tension layer of bars and left/right side bars. As amount of corrosion increases beyond 10% corrosion level, there is more reduction for the Case VI at tension controlled region. The reduction in the compression controlled region is almost equal in both two cases for all four deterioration stages. Since, tension bars have smaller stresses at compression controlled region, corrosion of those bars have little effect on load carrying capacity.

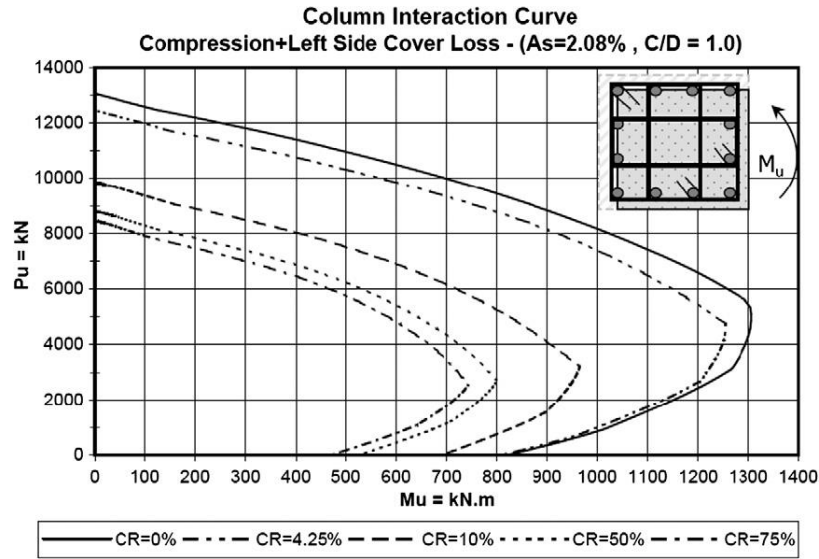


Fig. 77: Interaction diagram for pre-defined deterioration stages, where deterioration is on the compression and left side of the column section

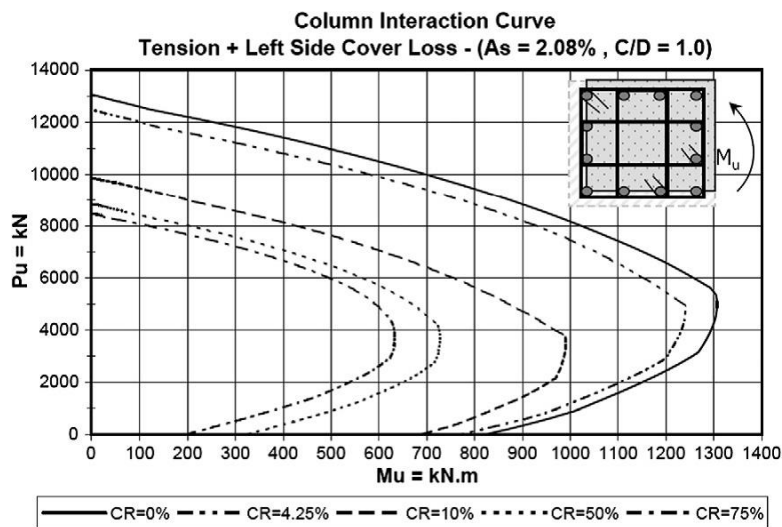


Fig. 78: Interaction diagram for pre-defined deterioration stages, where deterioration is on the tension and left side of the column section

The results of this study (Tapan and Aboutaha, 2011) suggest that for deteriorated columns the amount of strength loss depends on the location, and amount of the deterioration. Corrosion of steel bars on the compression side of column section reduces the effective depth, and therefore causing more reduction than left side or tension side deterioration, in compression controlled region. However, in general, corrosion of tension reinforcement causes more strength reduction than corrosion of reinforcement in compression or left/right side reinforcement, particularly, in tension controlled region. Corrosion on all four sides of the column section causes the most significant strength reduction.

Table 3: Strength reduction in different deterioration stages

Case number	Reduction in moment capacity for deteriorated column under an axial load = $0.4P_u$ (%)			
	Stage I	Stage II	Stage III–Stage IV	Stage IV
	CR = 4.25%	CR = 10%	CR = 50%	CR = 75%
Case I	7.27	36.88	46.75	49.87
Case II	7.27	31.43	43.64	48.57
Case III	6.23	29.09	34.55	36.62
Case IV	9.09	72.99	100.00	100.00
Case V	7.53	47.53	60.78	65.19
Case VI	7.53	43.90	58.44	63.12

CR = Corrosion rate, P_n = Nominal axial capacity.

5.4 Shear Capacity:

Experimental study on failure mode of reinforced concrete columns shows that columns subjected to axial and lateral load typically fail in shear (Ousalem et al., 2003). The first appeared cracks are flexural cracks because of initial flexural response of column; and then shear cracks are observed and developed which ultimately result in failure of column. In another word, if a column under lateral load has low shear capacity, it will fail immediately after flexural deformation, but if it has high shear capacity, shear failure occurs after large lateral deformation (Mostafaei et al., 2009). Shear load capacity of columns might decrease by corrosion faster than flexural load capacity, because transverse reinforcement has less concrete cover than longitudinal one, which may start to corrode first (Webster, 2000). All these factors together, make it difficult to predict the behavior of a corroded RC column.

According to ACI 318-11, nominal shear capacity of RC columns shall be defined as:

$$V_n = V_c + V_s \quad \text{Eq. 51}$$

V_c is nominal shear strength provided by concrete, which can be calculated using the following equations for concrete members subjected to axial compression loads.

$$V_c = (1.9\lambda\sqrt{f_c'} + 2500\rho_w \frac{V_u d}{M_m}) b_w d \leq 3.5\lambda\sqrt{f_c'} b_w d \sqrt{1 + \frac{N_u}{500A_g}} \quad \text{Eq. 52}$$

Where;

$$M_m = M_u - N_u \frac{4h-d}{8} \quad \text{Eq. 53}$$

For corroded section, Higgins et al. (2003) suggested using b_{eff} instead of b due to decrease in cross section of concrete.

$$b_{eff} = b - 2(c_v + d_s) + \frac{s}{5.5} \quad \text{if } s \leq 5.5c_v \quad \text{Eq. 54}$$

$$b_{eff} = b - \frac{5.5}{s}(c_v + d_s)^2 \quad \text{if } s > 5.5c_v \quad \text{Eq. 55}$$

where b is the original undamaged section width (in), c_v is the concrete cover (in), d_s is the stirrup diameter (in), and s is the stirrup spacing (in).

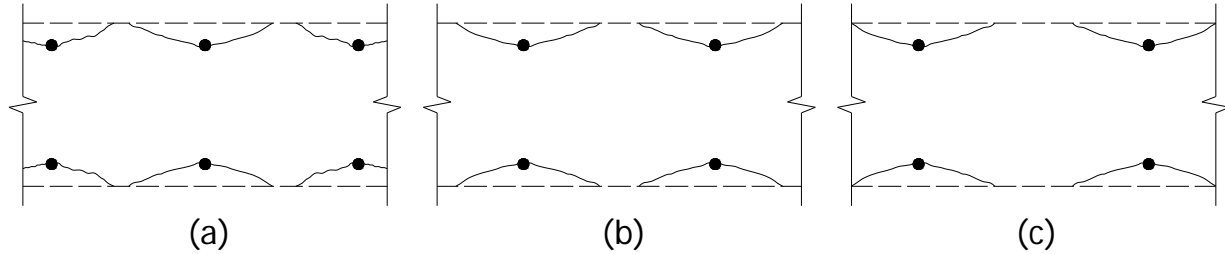


Fig. 79: Plan view of concrete cracking in beam web due to corrosion for three different stirrup spacing; (a) 8-in, (b) 10-in, and (c) 12-in (Higgins et al., 2003)

d is defined as distance from extreme compression fiber to centroid of longitudinal tension reinforcement; then for an un-symmetric cross-section:

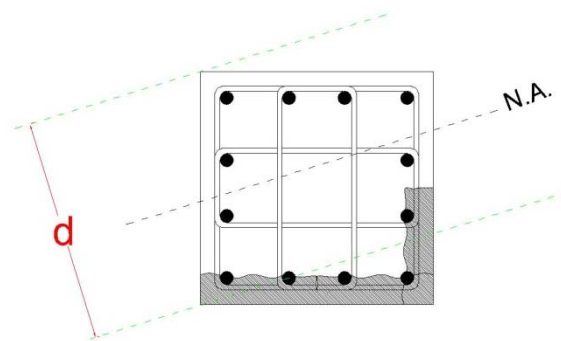


Fig. 80: Effective depth of unsymmetrical section

V_s is the nominal shear strength provided by shear reinforcement:

$$V_s = \frac{A_v f_y d}{s} \quad \text{Eq. 56}$$

For corroded RC section, A_v , the cross-sectional area of corroded stirrups can be calculated considering corrosion rate.

$$CR = \left(1 - \frac{d_{l0} - d_l}{d_{l0}}\right) \times 100\% \quad \text{Eq. 57}$$

Where; d_{l0} is the diameter of non-corroded stirrup, d_l is the diameter of corroded stirrup and CR is the corrosion rate. d , effective depth of corroded section shall be calculated as discussed above. s is the maximum spacing between stirrups in each section and should be checked with maximum allowable spacing according to ACI 318-11.

Stress in steel bar at ultimate limit state may change due to following reasons:

- Since the bond between concrete and steel is deteriorated in partial length of steel bars, stress along the bar is not constant. Variation of stress results in change of shear failure mode. It can convert from yielding or fracture of stirrups to shear compression failure or splitting along the corrosion-induced cracks (Wang et al., 2012)
- Pitting corrosion of reinforcement leads to incredible change in stresses which results in sudden fracture of rebars.

ACI equation for shear capacity of reinforced concrete doesn't include the stresses in longitudinal bars. Therefore, it is not able to consider bonded or un-bonded length of corroded longitudinal bars using this equation. Consequently, ACI equation shall be used for small rates of corrosion in which bond deterioration is negligible.

Rahal (2000) proposed a method to calculate the shear strength of RC members, which is more accurate than the ACI model. The proposed method compared with modified compression field theory and also checked with experimental data and showed good agreements.

In this method, shear resistance of longitudinal bars of the section is defined as the subtraction of tensile forces from the maximum resistant of longitudinal bars, which assumed $A_s f_{yL}$. Shear resistance of transverse reinforcement is also considered as yielding force of them, $A_v f_{yt}$. In flexural compression and tension zones of cross section, modified resistance of bars has been supposed as, respectively:

$$F_{co} = A'_s f'_{yL} - \frac{N}{2} + \frac{M}{d_v} \quad \text{Eq. 58}$$

$$F_{ten} = A_s f_{yL} - \frac{N}{2} - \frac{M}{d_v} \quad \text{Eq. 59}$$

The proposed method has two non-dimensional indexes:

$$\omega_L = \frac{2 \min\{F_{co}, F_{ten}\}}{b_w d_v f'_c} \quad \text{Eq. 60}$$

$$\omega_t = \frac{A_v f_{yt}}{b_w s f'_c} \quad \text{Eq. 61}$$

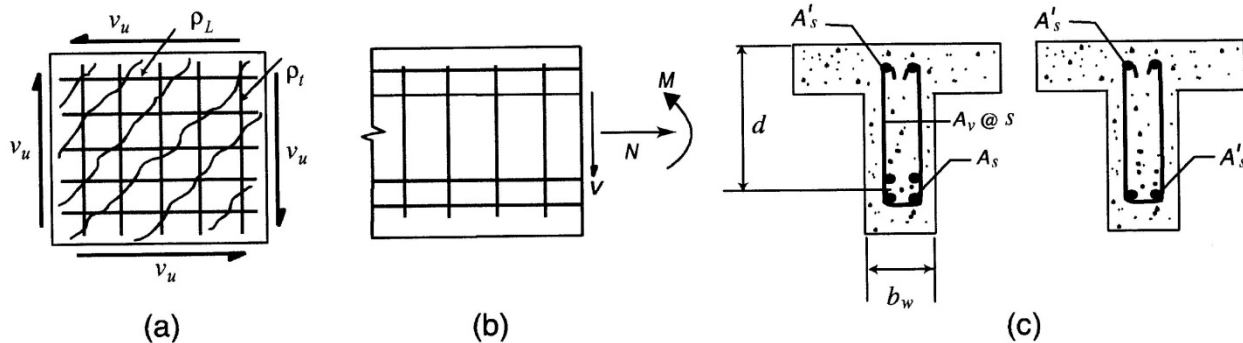


Fig. 81: Information for calculating transverse and longitudinal indexes w_t and w_L : (a) membrane element; (b) beam cross section under shear, bending, and axial load; and (c) unsymmetrically reinforced sections.

Shear strength of a reinforced concrete section due to both longitudinal and transverse bars can be defined using non-dimensional indexes ω_L and ω_t and referring to Fig. 82.

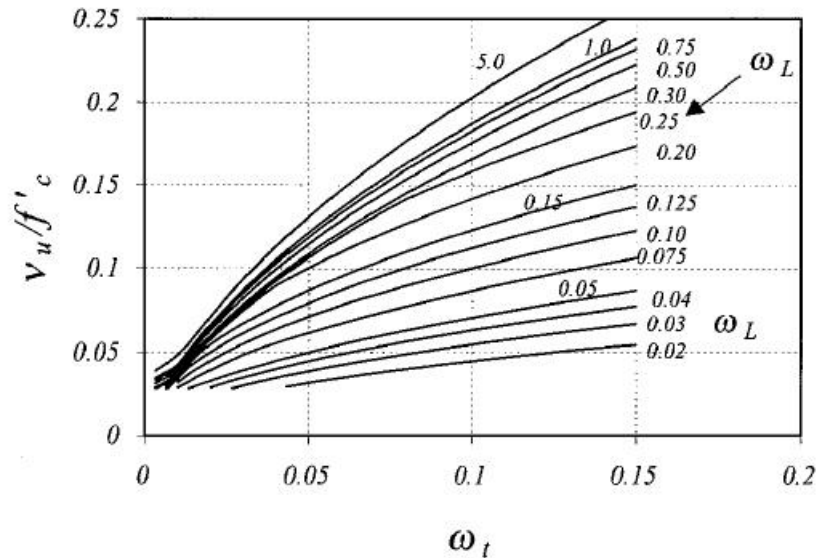


Fig. 82: Normalized shear strength curves (Rahal, 2000)

Based on this methodology, the approach can be applicable for corroded sections, too. Reduction in cross-section area of longitudinal and transverse reinforcement due to corrosion rate, reduction in effective width of the corroded section using Higgins et al. equations, and the most important, change in maximum stresses at bars due to debonding lead the investigator to be able to define shear capacity of corroded column.

5.5 Lap Splices:

Ductility of reinforced concrete members has an important role on seismic behavior of structural systems. Ductility is the ability of a structure or structural member to maintain its capacity during through post-elastic deformation. Past earthquakes indicate that non-ductile structures are more vulnerable to severe damages or even collapse (Aboutaha et al., 1999). Adequate detailing of reinforced concrete and well confinement of RC members at regions where formation of plastic hinges is more probable, can improve ductility of a RC member. Plastic hinges are formed at regions with high flexural moment demand, above the foundation footing in bridges; where the common practice is splicing the longitudinal reinforcing bars (Harajli and Khalili, 2008). Therefore, any deficiencies in lap spliced region like corrosion leads the column to a non-ductile behavior and vulnerability of columns in seismic regions.

The ideal form of failure of lap splices, in which the bars can develop their full potential strength before anchorage failure, is yielding of spliced bars and fracture near their loaded ends within the splice (Lin et al., 1998). Bond is the main problems of lap splices. Because of deficiencies such as short lap splices, small concrete covers and low amount of confining transverse reinforcement in most of the columns, failure of lap splice occurs due to loss of bond transfer and as a result, splitting of the concrete cover prior to yielding of longitudinal bars occurs.

Steel properties, concrete strength and cover, splice length and transverse reinforcement have significant influence on the behavior of lapped splices (Lin et al., 1998). Corrosion mainly changes the steel reinforcement section and ductility, integrates concrete and the most important, affects the concrete-steel interaction due to bond reduction (Rudriquez et al., 2006). Consequently, corrosion causes premature failure of lap splices.

As mentioned above, bond is the main parameter determining the behavior of lap splices; specially in corroded columns. Bond stresses in lapped splice produce longitudinal, radial and circumferential tensile stresses (Lutz and Gergely, 1967). When the resulting stresses exceed the tensile strength of concrete, more cracks are formed. Steel bars have volumetric expansion due to corrosion products. This expansion generates micro-cracking in concrete which results in less strength and ductility of concrete. Therefore, in a corroded concrete, formation of cracks is progressive. When cracks formed, they propagate widely which results in quick bond deterioration and loss of shear stress transfer between steel and concrete.

The ratio of concrete cover to bar diameter has an important role in defining the mode of failure of spliced bars; as the ratio is reduced due to corrosion, splitting of concrete cover is more probable to occur. Radial and circumferential tensile stresses tend to split the concrete cylinder cover around the lapped bars. Reduction in concrete area because of cracking and spalling of concrete in corroded column, decreases the effective cover thickness resulting in low bond strength. Therefore, low bond strength is achieved due to splitting of concrete cover because of corrosion-induced cracking (Coronelli and Gambarova, 2004).

If lap splices had sufficient length to develop high stresses, less splitting forces per unit length of bars are developed. So, short lap splices doesn't allow the stress in longitudinal bars to be developed to yielding stress. Bond deterioration proceeds progressively due to short lap splices which gets worse in corroded concrete elements. Furthermore, the amount and distribution of transverse reinforcement as confining parameter has a major effect on strength and energy dissipation of lapped splices. In addition, well-confined concrete core has increased compressive strength and delay crushing of concrete (Lin et al., 1998). For columns subjected to cyclic loading, confining reinforcement decreases deterioration of bond significantly (Fang et al., 2006).

During a seismic event, shear stresses transfer tensile stresses between starter bars and main column bars. Cracking and collection of rust products in corroded concrete decrease the shear capacity of it to carry these stresses (Aquino and Hawkins, 2007). Furthermore, bond stresses along the bars generate radial stresses which widen the cracks and causes more loss of bond, results in splitting of concrete cover. Therefore, lapped splices fail prior to yielding of longitudinal bars occurs.

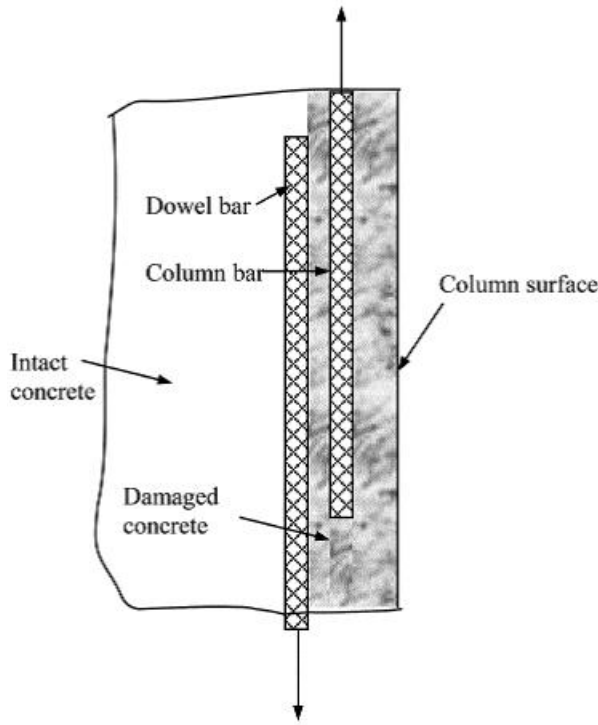


Fig. 83: Conceptual model for damage due to corrosion in column specimens (Aquino and Hawkins, 2007)

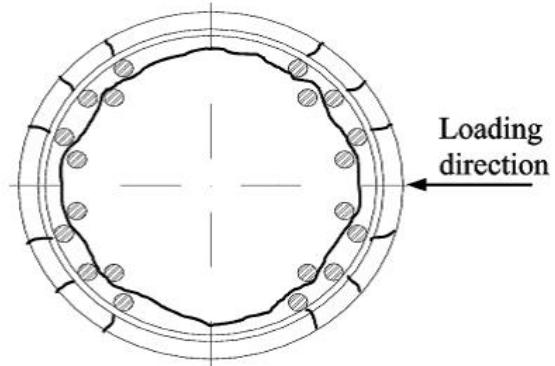


Fig. 84: Crack-damage pattern after corrosion and before cyclic load test. (Aquino and Hawkins, 2007)

In order to calculate the flexural and shear capacity of corroded RC column section at lap splice region, it is required to determine the stress in the lap spliced bars, which is less than yielding stress. Bond stress, τ , can be expressed in terms of stress in longitudinal bar, f_s , bar diameter, d_b , and embedment length, l_e , as:

$$\tau = \frac{f_s d_b}{4l_e} \quad \text{Eq. 62}$$

Several empirical models have been proposed to explain bond strength of corroded reinforcing bars. Cabrera (1996) presented bond strength of corroded RC specimens, τ_{cor} , based on pullout tests as:

$$\tau_{cor} = 23.478 - 1.313 C \quad (MPa) \quad \text{Eq. 63}$$

Where; C is the persantage of corrosion level:

$$C = \frac{\Delta w}{w} \times 100 \quad \text{Eq. 64}$$

Where; Δw is the average mass loss of corroded bars and w is the mass of original bars. Bond strength proposed by Lee et al. (2002) based on pullout tests of corroded RC specimens is as following:

$$\tau_{cor} = 5.21e^{(0.0561C)} \quad (MPa) \quad \text{Eq. 65}$$

Stanish et al. (1999) presented bond strength of corroded RC members based on flexure tests as:

$$\tau_{cor} = (0.77 - 0.027 C)\sqrt{f'_c} \quad (MPa) \quad \text{Eq. 66}$$

R, ratio of bond strength of corroded bar to bond strength of non-corroded bar was first defined by Chung et al. (2004) based on flexural tests:

$$R = 2.09 C^{(-1.06)} \quad \text{for } C > 2.0\% \quad \text{Eq. 67}$$

Bhargava et al. (2007) carried out experimental tests on corroded RC specimens based on both pullout and flexural tests and came about with the following equations:

$$\text{Model M-Pull (Based on pullout test)} \begin{cases} R = 1.0 & \text{for } C \leq 1.5\% \\ R = 1.192e^{-0.117C} & \text{for } C > 1.5\% \end{cases} \quad \text{Eq. 68}$$

$$\text{Model M-Flex (Based on flexural test)} \begin{cases} R = 1.0 & \text{for } C \leq 1.5\% \\ R = 1.346e^{-0.198C} & \text{for } C > 1.5\% \end{cases} \quad \text{Eq. 69}$$

The equations are valid for up to 10% corrosion level for model M-Flex and up to 30% corrosion level for model M-Pull. Using model M-Flex has been considered more conservative by Bhargava et al.

In current research, the M-Flex model proposed by Bhargava et al. has been used to present the stress of longitudinal bars in corroded lap splices.

$$R = \frac{\tau_{cor}}{\tau_{sound}} = \frac{\frac{f_{s(cor)}d_{b(cor)}}{4l_{e(cor)}}}{\frac{f_{s(sound)}d_{b(sound)}}{4l_{e(sound)}}} \quad \text{Eq. 70}$$

Considering embedment length of corroded and non-corroded bar is constant, the ratio can be simplified as:

$$R = \frac{f_{s(cor)}d_{b(cor)}}{f_{s(sound)}d_{b(sound)}} \quad \text{Eq. 71}$$

According to definition of corrosion level, C, ratio of corroded bar diameter to sound bar diameter can be expressed as:

$$\frac{d_{b(cor)}}{d_{b(sound)}} = 1 - \frac{C}{100} \quad \text{Eq. 72}$$

Stress at non-corroded bar depends on ratio of embedment length to developing length.

$$f_{s(sound)} = \frac{l_{e(sound)}}{l_{d(sound)}} f_{y(sound)} \quad \text{Eq. 73}$$

Eventually, stress of corroded bar can be proposed by the following equation:

$$\begin{cases} f_{s(cor)} = \frac{l_{e(sound)}}{l_{d(sound)}} f_{y(sound)} & \text{for } C \leq 1.5\% \\ f_{s(cor)} = \frac{1.346e^{-0.198C}}{1 - \frac{C}{100}} \frac{l_{e(sound)}}{l_{d(sound)}} f_{y(sound)} & \text{for } C > 1.5\% \end{cases} \quad \text{Eq. 74}$$

Fig. 85 show stress ratio of corroded bar to non-corroded bar in terms of corrosion. Stress in corroded bar reduces significantly by increasing corrosion level. When corrosion level is 10%, lap splice fails due to bond failure while the stress at the bar is about just 20% of yielding stress for embedment length equal to development length.

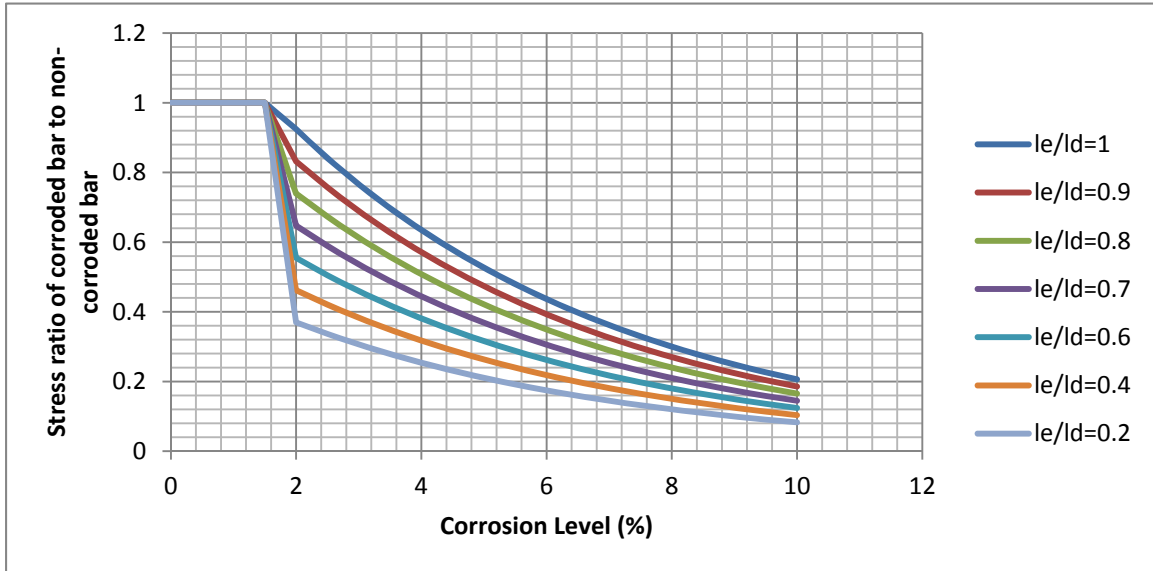


Fig. 85: Stress ratio of corroded bar to non-corroded bar

Table 4: Stress ratio of corroded bar to non-corroded bar

le/ld C	1	0.9	0.8	0.7	0.6	0.5	0.4	0.3	0.2	0.1
1	1.000	1.000	1.000	1.000	1.000	1.000	1.000	1.000	1.000	1.000
1.5	1.000	1.000	1.000	1.000	1.000	1.000	1.000	1.000	1.000	1.000
2	0.924	0.832	0.739	0.647	0.555	0.462	0.370	0.277	0.185	0.092
3	0.766	0.690	0.613	0.536	0.460	0.383	0.306	0.230	0.153	0.077
4	0.635	0.572	0.508	0.445	0.381	0.318	0.254	0.191	0.127	0.064
5	0.526	0.474	0.421	0.369	0.316	0.263	0.211	0.158	0.105	0.053
6	0.436	0.393	0.349	0.306	0.262	0.218	0.175	0.131	0.087	0.044
7	0.362	0.326	0.290	0.253	0.217	0.181	0.145	0.109	0.072	0.036
8	0.300	0.270	0.240	0.210	0.180	0.150	0.120	0.090	0.060	0.030
9	0.249	0.224	0.199	0.174	0.149	0.124	0.100	0.075	0.050	0.025
10	0.206	0.186	0.165	0.145	0.124	0.103	0.083	0.062	0.041	0.021

6 Inadequate Foundation Capacity:

6.1 Introduction:

The behavior of a bridge during seismic events is very dependent on the strength and stiffness of its foundation system. The foundation system refers to abutments/piers, footings, and piles (FHWA).

Deterioration in bridge foundation is usually more difficult to inspect compared to other bridge elements because it needs excavation above and around the footing and piles to visually inspect their integrity. There are many signs to indicate that the foundations are deteriorated or vulnerable to failure during an earthquake such as, but not limited to, tilting of a pier, flexural cracking of the column, sloughing of the fill around a footing, pulling away of the fill from a footing. However, the mode of failure is dependent on the type of soil as well as the detail of foundation (O'Connor 2010).

FHWA classifies footing failures in one of two ways, the first type of foundation failure is caused by instabilities created in the soil during the seismic event resulting in large displacements of the foundation material. This type of failure also includes liquefaction or slope instability.

The second type of foundation failure occurs due to excessive seismic forces transmitted from the structure itself, this type of failure involves the yielding or rupture of foundation elements. This type of failure includes concrete and/or steel failure, bearing failure of the soil, footing failure due to sliding or overturning, and pile failure. These types of failure may result in a ductile behavior or in a sudden brittle failure (FHWA).

However, mode of failure of footing usually depends on the type of footing. But even if the footing failure will not cause a total collapse of the structure, it is still important to be able to determine the capacity of the footing when evaluating a bridge.

The effect of corrosion on the two major types of footing in bridge construction which are: spread and pile footing will be discussed in this chapter.

6.2 Spread footings:

It is extremely important to determine the capacity of the footing to resist the loads transmitted from the column or pier. The following modes of failure usually occur in spread footing, Fig. 86, and govern the interaction between the vertical load and the moment capacity (FHWA):

- Tilting of the footing due to a soil bearing failure.
- Flexural yielding of footing reinforcing.
- Concrete shear failure of the footing.
- Bond failure of the main column steel.

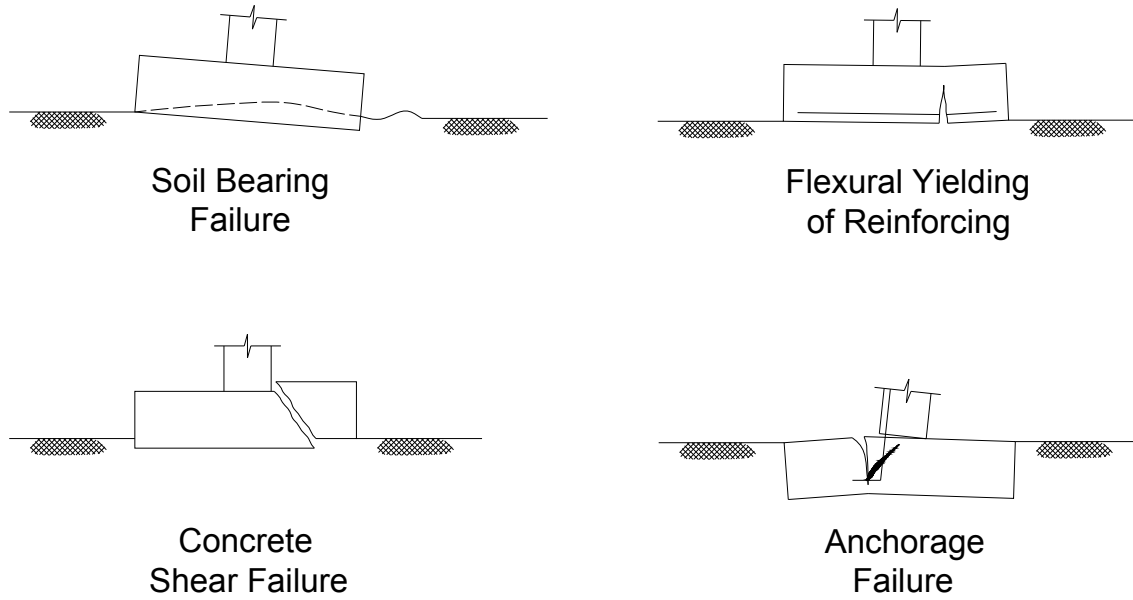


Fig. 86: Modes of failure for spread footings (FHWA)

6.2.1 Tilting of the footing due to a soil bearing failure:

Bearing capacity is the power of foundation soil to hold the forces from the superstructure without undergoing shear failure or excessive settlement.

This mode of failure is unlikely to occur in a deteriorated footing during an earthquake. This is because the deterioration of concrete and steel due to corrosion of steel reinforcement will decrease the strength, stiffness, and cross section of the footing, which will cause the footing to be vulnerable to other modes of failure during earthquake ground motion. However, according to the FHWA, this mode of failure will occur in an un-deteriorated footing if neither shear nor flexural failure occurs. By assuming that various areas of the footing are loaded with a uniform pressure equal to the ultimate soil pressure, one can calculate the interaction between axial force and moments at the yield capacity of the footing. This will produce an interaction surface that will indicate the possibility of bearing failure only at the locations where this surface falls within the column interaction surface factored for overstrength. Ultimate soil bearing pressure can usually be taken as three times the design allowable value (FHWA).

As mentioned above, this mode of failure is not critical. In fact, Caltrans considers this mode of failure to be acceptable because it does not cause a total collapse of the structure. FHWA states that if the bridge is not required to perform to a higher level, retrofitting would not be considered. In other words, retrofitting is required if the structure is expected to meet certain functionality criteria immediately following an earthquake.

However, according to AASHTO, the overturning demand due to forces associated with the plastic overstrength moment of a column or wall shall be less than the overturning resistance of

the footing, and the location of the resultant shall be limited as described below. Overturning shall be examined in each principal direction and satisfy the following requirement:

$$M_{po} + V_{po}H_f \leq \Phi P_u \left(\frac{L-a}{2} \right) \quad \text{Eq. 75}$$

in which:

$$a = \frac{P_u}{q_n B}$$

Where:

M_{po} = overstrength plastic moment capacity of the column calculated in accordance with AASHTO Guide Specifications for LRFD Seismic Bridge Design Article 8.5 (kip-ft)

V_{po} = overstrength plastic shear demand (kip)

H_f = depth of footing (ft)

P_u = axial force in column including the axial force associated with overstrength plastic hinging calculated in accordance to AASHTO Guide Specifications for LRFD Seismic Bridge Design Article 4.11 (kip)

L = length of footing measured in the direction of loading (ft)

B = width of footing measured normal to the direction of loading (ft)

q_n = nominal bearing capacity of supporting soil or rock (ksf)

Φ = resistance factor for overturning of footing taken as 1.0

In addition, AASHTO states that the location of the resultant of the reaction forces shall be located within the middle two-thirds of the base, if no live loads present. Otherwise, AASHTO Guide Specifications for LRFD Seismic Bridge Design Article 6.39 is applicable. If full live load is present, then the resultant shall be within the middle eight-tenth of the base. If live load acts to reduce eccentricity, then it shall not be included in the check of overturning. However, deterioration of footing due to corrosion of reinforcing steel bars will cause the length and the width, of the footing to decrease. This might increase the risk of risk of overturning of footing during an earthquake as shown in Fig. 87.

$$M_{po} + V_{po}H_f \leq \Phi P_u \left(\frac{L-a}{2} \right) \quad \text{Eq. 75}$$

Equation 76 must be satisfied at all times to insure that the footing is not subjected to overturning during seismic events.

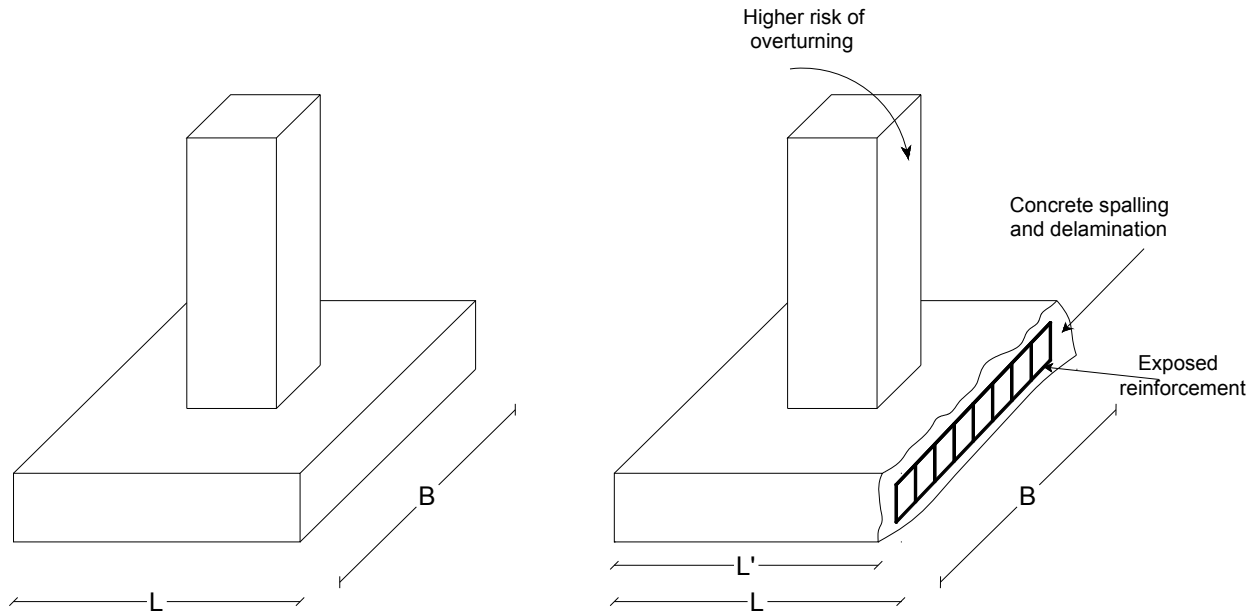


Fig. 87: Delamination of concrete leading to decrease the length of footing

6.2.2 Flexural yielding of footing reinforcement:

This mode of failure is caused by yielding of the main longitudinal bars in the footing. It is usually associated with localized concrete crushing of the top surface of the footing, near the pier column (O'Connor 2010). Unlike concrete shear failure, this mode of failure will not result in a sudden loss of overturning resistance. However, when designing a bridge, ductile yielding in the footing is avoided. This is because of the difficulties associated with inspecting and repairing the foundations. Unless it is particularly extensive, yielding of the main longitudinal bars in the footing will not cause a total collapse of the structure but will result in structural damage. Thus, the prospects of yielding in the footing do not justify seismic retrofitting existing structures. As a matter of fact, yielding of footing can have beneficial effect, because it can reduce shear and flexural in columns and therefore eliminate the chances of a sudden and brittle column failure (FHWA).

As mentioned above, extensive yielding of the main longitudinal bars in the footing might cause a total collapse of the structure. Taking into account the yield strength and the decreased cross-sectional area of the corroded bars, corrosion of longitudinal bars can result in a total collapse of the structure. This because corrosion results in less bar diameter as well as less yield strength, this means that the corroded reinforcing bars will yield and then rupture under smaller tensile force compared to the non-corroded bars. Assuming that there is a perfect bond between concrete and steel, corrosion will lead to loss in nominal moment capacity, the moment capacity must be checked in both the in the longitudinal and the transversal directions as follows (Fig. 88)

AASHTO LRFD Bridge Design Specifications Articles (5.7.3.2.1-1, 5.7.3.2.1-1):

$$M_r = \phi M_n$$

Eq. 76

$$M_n = A_{sp}f_{sp} \left(d_p - \frac{a}{2} \right) + A_s f_s \left(d_s - \frac{a}{2} \right) - A'_s f'_s \left(d'_s - \frac{a}{2} \right) + 0.85 f'_c (b - b_w) h_f \left(\frac{a}{2} - \frac{h_f}{2} \right) \quad \text{Eq. 77}$$

where:

A_{ps} = area of prestressing steel (in. ²)

f_{ps} = average stress in prestressing steel at nominal bending resistance specified in Eq. 5.7.3.1.1-1 (ksi)

d_p = distance from extreme compression fiber to the centroid of prestressing tendons (in.)

A_s = area of nonprestressed tension reinforcement (in. ²)

f_s = stress in the mild steel tension reinforcement at nominal flexural resistance (ksi) as specified in Article 5.7.2.1

d_s = distance from extreme compression fiber to the centroid of nonprestressed tensile reinforcement (in.)

A'_s = area of compression reinforcement (in. ²)

f'_s = stress in the mild steel compression reinforcement at nominal flexural resistance (ksi), as specified in Article 5.7.2.1

d'_s = distance from extreme compression fiber to the centroid of compression reinforcement (in.)

f'_c = specified compressive strength of concrete at 28 days, unless another age is specified (ksi)

b = width of the compression face of the member; for a flange section in compression, the effective width of the flange as specified in Article 4.6.2.6 (in.)

b_w = web width or diameter of a circular section (in.)

β_1 = stress block factor specified in Article 5.7.2.2

h_f = compression flange depth of an I or T member (in.)

$\alpha = c\beta_1$; depth of the equivalent stress block (in.)

The assumption of perfect bond between concrete and steel was drawn because with the loss of bond, there will be no yielding in the rebars and this mode of failure will not occur. The decrease of A_s, f_y , will lead to decrease in the footing capacity leading to yielding of the tensile reinforcement under a smaller loading. The above equation should be checked using the corroded steel cross-section area and yield strength. However, this should be checked at the moment critical section which is taken at the face of the column in accordance with AASHTO Article (5.13.3.4), (Fig. 88).

According to the AASHTO Specifications, the capacity should be sufficient to resist uniform footing pressures of 1.3 times the ultimate soil bearing capacity. Flexural yielding of the footing will cause the column shear force to be limited in order to satisfy static equilibrium.”

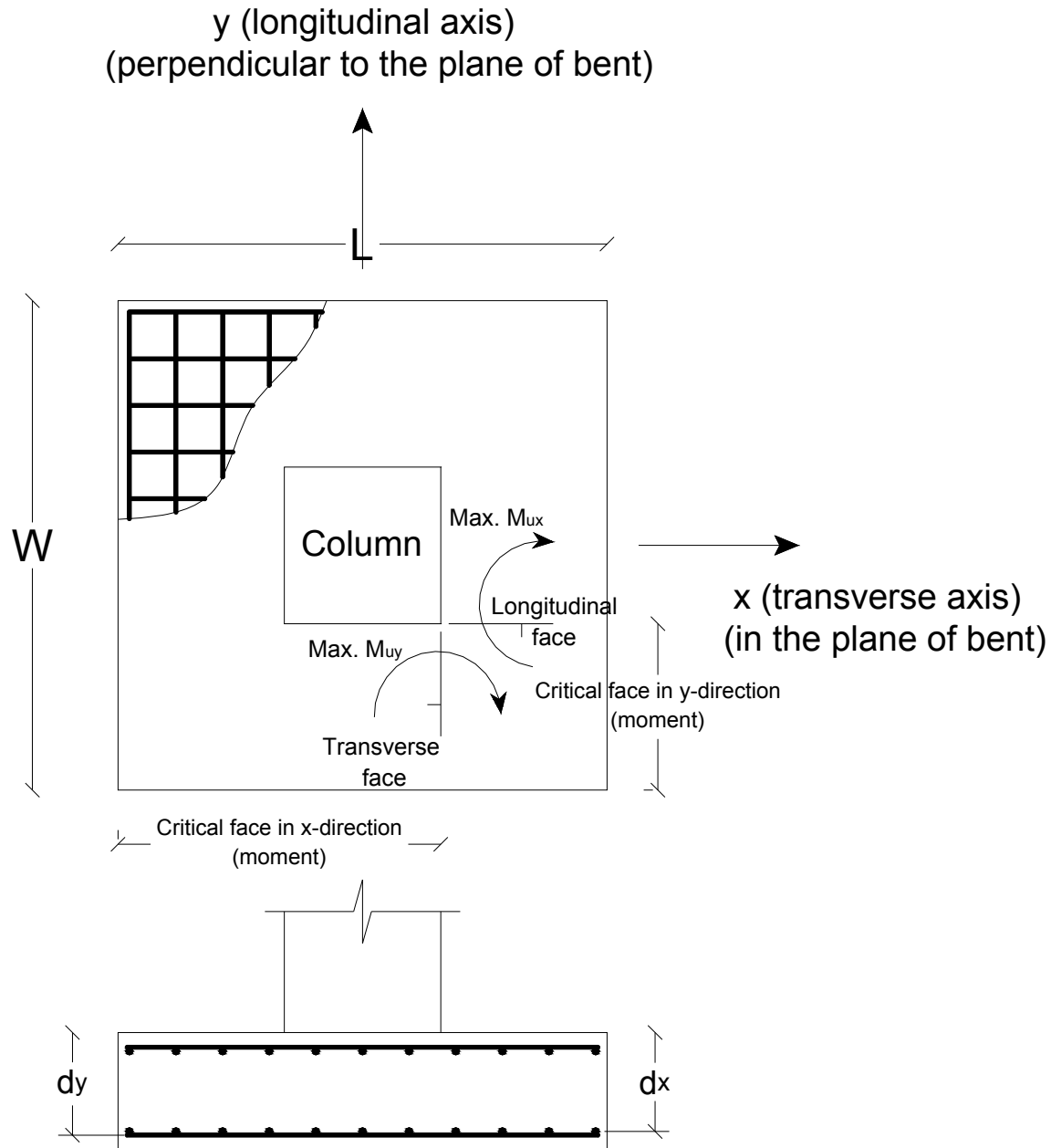


Fig. 88: Reinforcement of footing in longitudinal and transversal directions

6.2.3 Shear failure of Concrete footing:

This mode of failure could be very serious because it can cause a sudden loss of overturning resistance. In order to prevent shear failure, the shear capacity at the critical section determined according to the AASHTO specifications must be sufficient to resist a uniform pressure equal to 1.3 times the ultimate soil bearing capacity (FHWA).

Check design shear strength AASHTO Article (5.8.3.3)

According to AASHTO Article (5.13.3.6.1), the most critical of the following conditions shall govern the design for shear:

- One-way action, with a critical section extending in a plane across the entire width and located at a distance taken as specified in Article (5.8.3.2). This distance d_v is from the internal face of the support.
- Two-way action, with a critical section perpendicular to the plane of the slab and located so that its perimeter, b_o , is a minimum but not closer than $0.5d_v$ to the perimeter of the concentrated load or reaction area.

in which:

$$d_v = \frac{M_n}{A_{ps}f_{ps} + A_s f_y} \quad \text{Eq. 78}$$

When determining the one-way shear resistance, it must be calculated for longitudinal and transversal faces and it must be satisfy the requirements specified in AASHTO Article 5.8.3.

Where the factored shear resistance V_r shall be taken as AASHTO Article (5.8.2.1-2):

$$V_r = \phi V_n \quad \text{Eq. 79}$$

The nominal shear resistance for longitudinal face, V_{nx} , is taken as the lesser of AASHTO Article (S5.8.3.3):

$$V_n = V_c + V_s + V_p \quad \text{Eq. 80}$$

Or

$$V_n = 0.25f'_c b_v d_v + V_p \quad \text{Eq. 81}$$

in which:

$$V_c = 0.0316\beta \sqrt{f'_c} b_v d_v \quad \text{Eq. 82}$$

if the procedures of Articles 5.8.3.4.1 or 5.8.3.4.2 are used

and $V_c =$ the lesser of V_{ci} and V_{cw} if the procedures of Article 5.8.3.4.3 are used

$$V_s = \frac{A_v f_y d_v (\cot \theta + \cot \alpha)}{s} \quad \text{Eq. 83}$$

Where transverse reinforcement consists of a single longitudinal bar or a single group of parallel longitudinal bars bent up at the same distance from the support, the shear resistance V_s provided by these bars shall be determined as:

$$V_s = A_v f_y \sin \alpha \leq 0.095 \sqrt{f'_c} b_v d_v \quad \text{Eq. 84}$$

where:

$b_v =$ effective web width taken as the minimum web width within the depth d_v as determined in Article 5.8.2.9 (in.)

$d_v =$ effective shear depth as determined in Article 5.8.2.9 (in.)

s = spacing of transverse reinforcement measured in a direction parallel to the longitudinal reinforcement (in.)

β = factor indicating ability of diagonally cracked concrete to transmit tension and shear as specified in Article 5.8.3.4

θ = angle of inclination of diagonal compressive stresses as determined in Article 5.8.3.4 (degrees); if the procedures of Article 5.8.3.4.3 are used, $\cot \theta$ is defined therein

α = angle of inclination of transverse reinforcement to longitudinal axis (degrees)

A_v = area of shear reinforcement within a distance s (in.²)

V_p = component in the direction of the applied shear of the effective prestressing force; positive if resisting the applied shear; $V_p = 0$ when Article 5.8.3.4.3 is applied (kip)

In the same article 5.8.2.9, AASHTO Specifications also state that where bent longitudinal reinforcement is used, only the center three-fourths of the inclined portion of the bent bar shall be considered effective for transverse reinforcement. Where more than one type of transverse reinforcement is used to provide shear resistance in the same portion of a member, the shear resistance V_s shall be determined as the sum of V_s values computed from each type. Where shear resistance is provided by bent longitudinal reinforcement or a combination of bent longitudinal reinforcement and stirrups, the nominal shear resistance shall be determined using the simplified procedure in accordance with Article 5.8.3.4.1.

AASHTO Article 5.13.3.6.3 states that for two-way action for sections without transverse reinforcement, the nominal shear resistance, V_n in Kips, of the concrete shall be taken as:

$$V_n = \left(0.063 + \frac{0.126}{\beta_c}\right) \sqrt{f'_c} b_o d_v \leq 0.126 \sqrt{f'_c} b_o d_v \quad \text{Eq. 85}$$

where:

β_c = ratio of long side to short side of the rectangle through which the concentrated load or reaction force is transmitted

b_o = perimeter of the critical section (in.)

d_v = effective shear depth (in.)

For two-way action for sections with transverse reinforcement, the nominal shear resistance, V_n in Kips, of the concrete shall be taken as:

$$V_n = V_c + V_s \leq 0.192 \sqrt{f'_c} b_o d_v \quad \text{Eq. 86}$$

in which:

$$V_c = 0.0632 \beta \sqrt{f'_c} b_o d_v \quad \text{Eq. 87}$$

$$V_s = \frac{A_v f_y d_v}{s} \quad \text{Eq. 88}$$

where:

A_v = area of shear reinforcement within a distance s (in.²)

f_y = yield strength

d_v = effective shear depth as determined in Article 5.8.2.9 (in.)

s = spacing of transverse reinforcement measured in a direction parallel to the longitudinal reinforcement (in.)

Higgins et al., (2003), suggested two methods for calculating the residual shear capacity of a deteriorated section, average area and local minimum area within a shear length of d . The first method depends on determining the average area within a shear length of d by calculating the number of stirrups, n , crossing a potential diagonal crack oriented at an angle of 45° as:

$$n = \frac{d}{s} \quad \text{Eq. 89}$$

where:

n = number of stirrups crossing a potential diagonal crack oriented at an angle of 45°

s = stirrup spacing

d = depth of the section

Then the average area (\tilde{A}_{vi}) for each stirrup was determined by summing the average area measurements of each leg:

$$\tilde{A}_{vi} = \tilde{A}_{leg1} + \tilde{A}_{leg2} \quad \text{Eq. 90}$$

The average stirrup area within the region is determined by computing an equivalent stirrup area to be applied at the same spacing as that of the undamaged stirrups:

$$\tilde{A}_v = \frac{\sum_{i=1}^n \tilde{A}_{vi}}{n} \quad \text{Eq. 91}$$

According to Higgins et al., 2003, this method can provide a decent estimation of the residual capacity. However, for beams with wider spacing of stirrups and more than one sequential stirrup completely corroded, the smallest area for each stirrup (\hat{A}_{vi}) is determined by summing the local minimum area measurements for each leg:

$$\hat{A}_{vi} = \hat{A}_{leg1} + \hat{A}_{leg2} \quad \text{Eq. 92}$$

And the minimum stirrup area within the region is determined by computing an equivalent stirrup area to be applied at the same spacing as that of the undamaged stirrups:

$$\hat{A}_v = \frac{\sum_{i=1}^n \hat{A}_{vi}}{n} \quad \text{Eq. 93}$$

Both of the above method can be used in the case of stirrups or bent up bars by taking the average area of the corroded bent up bars within a width of 12 in. which can be considered the width of the cross-section and within a shear length of d .

In addition, Higgins et al., 2003, in their experimental study estimated the concrete damage due to corrosion as shown in Fig. 79. They found that when the spacing between stirrups is large enough, there is non-overlapping spall damage, on the other hand, when the space between stirrups is small, spall wedges will begin to interact and the entire cover area may spall. They also found that the angle of discrete spalls is approximately 20° .

Therefore they estimated the effective concrete width of the beam available to resist shear as:

$$b_{eff} = b - 2(c_v + \phi_v) + \frac{s}{5.5} \quad \text{if } s \leq 5.5 \cdot c \quad \text{Eq. 94}$$

$$b_{eff} = b - \frac{s}{5.5} (c_v + \phi_v)^2 \quad \text{if } s > 5.5 \cdot c \quad \text{Eq. 95}$$

where:

b = original undamaged beam width (in.)

c_v = concrete cover (in.)

ϕ_v = stirrup diameter (in.)

s = stirrup spacing (in.)

This effective width can be used in computing the residual nominal shear resistance of the concrete.

6.2.4 Bond failure of the main column steel:

Bond or anchorage failure is caused by pullout of the column main longitudinal bars from the pile cap, as well as concrete conical failure at individual bars (O'Connor 2010).

This mode of failure could result in serious consequences such as a structural collapse.

Moreover, this mode of failure is considered to be the most critical of all foundations' collapse modes and the strength of anchorage of the column main reinforcement in the footing must be evaluated in order to prevent this mode of failure. Bond failure usually occurs when the anchorage is not sufficient, this means the yield capacity of the reinforcement cannot be reached and the failure will occur before the column reaches its ultimate capacity. However, because the concrete tensile strength is usually sufficient to prevent cracking, a reduction in the effectiveness for the unanchored spread footing is usually not a problem (FHWA).

This mode of failure causes a sudden loss of flexural strength due to the loss of anchorage.

AASHTO states that column longitudinal reinforcement shall be extended into footing and cap beams as close as practically possible to the opposite face of the footing or the cap beam. In addition, the anchorage length for longitudinal column bars developed into the cap beam or footing for seismic loads shall satisfy:

$$l_{ac} = \frac{0.79d_{bl}f_{ye}}{\sqrt{f'_c}} \quad \text{Eq. 96}$$

Where:

l_{ac} = anchored length of longitudinal reinforcing bars into the cap beam or footing (in.)

d_{bl} = diameter of the longitudinal column bar (in.)

f_{ye} = expected yield strength of the longitudinal reinforcement (ksi)

f'_c = nominal compressive strength of concrete (ksi)

For SDC D, the anchorage length should not be reduced by means of adding hooks or mechanical anchorage devices. If hooks are provided, the tails should be pointed inward toward the joint core.

However, FHWA states that the effective anchorage length for straight anchorage, in mm or in. is given by:

$$L_a(d) = \frac{2.626K_s d_b}{\left(1 + \frac{2.5c}{d_b} + K_{tr}\right) \sqrt{f'_c}} \geq 30d_b \quad (mm, kPa) \quad \text{Eq. 97}$$

$$L_a(d) = \frac{K_s d_b}{\left(1 + \frac{2.5c}{d_b} + K_{tr}\right) \sqrt{f'_c}} \geq 30d_b \quad (\text{in, psi}) \quad \text{Eq. 98}$$

where:

k_s = constant for reinforcing steel with a yield stress of f_y (kPa or psi), i.e.,

$$\frac{f_y - 75,845}{33.1} \text{ kPa} \quad \text{or} \quad \frac{f_y - 11,000}{4.8} \text{ psi}$$

d_b = nominal bar diameter (mm or in.)

f'_c = concrete compression strength (kPa or psi)

c = lesser of the clear cover over the bar, or half the clear spacing between adjacent bars

$$k_{tr} = \frac{A_{tr}(c) f_{yt}}{4137s d_b} \leq 2.5 \quad (\text{mm, kPa}) \quad \text{Eq. 99}$$

$$k_{tr} = \frac{A_{tr}(c) f_{yt}}{600s d_b} \leq 2.5 \quad (\text{in, psi}) \quad \text{Eq. 100}$$

$A_{tr}(c)$ = area of transverse reinforcing normal to potential splitting cracks (when splitting will occur between several bars in a row, $A_{tr}(c)$ is the total of the transverse steel crossing the potential crack divided by the number of longitudinal bars in the row)

f_{yt} = yield stress of transverse reinforcement (kPa or psi)

s = spacing of transverse reinforcement (mm or in)

Note that the value for c/d_b should not be taken more than 2.5.

For anchorage with 90° standard hooks, the effective anchorage length, in mm or in, is:

$$L_a(d) = 1200k_m d_b \left(\frac{(2.626)f_y}{6000\sqrt{f'_c}} \right) \geq 15d_b \quad (\text{mm, kPa}) \quad \text{Eq. 101}$$

$$L_a(d) = 1200k_m d_b \left(\frac{f_y}{6000\sqrt{f'_c}} \right) \geq 15d_b \quad (\text{in, psi}) \quad \text{Eq. 102}$$

where k_m is 0.7 for #11 bars or smaller, when the side cover (normal to plane of the hook) is not less than 63 mm (2.5 in), and the cover on the bar extension beyond the hook is not less than 50 mm (2 in), and 1.0 for all other cases (FHWA 2006).

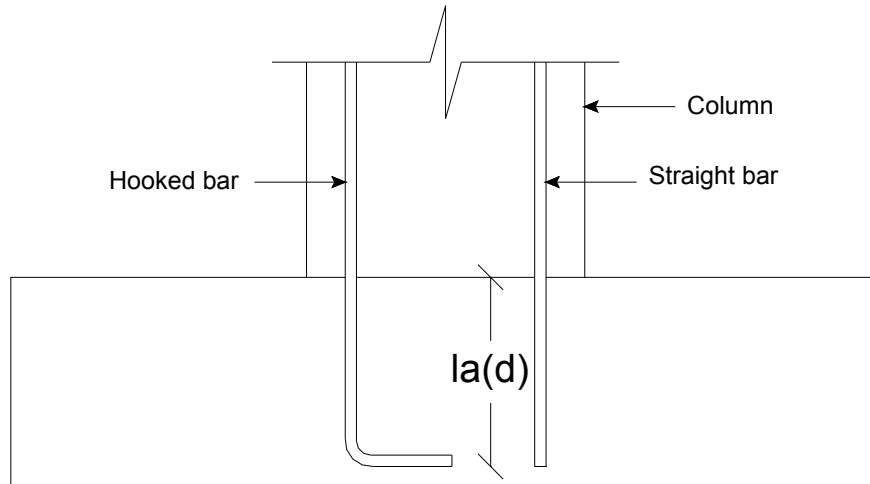


Fig. 89: Effective anchorage length of longitudinal reinforcement (EHWA 2006)

Note that in equations by AASHTO and FHWA, the effective anchorage length is a function of bar diameter, concrete compressive strength, and yield strength for steel. However, FHWA equations take into account area, bar spacing, and yield strength of transverse reinforcement. The above equations are based on the assumption that the bond between steel and concrete is perfect. Corrosion decreases this bond because it causes degradation of the rib height of the deformed bars, which in turn decreases the interlocking forces between the ribs of the deformed bars and the surrounding concrete. This reduces the bond between concrete and steel causing a bond failure under smaller loads. Many researchers investigated the relationship between the reinforcement corrosion and the bond strength in reinforced concrete, some of them presented empirical equations to calculate the bond strength based on pullout tests or based on flexural tests on concrete reinforced specimens.

Cabrera (1996) suggested an equation for the bond strength for normal Portland cement concrete based on corrosion level as follows:

$$\tau_{bu} = 23.478 - 1.313X_p \text{ (MPa)} \quad \text{Eq. 103}$$

Lee et al. (2002) presented the following equation:

$$\tau_{bu} = 5.21e^{0.0561X_p} \text{ (MPa)} \quad \text{Eq. 104}$$

Stanish et al. (1999) suggested the following equation that takes into account the concrete compressive strength:

$$\tau_{bu} = \sqrt{f'_c}(0.77 - 0.027X_p) \quad \text{Eq. 105}$$

where:

τ_{bu} = bond strength

X_p = corrosion level

f'_c = concrete compressive strength

Chung et al. (2004), proposed the normalized bond strength which is the ratio of bond strength at any corrosion level to the original bond strength for an un-corroded specimen in the following equation:

$$R = 2.09X_p^{(-1.06)} \quad \text{for } X_p \geq 2.0\% \quad \text{Eq. 106}$$

where:

R = normalized bond strength

X_p = corrosion level

Bhargava et al. (2007) presented the following equations based on pullout tests:

$$R = 1.0 \quad \text{for } X_p \leq 1.5\% \quad \text{Eq. 107}$$

$$R = 1.192e^{-0.117X_p} \quad \text{for } X_p \geq 1.5\% \quad \text{Eq. 108}$$

Bhargava et al. (2007) also suggested the following equations based on flexural tests:

$$R = 1.0 \quad \text{for } X_p \leq 1.5\% \quad \text{Eq. 109}$$

$$R = 1.346e^{-0.198X_p} \quad \text{for } X_p \geq 1.5\% \quad \text{Eq. 110}$$

Chung et al. (2004), also presented an analytical model to calculate the residual flexural strength of beams. AASHTO equations, discussed above, for the effective anchorage length of the column reinforcing bars that should be imbedded in the footing are based on a perfect bonding between concrete and steel. This will allow steel to reach its yielding strength prior to failure. With the decrease of yield strength of steel, and bond between steel and concrete due to corrosion, the collapse will occur under lower loads, and the steel will not be able to reach its yield strength before collapse. The decrease in bond strength can be estimated from the above equations.

6.3 Pile footing:

Fig. 90 shows the different potential modes of failure of bridge foundations during ground motion. These modes can be listed as follows:

- Pile Overload
- Concrete shear failure
- Flexural yielding of reinforcement
- Pile pullout
- Anchorage failure
- Pile flexural and/or shear failure

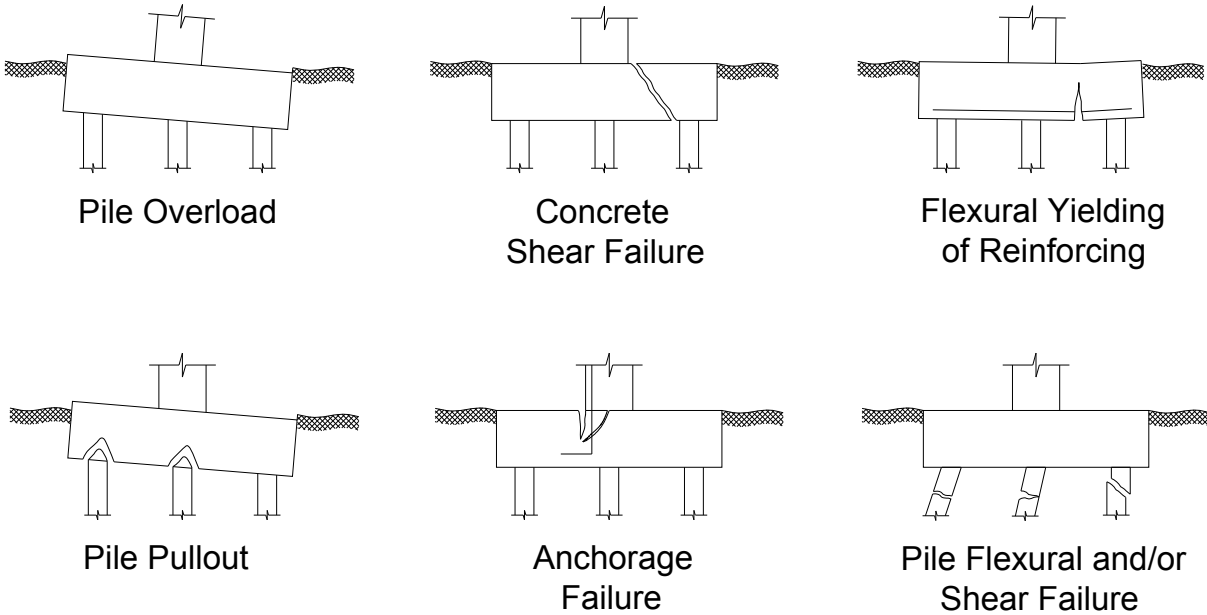


Fig. 90: Different types of foundation failure (Saad et al. 2010)

6.3.1 Pile pullout:

Pile Pullout is caused by anchorage failure of the pile main longitudinal bar due to inadequate embedment into the pile cap. Such mode of failure is associated with tilting of the pile cap (O'Connor 2010). The footing capacity will be controlled by pile failure if neither shear nor flexural failure occurs in the footing. A lower ductility indicator is suggested when there is a risk of pullout failure. This is because of the brittle nature of this type of failure. However, this mode of failure does not cause a total collapse of the structure, and thus considered acceptable by Caltrans. Retrofitting is required only if the bridge is expected to perform at a higher level. In other words, retrofitting is considered if the structure is required to meet certain functionality criteria immediately after the earthquake (FHWA 2006). The damage at the pile to cap connection usually occurs due to excessive displacements and bending strains concentrated near pile head, especially when combined with large structural inertial loads.

AASHTO Specifications indicate that the tops of piles shall project at least 12 in. into the pile cap after all damaged material has been removed. If the pile is attached to the cap by embedded bars or strands, the pile shall extend no less than 6 in. into the cap. Where a reinforced concrete beam is cast-in-place and used as a bent cap supported by piles, the concrete cover on the sides of the piles shall not be less than 6 in., plus an allowable for permissible pile misalignment. Where pile reinforcement is anchored in the cap satisfying the requirements of Article 5.13.4.1 which states that the reinforcement shall be developed sufficiently to resist $1.25f_yA_s$, the projection may be less than 6 in. However, AASHTO Guide Specifications for LRFD Seismic Bridge Design, Article 6.6.4 states that embedment of pile reinforcement in the footing cap shall be in accordance with Article 8.8.4 which requires the anchorage length for longitudinal column bars developed into the cap beam or footing for seismic loads for SDCs C and D shall satisfy:

$$l_{ac} \geq \frac{0.79d_{bl}f_{ye}}{\sqrt{f'_c}} \quad \text{Eq. 111}$$

where:

l_{ac} = anchored length of longitudinal reinforcing bars into the cap beam or footing (in.)

d_{bl} = diameter of the longitudinal column bar (in.)

f_{ye} = expected yield stress of the longitudinal reinforcement

f'_c = nominal compressive strength of concrete (ksi)

For SDC D, the anchorage length shall not be reduced by means of adding hooks or mechanical anchorage devices. If hooks are provided, the tails should be pointed inward toward the joint core. With corrosion of longitudinal reinforcement of the pile, the bar diameter and yield stress of the bars will decrease as discussed in Eqs. 2, 3. Corrosion will also decrease the bond between steel and concrete which will cause the pile pull out from the footing causing a local collapse. However, as mentioned above, this mode of failure does not cause a total collapse of the structure, and thus considered acceptable by Caltrans. Retrofitting is required only if the bridge is expected to perform at a higher level. In other words, retrofitting is considered if the structure is required to meet certain functionality criteria immediately after the earthquake (FHWA 2006).

6.3.2 Pile flexural and/or shear failure:

This mode of failure is stated by FHWA as a pile flexural and/or shear failure. However, O'Conner didn't consider pile flexural failure as a seismic collapse mechanism. This is because pile shear failure is more common and critical than flexural failure. "Pile Shear Failure is caused by lateral movement of the pile cap and inadequate pile shear strength due to lack of adequate shear reinforcement. This mode of failure is associated with lateral movement of the pile cap" (O'Conner 2010).

AASHTO Guide Specifications for LRFD Seismic Bridge Design, Article 8.16.1 states that for SDC C or D where piles are not designed as capacity-protected members (i.e., piles, pile shafts, pile extensions where plastic hinging is allowed in soft soil E or F, liquefaction case), the upper portion of every pile shall be reinforced and confined as a potential plastic region as specified in Article 4.11.

The above Article also requires spiral reinforcement or equivalent ties of not less than NO. 3 bars shall be provided at a pitch not exceeding 9.0 in., except that a 3.0-in. pitch shall be used within a confinement length of not less than 4.0 ft below the pile cap reinforcement. For cast-in-place piles, the 3.0-in. pitch may be extended to 4.0 in. For cast-in-place and precast concrete piles, longitudinal steel shall be provided for the full length of the pile. In the upper two-thirds of the pile, the longitudinal steel ratio shall not be less than 0.007. Longitudinal reinforcement shall be provided by no fewer than four bars. However, AASHTO states that the shear reinforcement requirements specified in Article 8.6 shall apply.

Article 8.6 states that the column shear capacity within the plastic hinge region as specified in Article 4.11.7 shall be calculated on the basis of the nominal material strength properties and shall satisfy:

$$\Phi_s V_n \geq V_u \quad \text{Eq. 112}$$

in which:

$$V_n = V_c + V_s \quad \text{Eq. 113}$$

where:

$\phi_s = 0.90$ for shear capacity of member

V_n = nominal shear capacity of member (kips)

V_c = concrete contribution to shear capacity (kips)

V_s = reinforcing steel contribution to shear capacity (kips)

The concrete shear capacity, V_c , of members designed for SDCs B, C, and D shall be taken as:

$$V_c = v_c A_e \quad \text{Eq. 114}$$

in which:

$$A_e = 0.8A_g \quad \text{Eq. 115}$$

If P_u is compressive:

$$v_c = 0.032\alpha' \left(1 + \frac{P_u}{2A_g} \right) \sqrt{f'_c} \leq \min \begin{cases} 0.11\sqrt{f'_c} \\ 0.047\alpha'\sqrt{f'_c} \end{cases} \quad \text{Eq. 116}$$

otherwise:

$$v_c = 0$$

For circular columns with spiral or hoop reinforcing:

$$0.3 \leq \alpha' = \frac{f_s}{0.15} + 3.67 - \mu_D \leq 3 \quad \text{Eq. 117}$$

$$f_s = \rho_s f_{yh} \leq 0.35 \quad \text{Eq. 118}$$

$$\rho_s = \frac{4A_{sp}}{sD'} \quad \text{Eq. 119}$$

For rectangular columns with ties:

$$0.3 \leq \alpha' = \frac{f_w}{0.15} + 3.67 - \mu_D \leq 3 \quad \text{Eq. 120}$$

$$f_s = 2\rho_w f_{yh} \leq 0.35 \quad \text{Eq. 121}$$

$$\rho_w = \frac{A_v}{bs} \quad \text{Eq. 122}$$

where:

A_g = gross area of member cross-section (in.²)

P_u = ultimate compressive force acting on section (kips)

A_{sp} = area of spiral or hoop reinforcing bar (in.²)

s = pitch of spiral or spacing of hoops or ties (in)

For members that are reinforced with circular hoops, spirals, or interlocking hoops or spirals, the nominal shear reinforcement strength, V_s , shall be taken as:

$$V_s = \frac{\pi}{2} \left(\frac{nA_{sp}f_{yh}D'}{s} \right) \quad \text{Eq. 123}$$

where:

n = number of individual interlocking spiral or hoop core sections

A_{sp} = area of spiral or hoop reinforcing bar (in.)

f_{yh} = yield stress of spiral or hoop reinforcement (ksi)

D' = core diameter of column measured from center of spiral or hoop (in)

s = pitch of spiral or spacing of hoop reinforcement (in.)

The same method suggested by Higgins et al., 2003, and discussed above in “Concrete shear failure of footing” can be applied to members that are reinforced circular hoops, spirals, or interlocking hoops or spirals.

In this case the average area of each hoop or 360° circle spiral can be taken using few measurements, and then the average stirrup area within the region of D (pile diameter) is determined by computing an equivalent stirrup area to be applied at the same spacing as that of the undamaged stirrups:

$$\tilde{A}_v = \frac{\sum_{i=1}^n \tilde{A}_{vi}}{n} \quad \text{Eq. 124}$$

where:

\tilde{A}_{vi} = average area of corroded spiral or hoop reinforcing bar by taking measurements at different locations

n = number of stirrups crossing a potential diagonal crack oriented at an angle of 45°

$$n = \frac{d}{s}$$

where:

s = stirrup spacing

d = depth of the section

The same procedure as above can be used when minimum areas are to be computed when more than one sequential stirrup is completely corroded. In this case the minimum area of each hoop or 360° circle spiral is measured and then average stirrup area within the region of D (pile diameter) is determined by computing an equivalent stirrup area to be applied at the same spacing as that of the undamaged stirrups.

The effective concrete width of the beam available to resist shear can be calculated using

$$b_{eff} = b - 2(c_v + \phi_v) + \frac{s}{5.5} \quad \text{if } s \leq 5.5 \cdot c \quad \text{Eq. 94}$$

$$b_{eff} = b - \frac{s}{5.5} (c_v + \phi_v)^2 \quad \text{if } s > 5.5 \cdot c \quad \text{Eq. 95.}$$

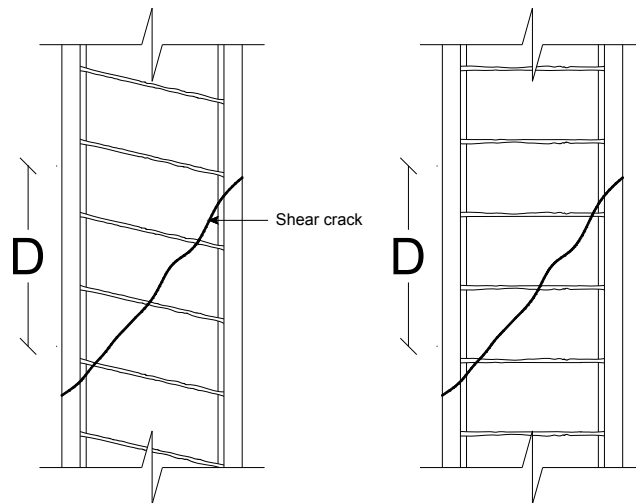


Fig. 91: stirrup area within the region of D (pile diameter)

7 SEISMIC RETROFIT OF CONCRETE BRIDGES WITH CFRP COMPOSITES

Reinforced concrete bridges constructed prior to 1970 are very vulnerable to earthquakes. Corrosion of steel bars compounds the deficiencies of concrete bridge columns. The first main step for seismic retrofit of deteriorated concrete bridge components is the restoration of the original condition of the bridge. Lost steel sections and spalled concrete should be replaced, and the bond between the steel rebars and the surrounding concrete should be restored. This is very critical for superstructure joints, and columns with corroded lap splice in the longitudinal reinforcement. Restoration to the original condition should be associated with adoption of corrosion protection system. Depending on the details of the pedestals, restrainers and or support extension near the bearings (under the girders) might be needed.

In corrosive environments, deterioration of bridge columns starts with the corrosion of the transverse reinforcement, as they are the closest to the exterior surface of the column. Corrosion and lack of adequate amount of transverse reinforcement are major deficiencies that lead to one or combination of the followings during a seismic event:

1. **Crushing of flexural plastic hinge region(s).** This mode of failure is typically associated with flexural cracking, crushing and spalling of concrete cover, buckling of longitudinal steel rebars, and possibly crushing of the concrete core.
2. **Shear failure.** Lack of adequate amount of transverse shear reinforcement results in shear strength much smaller than the shear demand associated with the development of the flexural strength, and consequently resulting in shear failure. This brittle mode of failure is typically associated with diagonal cracks, spalling of concrete cover, and rupture or opening of the transverse reinforcement.

3. **Premature flexural failure due to inadequate lap splice in the longitudinal rebars.** For ease of construction, the longitudinal rebars of bridge columns are lap spliced at the bottom of the column (in a potential plastic hinge region). The fact that the flexural demand in the plastic hinge regions is fairly high, premature failure of the lap splice results in limited ductility and strength. This mode of failure is typically associated with formation of vertical cracks in the vicinity of the lap-splice, which ultimately leads to debonding between the concrete cover and the spliced rebars along the lap splice.

As presented above, lack of adequate amount of transverse reinforcement contributes to all modes of column failures during a seismic event. Therefore, wrapping columns with CFRP composite jackets would prevent such failures. However, it is important to note here that all modes of failure must be investigated and considered when designing a CFRP retrofit system since retrofitting for one deficiency may only change the mode of failure without improving the overall performance of the column. Therefore, the thickness of the CFRP jacket along the height of the column may vary. Fig. 92 and Fig. 93 show the forces and CFRP jacket regions for bridge column retrofit for single bending and double bending, respectively. The CFRP jacket may have to be extended along the full height of the column to prevent shear failure, particularly, for short columns.

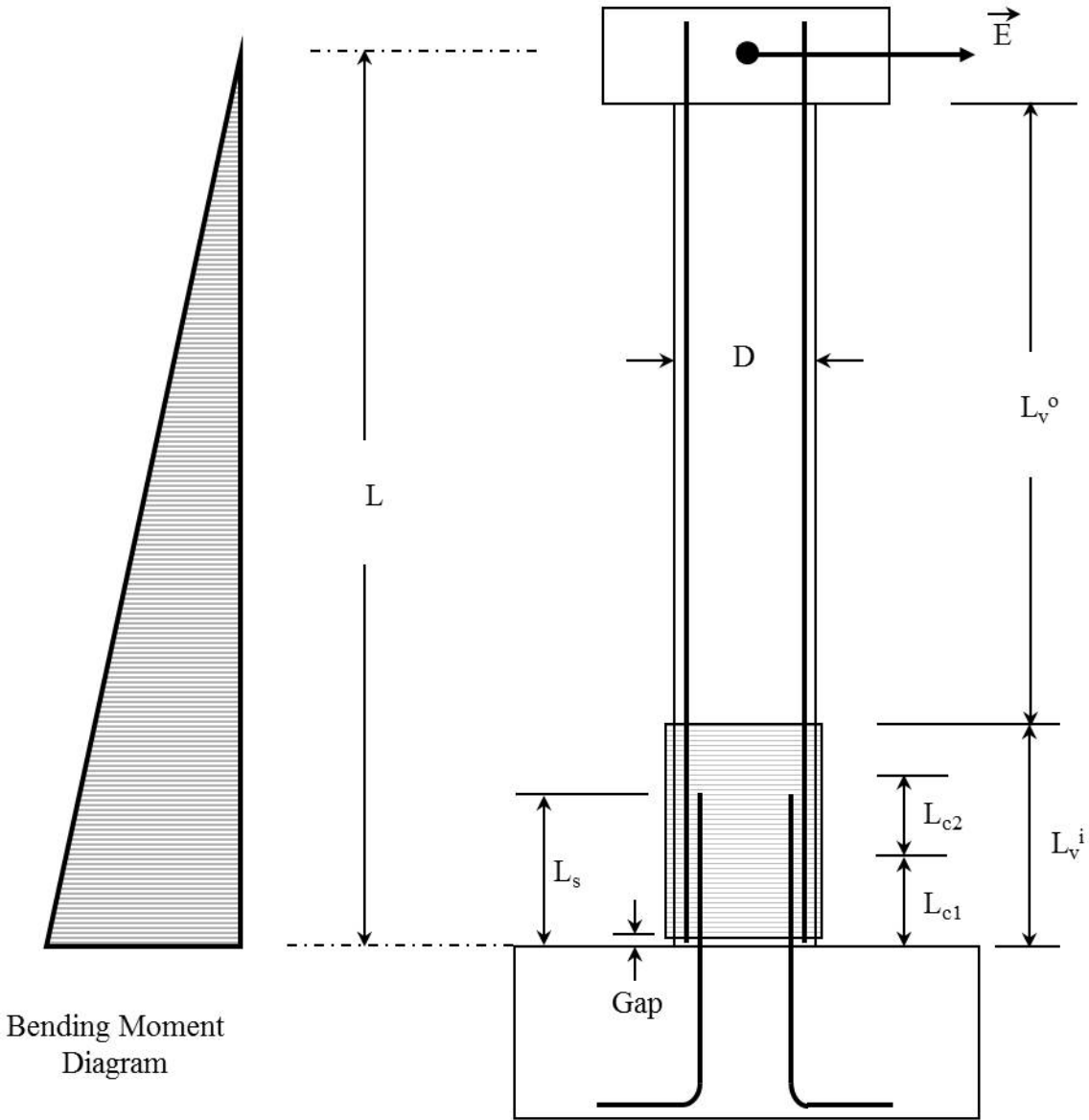
Design of a seismic retrofit CFRP jacket depends on the type of structural deficiency. The followings are general design guidelines for estimating the thickness of the CFRP jacket for the different column regions, (Seible et al, 1996).

7.1 Seismic Shear Design of CFRP Jacket

The shear failure of a column is a strength and dilation problem. Shear strength can be added to concrete columns by hoop or horizontal reinforcement of the FRP composites. The loss of aggregate interlock due to the opening of the inclined cracks can be controlled by the limitation of the column dilation in the loading direction ($\epsilon_d < 0.004$). The jacket thickness for shear strengthening can be determined based on the following equations for circular and for rectangular columns as;

$$\text{Circular column : } t_f = \frac{\frac{V_o}{\phi_v} - (V_c + V_s + V_p)}{\frac{\pi}{2}(0.004E_f D)} \quad \text{Eq.97}$$

$$\text{Rectangular column : } t_f = \frac{\frac{V_o}{\phi_v} - (V_c + V_s + V_p)}{2(0.004E_f D)} \quad \text{Eq.98}$$



$$L_v^i = 1.50 D$$

$$L_{c1} \geq \begin{cases} 0.50D \\ L/8 \end{cases}$$

$L_s > \text{or} =$ to Lap splice length

$$L_{c2} \geq \begin{cases} 0.50D \\ L/8 \end{cases}$$

i = inside hinge region
o = outside hinge region

Fig. 92 CFRP composite jacket for bridge column retrofit – Single Bending

Where,

V_o = Column shear demand based on full flexural over-strength in the potential plastic hinges

Φ_v = Shear capacity reduction factor (typically taken as 0.85)

V_c , V_s , and V_p = Three shear capacity contributions from the concrete, horizontal steel reinforcement, and axial load based on the UCSD three-component shear model (Priestley et al 1996) with reductions for the concrete component V_c in the flexural plastic region, based on the ductility demand

E_f and D = Composite jacket modulus and the column dimension in the loading direction, respectively

The proportional relationship for composite jacket thickness for shear retrofit can be expressed as;

$$t_f^* \approx \frac{1}{E_f D} C_v \quad \text{Eq. 99}$$

Where,

C_v = denotes the remaining general coefficient derived from the previously equations. Appendix “K” presents an example for seismic shear strengthening of rectangular concrete column.

7.2 Seismic Design of Flexural Hinge Confinement Jacket

Inelastic deformation capacity of flexural plastic hinge regions can be increased by confinement of the column concrete with hoop reinforcement from a FRP jacket system. The required jacket thickness of circular columns can be written as;

$$t_f = 0.09 \frac{D(\varepsilon_{cu} - 0.004)f_{cc}'}{\phi_f f_{fu} \varepsilon_{fu}} \quad \text{Eq.100}$$

Where,

f_{cc}' = Confined concrete compression strength that depends on the effective lateral continuing stress and the nominal concrete strength and can be conservatively taken as $1.5f_c'$ for most retrofit designs (Priestley et al. 1996)

f_{fu} and ε_{fu} = Strength and deformation capacity of the composite jacket in the hoop direction

Φ_f = flexural capacity reduction factor (typically taken as 0.9)

ε_{cu} = Ultimate concrete strain that depends on the level of confinement provided by the composite jacket and can be determined as;

$$\varepsilon_{cu} = 0.004 + \frac{2.8\rho_f \varepsilon_{fu} f_{fu}}{f_{cc}'} \quad \text{Eq.101}$$

With ρ_f representing the volumetric jacket reinforcement ratio. In turn, ε_{cu} can be obtained from

$$\varepsilon_{cu} = \Phi_u c_u \quad \text{Eq.102}$$

Based on the ultimate section curvature Φ_u and the corresponding neutral axis depth c_u , both of which can be determined from a sectional moment-curvature analysis and directly related to a structural member ductility factor as follows;

$$\mu_{\Delta} 1 + 3 \left(\frac{\Phi_u}{\Phi_y} - 1 \right) \left(\frac{L_p}{L} \right) \left(1 - 0.5 \frac{L_p}{L} \right) \quad \text{Eq.103}$$

$$L_p = 0.08L + 0.022 f_{sy} d_b \quad \text{Eq.104}$$

Where,

L= Represents the shear span to the plastic hinge

Φ_y = Section yield curvature

f_{sy} and d_b = yield strength and bar diameter of the main column reinforcement (Priestley et al.1996)

The proportional relationship for composite jacket for flexural hinge confinement retrofit can be expressed as;

$$t_f^c \approx \frac{D}{f_{fu} \varepsilon_{fu}} C_c \quad \text{Eq.105}$$

Where,

D= the column dimension in the loading direction. Appendix “L” presents an example for seismic strengthening of rectangular concrete column with inadequate confinement.

7.3 Seismic Design of Lap-Splice Clamping Jacket

Lap splice clamping requires sufficient lateral pressure onto the splice region to prevent the concrete prisms that adhere to the starter bars and the column reinforcement to slip relative to each other.

Limiting dilation strain levels to 0.001, the composite jacket thickness to ensure lap splice clamping can be derived as;

$$t_f = 500 \frac{D(f_l - f_h)}{E_f} \quad \text{Eq.106}$$

$$f_l = \frac{A_s f_{sy}}{\left[\frac{P}{2n} + 2(d_b + cc) \right] L_s} \quad \text{Eq.107}$$

Where,

f_h = Represents the horizontal stress level provided by the existing hoop reinforcement in a circular column at a strain of 0.1%

f_l = The later clamping pressure over the lap splice(L_s)

p = Perimeter line in the column cross section along the lap-spliced bar locations

n = number of spliced bars along p

A_s = Area of one main column reinforcing bar

cc = Concrete cover to the main column reinforcement with diameter d_b .

In terms of a proportional relationship, the required composite jacket thickness is expressed as;

$$t_f^s \approx \frac{D}{E_f} C_s \quad \text{Eq.108}$$

Where,

E_f = the jacket modulus in the hoop direction. Appendix “M” presents an example for seismic strengthening of circular concrete column with inadequate lap splice in the longitudinal reinforcement.

Appendices “A” through “M” present examples for retrofit of reinforced concrete bridge components with CFRP polymer composites, for both gravity and lateral load resisting members, as both types of members are affected by corrosion and require retrofit.

7.4 DETAILING OF EXTERNALLY BONDED FRP REINFORCEMENT

In general, detailing of externally bonded FRP reinforcement depends on the one or more of the followings:

1. Geometry and type of the concrete structural member,
2. Quality and soundness of the concrete substrate,
3. The condition of the surrounding environment,
4. The direction of the tensile stresses in concrete, and
5. The required amount of FRP tensile reinforcement

Separation of an FRP system from the concrete substrate may be caused by one or more of the followings:

1. Lack of adequate bond surface area (limited interface area), particularly, for multi-layer FRP system,

2. Poor concrete quality concrete substrate, which may result in tension-shear failure within the concrete substrate, and
3. Corrosion activities, which may cause premature splitting crack in the plane of tension steel rebars, and complete separation of the FRP system along with the concrete cover.

Based on several past research studies, the concrete substrate is the most critical link in an FRP strengthened concrete system. Therefore, the concrete substrate should be thoroughly inspected and well prepared to receive the FRP system. For bridges located in corrosive environments, including those subjected to deicing salts, FRP reinforcement should be anchored away from the existing steel reinforcing bars.

In order to prevent premature failure of externally bonded FRP systems some general guidelines for detailing of FRP reinforcement should followed:

1. FRP reinforcement should not be run continuous over an inside corner,
2. Externally wrapped outside corners should be rounded to at least a radius of two inch,
3. Wherever splicing of FRP reinforcement is required, laminate overlap should have sufficient length,
4. The individual layers of a multi-layered FRP system should not be terminate at one section, at least a 6.0 inch offset should be maintained, and
5. For bond critical applications, FRP anchor systems should be used in corrosive environments.

To ensure the continuity of the FRP reinforcement, laminate(s) may have to be spliced, which could be maintained by overlapping laminates to form a lap splice. For uniaxial FRP reinforcement, the longitudinal axis of the lap splice should in the direction of the fibers. The lap splice length depends on the tensile strength and thickness of the laminate, and the bond strength at the interface between the laminates. The required lap splice length should be according to the manufacturer recommendations but no shorter than 12 inches.

8 REFERENCES

1. ACI 318-08. "Building Code Requirements for Structural Concrete (ACI 318-05) and Commentary (ACI 318R-05), American Concrete Institute, MI, USA.
2. Aboutaha R. S, Engelhardt M.D, Jirsa J.O, Kreger M.E. "Experimental Investigation of Seismic Repair of Lap Splice Failures in Damaged Concrete Columns," ACI Structural Journal, 1999, V. 96, No. 2, pp. 297-306.
3. Aboutaha R.S. (2004). "Guide for Maintenance, and Rehabilitation of Concrete Bridge Components with FRP Composites-Research into Practice," TIRC & NYSDOT, NY, USA.
4. Albrecht, P., and Naemi, A. _1984_. Performance of weathering steel in bridges, National

Cooperative Highway Research Program, Washington, D.C.

5. Aquino W, Hawkins N.M. "Seismic retrofitting of corroded Reinforced Concrete Columns Using Carbon Composites," *ACI Structural Journal*, 2007, V. 104, No. 3, pp. 348-356.
6. Asri B.D, Ou Y.C. "Seismic Evaluation of Reinforced Concrete Bridges with Corroded Steel Reinforcement using Pushover Analysis," 2011, Thesis for Master Degree, National Taiwan University of Science and Technology, Taiwan.
7. Beal, D. B. and Chamberlin, W. P. Effects of concrete deterioration on bridge response. *Concrete Analysis and Deterioration*, Transportation Research Record 853, Transportation Research Board, 1982, pp. 43-47.
8. Bhargava K, Ghosh A K, Mori Y, Ramanujam S. "Corrosion-induced bond strength degradation in reinforced concrete—Analytical and empirical models," 2007, *Nuclear Engineering and Design Journal*, pp. 1140-1157.
9. Brunson, D. R., Davey, R. A., Graham, C. J., Sidwell, G. K., Villamor, P., White, R. H., and Zhao, J. X., 2000. The Chi-Chi Taiwan earthquake of 21 September 1999; Report of the NZSEE Reconnaissance Team, *Bull. N. Z. Soc. Earthquake Eng.* 33 (2), June, 105–167.
10. Cabrera J G. "Deterioration of concrete due to reinforcement steel corrosion," 1996, *Cement and Concrete Composite Journal*, Vol.18, No. 1, pp. 47–59.
11. Caltrans, 1989, *Bridge Design Aids - Equivalent Static Analysis of Restrainers*, California Department of Transportation, Sacramento, California, pp 14-11 to 14-25.
12. Caltrans, 1990, "Competing Against Time," Report to Governor George Deukmejian by the Governor's Board of Inquiry on the 1989 Loma Prieta Earthquake, Department of General Services, North Highlands, California.
13. Caltrans, 1995, *Standard Specifications*, California Department of Transportation, Sacramento, California.
14. Caltrans, 1996, *Earthquake Retrofit Guidelines for Bridges*, Memo to Designers 20-4, California Department of Transportation, Sacramento, California.
15. Caltrans, 1999, *Seismic Design Methodology*, Memo to Designers 20-1, California Department of Transportation, Sacramento, California, 14 pp.
16. Caltrans Seismic Advisory Board Ad Hoc Committee on Soil-Foundation-Structure Interaction (CSABAC), 1999, *Seismic Soil-Foundation-Structure Interaction: Final Report*, prepared for California Department of Transportation, February.
17. Contecvet, "A Validate User's Manual for Assessing the Residual Service Life of Concrete Structures", EC INNOVATION PROGRAMME, GEOCISA, GEOTECNIA Y CIMENTOS, S.A.
18. "Durability of Concrete Road Bridges", Organization for Economic Co-operation and development (OECD), Paris, France, 1989.
19. Coronelli D, Gambarova P. "Structural Assessment of Corroded Reinforced Concrete Beams: Nodeling Guidelines," *Journal of Structural Engineering*, 2004, Vol. 130, No. 8, pp. 1214-1224.
20. Du, Y. G., Clark, L. A., and Chan, A. H. C. (2005a). "Residual capacity of corroded reinforcing bars." *Mag. Concr. Res.*, 57(3), 135–147.
21. Du, Y. G., Clark, L. A., and Chan, A. H. C. (2005b). "Effect of corrosion on ductility of reinforcing bars." *Mag. Concr. Res.*, 57(7), 407–419.
22. Enright, M. P., and Frangopol, D. M. (1998). "Probabilistic analysis of resistance degradation of reinforced concrete bridge beams under corrosion." *Eng. Struct.*, 20(11), 960-971.

23. Fang C., Lundgren K., Chen L., Zhu C. "Corrosion Influence on Bond in Reinforced Concrete", 2004, Cement and Concrete Research, Vol. 34, No. 11, pp. 2159-2167.
24. FEMA 451, Federal Emergency Management Agency (FEMA), "NEHRP Recommended Provisions: Design Examples", 2006, Washington, DC, USA.
25. FHWA Bridge Maintenance: Substructure, Mark Rossow, PhD, PE, Course No: S04-012. Continuing Education and Development, Inc. 9 Greyridge Farm Court, Stony Point, NY 10980.
26. FHWA, Federal Highway Administration, "Seismic Retrofitting Manual for Highway Structures: Part 1 – Bridges", PUBLICATION NO. FHWA-HRT-06-032, JANUARY 2006.
27. Ghosh, Jayadipta, and Padgett, Jamie, E., "Aging Considerations in the Development of Time-Dependent Seismic Fragility Curves", JOURNAL OF STRUCTURAL ENGINEERING © ASCE / DECEMBER 2010 / 1497.
28. Harajli M. H, Khalili Z. "Seismic FRP Retrofit of Bond-Critical Regions in Circular RC Columns: Validation of Proposed Design Methods," ACI Structural Journal, 2008, V. 105, No. 6, pp. 760-769.
29. Higgins C., Farrow III W. C., Potisuk T., Miller T.H., Yim S. C., Holcomb G. R., Cramer S. D., Covino B. S., Bullard S. J., Moroz M. Z., and Matthes S. A. (2003). "Shear Capacity Assessment of Corrosion Damaged Reinforced Concrete Beams", Oregon Department of Transportation Research Unit and FHWA, Washington, DC, US.
30. Hoeke, L. J. L., Singh, P. M., Moser, R. D., Kahn, L. F., and Kurtis, K. E. _2009_. "Degradation of steel girder bridge bearing systems by corrosion." Corrosion 2009, NACE— Int. Corrosion Conf. Series, National Association of Corrosion Engineers International, Atlanta, Ga.
31. Hover, Kenneth C., "Special problems in evaluating the safety of concrete bridges and concrete bridge components", Construction and Building Materials, Vol. 10, No. I, pp. 39-43, 1996, Copyright © 1996 Elsevier Science Ltd, Printed in Great Britain.
32. Itani, Rafik and Liao Xin, "EFFECTS OF RETROFITTING APPLICATIONS ON REINFORCED CONCRETE BRIDGES" Washington State Transportation Commission Department of Transportation and in cooperation with U.S. Department of Transportation Federal Highway Administration August, 2003.
33. Kawashima, K., Nishikawa, K., Nakano, M., Unjoh, S., Kimura, Y., Hoshikuma, J. I., 1996. Guide specifications for reconstruction and repair of highway bridges which suffered damage due to the Hyogo-Ken Nanbu earthquake, Proceedings of the 28th Joint Meeting of the U.S.-Japan Cooperative Program in Natural Resources Panel on Wind and Seismic Effects, NIST, Gaithersburg, MD, August, 159–174.
34. Kamal, S., O. Salama, and S. El-Abiary. 1992. Deteriorated concrete structure and methods of repair. University Publishing House, Egypt.
35. Komp, M. (1987). "Atmospheric corrosion ratings of weathering steels calculation and significance." Materials Performance, 26(7), 42–44.
36. Lee H.S, Kage T, Noguchi T, Tomosawa F. "An experimental study on the retrofitting effects of reinforced concrete columns damaged by rebar corrosion strengthened with carbon fiber sheets", Cement and Concrete Research, 2003, No. 33, pp 563-570.
37. Lee H S, Noguchi T, Tomosawa F. "Evaluation of the Bond Properties Between Concrete and Reinforcement as a Function of the Degree of Reinforcement Corrosion," 2002, Cement and Concrete Composite Journal, Vol. 32, No. 8, pp. 1313–1318.
38. Li J, Gong J, Wang L. "Seismic Behavior of Corrosion-damaged Reinforced Concrete Columns Strengthened Using Combined Carbon Fiber-reinforced Polymer and Steel Jacket",

- 2009, *Journal of Construction and Building Materials*, No. 23, pp. 2653-2663.
39. Lin Y, Gamble W.L, Hawkins N.M. "SEISMIC BEHAVIOR OF BRIDGE COLUMN NON-CONTACT LAP SPLICES," Report to the Illinois Department of Transportation, 1998.
40. Lindquist, Lisa, "CORROSION OF STEEL BRIDGE GIRDER ANCHOR BOLTS", Aug 2008, School of Civil and Environmental Engineering Georgia Institute of Technology, <http://hdl.handle.net/1853/24649>.
41. Lutz L.A, Gergely P. "Mechanics of Bond and Slip of Deformed Bars in Concrete," *ACI Journal*, 1967, Title No. 64-62, pp. 711-721.
42. Ma Y, Che Y, Gong J. "Behaviour of Corrosion Damaged Circular Reinforced Concrete Columns under Cyclic Loading", *Construction and Building Materials*, 2012, No. 29, pp. 548-556.
43. Mander, J. B., Kim, D., Chen, S., and Premus, G. (1996). Response of steel bridge bearings to reversed cyclic loading, NCEER, Buffalo.
44. Moehle, J.P., Eberhard, M.O. "Earthquake Damage to Bridges." *Bridge Engineering Handbook*. Ed. Wai-Fah Chen and Lian Duan Boca Raton: CRC Press, 2000.
45. Moehle, J. P. (1995). "Northridge earthquake of January 17, 1994: Reconnaissance report, Volume 1—Highway bridges and traffic management." *Earthquake Spectra*, 11(3), 287–372.
46. Montemor, M. F., Simões, A. M. P., and Ferreira, M. G. S. (2002). "Chloride-induced corrosion on reinforcing steel: From the fundamentals to the monitoring techniques." *Cem. Concr. Compos.*, 25(4– 5), 491–502.
47. Morinaga, S. (1989). "Prediction of Service Lives of Reinforced Concrete Buildings Based on Rate of Corrosion of Reinforcing Steel,S" special Report of the Institute of Technology, Skimiza Corporation, Japan.
48. Mostafaei H, Vecchio F.J, Kabeyasawa T. "A Simplified Axial-Shear-Flexure Interaction Approach for Load and Displacement Capacity of Reinforced Concrete Columns", 2009, Improving the Seismic Performance of Existing Buildings and other Structures, Applied Technology Council and the Structural Engineering Institute of ASCE, San Francisco, pp. 12.
49. NATIONAL COOPERATIVE HIGHWAY RESEARCH PROGRAM, NCHRP REPORT 519, Connection of Simple- Span Precast Concrete Girders for Continuity, TRANSPORTATION RESEARCH BOARD EXECUTIVE COMMITTEE 2004.
50. NYSDOT, New York State Department of Transportation, "New York State's Bridge Program in Brief".
51. O'Connor, Jerome S., "Post-Earthquake Bridge Inspection Guidelines", University at Buffalo, October 2010, Final Report for NYSDOT SPR Project # C-06-14, Development of Post-Earthquake Bridge Inspection Guidelines, Cornell Transportation Infrastructure Research Consortium (TIRC) Subcontract, 53740-8411.
52. Ousalem H, Kabeyasawa T, Tasai A, Iwamoto J. "Effect of Hysteretic Reversals on Lateral and Axial Capacities of Reinforced Concrete Columns", 2003, Proceedings of the Japan Concrete Institute, Vol. 25, No. 2, pp. 367-372.
53. Padgett, Jamie E., DesRoches, Reginald., and Hodgson, Darl "Large-Scale Testing of Superelastic Shape Memory Alloy Recentering Devices for Multi Span Bridges", International Conference on Shape Memory and Superelastic Technologies, May 7-11, 2006, Pacific Grove, CA, USA.
54. Priestley M. J. N, Seible F. (1991). "Design of Seismic Retrofit Measures for Concrete Bridges," *Seismic Assessment and Retrofit of Bridges*, SSRP 91/03, University of California, San Diego, pp. 197-234.

55. Rashidi, S., and Saadeghvaziri, M. (1997). "Seismic Modeling of Multi-Span Simply Supported Bridges Using ADINA", *Journal of Computers and Structures*, Vol. 64 No. 5/6, p1025-1039.
56. Rudriguez J, Ortega L, Izquierdo D, Andrade C. "Calculation of Structural Degradation Due to Corrosion of Reinforcements," *Measuring, Monitoring and Modeling Concrete Properties*, 2006, Springer, pp. 527-536.
57. Saad, Tom, Maswoswe, Justice, and Derrell Manceaux, FHWA Seismic Retrofitting Seminar, Indianapolis, IN, October 19-20, 2010.
58. Saadeghvaziri, M. Ala, Yazdani-Motlaghb, A.R., "Seismic behavior and capacity/demand analyses of three multi-span simply supported bridges" Nishkian and Associates Inc., 1200 Folsom St., San Francisco, CA 94103, United States, 2007.
59. Saiidi, M., Maragakis, E., Abdel-Ghaffar, S., Feng, S., and O'Connor, D. (1993). "Response of bridge hinge restrainers during earthquakes-field performance, analysis, and design." Rep. No. CCEER 93/06, Ctr. for Civ. Engrg. Earthquake Research, University of Nevada, Reno, Nev.
60. Saiidi, M., Maragakis, E., and Feng, S. (1996). "Parameters in bridge restrainer design for seismic retrofit." *J. Struct. Engrg.*, ASCE, 122(1), 61–68.
61. Silano, L. G., and Brinckerhoff, P. (1993). "Bridge inspection and rehabilitation", Wiley-IEEE, New York.
62. Stanish K, Hooton R D, Pantazopoulou S J. "Corrosion effects on bond strength in reinforced concrete," *ACI Structural Journal*, 1999, Vol. 96, No. 6, pp. 915–921.
63. Stewart, M. G., and Rosowsky, D. V. (1998). "Time-dependent reliability of deteriorating reinforced concrete bridge decks." *Struct. Safety*, 20(1), 91-109.
64. Tapan M, Aboutaha R.S. "Strength Evaluation of Deteriorated Reinforced Concrete Bridge Columns", 2008, Doctor of Philosophy Thesis, Syracuse University, Syracuse, NY, USA.
65. Val D.V., Stewart M.G., Melchers R.E., "Effect of Reinforcement Corrosion on Reliability of Highway Bridges", *Engineering Structures*, Vol.20, No.11, 1998.
66. Weyers, R. E., Fitch, M., Larsen, E., Al-Qadi, I., and Hoffman, P. 1994. "Concrete bridge protection and rehabilitation: Chemical and physical techniques." *Service life estimates, Strategic Highway Research Program*, Washington D.C., 357.
67. Webster M.P. "The Assessment of Corrosion-Damaged Concrete Structures," 2000, Doctor of Philosophy Thesis, University of Birmingham, School of Civil Engineering, Birmingham, UK.
68. WSDOT (2001). "Rapid Repair Design of Temporary Support System for Bridges Damaged by Earthquakes in the State of Washington," *Research Project Contract Report No. T1804-9, Emergency Bridge Repair*.
69. WSDOT, Washington State Department of Transportation (2001). "Rapid Repair Design of Temporary Support Systems for Bridges Damaged by Earthquakes in the State of Washington, Appendix A – Design Manual," WA-RD 542.2.

APPENDICES

**ANALYSIS AND DESIGN OF CFRP STRENGTHENED
CONCRETE BRIDGE COMPONENTS**

(Aboutaha, 2004)

**ANALYSIS AND DESIGN OF CFRP STRENGTHENED
CONCRETE BRIDGE COMPONENTS**

- Appendix “A” Flexural Strengthening of a Simply Supported reinforced Concrete Beam with Inadequate Flexural Tension Reinforcing Steel Rebars.
- Appendix “B” Flexural Strengthening of a Cantilever reinforced Concrete Beam with Inadequate Flexural Tension Reinforcing Steel Rebars.
- Appendix “C” Shear Strengthening of a Cantilever reinforced Concrete Beam with Inadequate Shear Reinforcement (Complete wrapping scheme).
- Appendix “D” Shear Strengthening of a Cantilever reinforced Concrete Beam with Inadequate Shear Reinforcement (Three side U-wrapping scheme).
- Appendix “E” Shear Strengthening of a Cantilever reinforced Concrete Beam with Inadequate Shear Reinforcement (Three side U-wrapping scheme – ignore the contribution of the existing transverse reinforcement).
- Appendix “F” Shear Strengthening of a Cantilever reinforced Concrete Beam with Inadequate Shear Reinforcement (Two side bonding scheme).
- Appendix “G” Shear Strengthening of a rectangular reinforced Concrete Column with Inadequate Shear Reinforcement (Complete wrapping scheme).
- Appendix “H” Shear Strengthening of a rectangular reinforced Concrete Column with Inadequate Shear Reinforcement (Complete wrapping scheme – ignore the contribution of the existing transverse reinforcement).

- Appendix “I” Axial Strengthening of a Circular reinforced Concrete Column with Inadequate Axial Load Carrying Capacity.
- Appendix “J” Axial Strengthening of a Rectangular reinforced Concrete Column with Inadequate Axial Load Carrying Capacity.
- Appendix “K” Seismic Retrofit of a Rectangular Reinforced Concrete Column with Inadequate Shear Strength and Ductility.
- Appendix “L” Seismic Retrofit of a Rectangular Reinforced Concrete Column with Poorly Confined Plastic Hinge Regions.
- Appendix “M” Seismic Retrofit of a Circular Reinforced Concrete Column with Inadequate Lap Splice in the Longitudinal Steel Reinforcing Rebars.

MAINTENANCE AND REHABILITATION WITH FRP COMPOSITES

NOTATIONS

A_f	= area of FRP reinforcement, in ² (mm ²) $A_f = n t_f w_f$
A_{fv}	= area of FRP shear reinforcement within spacing s , in ² (mm ²)
A_g	= gross area of section, in ² (mm ²)
A_s	= area of non-prestressed steel reinforcement, in ² (mm ²)
b	= width of a rectangular cross-section, in (mm)
c	= distance from extreme compression fiber to the neutral axis, in (mm)
C_E	= environmental reduction factor
d	= distance from extreme compression fiber to the centroid of the non-prestressed steel tension reinforcement, in (mm)
d_f	= depth of FRP shear reinforcement, in (mm)
E_c	= modulus of elasticity of concrete, psi (MPa)
E_f	= tensile modulus of elasticity of FRP, psi (MPa)
E_s	= modulus of elasticity of steel, psi (MPa)
f_c	= compressive stress in concrete, psi (MPa)
f'_c	= specified compressive strength of concrete, psi (MPa)
$\sqrt{f'_c}$	= square root of specified compressive strength of concrete, psi (MPa)
f'_{cc}	= apparent compressive strength of confined concrete, psi (MPa)
f_f	= stress level in the FRP reinforcement, ksi (MPa)
$f_{f,s}$	= stress level in the FRP caused by a moment within the elastic range of the member, psi (MPa)
$F_{f,s}$	= creep rupture stress limit in the FRP, psi (MPa)
f_{fe}	= effective stress in the FRP, psi (MPa)
f_{fu}^*	= ultimate tensile strength of the FRP material as reported by the manufacturer, psi (MPa)
f_{fu}	= design ultimate tensile strength of FRP, psi (MPa)
\bar{f}_{fu}	= mean ultimate tensile strength of FRP based on a population of 20 or more tensile tests per ASTM D 3039, psi (MPa)
f_i	= confining pressure due to FRP jacket, psi (MPa)
f_s	= stress in non-prestressed steel reinforcement, psi (MPa)
$f_{s,s}$	= stress level in non-prestressed steel reinforcement at service loads, psi (MPa)
f_y	= specified yield stress of non-prestressed steel reinforcement, psi (MPa)
h	= overall thickness of a member, in (mm)
k	= ratio of the depth of the neutral axis to the reinforcement depth
k_f	= stiffness per unit width per ply of the FRP reinforcement, lb/in (N/mm) $k_f = E_f t_f$
k_1	= modification factor applied to κ_v to account for the concrete strength
k_2	= modification factor applied to κ_v to account for the wrapping scheme
L_e	= active bond length of FRP laminate, in (mm)
M_n	= nominal moment capacity, in-lbs (N-mm)

M_s	= moment within the elastic range of the member, in-lbs (N-mm)
M_u	= moment demand based on factored loads, in-lbs (N-mm)
n	= number of plies of FRP reinforcement
p_{fu}^*	= ultimate tensile strength per unit width per ply of the FRP reinforcement, lb/in (N/mm) $p_{fu}^* = f_{fu}^* t_f$
P_n	= nominal axial load capacity at given eccentricity, lb (N)
r	= radius of the edges of a square or rectangular section confined with FRP, in (mm)
$R_{n\theta}$	= nominal capacity of a member subjected to the elevated temperatures associated with a fire
s_f	= stirrup spacing or pitch of continuous spirals, in (mm)
t_f	= nominal thickness of one ply of the FRP reinforcement, in (mm)
T_g	= glass transition temperature, °F (°C)
V_c	= shear resistance provided by concrete with steel flexural reinforcement, lb (N)
V_n	= nominal shear strength, lb (N)
V_s	= shear resistance provided by steel stirrups, lb (N)
V_f	= shear resistance provided by FRP stirrups, lb (N)
V_u	= shear demand based on factored loads, lb (N)
w_f	= width of the FRP shear reinforcing plies, in (mm)
α	= angle of inclination of stirrups or spirals, degrees
α_L	= longitudinal coefficient of thermal expansion, in/in/°F (mm/mm/°C)
α_T	= transverse coefficient of thermal expansion, in/in/°F (mm/mm/°C)
β_I	= ratio of the depth of the equivalent rectangular stress block to the depth to the neutral axis
ϵ_b	= strain level in the concrete substrate developed by a given bending moment (tension is positive), in/in (mm/mm)
ϵ_{bi}	= strain level in the concrete substrate at the time of the FRP installation (tension is positive), in/in (mm/mm)
ϵ_c	= strain level in the concrete, in/in (mm/mm)
ϵ_{cu}	= maximum usable compressive strain of concrete, in/in (mm/mm)
ϵ_f	= Strain level in the FRP reinforcement, in/in (mm/mm)
ϵ_{fe}	= effective strain level in FRP reinforcement attained at section failure, in/in (mm/mm)
ϵ_{fu}^*	= ultimate rupture strain of the FRP reinforcement, in/in (mm/mm)
ϵ_{fu}	= design rupture strain of FRP reinforcement, in/in (mm/mm)
$\overline{\epsilon}_{fu}$	= mean rupture strain of FRP reinforcement based on a population of 20 or more tensile tests per ASTM D 3039, in/in (mm/mm)
ϵ_s	= strain level in the mild steel reinforcement, in/in (mm/mm)
ϵ_{sy}	= strain corresponding to the yield point of non-prestressed steel reinforcement, in/in (mm/mm)
ϕ	= strength reduction factor
γ	= Multiplier on f'_c to determine the intensity of an equivalent rectangular stress distribution for concrete
κ_a	= efficiency factor for FRP confinement (based on the section geometry)
κ_m	= bond dependent coefficient for flexure
κ_v	= bond dependent coefficient for shear
ρ_f	= FRP confinement reinforcement ratio

- ρ_g = ratio of the area of longitudinal steel reinforcement to the cross-sectional area of a compression member
- σ = standard deviation
- Ψ_f = additional FRP strength reduction factor

Appendix "A"

Flexural strengthening of a simply supported reinforced concrete beam with CFRP

A simply-supported concrete beam reinforced with 5-#9 bars (see Figures A1 & A2 on Pages 498 & 499) is carrying 1.25 k/ft. dead load, and 1.5 k/ft. live load. Design a CFRP system to allow for an increase in the live load carrying requirements by 1.0 k/ft. An analysis of the existing beam indicates that the beam still has sufficient shear strength to resist the new shear demand and meets the deflection and crack control serviceability requirements. However its flexural strength is inadequate to carry the new live load. Ignore the contribution of the compression steel rebars.

$$f'_c = 5,000 \text{ psi}$$

$$E_c = 57,000\sqrt{f'_c} = 4030.5 \text{ ksi}$$

$$f_y = 65,000 \text{ psi}$$

$$A_s, 5\#9: A_s = 5.0 \text{ in}^2$$

$$b = 16 \text{ in.}$$

$$d = 27 \text{ in.}$$

$$\phi M_n = 600 \text{ k-in (without CFRP)}$$

Nominal flexural capacity of the concrete section without CFRP

$$A_s = 5 (1.00 \text{ in}^2) = 5.0 \text{ in}^2$$

$$d = 27 \text{ in}$$

Equation of Equilibrium

$$C = T$$

$$(0.85 f'_c) b a = A_s f_y$$

$$\therefore a = \frac{A_s f_y}{0.85 f'_c b} = \frac{5.0(65)}{0.85 (5)(16)}$$

$$\therefore a = 4.78 \text{ in.}$$

$$\left(d - \frac{a}{2}\right) = 27 - \left(\frac{4.78}{2}\right) = 24.61 \text{ in}$$

$$M_n = T \left(d - \frac{a}{2}\right) = 5.0 (65)(24.61") = 7998.25 \text{ k-in} = 666.5 \text{ k-ft}$$

$$\phi M_n = 0.9 (666.5) = 600 \text{ k-ft}$$

Loadings

Dead Load

$$w_{GDL} = \left(\frac{16" \times 30"}{144}\right) 1.0 \times 0.15 = 0.50 \text{ k / ft}$$

$$\text{Super imposed dead load: } w_{SDL} = 0.75 \text{ k / ft}$$

$$\text{Total dead load: } w_{DL} = 1.25 \text{ k / ft}$$

Live Load

$$w_{LL} = 1.5 \text{ k / ft}$$

$$\text{New } w_{LL} = 2.5 \text{ k / ft}$$

Service Loads

$$\text{Existing } w_s = 1.25 + 1.5 = 2.75 \text{ k / ft}$$

$$\text{New } w_s = 1.25 + 2.5 = 3.75 \text{ k / ft}$$

Factored Loads

$$\text{Existing } w_u = 1.4(1.25) + 1.7(1.5) = 4.30 \text{ k / ft}$$

$$\text{New } w_u = 1.4(1.25) + 1.7(2.5) = 6.0 \text{ k / ft}$$

Dead Load Moments (M_{DL})

$$\text{Existing } M_{DL} = \frac{1.25(30)^2}{8} = 140.6 \text{ k - ft}$$

$$\text{New } M_{DL} = 140.6 \text{ k - ft}$$

Service Load Moments (M_s)

$$\text{Existing } M_s = \frac{2.75(30)^2}{8} = 309.4 \text{ k-ft}$$

$$\text{New } M_s = \frac{3.75(30)^2}{8} = 421.9 \text{ k-ft}$$

Factored Load Moments (M_u)

$$\text{Existing } M_u = \frac{4.30(30)^2}{8} = 483.8 \text{ k-ft}$$

$$\text{New } M_u = \frac{6.0(30)^2}{8} = 675.0 \text{ k-ft}$$

Loading/ Moments	Existing	New
Dead Loads (w_{DL})	1.25 k/ft	1.25 k/ft
Live Loads (w_{LL})	1.50 k/ft	2.50 k/ft
Service Loads ($w_{DL} + w_{LL}$)	2.75 k/ft	3.75 k/ft
Factored Loads ($1.4w_{DL} + 1.7w_{LL}$)	4.30 k/ft	6.00 k/ft
Dead Load Moments (M_{DL})	140.6 k-ft	140.6 k-ft
Service Load Moments (M_s)	309.4 k-ft	421.9 k-ft
Factored Load Moments (M_u)	483.8 k-ft	675.0 k-ft

CFRP Material

$$t_f = 0.0066 \text{ in / layer}$$

$$E_f = 33,400 \text{ ksi}$$

$$\varepsilon_{fu}^* = 0.017 \text{ in / in}$$

$$n_f = \frac{E_f}{E_s} = \frac{33,400}{4030.5} = 8.29$$

$$\varepsilon_{fu} = C_E \varepsilon_{fu}^* = 0.85(0.017 \text{ in / in}) = 0.0144 \text{ in / in}$$

(C_E : Environmental factor for Exterior exposure)

$$f_{fu} = \varepsilon_{fu} E_f = 0.0144(33,400) = 481 \text{ ksi}$$

∴ CFRP Ultimate Design Values

$$\varepsilon_{fu} = 0.0144 \text{ in / in}$$

$$f_{fu} = 481 \text{ ksi}$$

$$E_{fu} = 33,400 \text{ ksi}$$

Concrete and Steel Properties

Concrete

$$f_c' = 5000 \text{ psi}$$

$$E_c = 57,000\sqrt{f_c'} = 57000\sqrt{5000} * 10^{-3} = 4030.5 \text{ ksi}$$

$$\beta_1 = 0.85 - 0.05\left(\frac{f_c' - 4000}{1000}\right) = 0.85 - 0.05\left(\frac{5000 - 4000}{1000}\right) = 0.80$$

Steel

$$f_y = 65,000 \text{ psi}$$

$$A_s = 5(1.0 \text{ in}^2 \text{ per bar}) = 5.0 \text{ in}^2$$

$$\rho_s = \frac{A_s}{bd} = \frac{5.0 \text{ in}^2}{(16)(27)} = 0.01157$$

$$n_s = \frac{E_s}{E_c} = \frac{29,000 \text{ ksi}}{4030.5 \text{ ksi}} = 7.195$$

$$\rho_s n_s = (0.01157)(7.195) = 0.0832$$

Design of the Amount of CFRP

Preliminary Estimate

$$h = 30 \text{ in}$$

$$d = 30 - 3.0 = 27 \text{ in}$$

$$\left(d - \frac{a}{2}\right) \approx 0.87d \approx 0.87(27) = 23.5 \text{ in}$$

$$\left(h - \frac{a}{2}\right) \approx 0.87d + 3.0 = 26.5 \text{ in}$$

$$M_n = A_s f_s \left(d - \frac{a}{2}\right) + \psi_f A_f f_{fe} \left(h - \frac{a}{2}\right)$$

$$\therefore A_f = \frac{\frac{M_u}{\phi} - A_s f_s \left(d - \frac{a}{2}\right)}{\psi_f f_{fe} \left(h - \frac{a}{2}\right)}$$

$$M_u (\text{New}) = 675 \text{ ft} - k, \phi = 0.9$$

$$\therefore A_f = \frac{675(12,000) / 0.9 - 5.0(65000)(23.5)}{0.85(0.85 * 481,000)(26.5)} = 0.1479 \text{ in}^2$$

Beam width = 16 in, Use $b_f = 14$ in

$$\text{Number of Re plark 30 layers} = \frac{A_f}{b_f * t_f / \text{layer}}$$

$$N = \frac{0.1479 \text{ in}^2}{(14 \text{ in})(0.0066 \text{ in})} = 1.6$$

\therefore Use 2 layers

$$A_f = n t_f w_f = (2 \text{ plies})(0.0066 \text{ in})(14 \text{ in}) = 0.1848 \text{ in}^2$$

$$\rho_f = \frac{A_f}{bd} = \frac{0.1848 \text{ in}^2}{(14 \text{ in})(27 \text{ in})} = 0.00049$$

$$n_f = \frac{E_f}{E_c} = \frac{33,400 \text{ ksi}}{4030.5 \text{ ksi}} = 8.29$$

$$\rho_f n_f = (0.00049)(8.29) = 0.00406$$

Determine the strain in concrete at the level of CFRP (Initial strain before the installation of CFRP) – ϵ_{bi}

$$K = \sqrt{(n_s \rho_s)^2 + 2n_s \rho_s} - n_s \rho_s$$

$$n_s \rho_s = 0.0832$$

$$\therefore K = \sqrt{(0.0832)^2 + 2(0.0832)} - (0.0832) = 0.333$$

$$I_{cr} = \left[\frac{b}{12} (kd)^3 + b(kd) \left(\frac{kd}{2} \right)^2 \right] + nA_s (kd - d)^2 = \left[\frac{16}{12} \left(\frac{27}{3} \right)^3 + (16) \left(\frac{27}{3} \right) \left(\frac{27}{3 \cdot 2} \right)^2 \right] + (7.195)(5) \left(\frac{27}{3} - 27 \right)^2$$

$$\therefore I_{cr} = 15,543.90 \text{ in}^4$$

$$\text{Normal Stress: } f_{bi} = \frac{M_{DL}}{I_{cr}} y_{bottom} = E_c \epsilon_{bi}$$

Assuming that the Dead Load is the only load on the beam at the time the CFRP is applied.

$$\epsilon_{bi} = \frac{M_{DL}(h - kd)}{I_{cr} E_c} = \frac{(140.6 \text{ ft} - k * 12)(30 \text{ in} - (0.333)(27 \text{ in}))}{15,543.90 \text{ in}^4 * 4030.5 \text{ ksi}} = 0.0005658$$

Determine the bond-dependent coefficient of the CFRP system

$$n = \frac{1,200,000}{E_f t_f} \leq 2.0$$

$$n = \frac{1,200,000}{(33,400,000)(0.0066)} = 5.44$$

\therefore Use $n = 2.0$

$$k_m = 1 - \frac{nE_f t_f}{2,400,000} = 1 - \frac{(2)(33,400,000)(0.0066)}{2,400,000} = 0.8163$$

In order to determine the nominal flexural capacity of the strengthened section we need to determine the location of the neutral axis at ultimate state. Of course, equilibrium, strain compatibility and material constitutive laws should be satisfied.

To simplify the analysis, it is assumed that the concrete strain at the extreme compression fiber is equal to 0.003.

Steps of analysis;

1. Plot the strain distribution diagram and start with $\varepsilon_{cu} = 0.003$
2. Assume the depth of the neutral axis, which is the distance from the extreme compression fiber to the neutral axis(c)
3. Draw the strain distribution diagram.
4. Calculate ε_s and ε_{fe} using similar triangles.
5. Use the constitutive laws to calculate the stresses in the steel & CFRP (f_s and f_{fe}).
Multiply the area of steel bars with f_s to get T_s , and multiply f_{fe} with A_f to get T_{fe} .
6. Use the equilibrium equation to determine the depth of the neutral axis (c), which was assumed in step 2.

$$C = T_s + T_f$$

$$0.85 f_c' b \beta_1 c = T_s + T_f$$

$$\therefore c = \frac{A_s f_s + A_f f_{fe}}{0.85 f_c' b \beta_1}$$

Compare the calculated “c” in step 6 with the assumed “c” in step 2.

If the calculated “c”, then go to step 7 and calculate M_n . Otherwise, go to step 2 and assume new “c”.

7. Calculate M_n .

$$\phi M_n = \phi \left[A_s f_s \left(d - \frac{\beta_1 c}{2} \right) + \psi A_f f_{fe} \left(h - \frac{\beta_1 c}{2} \right) \right], \quad \phi = 0.9 \text{ and } \psi = 0.85$$

The procedure shown above is true for analysis of reinforced concrete beam reinforced tension steel bars only, and strengthened with CFRP sheets on the tension side only.

Assume “c” the depth of the neutral axis.

Say, $c = 0.25 d$

Therefore, $c = 0.25(27 \text{ in}) = 6.75 \text{ in}$

Draw the Strain Distribution Diagram.

Calculate the steel strain “ ϵ_s ”

$$\frac{\epsilon_s}{(d - c)} = \frac{0.003}{c}$$

$$\therefore \epsilon_s = \frac{(d - c)}{c} (0.003) = \frac{20.25 \text{ in.}}{6.75 \text{ in.}} (0.003) = 0.009$$

$$\epsilon_y = \frac{f_y}{E_s} = \frac{65,000}{29,000,000} = 0.00224$$

$$\therefore \epsilon_s \gg \epsilon_y$$

$$\therefore f_s = f_y = 65,000 \text{ psi : Stress level in steel bars}$$

Please Note that

if $\epsilon_s \leq \epsilon_y$, then $f_s = \epsilon_s E_s$ and if $\epsilon_s \geq \epsilon_y$ then $f_s = f_y$

Calculate the CFRP strain “ ϵ_{fe} ”

From the strain distribution diagram

$$\epsilon_{fe} + \epsilon_{bi} = \frac{(h - c)}{c} (0.003)$$

$$\therefore \epsilon_{fe} = \frac{(h - c)}{c} (0.003) - \epsilon_{bi} \leq k_m \epsilon_{fu}$$

$$\epsilon_{fe} = \frac{23.25}{6.75} (0.003) - 0.0005658 = 0.00976$$

$$k_m \epsilon_{fu} = 0.8163(0.0144) = 0.01175$$

$$\therefore \epsilon_{fe} = 0.00976$$

Calculate the stress level in the CFRP

$$f_{fe} = \varepsilon_{fe} E_f = 0.00976(33,400 \text{ ksi}) = 325.984 \approx 326 \text{ ksi}$$

Calculate the depth of the neutral axis “c”

Use the equilibrium equation,

$$c = \frac{A_s f_s + A_f f_{fe}}{0.85 f_c' b \beta_1}$$

$$\text{for } f_c' = 5000 \text{ psi} \Rightarrow \beta_1 = 0.80$$

$$c = \frac{(5.0 \text{ in}^2)(65) + (0.1848 \text{ in}^2)(326 \text{ ksi})}{0.85(5)(16 \text{ in.})(0.80)} = \frac{325 + 60.24}{54.4} = 7.08 \text{ in}$$

Assumed "c = 6.75 in" ≠ calculated" c = 7.08 in"

Assume c = 7.023 in and f_s = f_y

$$\varepsilon_{fe} = 0.009249 \text{ and } f_{fe} = 308.924 \text{ ksi}$$

$$c = \frac{325 + (0.1848 \text{ in}^2)(308.924)}{54.4} = 7.023 \text{ in.}$$

Calculate the nominal flexural strength “M_n”

$$\begin{aligned}
M_n &= A_s f_s \left(d - \frac{\beta_1 c}{2}\right) + \psi A_f f_{fe} \left(h - \frac{\beta_1 c}{2}\right) \\
&= (5)(65) \left(27 - \frac{0.8(7.023)}{2}\right) + 0.85(0.1848)(308.924) \left(30 - \frac{0.8(7.023)}{2}\right) \\
&= 7862.01 + 1319.45 \\
&= 9181.46 \text{ k-in} \\
&= 765.12 \text{ k-ft}
\end{aligned}$$

$$\phi M_n = 0.9(765.12) = 688.6 \text{ k-ft}$$

$$M_u = 675 \text{ k-ft}$$

$$\phi M_n > M_u \quad \text{Good!!!}$$

Check service stresses in the reinforcing steel and the CFRP

We need to determine the depth of the elastic neutral axis for a reinforced section strengthened with CFRP.

$$\begin{aligned}
k &= \sqrt{(\rho_s n_s + \rho_f n_f)^2 + 2(\rho_s n_s + \rho_f n_f \left(\frac{h}{d}\right))} - (\rho_s n_s + \rho_f n_f) \\
&= \sqrt{(0.0832 + 0.00406)^2 + 2(0.0832 + 0.00406 \left(\frac{30}{27}\right))} - (0.0832 + 0.00406) \\
&= 0.340
\end{aligned}$$

$$kd = 0.340(27) = 9.18 \text{ in}$$

Stress in steel under service load “ $f_{s,s}$ ”

$$\begin{aligned}
 f_{s,s} &= \frac{[M_s + \varepsilon_{bi} A_f E_f (h - \frac{kd}{3})](d - kd) E_s}{A_s E_s (d - \frac{kd}{3})(d - kd) + A_f E_f (h - \frac{kd}{3})(h - kd)} \\
 &= \frac{[(421.9 * 12) + (0.0005658)(0.1848)(33,400)(30 - \frac{9.18}{3})](27 - 9.18)29,000}{5(29,000)(27 - \frac{9.18}{3})(27 - 9.18) + 0.1848(33,400)(30 - \frac{9.18}{3})(30 - 9.18)} \\
 &= \frac{2,664,973,751}{61,858,566 + 3,461,997.5} \\
 &= 40.80 \text{ ksi}
 \end{aligned}$$

$$0.80 f_y = 0.80(65) = 52 \text{ ksi}$$

$$f_{s,s} = 40.80 \text{ ksi} < 0.80 f_y = 52 \text{ ksi}$$

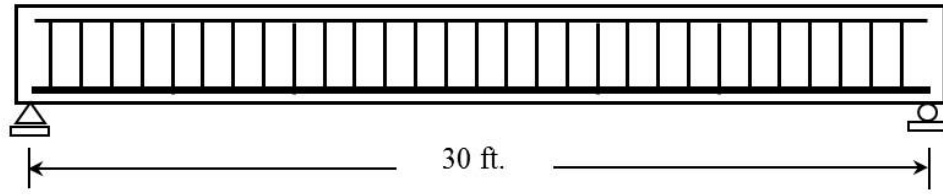
Stress in CFRP under service load “ $f_{f,s}$ ”

$$\begin{aligned}
 f_{f,s} &= f_{s,s} \left[\frac{E_f}{E_s} \right] \left[\frac{h - kd}{d - kd} \right] - \varepsilon_{bi} E_f \\
 &= 40.8 \left[\frac{33,400}{29,000} \right] \left[\frac{30 - 9.18}{27 - 9.18} \right] - (0.0005658)(33,400) \\
 &= 36.00 \text{ ksi}
 \end{aligned}$$

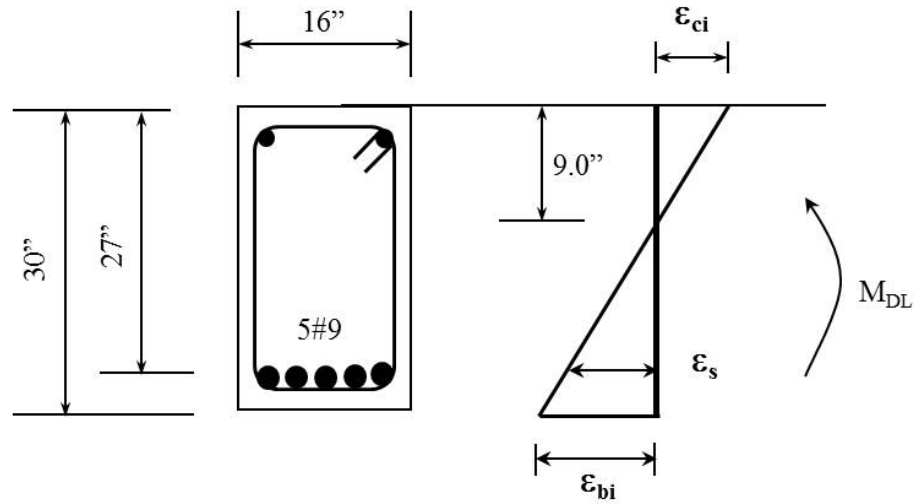
$$0.55 f_{fu} = 0.55(481 \text{ ksi}) = 264.55 \text{ ksi}$$

$$f_{f,s} = 36 \text{ ksi} \ll 0.55 f_{fu} = 264.55 \text{ ksi}$$

Appendix "A"



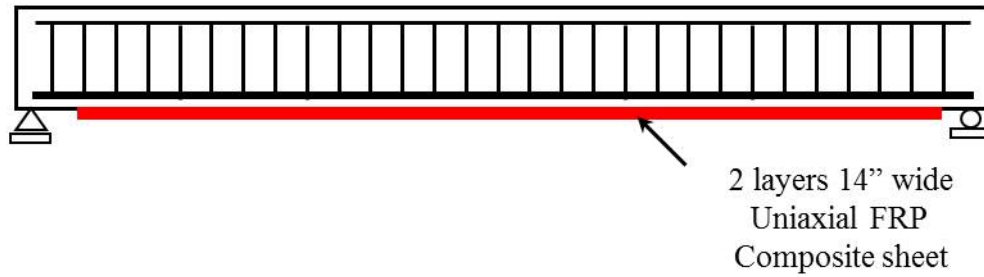
(a) Elevation of the existing beam



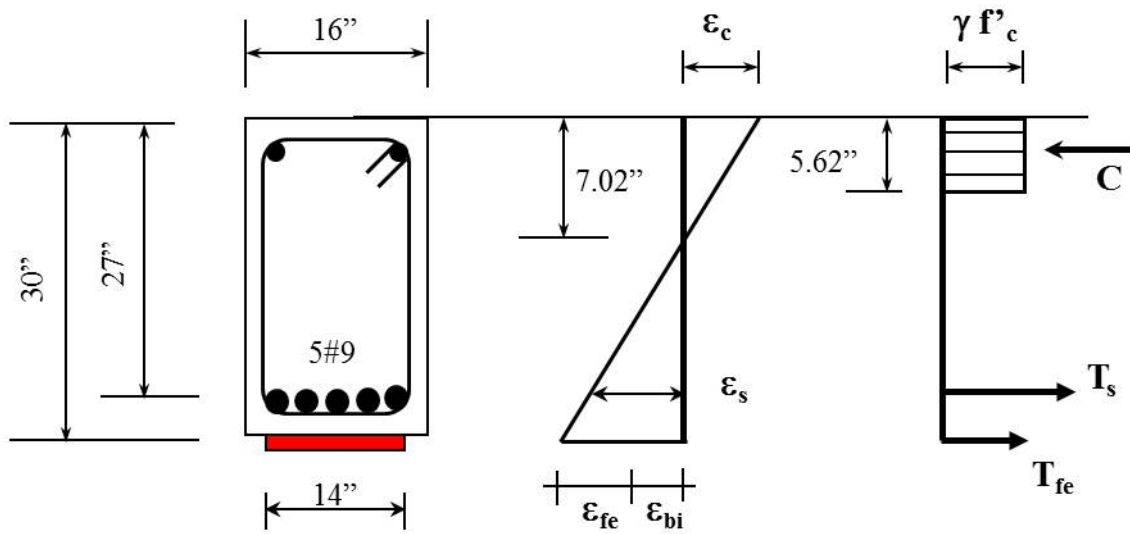
(b) Strain and stress distribution diagrams under sustained loads (Dead loads)

Figure A1. State of strains in the existing beam during installation of the CFRP Composite sheets.

Appendix "A"



(a) Elevation of the strengthened beam



(b) Strain and stress distribution diagrams

Figure A2. State of strains and stresses in the retrofitted beam at ultimate state.

Appendix “B”

Flexural strengthening of a reinforced concrete cantilever beam with CFRP

A cantilever concrete beam reinforced with 10#10 bars (see Figures B1-B3 on Pages 500-502) is carrying 1.95 k/ft. dead load, and 44.13 k/ft. live load. Design a CFRP system to allow for an increase in the dead and live load carrying requirements by 0.2 k/ft. and 4.41 k/ft, respectively. An analysis of the existing beam indicates that the beam still has sufficient shear strength to resist the new shear demand and meets the deflection and crack control serviceability requirements. However its flexural strength is inadequate to carry the new loads. Ignore the contribution of the compression steel rebars.

$$f_c' = 5,000 \text{ psi}$$

$$E_c = 57,000\sqrt{f_c'} = 4030.5 \text{ ksi}$$

$$f_y = 65,000 \text{ psi}$$

$$A_s, 10\#10: A_s = 12.7 \text{ in}^2, A_v = 0.31 * 4 = 1.24 \text{ in}^2, s(\text{spacing}) = 6 \text{ in}$$

$$b = 24 \text{ in}, L = 8 \text{ ft}$$

$$d = 44.23 \text{ in}$$

$$\phi M_n = 2487.857 \text{ k-ft (without CFRP)}$$

Nominal flexural capacity of the concrete section without CFRP

$$A_s = 10 (1.27 \text{ in}^2) = 12.7 \text{ in}^2$$

$$d = 44.23 \text{ in}$$

Equation of Equilibrium

$$C = T$$

$$(0.85 f_c') b a = A_s f_y$$

$$\therefore a = \frac{A_s f_y}{0.85 f_c' b} = \frac{12.7(65)}{0.85(5)(24)}$$

$$\therefore a = 8.093 \text{ in.}$$

$$\left(d - \frac{a}{2}\right) = 44.23 - \left(\frac{8.093}{2}\right) = 40.183 \text{ in.}$$

$$M_n = T(d - \frac{a}{2}) = 12.7 (65)(40.183") = 33172.42 k - in = 2764.285 k - ft$$

$$\phi M_n = 0.9 (2764.285) = 2487.857 k - ft$$

$$V_n = \frac{M_n}{L} = 691.07 kips$$

$$\phi V_{n,reqd} = (0.9)(691.07) = 587.41 kips (required)$$

$$V_c = 150.12 kips \text{ and } V_s = 594.16 kips$$

$$\phi V_{n,designed} = 632.64 kips$$

Loadings

Dead Load

$$w_{GDL} = (\frac{24" \times 48"}{144}) 1.0 \times 0.15 = 1.20 k / ft$$

$$\text{Super imposed dead load: } w_{SDL} = 0.75 k / ft$$

$$\text{Total dead load: } w_{DL} = 1.95 k / ft$$

$$\text{New total dead load: } w_{DL} = 2.15 k / ft$$

Live Load

$$\text{Existing } w_{LL} = 44.13 k / ft$$

$$\text{New } w_{LL} = 48.54 k / ft$$

Service Loads

$$\text{Existing } w_s = 1.95 + 44.13 = 46.08 k / ft$$

$$\text{New } w_s = 2.15 + 48.54 = 50.69 k / ft$$

Factored Loads

$$\text{Existing } w_u = 1.4(1.95) + 1.7(44.13) = 77.75 \text{ k/ft}$$

$$\text{New } w_u = 1.4(2.15) + 1.7(48.54) = 85.52 \text{ k/ft}$$

Dead Load Moments (M_{DL})

$$\text{Existing } M_{DL} = \frac{1.95(8)^2}{2} = 62.4 \text{ k-ft}$$

$$\text{New } M_{DL} = \frac{2.15(8)^2}{2} = 68.6 \text{ k-ft}$$

Service Load Moments (M_s)

$$\text{Existing } M_s = \frac{46.08(8)^2}{2} = 1474.6 \text{ k-ft}$$

$$\text{New } M_s = \frac{50.68(8)^2}{2} = 1621.8 \text{ k-ft}$$

Factored Load Moments (M_u)

$$\text{Existing } M_u = \frac{77.75(8)^2}{2} = 2488.0 \text{ k-ft}$$

$$\text{New } M_u = \frac{85.52(8)^2}{2} = 2736.6 \text{ k-ft}$$

Loading/ Moments	Existing	New
Dead Loads (w_{DL})	1.95 k/ft	2.15 k/ft
Live Loads (w_{LL})	44.13 k/ft	48.54 k/ft
Service Loads ($w_{DL} + w_{LL}$)	46.08 k/ft	50.68 k/ft
Factored Loads ($1.4w_{DL} + 1.7w_{LL}$)	77.75 k/ft	85.52 k/ft
Dead Load Moments (M_{DL})	62.4 ft-k	68.6 ft-k

Service Load Moments (M_S)	1474.6 ft-k	1621.8 ft-k
Factored Load Moments (M_u)	2488.0 ft-k	2736.6 ft-k

CFRP Material

$$t_f = 0.0066 \text{ in / layer}$$

$$E_f = 33,400 \text{ ksi}$$

$$\varepsilon_{fu}^* = 0.017 \text{ in. / in.}$$

$$n_f = \frac{E_f}{E_s} = \frac{33,400}{4030.5} = 8.29$$

$$\varepsilon_{fu} = C_E \varepsilon_{fu}^* = 0.85(0.017 \text{ in. / in.}) = 0.0144 \text{ in. / in.}$$

(C_E : Environmental factor for Exterior exposure)

$$f_{fu} = \varepsilon_{fu} E_f = 0.0144(33,400) = 481 \text{ ksi}$$

∴ CFRP Ultimate Design Values

$$\varepsilon_{fu} = 0.0144 \text{ in. / in.}$$

$$f_{fu} = 481 \text{ ksi}$$

$$E_{fu} = 33,400 \text{ ksi}$$

Concrete and Steel Properties

Concrete

$$f_c' = 5000 \text{ psi}$$

$$E_c = 57,000\sqrt{f_c'} = 57000\sqrt{5000} * 10^{-3} = 4030.5 \text{ ksi}$$

$$\beta_1 = 0.85 - 0.05\left(\frac{f_c' - 4000}{1000}\right) = 0.85 - 0.05\left(\frac{5000 - 4000}{1000}\right) = 0.80$$

Steel

$$f_y = 65,000 \text{ psi}$$

$$A_s = 10(1.27 \text{ in}^2 \text{ per bar}) = 12.7 \text{ in}^2$$

$$\rho_s = \frac{A_s}{bd} = \frac{12.7 \text{ in}^2}{(24)(44.23)} = 0.01196$$

$$n_s = \frac{E_s}{E_c} = \frac{29,000 \text{ ksi}}{4030.5 \text{ ksi}} = 7.195$$

$$\rho_s n_s = (0.01157)(7.195) = 0.0861$$

Design of the Amount of CFRP

Preliminary Estimate

$$h = 48 \text{ in.}$$

$$d = 48 - 1.5 - 0.5 - 1.27 - 0.5 = 44.23 \text{ in}$$

$$\left(d - \frac{a}{2}\right) \approx 0.87d \approx 0.87(44.23) = 38.48 \text{ in}$$

$$\left(h - 8 - \frac{a}{2}\right) \approx 0.87d + 3.77 - 8 = 34.25 \text{ in}$$

$$M_n = A_s f_s \left(d - \frac{a}{2}\right) + \psi_f A_f f_{fe} \left(h - \frac{a}{2}\right)$$

$$\therefore A_f = \frac{\frac{M_u}{\phi} - A_s f_s \left(d - \frac{a}{2}\right)}{\psi_f f_{fe} \left(h - \frac{a}{2}\right)}$$

$$M_u (\text{New}) = 2736.6 \text{ k-ft}, \phi = 0.9, \psi_f = 0.85$$

$$\therefore A_f = \frac{2736.6(12,000)/0.9 - 12.7(65000)(38.48)}{0.85(0.65 * 481,000)(34.25)} = 0.5224 \text{ in}^2$$

Beam width = 24 in, Use $b_f = 12$ in at each side

$$\text{Number of Re plark 30 layers} = \frac{A_f}{b_f * t_f / \text{layer}}$$

$$N = \frac{0.5224 \text{ in}^2}{(12 \text{ in.})(2 * 0.0066 \text{ in})} = 3.298$$

\therefore Use 4 layers each side of the beam (like U - shape wrap)

$$A_f = n t_f w_f = (2 * 4 \text{ plies})(0.0066 \text{ in.})(12 \text{ in.}) = 0.6336 \text{ in}^2$$

$$\rho_f = \frac{A_f}{bd} = \frac{0.6336 \text{ in}^2}{(24 \text{ in.})(44.23 \text{ in.})} = 0.000597$$

$$n_f = \frac{E_f}{E_c} = \frac{33,400 \text{ ksi}}{4030.5 \text{ ksi}} = 8.29$$

$$\rho_f n_f = (0.00041)(8.29) = 0.00495$$

Determine the strain in concrete at the level of CFRP (Initial strain before the installation of CFRP) – ϵ_{bi}

$$K = \sqrt{(n_s \rho_s)^2 + 2n_s \rho_s} - n_s \rho_s$$

$$n_s \rho_s = 0.0861$$

$$\therefore K = \sqrt{(0.0861)^2 + 2(0.0861)} - (0.0861) = 0.3377$$

$$I_{cr} = \left[\frac{b}{12} (kd)^3 + b(kd) \left(\frac{kd}{2} \right)^2 \right] + nA_s (kd - d)^2 = \left[\frac{24}{12} (14.94)^3 + (24)(14.94)(7.47)^2 \right] + (7.195)(12.7)(14.94 - 44.23)^2$$

$$\therefore I_{cr} = 39,956.3 \text{ in}^4$$

$$\text{Normal Stress: } f_{bi} = \frac{M_{DL}}{I_{cr}} y_{top} = E_c \epsilon_{bi}$$

Assuming that the Dead Load is the only load on the beam at the time the CFRP is applied.

$$\epsilon_{bi} = \frac{M_{DL}(h - 8 - kd)}{I_{cr} E_c} = \frac{(68.6 \text{ k} - \text{ft} * 12)(48 \text{ in} - 8 \text{ in} - (0.3377)(44.23 \text{ in}))}{39,956.3 \text{ in}^4 * 4030.5 \text{ ksi}} = 0.000128$$

Determine the bond-dependent coefficient of the CFRP system

$$n = \frac{1,200,000}{E_f t_f} \leq 2.0$$

$$n = \frac{1,200,000}{(33,400,000)(0.0066)} = 5.44$$

\therefore Use $n = 2.0$

$$k_m = 1 - \frac{nE_f t_f}{2,400,000} = 1 - \frac{(2)(33,400,000)(0.0066)}{2,400,000} = 0.8163$$

In order to determine the nominal flexural capacity of the strengthened section we need to determine the location of the neutral axis at ultimate state. Of course, equilibrium, strain compatibility and material constitutive laws should be satisfied.

To simplify the analysis, it is assumed that the concrete strain at the extreme compression fiber is equal to 0.003.

Steps of analysis;

1. Plot the strain distribution diagram and start with $\epsilon_{cu} = 0.003$
2. Assume the depth of the neutral axis, which is the distance from the extreme compression fiber to the neutral axis(c)
3. Draw the strain distribution diagram.
4. Calculate ϵ_s and ϵ_{fe} using similar triangles.
5. Use the constitutive laws to calculate the stresses in the steel & CFRP (f_s and f_{fe}).
Multiply the area of steel bars with f_s to get T_s , and multiply f_{fe} with A_f to get T_f .
6. Use the equilibrium equation to determine the depth of the neutral axis (c), which was assumed in step 2.

$$C = T_s + T_f$$

$$0.85 f_c' b \beta_1 c = T_s + T_f$$

$$\therefore c = \frac{A_s f_s + A_f f_{fe}}{0.85 f_c' b \beta_1}$$

Compare the calculated “c” in step 6 with the assumed “c” in step 2.

If the calculated “c”, then go to step 7 and calculate M_n . Otherwise, go to step 2 and assume new “c”.

7. Calculate M_n .

$$\phi M_n = \phi \left[A_s f_s \left(d - \frac{\beta_1 c}{2} \right) + \psi A_f f_{fe} \left(h - \frac{\beta_1 c}{2} \right) \right], \quad \phi = 0.9 \text{ and } \psi = 0.85$$

The procedure shown above is true for analysis of reinforced concrete beam reinforced tension steel bars only, and strengthened with CFRP sheets on the tension side only.

Assume “c” the depth of the neutral axis.

Say, $c = 0.25 d$

Therefore, $c = 0.25(44.23 \text{ in.}) = 11.06 \text{ in.}$

Draw the Strain Distribution Diagram.

Calculate the steel strain “ ϵ_s ”

$$\frac{\epsilon_s}{(d-c)} = \frac{0.003}{c}$$
$$\therefore \epsilon_s = \frac{(d-c)}{c}(0.003) = \frac{33.17 \text{ in.}}{11.06 \text{ in.}}(0.003) = 0.009$$
$$\epsilon_y = \frac{f_y}{E_s} = \frac{65,000}{29,000,000} = 0.00224$$
$$\therefore \epsilon_s \gg \epsilon_y$$
$$\therefore f_s = f_y = 65,000 \text{ psi : Stress level in steel bars}$$

Please Note that

if $\epsilon_s \leq \epsilon_y$, then $f_s = \epsilon_s E_s$ and if $\epsilon_s \geq \epsilon_y$ then $f_s = f_y$

Calculate the CFRP strain “ ϵ_{fe} ”

From the strain distribution diagram

$$\epsilon_{fe} + \epsilon_{bi} = \frac{(h-8-c)}{c}(0.003)$$
$$\therefore \epsilon_{fe} = \frac{(h-8-c)}{c}(0.003) - \epsilon_{bi} \leq k_m \epsilon_{fu}$$
$$\epsilon_{fe} = \frac{28.94}{11.06}(0.003) - 0.000128 = 0.00772$$
$$k_m \epsilon_{fu} = 0.8163(0.0144) = 0.01175$$
$$\therefore \epsilon_{fe} = 0.00772$$

Calculate the stress level in the CFRP

$$f_{fe} = \epsilon_{fe} E_f = 0.00772(33,400 \text{ ksi}) = 257.994 \approx 258 \text{ ksi}$$

Calculate the depth of the neutral axis “c”

Use the equilibrium equation,

$$c = \frac{A_s f_s + A_f f_{fe}}{0.85 f_c' b \beta_1}$$

$$\text{for } f_c' = 5000 \text{ psi} \Rightarrow \beta_1 = 0.80$$

$$c = \frac{(12.7 \text{ in}^2)(65) + (0.6336 \text{ in}^2)(258 \text{ ksi})}{0.85(5)(24\text{in})(0.80)} = 12.12 \text{ in}$$

Assumed "c = 11.06 in" ≠ calculated "c = 12.12 in."

Assume c = 11.92 in. and f_s = f_y

$$\varepsilon_{fe} = 0.00694 \text{ and } f_{fe} = 232 \text{ ksi}$$

$$c = \frac{825.5 + (0.6336 \text{ in}^2)(232)}{81.6} = 11.92 \text{ in.}$$

Calculate the nominal flexural strength “M_n”

$$\begin{aligned}
M_n &= A_s f_s \left(d - \frac{\beta_1 c}{2}\right) + \psi A_f f_{fe} \left(h - \frac{\beta_1 c}{2}\right) \\
&= (5)(65)\left(44.23 - \frac{0.8(11.92)}{2}\right) + 0.85(0.6336)(232)\left(48 - \frac{0.8(11.92)}{2}\right) \\
&= 36978.80 \text{ k-in} \\
&= 3081.6 \text{ k-ft}
\end{aligned}$$

$$\phi M_n = 0.9(3081.6) = 2773.4 \text{ k-ft}$$

$$M_u = 2773.4 \text{ k-ft}$$

$$\phi M_n > M_u = 2736.7 \text{ k-ft} \text{ Good!!!}$$

Check service stresses in the reinforcing steel and the CFRP

We need to determine the depth of the elastic neutral axis for a reinforced section strengthened with CFRP.

$$\begin{aligned}
k &= \sqrt{(\rho_s n_s + \rho_f n_f)^2 + 2(\rho_s n_s + \rho_f n_f \left(\frac{h}{d}\right))} - (\rho_s n_s + \rho_f n_f) \\
&= \sqrt{(0.0861 + 0.00495)^2 + 2(0.0861 + 0.00495\left(\frac{48}{44.23}\right))} - (0.0861 + 0.00495) \\
&= 0.3462
\end{aligned}$$

$$kd = 0.3462(44.23) = 15.31 \text{ in}$$

Stress in steel under service load “ $f_{s,s}$ ”

$$\begin{aligned} f_{s,s} &= \frac{[M_s + \varepsilon_{bi} A_f E_f (h - \frac{kd}{3})](d - kd) E_s}{A_s E_s (d - \frac{kd}{3})(d - kd) + A_f E_f (h - \frac{kd}{3})(h - kd)} \\ &= \frac{[(1621.8 * 12) + (0.000128)(0.6336)(33,400)(48 - \frac{15.31}{3})](44.23 - 15.31)29,000}{12.7(29,000)(44.23 - \frac{15.31}{3})(44.23 - 15.31) + 0.6336(33,400)(48 - \frac{15.31}{3})(48 - 15.31)} \\ &= 37.71 \text{ ksi} \end{aligned}$$

$$0.80 f_y = 0.80(65) = 52 \text{ ksi}$$

$$f_{s,s} = 37.71 \text{ ksi} < 0.80 f_y = 52 \text{ ksi}$$

Stress in CFRP under service load “ $f_{f,s}$ ”

$$\begin{aligned} f_{f,s} &= f_{s,s} \left[\frac{E_f}{E_s} \right] \left[\frac{h - kd}{d - kd} \right] - \varepsilon_{bi} E_f \\ &= 37.71 \left[\frac{33,400}{29,000} \right] \left[\frac{48 - 15.31}{44.23 - 15.31} \right] - (0.000128)(33,400) \\ &= 32.80 \text{ ksi} \end{aligned}$$

$$0.55 f_{fu} = 0.55(481 \text{ ksi}) = 264.55 \text{ ksi}$$

$$f_{f,s} = 32.80 \text{ ksi} \ll 0.55 f_{fu} = 264.55 \text{ ksi}$$

Appendix "B"

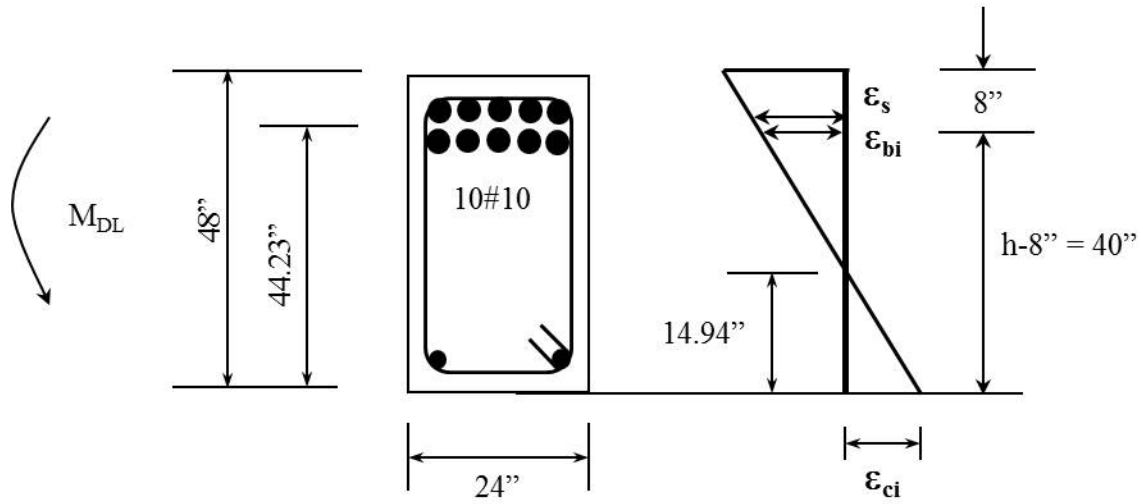
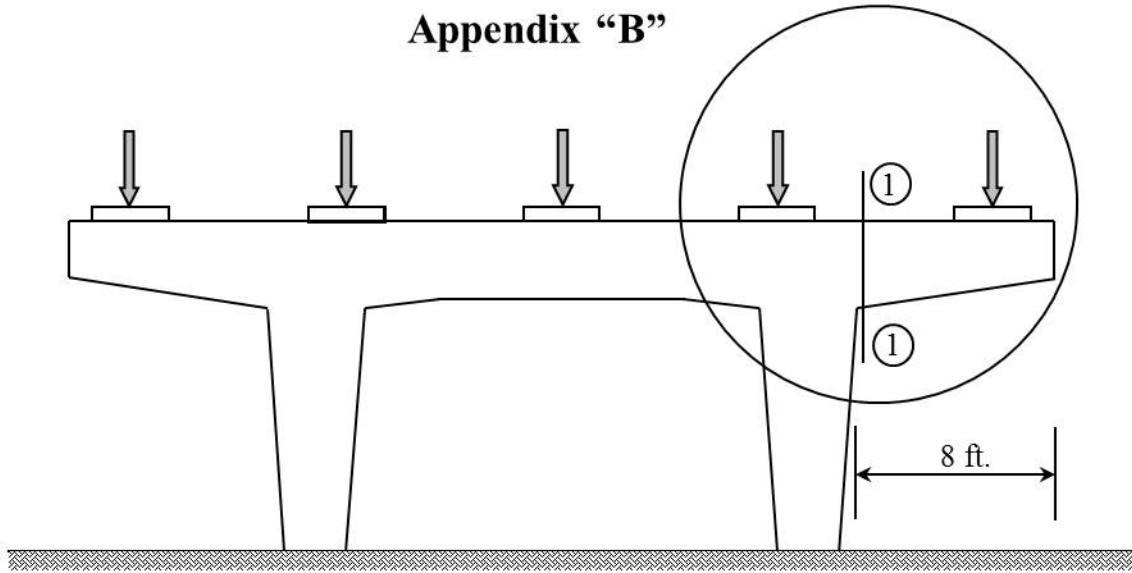


Figure B1. State of strains and stresses in the existing section under sustained loads.

Appendix "B"

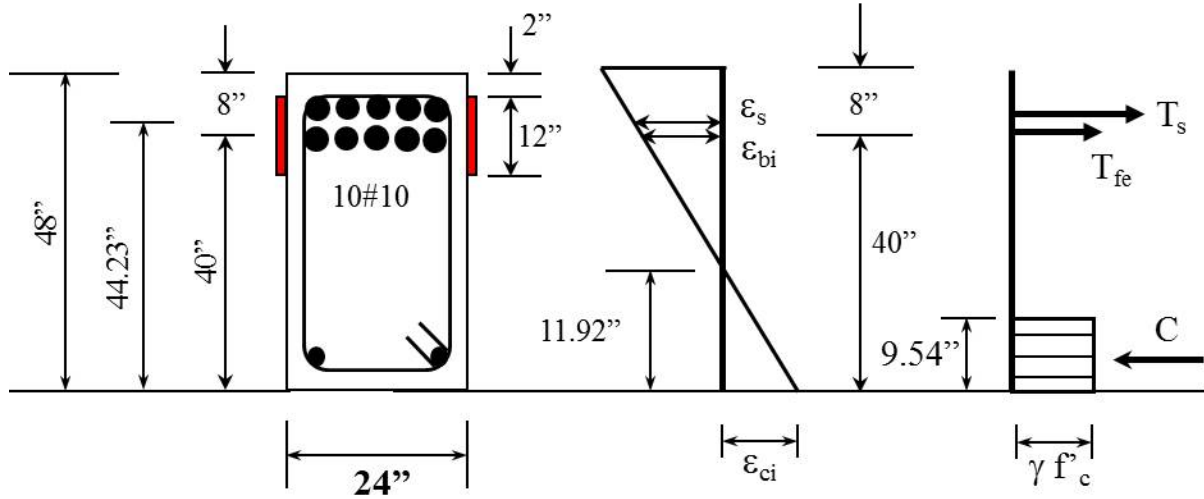


Figure B2. State of strains and stresses in the retrofitted beam at ultimate state.

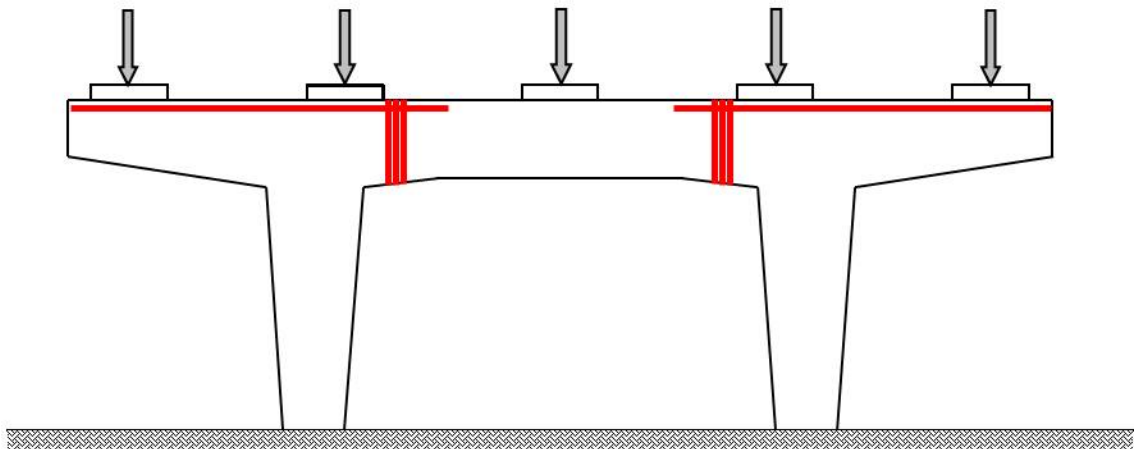
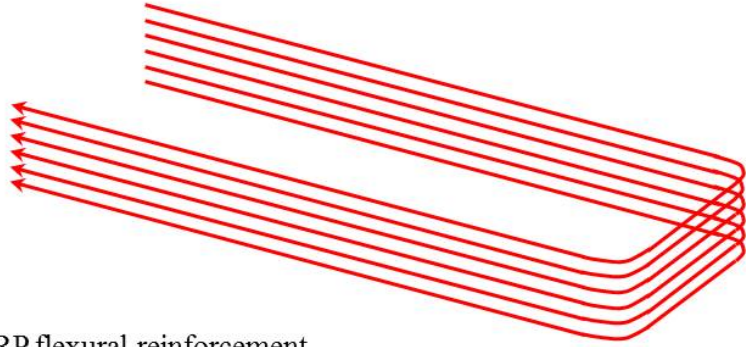
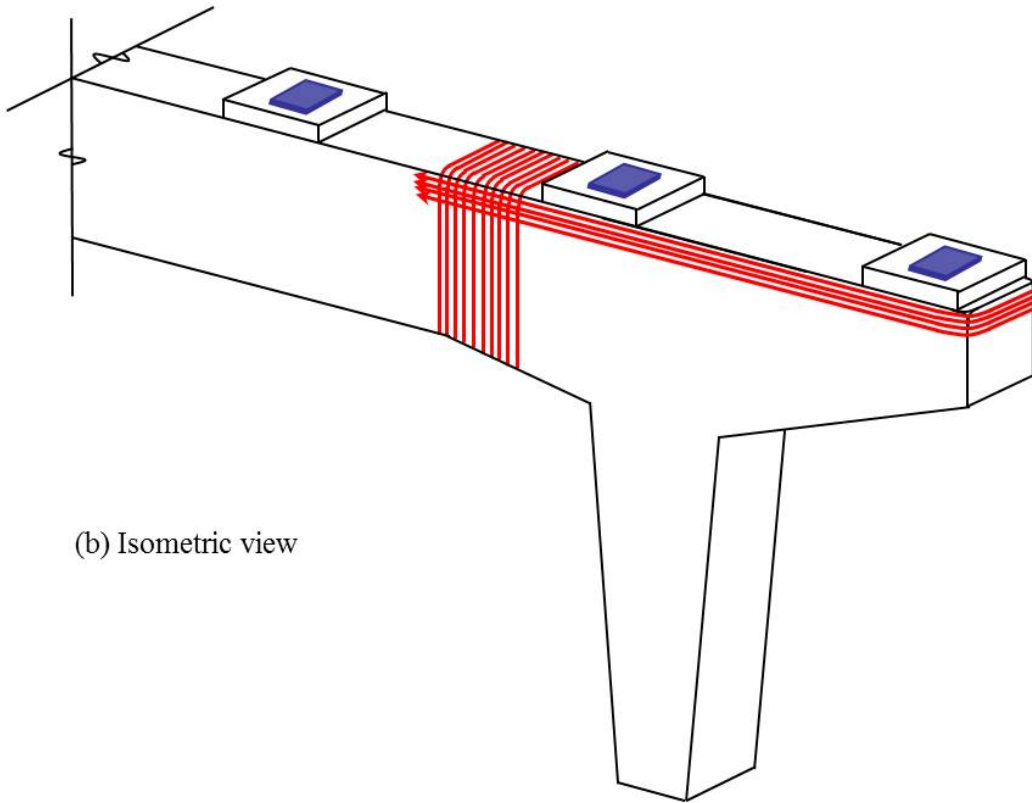


Figure B3. Elevation view of the strengthened concrete bridge pier showing the CFRP strengthened cantilever section

Appendix "B"



(a) The main CFRP flexural reinforcement for the cantilever section



(b) Isometric view

Figure B4. Isometric view of the CFRP strengthened cantilever section of the concrete bridge pier.

Appendix “C”

Shear Strengthening of a reinforced concrete cantilever beam with CFRP (ignoring internal steel shear reinforcement):

Completely wrapping scheme

A reinforced concrete cantilever beam is transversely reinforced with #3@12” shear reinforcement, (see Figures C1 & C2 on Pages 503 & 504). The beam section is subjected to an ultimate shear force of 192.4 kips. Assume that the internal shear rebars are corroded, and do not provide any shear resistance. Design a CFRP shear reinforcement system to resist the external ultimate shear force. Use a complete wrapping scheme.

Given Values

$$f_c' = 7000 \text{ psi} = 7 \text{ ksi}$$

$$\beta_1 = 0.85 - \frac{0.05(f_c' - 4000)}{1000} = 0.7$$

$$f_y = 65000 \text{ psi} = 65 \text{ ksi}$$

$$E_c = 57000\sqrt{f_c'} = 4768962 \text{ psi} = 4769.0 \text{ ksi}$$

$$E_s = 29000000 \text{ psi} = 29000 \text{ ksi}$$

$$A_s (8\#7 \text{ bars}) = 4.8 \text{ in}^2$$

$$h = 48 \text{ in}$$

$$d = 44.625 \text{ in}$$

$$b = 24 \text{ in}$$

Step 1 Compute the design material properties.

$$C_E = 0.85 \text{ for Environmental factor of exterior exposure}$$

$$t_f = 0.0066 \text{ in a layer}$$

$$E_f = 33400000 \text{ psi} = 33400 \text{ ksi}$$

$$\varepsilon_{fu}^* = 0.017$$

$$\varepsilon_{fu} = C_E \varepsilon_{fu}^* = 0.0144$$

$$f_{fu} = \varepsilon_{fu} E_f = 480960 \text{ psi} = 481 \text{ ksi}$$

$$n_f = \frac{E_f}{E_c} = \frac{33400}{4769.0} = 7$$

Step 2 Calculate the effective strain level in the CFRP shear reinforcement for the completely wrapping scheme.

$$\varepsilon_{fe} = 0.004 \leq 0.75\varepsilon_{fu} = 0.0108 \text{ O.K.}$$

Step3 Calculate the contribution of the CFRP reinforcement to the shear strength.

$$A_{vf} = 2nt_f w_f = 2(1)(0.0066)(10) = 0.132 \text{ in}^2$$

$$f_{fe} = \varepsilon_{fe} E_f = 0.004 * 33400 = 133.6 \text{ ksi}$$

$$V_f = \frac{A_f f_{fe} d_f (\sin \alpha + \cos \alpha)}{s_f} = \frac{(0.132)(133.6)(44.625)(\sin 45 + \cos 45)}{18} = 61.83 \text{ kips}$$

Step 4 Calculate the shear strength of the section.

Ignore the internal shear reinforcement due to corrosions.

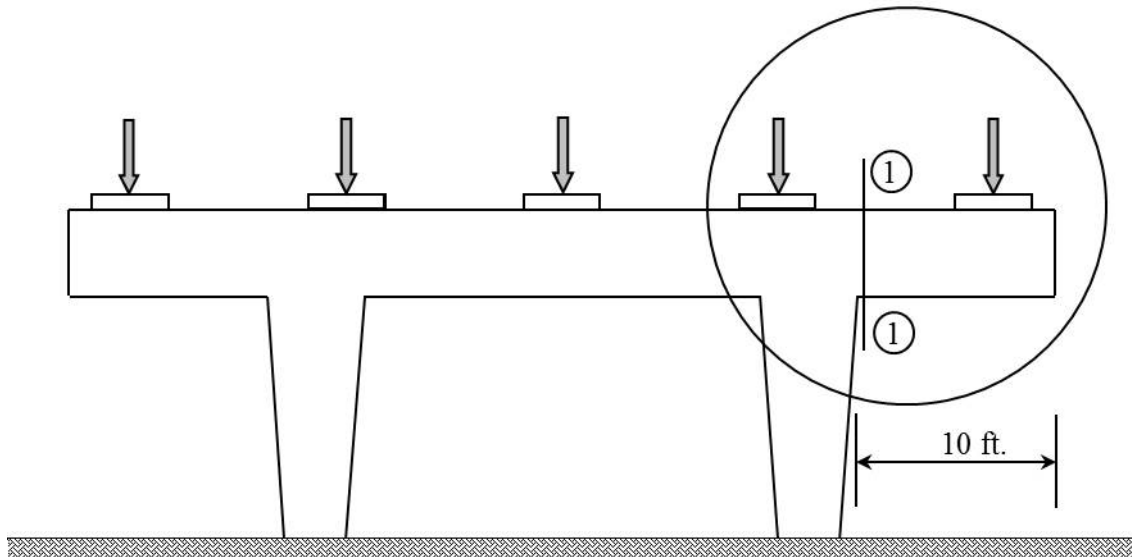
$$\phi = 0.85 \text{ and } \psi_f = 0.95$$

$$V_s = \frac{A_v f_y d}{s} = 0 \text{ kips}$$

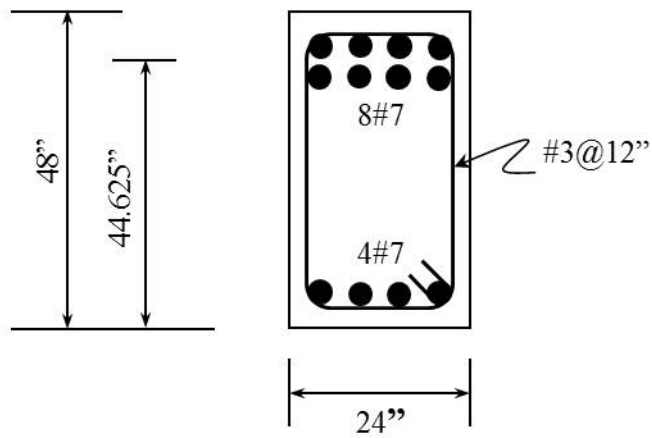
$$V_c = 2\sqrt{f_c'}bd = 2(\sqrt{7000})(24)(44.625) = 179.2 \text{ kips}$$

$$\phi V_n = \phi(V_c + V_s + \psi_f V_f) = 0.85(179.2 + 0 + 0.95(61.8)) = 202.3 \text{ kips} \geq V_u = 192.4 \text{ kips} \text{ O.K.}$$

Appendix "C, D, E, & F"



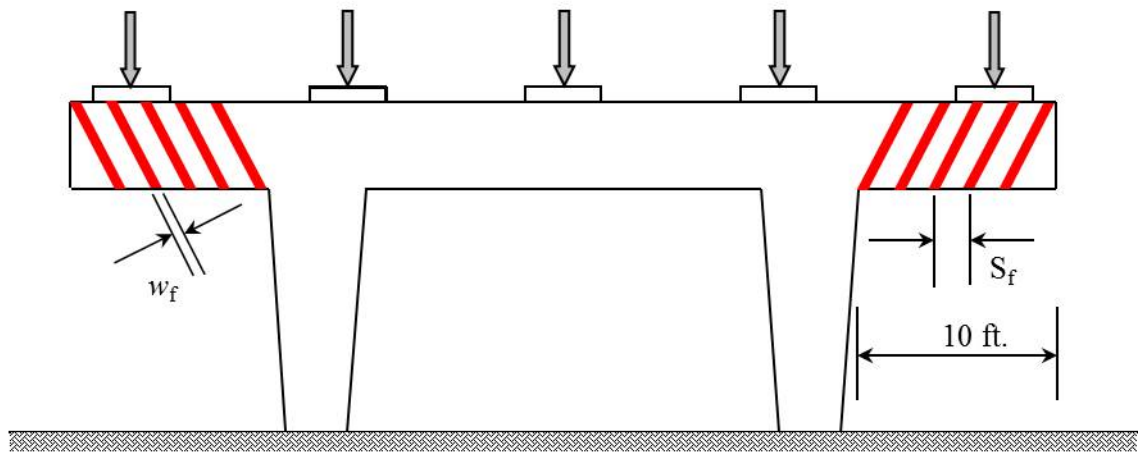
(a) Elevation view of the existing bridge pier



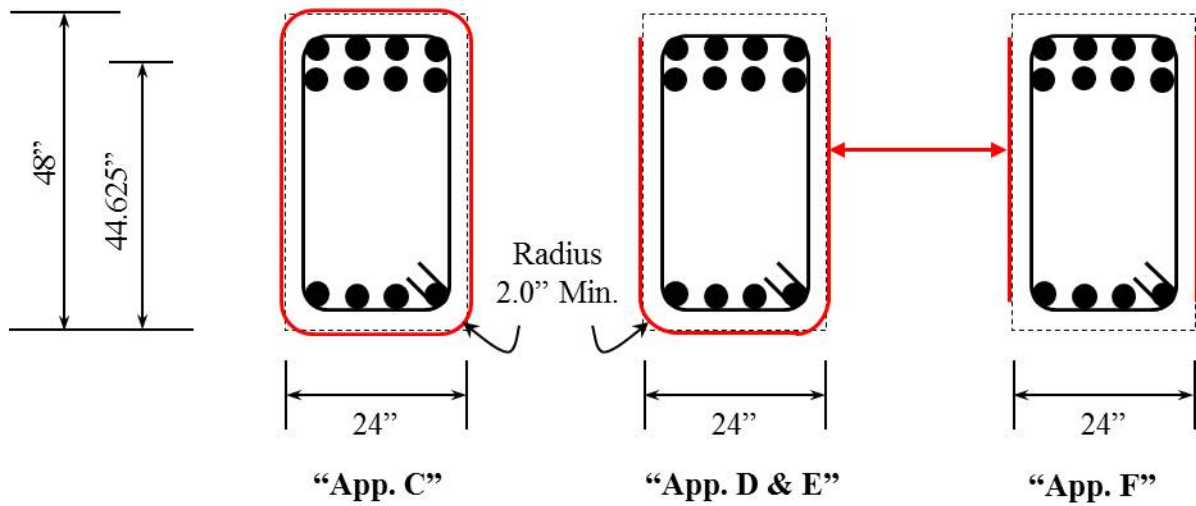
(b) Section 1-1

Figure C1. Concrete bridge pier cap beam with inadequate shear strength.

Appendix “C, D, E, & F”



(a) Elevation view of the existing bridge pier



(b) Section 1-1

Figure C2. Concrete bridge pier cap beam with inadequate shear strength.

Appendix “D”

Shear Strengthening of a reinforced concrete cantilever beam with CFRP (considering internal steel shear reinforcement):

U-shape wrapping scheme

A reinforced concrete cantilever beam is transversely reinforced with #3@12” shear reinforcement, (see Figures C1 & C2 on Pages 501 & 502). The beam section is subjected to an ultimate shear force of 192.4 kips. Design a CFRP shear reinforcement system to resist the external ultimate shear force. Use a U-shaped wrapping scheme.

Given Values

$$f_c' = 7000 \text{ psi} = 7 \text{ ksi}$$

$$\beta_1 = 0.85 - \frac{0.05(f_c' - 4000)}{1000} = 0.7$$

$$f_y = 65000 \text{ psi} = 65 \text{ ksi}$$

$$E_c = 57000\sqrt{f_c'} = 4768962 \text{ psi} = 4769.0 \text{ ksi}$$

$$E_s = 29000000 \text{ psi} = 29000 \text{ ksi}$$

$$A_s (8\#7 \text{ bars}) = 4.8 \text{ in}^2$$

$$h = 48 \text{ in}$$

$$d = 44.625 \text{ in}$$

$$b = 24 \text{ in}$$

$$A_v (\#3 @ 12 \text{ in}) = 0.22 \text{ in}^2$$

$$s(\text{spacing}) = 12 \text{ in}$$

Step 1 Compute the design material properties.

$$C_E = 0.85 \text{ for Environmental factor of exterior exposure}$$

$$t_f = 0.0066 \text{ in / a layer}$$

$$E_f = 33400000 \text{ psi} = 33400 \text{ ksi}$$

$$\varepsilon_{fu}^* = 0.017$$

$$\varepsilon_{fu} = C_E \varepsilon_{fu}^* = 0.0144$$

$$f_{fu} = \varepsilon_{fu} E_f = 480960 \text{ psi} = 481 \text{ ksi}$$

$$n_f = \frac{E_f}{E_c} = \frac{33400}{4769} = 7.00$$

Step 2 Calculate the effective strain level in the CFRP shear reinforcement for the completely wrapping scheme.

$$L_e = \frac{2500}{\sqrt[0.58]{nt_f E_f}} = \frac{2500}{\sqrt{(2)(0.0066)(33400000)}} = 1.33 \text{ in}$$

$$k_1 = \sqrt[2/3]{\frac{f'_c}{4000}} = \sqrt[2/3]{\frac{7000}{4000}} = 1.45$$

$$k_2 = \frac{d_f - L_e}{d_f} = \frac{44.625 - 1.33}{44.625} = 0.970$$

$$k_v = \frac{k_1 k_2 L_e}{468 \varepsilon_{fu}} = \frac{(1.45)(0.970)(1.33)}{(468)(0.0144)} = 0.278 \leq 0.75 \text{ O.K.}$$

$$\varepsilon_{fe} = k_v \varepsilon_{fu} = (0.278)(0.0144) = 0.0040 \leq 0.004 \text{ O.K.}$$

Step3 Calculate the contribution of the CFRP reinforcement to the shear strength.

$$A_{vf} = 2nt_f w_f = 2(2)(0.0066)(10) = 0.264 \text{ in}^2$$

$$f_{fe} = \varepsilon_{fe} E_f = 0.004 * 33400 = 133.8 \text{ ksi}$$

$$V_f = \frac{A_f f_{fe} d_f (\sin \alpha + \cos \alpha)}{s_f} = \frac{(0.264)(133.8)(44.625)(\sin 45 + \cos 45)}{18} = 87.6 \text{ kips}$$

Step 4 Calculate the shear strength of the section.

Ignore the internal shear reinforcement due to corrosions.

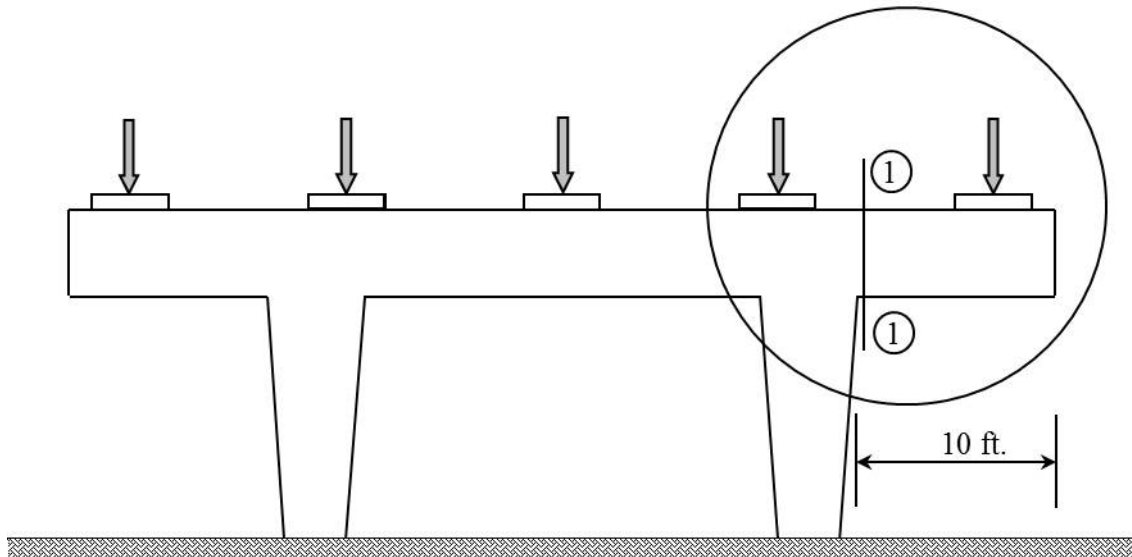
$$\phi = 0.85 \text{ and } \psi_f = 0.85$$

$$V_s = \frac{A_v f_y d}{s} = 53.2 \text{ kips}$$

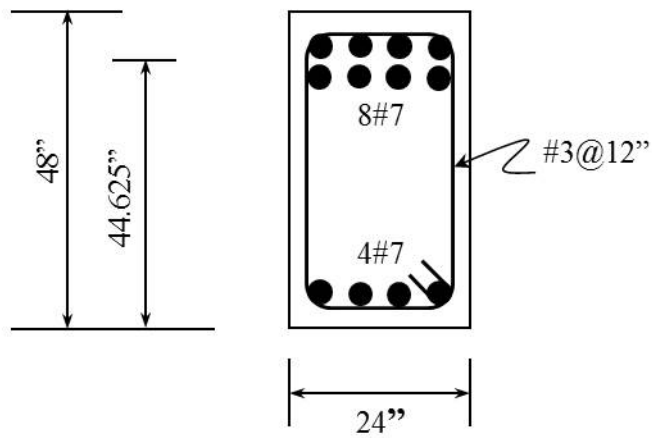
$$V_c = 2\sqrt{f'_c} bd = 2(\sqrt{7000})(24)(44.625) = 179.2 \text{ kips}$$

$$\phi V_n = \phi(V_c + V_s + \psi_f V_f) = 0.85(179.2 + 53.2 + 0.85(87.6)) = 260.8 \text{ kips} \geq V_u = 240.5 \text{ kips} \text{ Good.}$$

Appendix "C, D, E, & F"



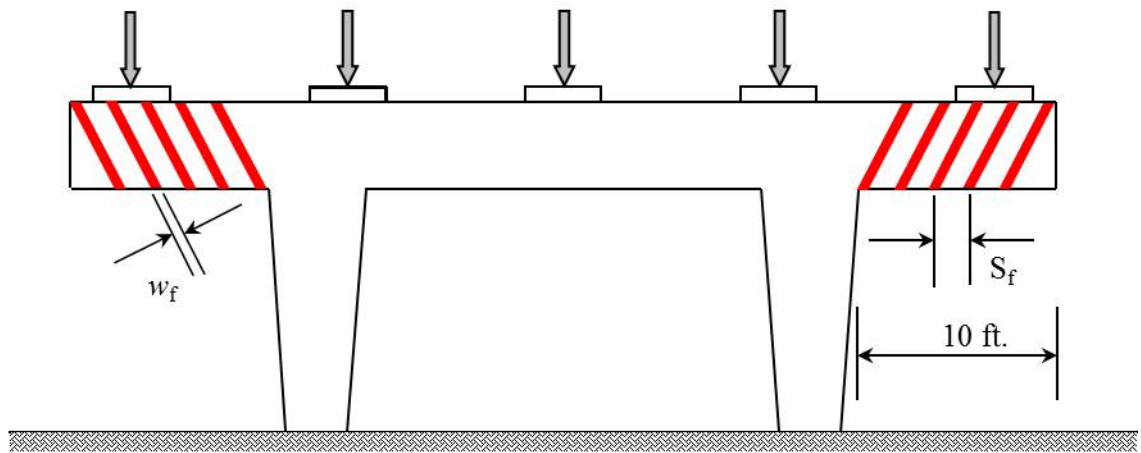
(a) Elevation view of the existing bridge pier



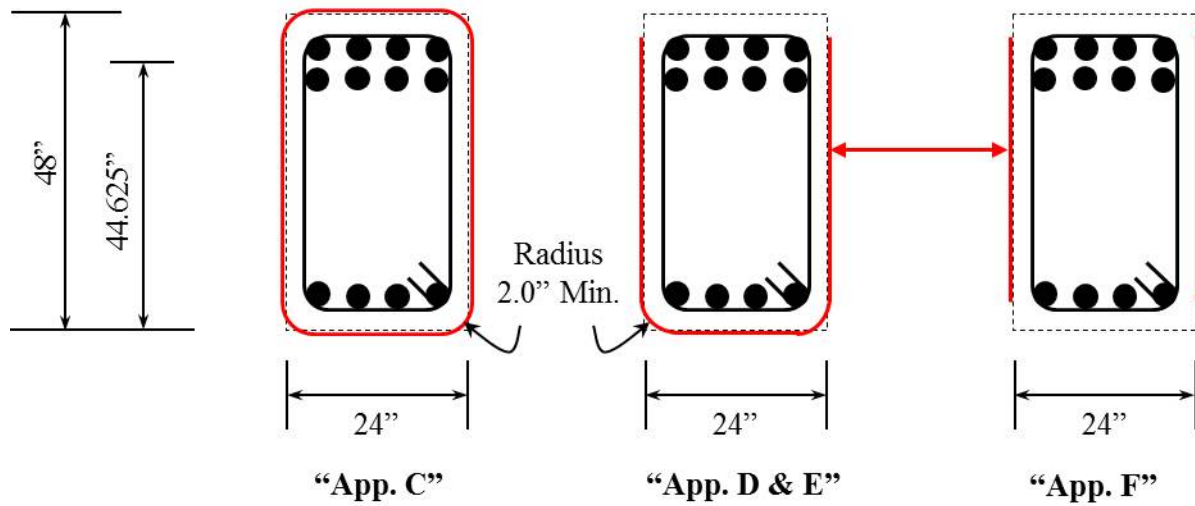
(b) Section 1-1

Figure C1. Concrete bridge pier cap beam with inadequate shear strength.

Appendix “C, D, E, & F”



(a) Elevation view of the existing bridge pier



(b) Section 1-1

Figure C2. Concrete bridge pier cap beam with inadequate shear strength.

Appendix “E”

Shear Strengthening of a reinforced concrete cantilever beam with CFRP (ignoring internal steel shear reinforcement):

U-shape wrapping scheme

A reinforced concrete cantilever beam is transversely reinforced with #3@12” shear reinforcement, (see Figures C1 & C2 on Pages 501 & 502). The beam section is subjected to an ultimate shear force of 192.4 kips. Assume that the internal shear rebars are corroded, and do not provide any shear resistance. Design a CFRP shear reinforcement system to resist the external ultimate shear force. Use a U-shaped wrapping scheme.

Given Values

$$f_c' = 7000 \text{ psi} = 7 \text{ ksi}$$

$$\beta_1 = 0.85 - \frac{0.05(f_c' - 4000)}{1000} = 0.7$$

$$f_y = 65000 \text{ psi} = 65 \text{ ksi}$$

$$E_c = 57000\sqrt{f_c'} = 4768962 \text{ psi} = 4769.0 \text{ ksi}$$

$$E_s = 29000000 \text{ psi} = 29000 \text{ ksi}$$

$$A_s (8\#7 \text{ bars}) = 4.8 \text{ in}^2$$

$$h = 48 \text{ in}$$

$$d = 44.625 \text{ in}$$

$$b = 24 \text{ in}$$

Step 1 Compute the design material properties.

$$C_E = 0.85 \text{ for Environmental factor of exterior exposure}$$

$$t_f = 0.0066 \text{ in / a layer}$$

$$E_f = 33400000 \text{ psi} = 33400 \text{ ksi}$$

$$\varepsilon_{fu}^* = 0.017$$

$$\varepsilon_{fu} = C_E \varepsilon_{fu}^* = 0.0144$$

$$f_{fu} = \varepsilon_{fu} E_f = 480960 \text{ psi} = 481 \text{ ksi}$$

$$n_f = \frac{E_f}{E_c} = \frac{33400}{4769} = 7.00$$

Step 2 Calculate the effective strain level in the CFRP shear reinforcement for the completely wrapping scheme.

$$L_e = \frac{2500}{\sqrt[0.58]{nt_f E_f}} = \frac{2500}{\sqrt{(2)(0.0066)(33400000)}} = 1.33 \text{ in}$$

$$k_1 = \sqrt[2/3]{\frac{f'_c}{4000}} = \sqrt[2/3]{\frac{7000}{4000}} = 1.45$$

$$k_2 = \frac{d_f - L_e}{d_f} = \frac{44.625 - 1.33}{44.625} = 0.945$$

$$k_v = \frac{k_1 k_2 L_e}{468 \varepsilon_{fu}} = \frac{(1.45)(0.945)(1.33)}{(468)(0.0144)} = 0.271 \leq 0.75 \text{ O.K.}$$

$$\varepsilon_{fe} = k_v \varepsilon_{fu} = (0.271)(0.0144) = 0.0039 \leq 0.004 \text{ O.K.}$$

Step3 Calculate the contribution of the CFRP reinforcement to the shear strength.

$$A_{vf} = 2 n t_f w_f = 2(2)(0.0066)(10) = 0.264 \text{ in}^2$$

$$f_{fe} = \varepsilon_{fe} E_f = 0.0039 * 33400 = 130.31 \text{ ksi}$$

$$V_f = \frac{A_f f_{fe} d_f (\sin \alpha + \cos \alpha)}{s_f} = \frac{(0.264)(130.31)(44.625)(\sin 45 + \cos 45)}{18} = 64.87 \text{ kips}$$

Step 4 Calculate the shear strength of the section.

Ignore the internal shear reinforcement due to corrosions.

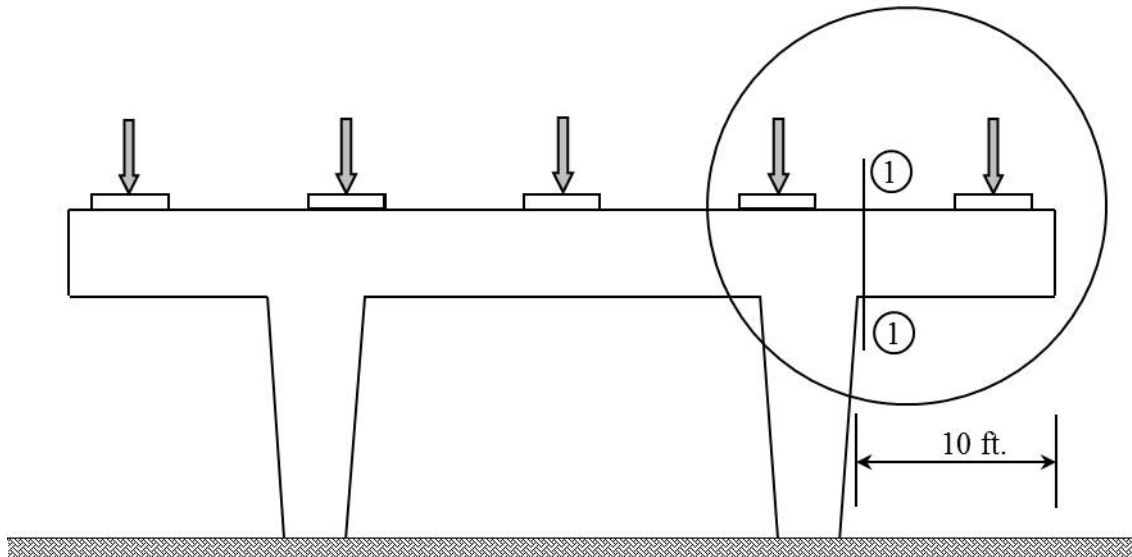
$$\phi = 0.85 \text{ and } \psi_f = 0.85$$

$$V_s = \frac{A_v f_y d}{s} = 0 \text{ kips}$$

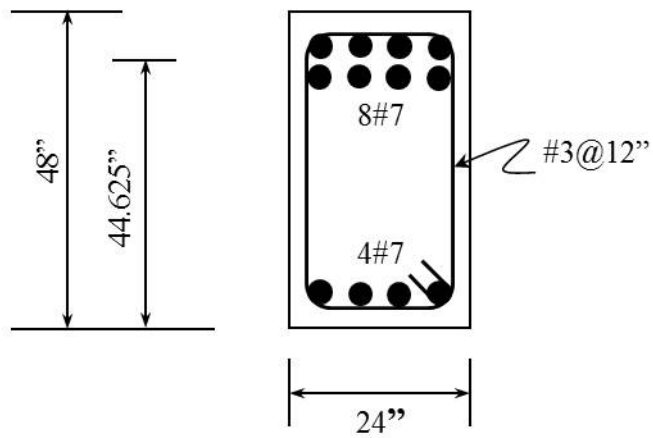
$$V_c = 2\sqrt{f'_c} b d = 2(\sqrt{7000})(24)(44.625) = 179.2 \text{ kips}$$

$$\phi V_n = \phi(V_c + V_s + \psi_f V_f) = 0.85(179.2 + 0 + 0.85(64.87)) = 199.2 \text{ kips} \geq V_u = 192.4 \text{ kips} \text{ Good.}$$

Appendix "C, D, E, & F"



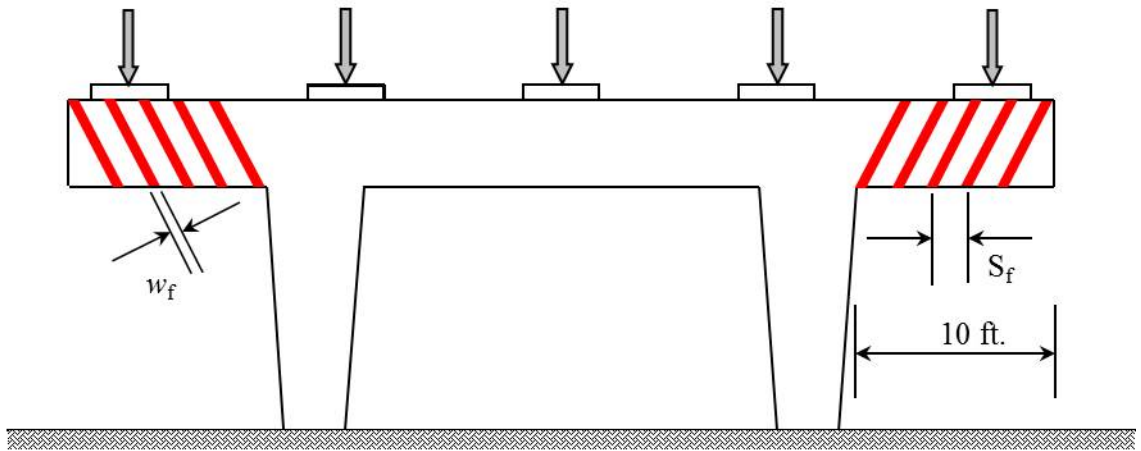
(a) Elevation view of the existing bridge pier



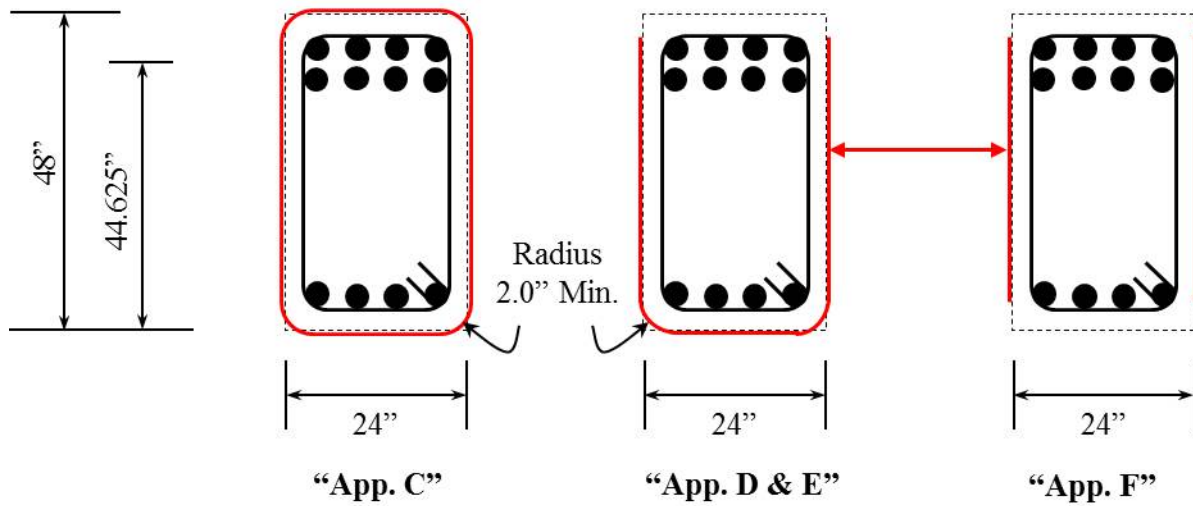
(b) Section 1-1

Figure C1. Concrete bridge pier cap beam with inadequate shear strength.

Appendix “C, D, E, & F”



(a) Elevation view of the existing bridge pier



(b) Section 1-1

Figure C2. Concrete bridge pier cap beam with inadequate shear strength.

Appendix “F”

Shear Strengthening of a reinforced concrete cantilever beam with CFRP ignored internal shear reinforcement:

Two-side bonded scheme

A reinforced concrete cantilever beam is transversely reinforced with #3@12” shear reinforcement, (see Figures C1 & C2 on Pages 501 & 502). The beam section is subjected to an ultimate shear force of 192.4 kips. Assume that the internal shear rebars are corroded, and do not provide any shear resistance. Design a CFRP shear reinforcement system to resist the external ultimate shear force. Use a two-sided FRP reinforcement scheme.

Given Values

$$f_c' = 7000 \text{ psi} = 7 \text{ ksi}$$

$$\beta_1 = 0.85 - \frac{0.05(f_c' - 4000)}{1000} = 0.7$$

$$f_y = 65000 \text{ psi} = 65 \text{ ksi}$$

$$E_c = 57000 \sqrt{f_c'} = 4768962 \text{ psi} = 4769.0 \text{ ksi}$$

$$E_s = 29000000 \text{ psi} = 29000 \text{ ksi}$$

$$A_s (8\#7 \text{ bars}) = 4.8 \text{ in}^2$$

$$h = 48 \text{ in}$$

$$d = 44.625 \text{ in}$$

$$b = 24 \text{ in}$$

Step 1 Compute the design material properties.

$$C_E = 0.85 \text{ for Environmental factor of exterior exposure}$$

$$t_f = 0.0066 \text{ in / a layer}$$

$$E_f = 33400000 \text{ psi} = 33400 \text{ ksi}$$

$$\varepsilon_{fu}^* = 0.017$$

$$\varepsilon_{fu} = C_E \varepsilon_{fu}^* = 0.0144$$

$$f_{fu} = \varepsilon_{fu} E_f = 480960 \text{ psi} = 481 \text{ ksi}$$

$$n_f = \frac{E_f}{E_c} = \frac{33400}{4769} = 7.00$$

Step 2 Calculate the effective strain level in the CFRP shear reinforcement for the completely wrapping scheme.

$$L_e = \frac{2500}{\sqrt[0.58]{nt_f E_f}} = \frac{2500}{\sqrt{(2)(0.0066)(33400000)}} = 1.33 \text{ in}$$

$$k_1 = \sqrt[2/3]{\frac{f'_c}{4000}} = \sqrt[2/3]{\frac{7000}{4000}} = 1.45$$

$$k_2 = \frac{d_f - 2L_e}{d_f} = \frac{44.625 - 2(1.33)}{44.625} = 0.889$$

$$k_v = \frac{k_1 k_2 L_e}{468 \varepsilon_{fu}} = \frac{(1.45)(0.889)(1.33)}{(468)(0.0144)} = 0.255 \leq 0.75 \text{ O.K.}$$

$$\varepsilon_{fe} = k_v \varepsilon_{fu} = (0.255)(0.0144) = 0.0037 \leq 0.004 \text{ O.K.}$$

Step3 Calculate the contribution of the CFRP reinforcement to the shear strength.

$$A_{vf} = 2nt_f w_f = 2(2)(0.0066)(10) = 0.264 \text{ in}^2$$

$$f_{fe} = \varepsilon_{fe} E_f = 0.0037 * 33400 = 122.66 \text{ ksi}$$

$$V_f = \frac{A_f f_{fe} d_f (\sin \alpha + \cos \alpha)}{s_f} = \frac{(0.264)(122.66)(44.625)(\sin 45 + \cos 45)}{18} = 61.06 \text{ kips}$$

Step 4 Calculate the shear strength of the section.

Ignore the internal shear reinforcement due to corrosions.

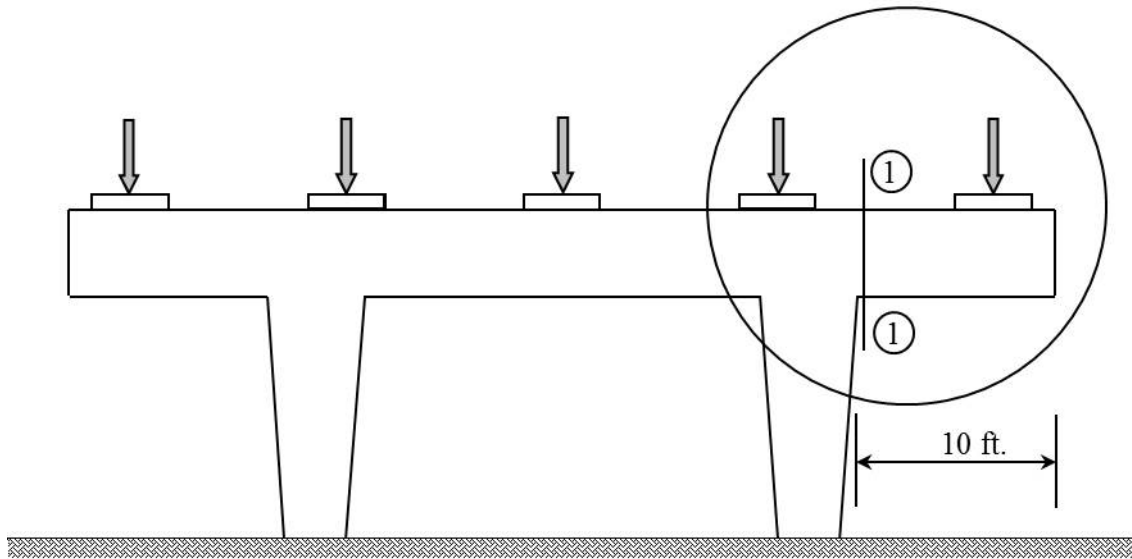
$$\phi = 0.85 \text{ and } \psi_f = 0.85$$

$$V_s = \frac{A_v f_y d}{s} = 0 \text{ kips}$$

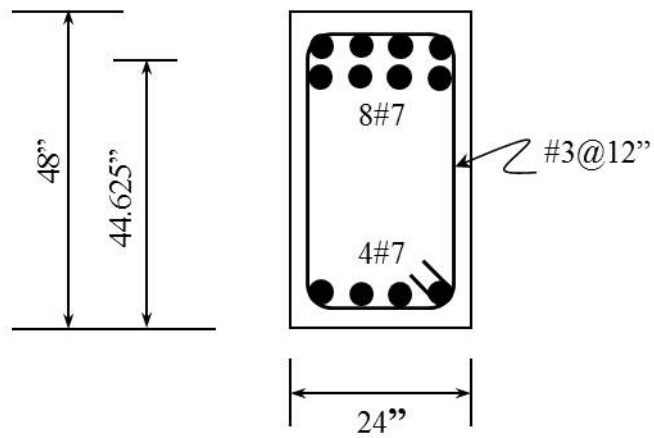
$$V_c = 2\sqrt{f'_c} bd = 2(\sqrt{7000})(24)(44.625) = 179.2 \text{ kips}$$

$$\phi V_n = \phi(V_c + V_s + \psi_f V_f) = 0.85(179.2 + 0 + 0.85(61.06)) = 196.4 \text{ kips} \geq V_u = 192.4 \text{ kips Good.}$$

Appendix "C, D, E, & F"



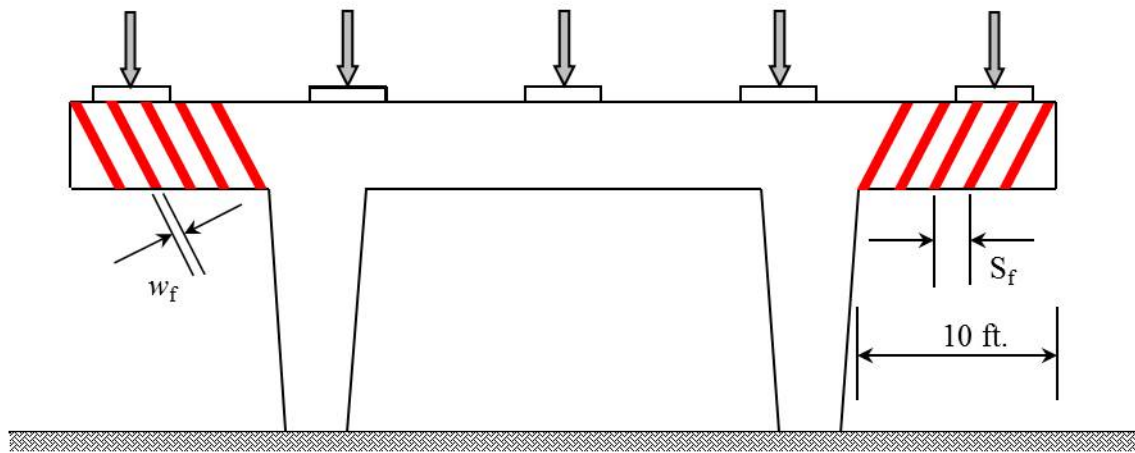
(a) Elevation view of the existing bridge pier



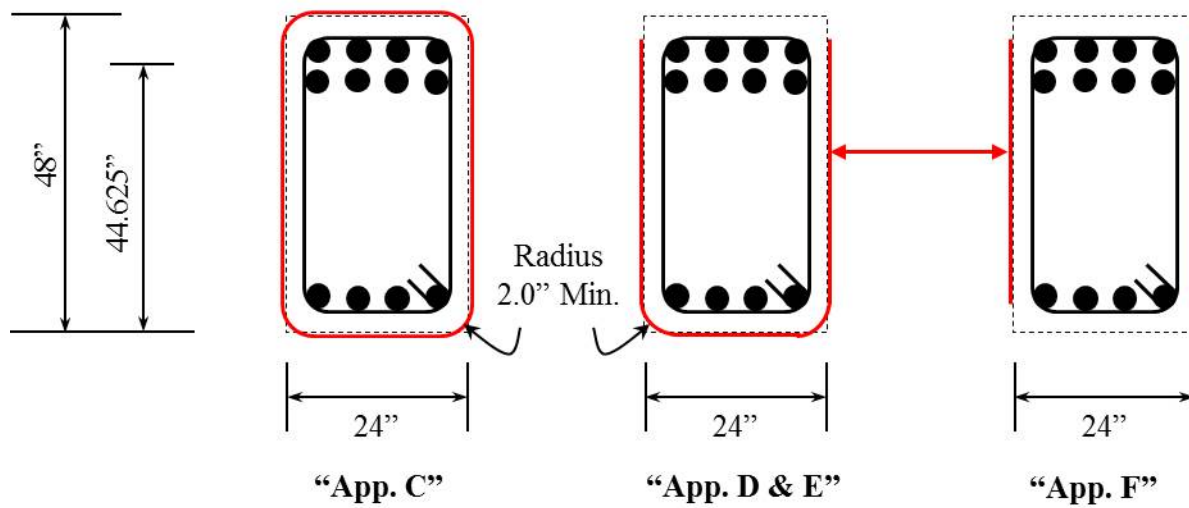
(b) Section 1-1

Figure C1. Concrete bridge pier cap beam with inadequate shear strength.

Appendix “C, D, E, & F”



(a) Elevation view of the existing bridge pier



(b) Section 1-1

Figure C2. Concrete bridge pier cap beam with inadequate shear strength.

Appendix “G”

Column Shear Strengthening with CFRP (considering internal steel shear reinforcement):

Complete wrapping scheme

A 24” x 48” rectangular column is longitudinally reinforced with 10# 10 rebars, and transversely reinforced with #4@8.0 inches., (see Figure G1 on Page 505). Design a CFRP shear reinforcement system to allow the column to resist a 25% increase over its existing ultimate shear strength.

Given Values

$$f_c' = 5000 \text{ psi} = 5 \text{ ksi}$$

$$\beta_1 = 0.85 - \frac{0.05(f_c' - 4000)}{1000} = 0.8$$

$$f_y = 65000 \text{ psi} = 65 \text{ ksi}$$

$$E_c = 57000\sqrt{f_c'} = 4030508 \text{ psi} = 4030.5 \text{ ksi}$$

$$E_s = 29000000 \text{ psi} = 29000 \text{ ksi}$$

$$A_s (10\#10 \text{ bars}) = 12.7 \text{ in}^2$$

$$A_v (\#4@8 \text{ in}) = 0.4 \text{ in}^2$$

$$h = 48 \text{ in}$$

$$d = 44.625 \text{ in}$$

$$b = 24 \text{ in}$$

Step 1 Compute the design material properties.

$C_E = 0.85$ for Environmental factor of exterior exposure

$t_f = 0.0066$ in a layer

$E_f = 33400000$ psi = 33400 ksi

$\varepsilon_{fu}^* = 0.017$

$\varepsilon_{fu} = C_E \varepsilon_{fu}^* = 0.0144$

$f_{fu} = \varepsilon_{fu} E_f = 480960$ psi = 481 ksi

$$n_f = \frac{E_f}{E_c} = \frac{33400}{4030.5} = 8.29$$

Step 2 Calculate the effective strain level in the CFRP shear reinforcement for the completely wrapping scheme.

$$\varepsilon_{fe} = 0.004 \leq 0.75 \varepsilon_{fu} = 0.0108 \text{ O.K.}$$

Step 3 Calculate the shear strength of the section.

$\phi = 0.85$ and $\psi_f = 0.95$

$$V_s = \frac{A_v f_y d}{s} = 145.8 \text{ kips}$$

$N_u = 0$ kips assumed

$$V_c = 2\sqrt{f_c'} bd = 2(\sqrt{5000})(24)(44.865) = 152.3 \text{ kips}$$

$$\phi V_n = \phi(V_c + V_s) = 0.85(152.3 + 145.8) = 253.4 \text{ kips (without CFRP)}$$

Increase 25% of original shear strength.

$$1.25 \phi V_n = 316.7 \text{ kips}$$

$$\Delta V_u = 1.25 \phi V_n - \phi(V_c + V_s) = 63.3 \text{ kips}$$

Step 4 Calculate the contribution of the CFRP reinforcement to the shear strength.

$$V_{f,reqd} = \frac{\Delta V_u}{(\phi\psi)} = \frac{63.3}{(0.85)(0.95)} = 78.4 \text{ kips}$$

$$A_{fv,reqd} = \frac{V_{f,reqd} s_f}{\varepsilon_{fe} E_f d_f} = \frac{78.4 s_f}{(0.004)(33400)(48)} = 0.01 s_f \text{ in}^2$$

Step 5 Determine the number of plies and strip width and spacing.

$$n = \frac{A_{f,reqd}}{2t_f w_f} = \frac{0.01 s_f}{2(0.0066)(w_f)} = 0.93 \text{ (} s_f = w_f \text{ : Continuously wrapped)}$$

$$n = 1$$

Use one ply (n=1) continuously along the height of the column.

Appendix "G"

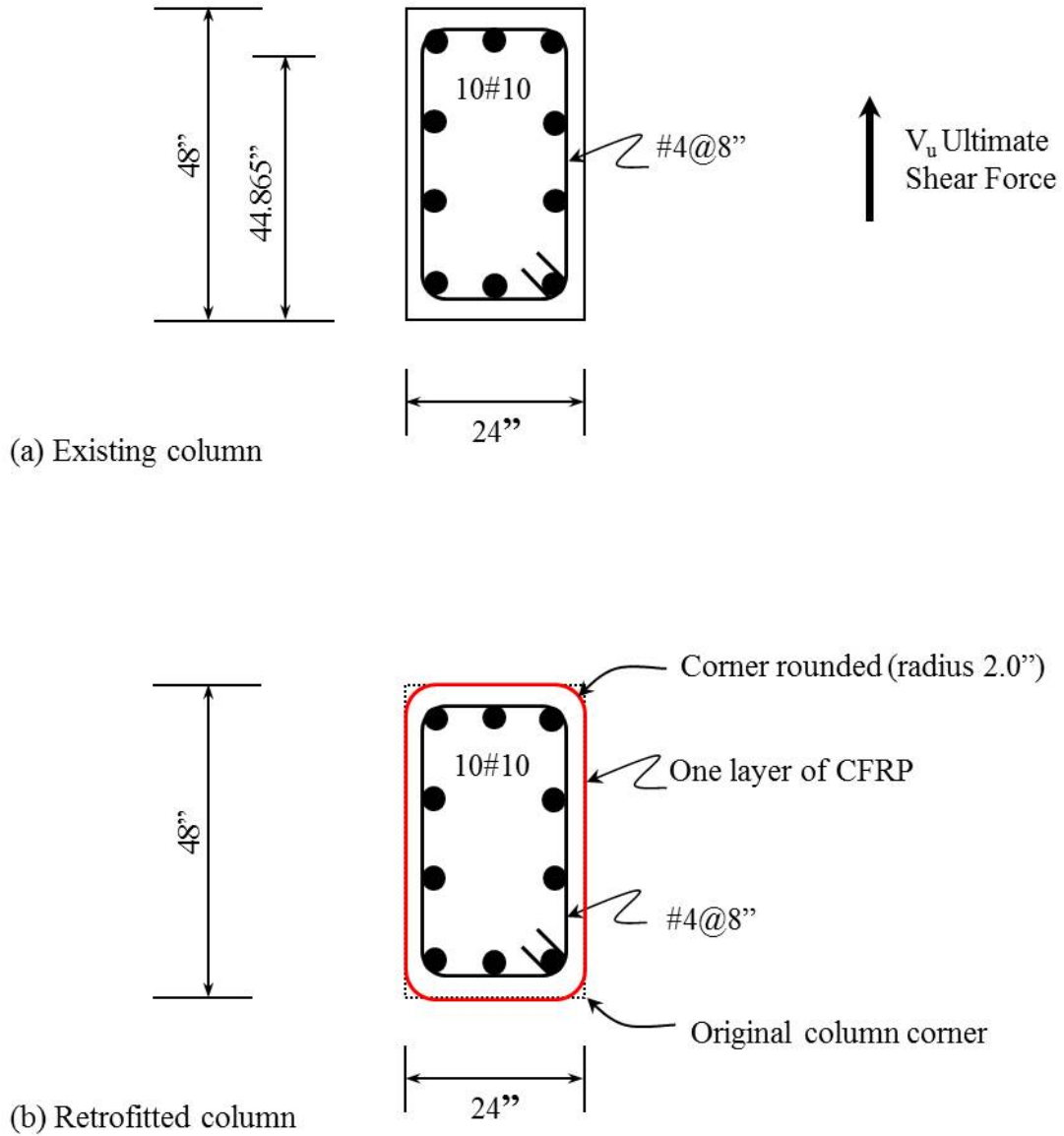


Figure G1. Shear Strengthening of rectangular concrete column.

Appendix “H”

Column Shear Strengthening with CFRP (ignoring internal steel shear reinforcement):

Complete wrapping scheme

A 24” x 48” rectangular column is longitudinally reinforced with 10# 10 rebars, and transversely reinforced with #4@8.0 inches., (see Figure H1 on Page 506). Assume that the internal shear rebars are corroded, and do not provide any shear resistance. Design a CFRP shear reinforcement system to resist an ultimate shear force of 253.4 kips.

Given Values

$$f_c' = 5000 \text{ psi} = 5 \text{ ksi}$$

$$\beta_1 = 0.85 - \frac{0.05(f_c' - 4000)}{1000} = 0.8$$

$$f_y = 65000 \text{ psi} = 65 \text{ ksi}$$

$$E_c = 57000\sqrt{f_c'} = 4030508 \text{ psi} = 4030.5 \text{ ksi}$$

$$E_s = 29000000 \text{ psi} = 29000 \text{ ksi}$$

$$A_s (10\#10 \text{ bars}) = 12.7 \text{ in}^2$$

$$A_v (\#4 @ 8 \text{ in}) = 0.4 \text{ in}^2$$

$$h = 48 \text{ in}$$

$$d = 44.625 \text{ in}$$

$$b = 24 \text{ in}$$

Step 1 Compute the design material properties.

$$C_E = 0.85 \text{ for Environmental factor of exterior exposure}$$

$$t_f = 0.0066 \text{ in a layer}$$

$$E_f = 33400000 \text{ psi} = 33400 \text{ ksi}$$

$$\varepsilon_{fu}^* = 0.017$$

$$\varepsilon_{fu} = C_E \varepsilon_{fu}^* = 0.0144$$

$$f_{fu} = \varepsilon_{fu} E_f = 480960 \text{ psi} = 481 \text{ ksi}$$

$$n_f = \frac{E_f}{E_c} = \frac{33400}{4030.5} = 8.29$$

Step 2 Calculate the effective strain level in the CFRP shear reinforcement for the completely wrapping scheme.

$$\varepsilon_{fe} = 0.004 \leq 0.75\varepsilon_{fu} = 0.0108 \text{ O.K.}$$

Step 3 Calculate the shear strength of the section.

Ignore the internal shear reinforcement due to corrosions.

$$\phi = 0.85 \text{ and } \psi_f = 0.95$$

$$V_s = \frac{A_v f_y d}{s} = 0 \text{ kips}$$

$$N_u = 0 \text{ kips assumed}$$

$$V_c = 2\sqrt{f_c'}bd = 2(\sqrt{5000})(24)(44.865) = 152.3 \text{ kips}$$

$$\phi V_c = 0.85(152.3) = 129.46 \text{ kips}$$

$$\phi V_s = 0 \text{ kips}$$

$$V_u = 253.4 \text{ kips}$$

$$\Delta V_f = V_u - \phi V_c - \phi V_s = 123.94 \text{ kips}$$

Step 4 Calculate the contribution of the CFRP reinforcement to the shear strength.

$$V_{f,reqd} = \frac{\Delta V_f}{(\phi\psi)} = \frac{123.94}{(0.85)(0.95)} = 153.49 \text{ kips}$$

$$A_{fv,reqd} = \frac{V_{f,reqd} s_f}{\varepsilon_{fe} E_f d_f} = \frac{153.49 s_f}{(0.004)(33400)(48)} = 0.02 s_f \text{ in}^2$$

Step 5 Determine the number of plies and strip width and spacing.

$$n = \frac{A_{f,reqd}}{2t_f w_f} = \frac{0.02s_f}{2(0.0066)(w_f)} = 1.81 \quad (s_f = w_f : \text{Continuously wrapped})$$

$$n = 2$$

Use two plies (n=2) continuously along the height of the column.

Appendix "H"

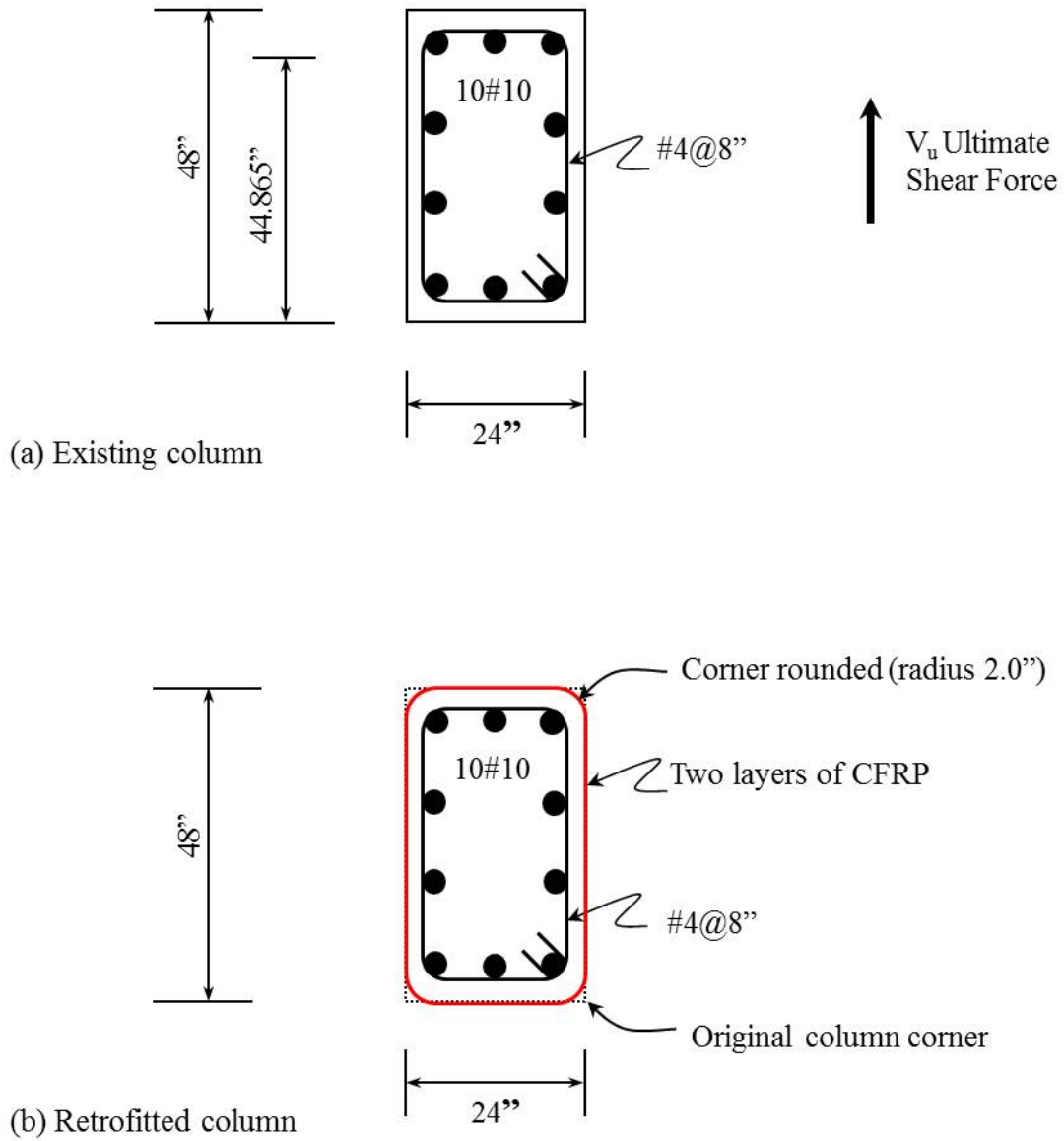


Figure H1. Shear Strengthening of rectangular concrete column, (Ignore internal transverse steel stirrups).

Appendix “I”

Retrofit of a Circular Concrete Column

(Increasing axial capacity of the concrete column)

A circular column is constructed of concrete of a uniaxial compressive strength of $f_c' = 4$ ksi. The column diameter is 18 inches, and reinforced with 10#10 longitudinal deformed steel bars and #3 spiral hoop. Please see Figure I1 on Page 507.

The applied loads on the column are as follows;

- Dead load : 280 kips
- Live load : 300 kips

Due to changes in the use of the structure, the column is required to carry 40% more axial live load. Determine the amount of CFRP composite to be used as a column continuous wrap to achieve the requirement. Assume there is no column moment.

CFRP composite properties

- $t_f = 0.0066$ in a layer
- $E_f = 33400$ ksi
- $\varepsilon_{fu}^* = 0.017$ in/in (Provided by manufacturer)
- $C_E = 0.85$ (Environmental Exposure Reduction Factor for Exterior CFRP)

Calculate existing column capacity

$$\phi P_{n(Existing)} = 0.85\phi[0.85f_c'(A_g - A_{st}) + f_y A_{st}] \quad (ACI10.3.5.1)$$

$$A_g = \frac{\pi d^2}{4} = \frac{\pi(18in)^2}{4} = 254.5 in^2$$

$$A_{st} = (10 bars)(1.27 in^2) = 12.7 in^2$$

$$\phi = 0.75 \text{ for spiral reinf orced column (ACI 318 - 9.3.2.2b)}$$

$$\phi P_{n(Existing)} = 0.85(0.75)[0.85(4)(254.5 - 12.7) + (60)(12.7)] = 1009.9 \text{ kips}$$

Required ultimate column capacity

$$\phi P_{n(\text{Req'd.})} = 1.4(P_{DL(\text{Req'd.})}) + 1.7(P_{LL(\text{Req'd.})}) = (1.4)(280 \text{ kips}) + (1.7)(1.4)(300 \text{ kips}) = 1106 \text{ kips}$$

$$\phi P_{n(\text{Req'd.})} = 1106 \text{ kips} \geq \phi P_{n(\text{Existing})} = 1009.9 \text{ kips}$$

Strengthening of column required

Check existing column capacity versus reduced factored demand

$$\phi P_{n(\text{Existing})} \geq 1.2(P_{DL(\text{Req'd.})} + P_{LL(\text{Req'd.})})$$

$$1009.9 \text{ kips} \geq 1.2(280 \text{ kips} + 420 \text{ kips}) = 840 \text{ kips}$$

\therefore Column is eligible for strengthening.

General axial capacity equation for spirally reinforced column

$$\phi P_n = 0.85\phi[0.85\psi_f f_{cc}'(A_g - A_{st}) + f_y A_{st}]$$

Use FRP reduction factor $\psi_f = 0.95$

Calculate apparent concrete confining strength due to CFRP column wrap

$$f_{cc}' = f_c' \left[2.25 \sqrt{1 + 7.9 \frac{f_L}{f_c'} - 2 \frac{f_L}{f_c} - 1.25} \right] = (4 \text{ ksi}) \left[2.25 \sqrt{1 + 7.9 \frac{0.194}{4} - 2 \left(\frac{0.194}{4} \right) - 1.25} \right] = 5.2 \text{ ksi}$$

Where confining pressure provided by CFRP jacket, f_L , for a circular column can be calculated by :

$$f_L = \frac{\kappa_a \rho_f \varepsilon_{fe} E_f}{2} = \frac{(1)(0.00293)(0.004)(33400 \text{ ksi})}{2} = 0.194 \text{ ksi}$$

$\kappa_a = 1.0$ Efficiency factor for circular column

$$\rho_f = \frac{4nt_f}{D} = \frac{4(2 \text{ layers})(0.0066 \text{ in})}{18 \text{ in}} = 0.00194$$

$$\varepsilon_{fe} = 0.004 \leq 0.75 \varepsilon_{fu} = 0.75(0.0144 \text{ in/in}) = 0.011 \text{ in/in}$$

Calculate strengthened column axial capacity

$$\begin{aligned} \phi P_n &= 0.85 \phi [0.85 \psi_f f_{cc}' (A_g - A_{st}) + f_y A_{st}] \\ &= (0.85)(0.75) [(0.85)(0.95)(5.2 \text{ ksi})(254.5 - 12.7) + (60 \text{ ksi})(12.7)] \end{aligned}$$

$$\phi P_n = 1133 \text{ kips} \geq 1106 \text{ kips Good!}$$

Use 2 layers of CFRP composite sheets around column.

Appendix "I"

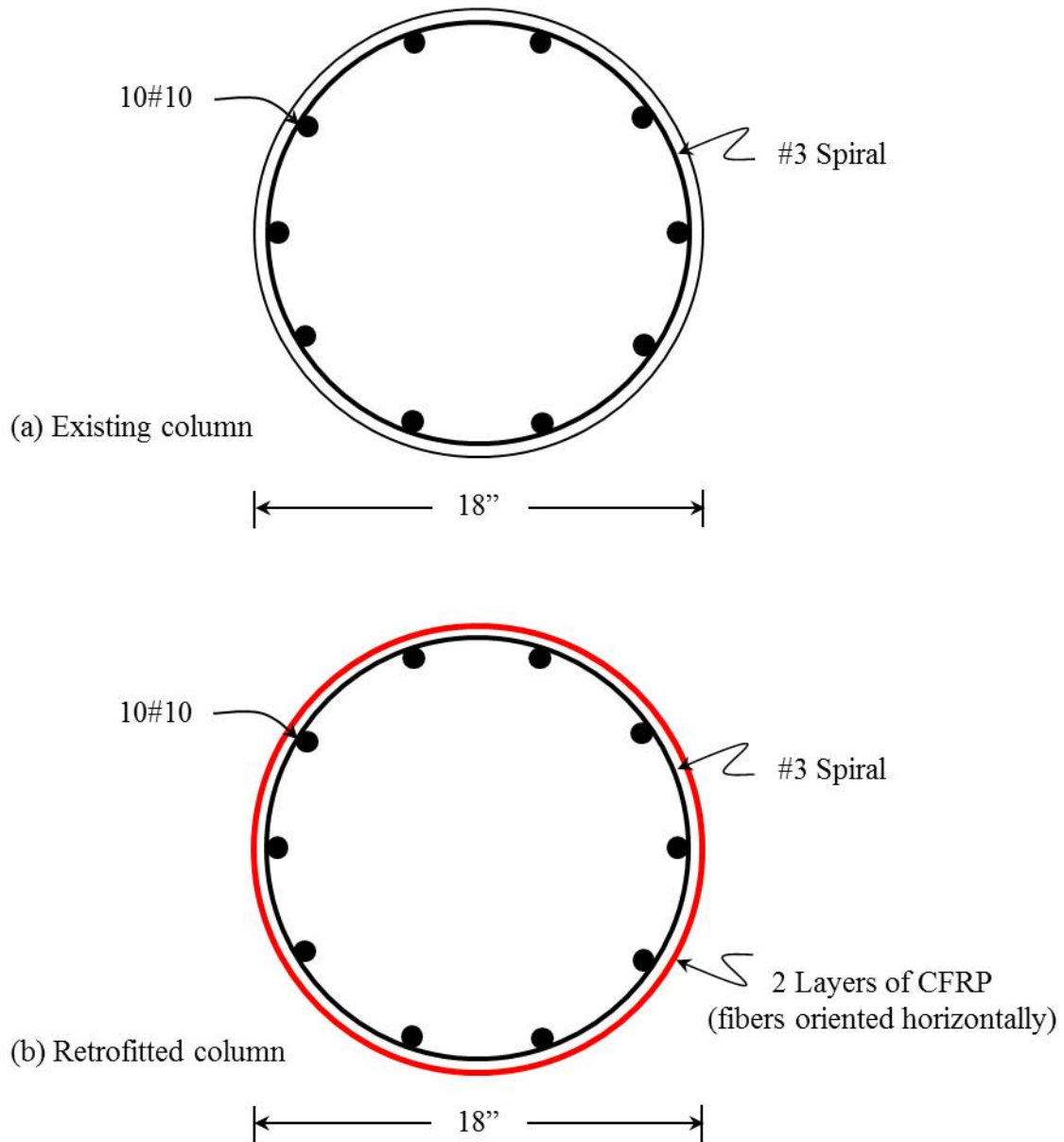


Figure II. Axial Strengthening of circular concrete column.

Appendix “J”

Retrofit of a Rectangular Concrete Column (Increasing axial capacity of the concrete column)

A rectangular column is constructed of concrete of a uniaxial compressive strength of $f_c' = 4$ ksi. The column is 18” by 30”, and reinforced with 10#10 longitudinal deformed steel bars and transversely reinforced with #3 tied hoops. Please see Figure J1 on Page 508.

The applied loads on the column are as follows;

- Dead load : 380 kips
- Live load : 400 kips

Due to changes in the use of the structure, the column is required to carry 40% more axial live load. Determine the amount of CFRP composite to be used as a column continuous wrap to achieve the requirement. Assume there is no column moment.

CFRP composite properties

- $t_f = 0.0066$ in a layer
- $E_f = 33400$ ksi
- $\epsilon_{fu}^* = 0.017$ in/in (Provided by manufacturer)
- $C_E = 0.85$ (Environmental Exposure Reduction Factor for Exterior CFRP)

Calculate existing column capacity

$$\phi P_{n(Existing)} = 0.80\phi[0.85f_c'(A_g - A_{st}) + f_y A_{st}] \quad (ACI318-10.3.6.2)$$

$$A_g = bh = (18)(30) = 540.0 \text{ in}^2$$

$$A_{st} = (10 \text{ bars})(1.27 \text{ in}^2) = 12.7 \text{ in}^2$$

$$\phi = 0.70 \text{ for tied reinforced column (ACI 318-9.3.2.2b)}$$

$$\phi P_{n(Existing)} = (0.8)(0.70)[0.85(4)(540.0 - 12.7) + (60)(12.7)] = 1430.7 \text{ kips}$$

Required ultimate column capacity

$$\phi P_{n(\text{Req'd.})} = 1.4(P_{DL(\text{Req'd.})}) + 1.7(P_{LL(\text{Req'd.})}) = (1.4)(380 \text{ kips}) + (1.7)(1.4)(400 \text{ kips}) = 1484.0 \text{ kips}$$

$$\phi P_{n(\text{Req'd.})} = 1484.0 \text{ kips} \geq \phi P_{n(\text{Existing})} = 1430.7 \text{ kips}$$

Strengthening of column is required

Check existing column capacity versus reduced factored demand

$$\phi P_{n(\text{Existing})} \geq 1.2(P_{DL(\text{Req'd.})} + P_{LL(\text{Req'd.})})$$

$$1430.7 \text{ kips} \geq 1.2(380 \text{ kips} + 560 \text{ kips}) = 1128 \text{ kips}$$

\therefore Column is eligible for strengthening.

General axial capacity equation for spirally reinforced column

$$\phi P_n = 0.80\phi [0.85\psi_f f_{cc}'(A_g - A_{st}) + f_y A_{st}]$$

Use FRP reduction factor $\psi_f = 0.95$

Calculate apparent concrete confining strength due to CFRP column wrap

$$f_{cc}' = f_c' \left[2.25 \sqrt{1 + 7.9 \frac{f_L}{f_c'}} - 2 \frac{f_L}{f_c'} - 1.25 \right] = (4 \text{ ksi}) \left[2.25 \sqrt{1 + 7.9 \frac{0.126}{4}} - 2 \left(\frac{0.126}{4} \right) - 1.25 \right] = 4.8 \text{ ksi}$$

Where confining pressure provided by CFRP jacket, f_L , for a rectangular column can be calculated by :

$$f_L = \frac{\kappa_a \rho_f \varepsilon_{fe} E_f}{2} = \frac{(0.8)(0.00235)(0.004)(33400 \text{ ksi})}{2} = 0.126 \text{ ksi}$$

$$\kappa_a = 1 - \frac{(b - 2r)^2 + (h - 2r)^2}{3bh(1 - \rho_g)} = 1 - \frac{(18 - (2)(17.5))^2 + (30 - (2)(17.5))^2}{(3)(18)(30)(1 - 0.0235)} = 0.8$$

$$\rho_g = \frac{A_{st}}{A_g} = \frac{12.7}{(18)(30)} = 0.0235$$

$$\rho_f = \frac{2nt_f(b + h)}{bh} = \frac{2(2 \text{ layers})(0.0066 \text{ in})(18 + 30)}{(18)(30)} = 0.00235$$

$$\varepsilon_{fe} = 0.004 \leq 0.75\varepsilon_{fu} = 0.75(0.0144 \text{ in/in}) = 0.011 \text{ in/in}$$

Calculate strengthened column axial capacity

$$\begin{aligned} \phi P_n &= 0.80 \phi [0.85 \psi_f f_{cc}' (A_g - A_{st}) + f_y A_{st}] \\ &= (0.80)(0.70) [(0.85)(0.95)(4.8 \text{ ksi})(540.0 - 12.7) + (60 \text{ ksi})(12.7)] \end{aligned}$$

$$\phi P_n = 1571 \text{ kips} \geq 1484 \text{ kips} \text{ Good!}$$

Use 2 layers of CFRP composite sheets around column.

Appendix “J”

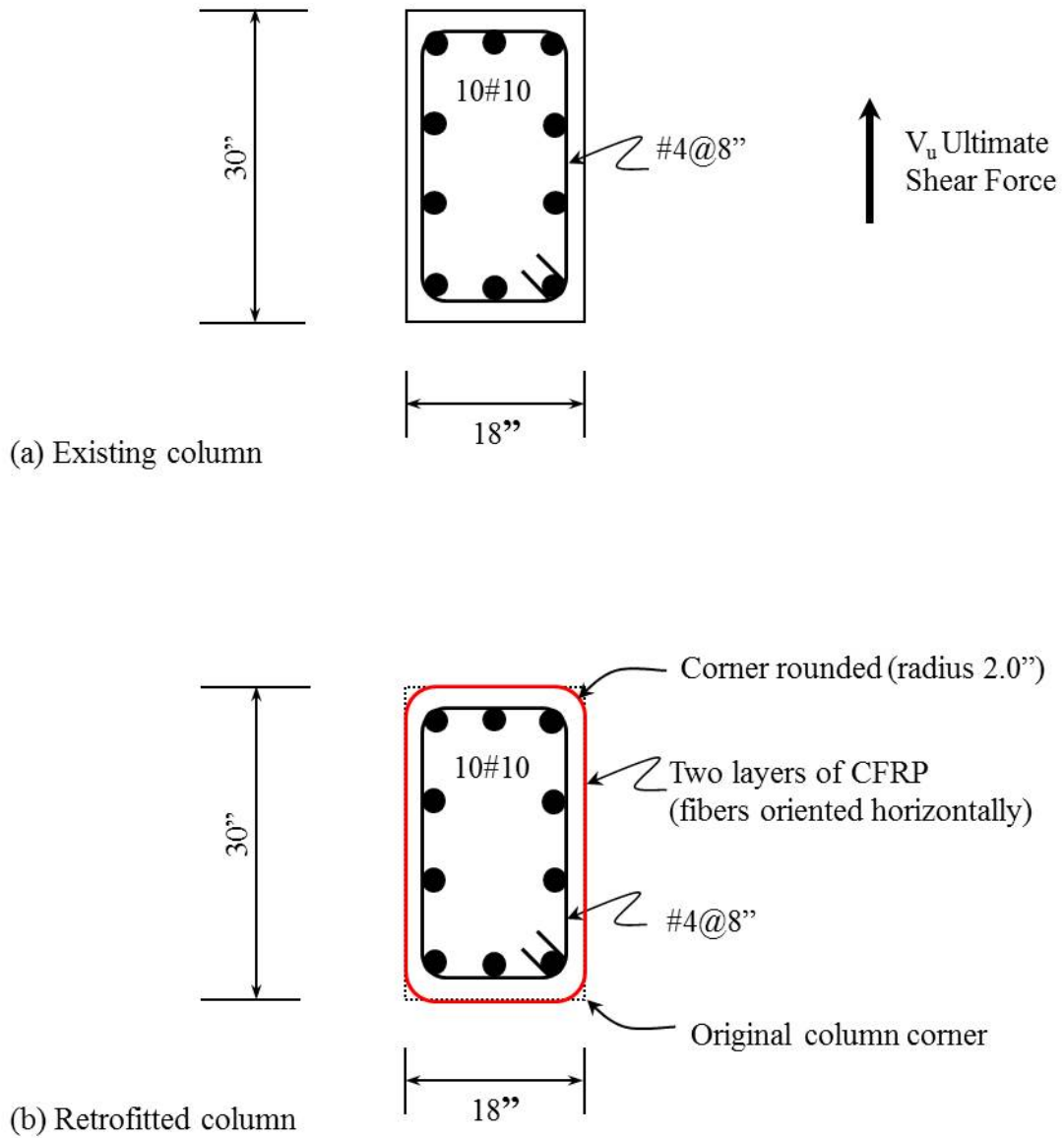


Figure J1. Axial Strengthening of rectangular concrete column.

Appendix “K”

Seismic Retrofit of a Rectangular Concrete Column With Inadequate Shear Strength

Figure K1 and K2 (on Pages 509 & 510) show the detail of a rectangular reinforced concrete column. It is required to provide the column with a carbon fiber reinforced jacket to convert the brittle shear failure to a ductile flexural failure with a target member displacement ductility of $\mu_{\Delta} \geq 8$.

Shear Strength Requirement

Maximum expected plastic shear demand including over-strength V_o equals

$$V_o = 1.5V_{yl} = 1.5 \frac{M_{yl}}{L} = 1.5 \frac{643}{1.250} = 771.6 \text{ kN}$$

Given values

$$H(\text{Height of column}) = 2.5 \text{ m}, L(\text{Length of shear span}) = 1.25 \text{ m}$$

$$D(\text{Column depth}) = 0.625 \text{ m}, B(\text{Column width}) = 0.420 \text{ m}$$

$$cc(\text{Concrete cover}) = 19 \text{ mm}, f_c'(\text{Concrete strength}) = 34.45 \text{ MPa}$$

$$\text{Longitudinal reinforcement (16\#7 bars of Grade 40)} : d_b = 22 \text{ mm} \& f_y = 303.16 \text{ MPa}$$

$$\text{Transverse reinforcement (Grade 40)} : d_b = 6 \text{ mm}, f_y = 303.16 \text{ MPa}, \& s = 127 \text{ mm}$$

$$P(\text{Axial load}) = 507 \text{ kN}, M_{yl} = 643 \text{ kN} - \text{m}$$

$$\phi_y(\text{Yield curvature}) = 0.0055 \text{ 1/m}, c_u(\text{Neutral axis depth}) = 115 \text{ mm}$$

$$V_c^i(\text{inside of the plastic region}) = 6 \text{ kN}$$

$$V_c^o(\text{Out side of the plastic region}) = 216 \text{ kN}$$

$$V_s = 183 \text{ kN}$$

$$V_p = 127 \text{ kN}$$

$$\phi_v = 0.85$$

$$E_f = 124 \text{ GPa}, f_{fu} = 1300 \text{ MPa}, \text{ and } \epsilon_{fu} = 0.01$$

The jacket thickness inside the plastic-hinge region (t_v^i) and outside the plastic-hinge region (t_v^o) can be determined as;

$$t_v^i = \frac{\frac{V_o}{\phi_v} - (V_c + V_s + V_p)}{2(0.004E_f D)} = \frac{\frac{772}{0.85} - (6 + 183 + 127)}{2 \times (0.004 \times 124020 \times 625)} \times 10^3 = 1.0 \text{ mm}$$

$$t_v^o = \frac{\frac{V_o}{\phi_v} - (V_c + V_s + V_p)}{2(0.004E_f D)} = \frac{\frac{772}{0.85} - (216 + 183 + 127)}{2 \times (0.004 \times 124020 \times 625)} \times 10^3 = 0.6 \text{ mm}$$

Flexural Plastic-Hinge Confinement Requirements

The confinement of the plastic hinge region was designed using a rectangular jacket with twice the jacket thickness required for an equivalent circular jacket with an effective diameter D_e of 753 mm.

Plastic hinge length (L_p)

$$L_p = 0.08L + 0.022f_{sy}d_b = 0.80 \times 1250 + 0.022 \times 303.16 \times 22 = 247 \text{ mm}$$

The required curvature ductility equals

$$\mu_\phi = 1 + \frac{8 - 1}{3(247/1250)[1 - 0.5(247/1250)]} = 14$$

The required ultimate strain is

$$\varepsilon_{cu} = \Phi_u c_u = \mu_\phi \Phi_y c_u = (14)(0.0055)(0.115) = 0.0089$$

The jacket thickness required to provide this ultimate concrete strain determined as;

$$t_{c1} = 0.09 \frac{D_e (\varepsilon_{cu} - 0.004) f_{cc}'}{\phi_f f_{fu} \varepsilon_{fu}} = 0.09 \frac{753(0.0089 - 0.004) \times 1.5 \times 34.45}{0.9 \times 1309 \times 0.01} \times 2 = 3.0 \text{ mm}$$

$$t_{c2} = t_{c1} / 2 = \frac{3.0}{2} = 1.5 \text{ mm}$$

Where,

t_{c1} and t_{c2} are the jacket thickness in the primary and secondary confinement regions, respectively. Because $L/D = 2.0 < 4.0$, the anti-bar buckling criteria is not necessary to be checked.

Summary of Jacket Thickness Specifications

$$L^i_v = 1.5D = 938 \text{ mm} \rightarrow t^i_v = 1.0 \text{ mm}$$

$$L^o_v = L - 2L^i_v = 625 \text{ mm} \rightarrow t^o_v = 0.60 \text{ mm}$$

$$L^t_{c1} = L^b_{c1} = 0.5D = 313 \text{ mm} \rightarrow t_{c1} = 3.0 \text{ mm}$$

$$L^t_{c2} = L^b_{c2} = 0.5D = 313 \text{ mm} \rightarrow t_{c2} = \frac{t_{c1}}{2} = 1.5 \text{ mm}$$

Appendix "K"

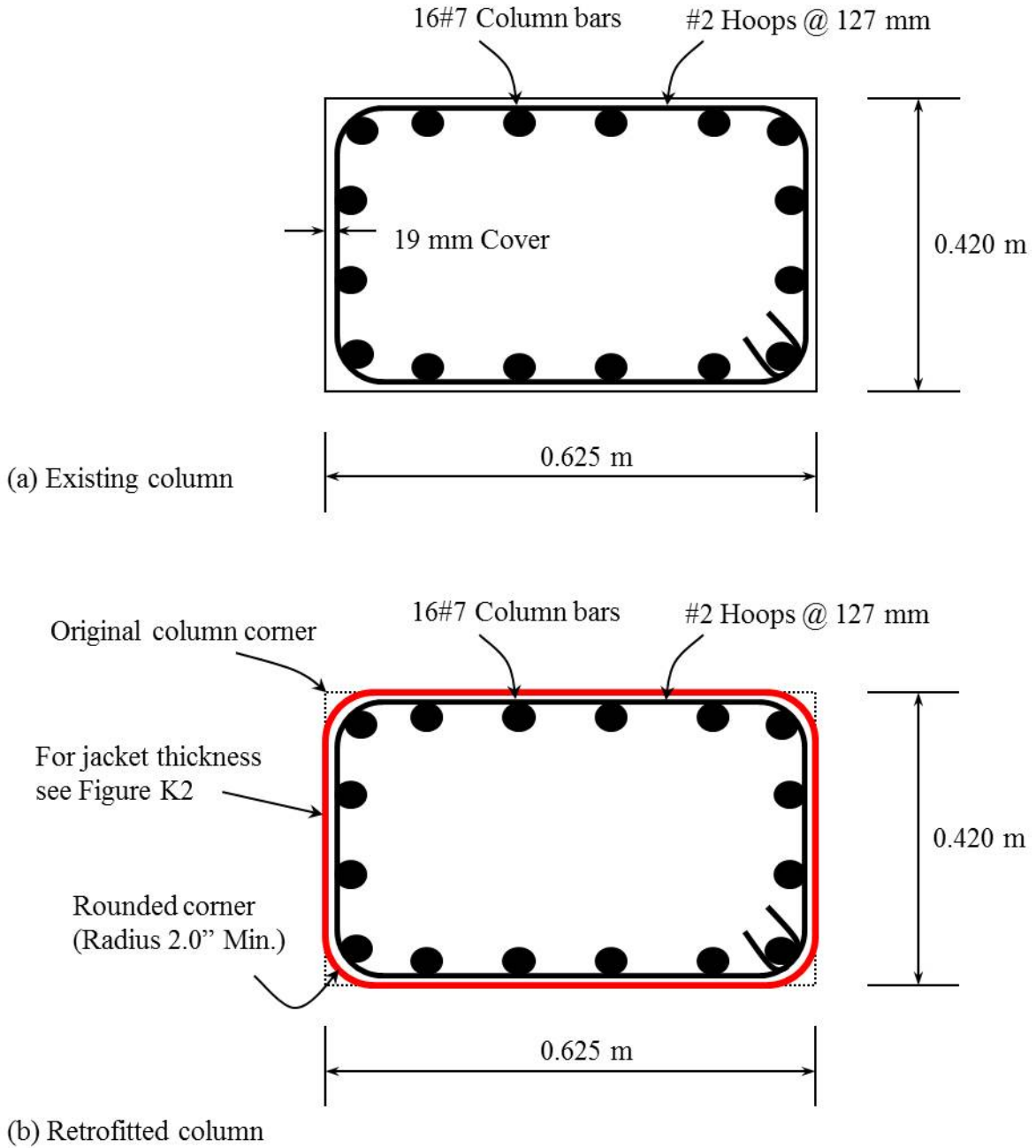
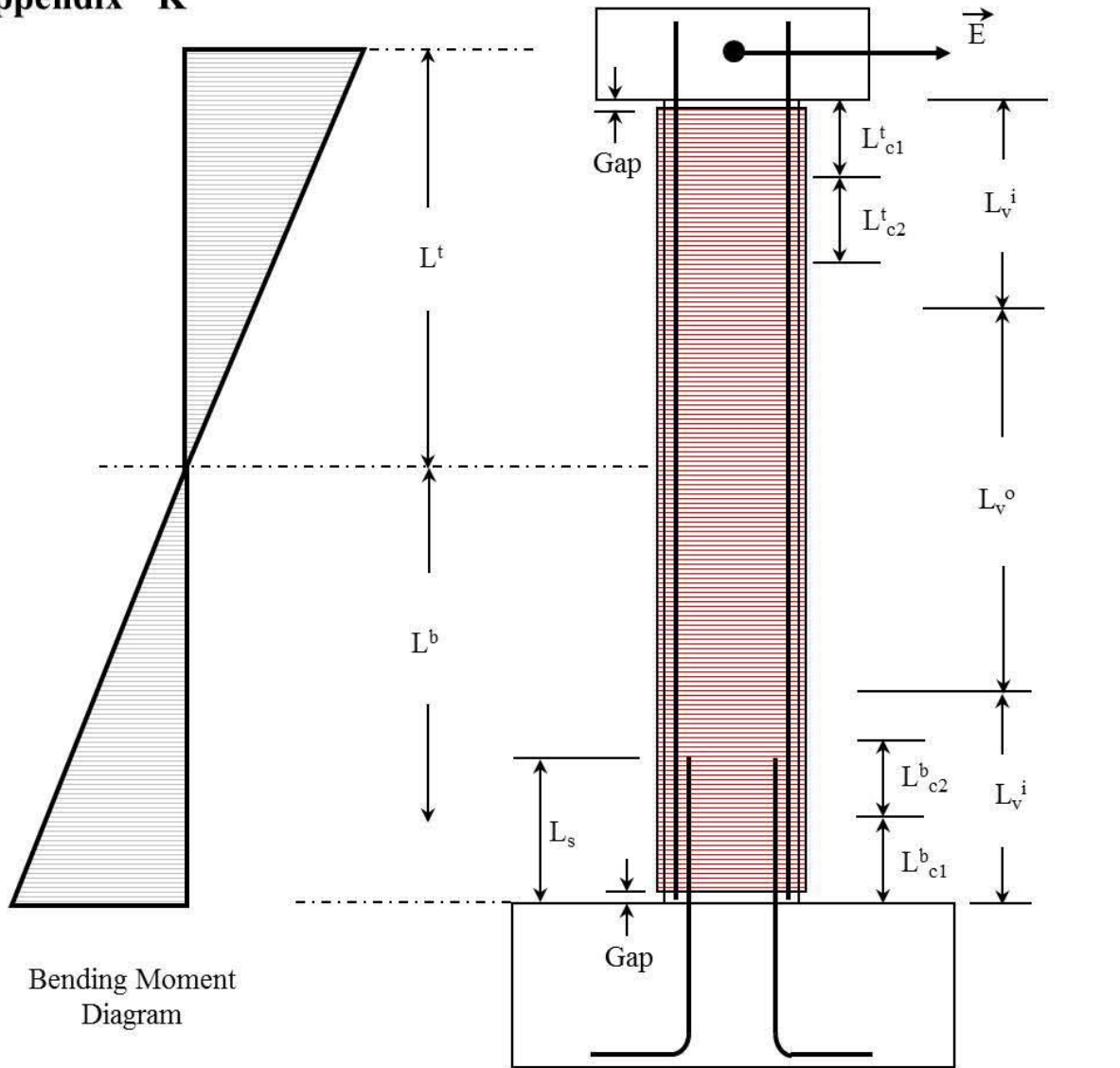


Figure K1. Shear Strengthening of rectangular concrete column.

Appendix “K”



$$L_v^i = 1.50 D$$

$L_s \geq$ or = to Lap splice length

$$L_{c1} \geq \begin{cases} 0.50D \\ L/8 \end{cases}$$

$$L_{c2} \geq \begin{cases} 0.50D \\ L/8 \end{cases}$$

$$L_v^i = 1.5D = 938 \text{ mm} \rightarrow t_v^i = 1.0 \text{ mm}$$

$$L_v^o = L - 2L_v^i = 625 \text{ mm} \rightarrow t_v^o = 0.60 \text{ mm}$$

$$L_{c1}^t = L_{c1}^b = 0.5D = 313 \text{ mm} \rightarrow t_{c1} = 3.0 \text{ mm}$$

$$L_{c2}^t = L_{c2}^b = 0.5D = 313 \text{ mm} \rightarrow t_{c2} = \frac{t_{c1}}{2} = 1.5 \text{ mm}$$

Figure K2 Seismic shear strengthening of concrete bridge column with CFRP.

Appendix “L”

Seismic Retrofit of a Rectangular Concrete Column With Poorly Confined Plastic Hinge Regions

Figure L1 and L2 (on Pages 511 & 512) show the detail of a rectangular reinforced concrete column with poorly confined plastic hinge regions. It is required to provide the column with a carbon fiber reinforced jacket to confine the plastic hinge regions and increase the column ductility to a target member displacement ductility of $\mu_{\Delta} \geq 6$.

Shear Strength Requirement

Maximum expected plastic shear demand including over-strength V_o equals

$$V_o = 1.5V_{yl} = 1.5 \frac{M_{yl}}{L} = 1.5 \frac{1808}{4.000} = 678 \text{ kN}$$

Given values

H (Height of column) = 4.0 m, L (Length of shear span) = 4.0 m

D (Column depth) = 0.750 m, B (Column width) = 0.500 m

cc (Concrete cover) = 19 mm, f_c' (Concrete strength) = 34.45 MPa

Longitudinal reinforcement(36#8 bars of Grade 40) : $d_b = 25 \text{ mm}$ & $f_y = 303.16 \text{ MPa}$

Transverse reinforcement(Grade 40) : $d_b = 6 \text{ mm}$, $f_y = 303.16 \text{ MPa}$, & $s = 127 \text{ mm}$

P (Axial load) = 1780 kN, $M_{yl} = 1808 \text{ kN} - \text{m}$

ϕ_y (Yield curvature) = 0.0047 1/m, c_u (Neutral axis depth) = 207 mm

V_c^i (inside of the plastic region) = 26 kN

V_c^o (Out side of the plastic region) = 555 kN

$V_s = 222 \text{ kN}$

$V_p = 167 \text{ kN}$

$\phi_v = 0.85$

$E_f = 124 \text{ GPa}$, $f_{fu} = 1300 \text{ MPa}$, and $\varepsilon_{fu} = 0.01$

The jacket thickness inside the plastic-hinge region (t_v^i) and outside the plastic-hinge region (t_v^o) can be calculated as;

$$t_v^i = \frac{\frac{V_o}{\phi_v} - (V_c + V_s + V_p)}{2(0.004E_f D)} = \frac{\frac{678}{0.85} - (26 + 222 + 167)}{2x(0.004x124020x750)} x10^3 = 0.5 \text{ mm}$$

$$t_v^o = \frac{\frac{V_o}{\phi_v} - (V_c + V_s + V_p)}{2(0.004E_f D)} = \frac{\frac{678}{0.85} - (555 + 222 + 167)}{2x(0.004x124020x750)} x10^3 = -0.2 \text{ mm}$$

Outside the plastic hinge region, the nominal shear capacity is greater than the factored ideal shear capacity, so no shear retrofit is necessary in this column region.

Flexural Plastic-Hinge Confinement Requirements

The confinement of the plastic hinge region was designed using a rectangular jacket with twice the jacket thickness required for an equivalent circular jacket with an effective diameter D_e of 901 mm.

Plastic hinge length (L_p)

$$L_p = 0.08L + 0.022f_{sy}d_b = 0.80x4000 + 0.022x303.16 * 25 = 487 \text{ mm}$$

The required curvature ductility equals

$$\mu_\phi = 1 + \frac{8-1}{3(487/4000)[1-0.5(487/4000)]} = 21$$

The required ultimate strain is

$$\varepsilon_{cu} = \Phi_u c_u = \mu_\phi \Phi_y c_u = 21x0.0055x0.207 = 0.021$$

The jacket thickness required to provide this ultimate concrete strain determined as;

$$t_{c1} = 0.09 \frac{D_e (\varepsilon_{cu} - 0.004) f_{cc}'}{\phi_f f_{fu} \varepsilon_{fu}} = 0.09 \frac{901(0.021 - 0.004)x1.5x34.45}{0.9x1309x0.01} 2 = 12.1 \text{ mm}$$

$$t_{c2} = t_{c1} / 2 = \frac{10.0}{2} = 6.0 \text{ mm}$$

Where,

t_{c1} and t_{c2} are the jacket thickness in the primary and secondary confinement regions, respectively.

Summary of Jacket Thickness Specifications

$$L_v^i = 1.5D = 1125 \text{ mm} \rightarrow t_v^i = 0.6 \text{ mm}$$

$$L_{c1}^t = 0.125L = 500 \text{ mm} \rightarrow t_{c1} = 10.0 \text{ mm}$$

$$L_{c2}^t = 0.125L = 500 \text{ mm} \rightarrow t_{c2} = \frac{t_{c1}}{2} = 5.0 \text{ mm}$$

Appendix "L"

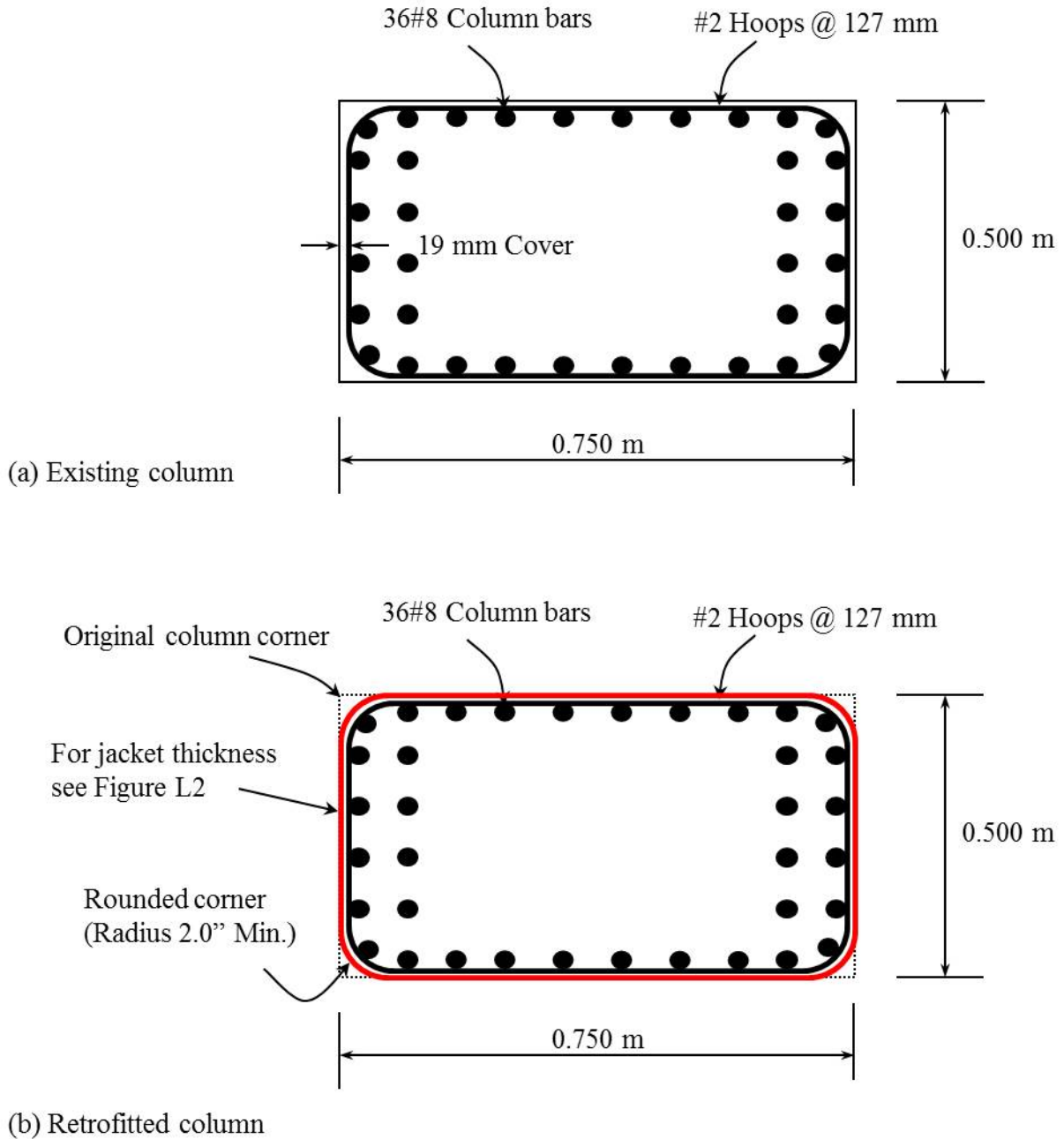
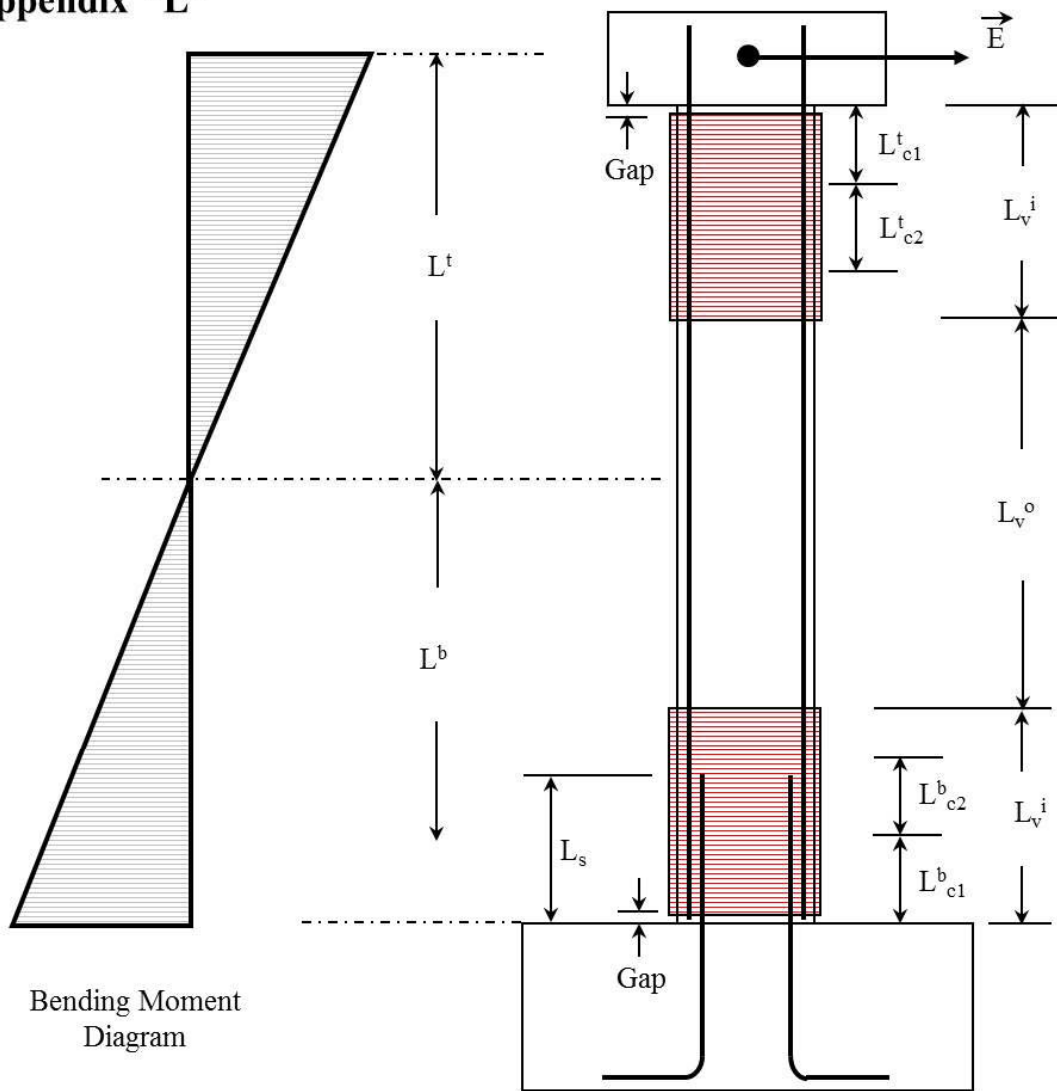


Figure L1. Seismic strengthening of plastic hinge regions of a rectangular concrete column.

Appendix "L"



$$L_v^i = 1.50 D$$

$L_s > \text{or} = \text{to Lap splice length}$

$$L_{c1} \geq \begin{cases} 0.50D \\ L/8 \end{cases}$$

$$L_{c2} \geq \begin{cases} 0.50D \\ L/8 \end{cases}$$

$$L_v^i = 1.50 D = 1125 \text{ mm} \rightarrow t_v^i = 0.6 \text{ mm}$$

$$L_{c1}^t = 0.125 L = 500 \text{ mm} \rightarrow t_{c1} = 10.0 \text{ mm}$$

$$L_{c2}^t = 0.125 L = 500 \text{ mm} \rightarrow t_{c2} = \frac{t_{c1}}{2} = 5.0 \text{ mm}$$

Figure L2. Seismic strengthening of plastic hinge regions of a rectangular concrete column.

Appendix “M”

Seismic Retrofit of a Circular Concrete Column With Inadequate Lap Splice in the Longitudinal Steel Rebars

Figure M1 and M2 (on Pages 511 & 512) show the detail of a circular reinforced concrete column with inadequate lap splice in the longitudinal reinforcement. It is required to provide the column with a carbon fiber reinforced jacket to confine the lap splice region to develop the full column capacity at a target member displacement ductility of $\mu_{\Delta} = 8$.

Shear Strength Requirement

Maximum expected plastic shear demand including over-strength V_o equals

$$V_o = 1.5V_{yl} = 1.5 \frac{M_{yl}}{L} = 1.5 \frac{933}{4.000} = 350 \text{ kN}$$

Given values

H (Height of column) = 4.0 m, L (Length of shear span) = 4.0 m

D (Column diameter) = 0.625 m

cc (Concrete cover) = 19 mm, f_c' (Concrete strength) = 34.45 MPa

Longitudinal reinforcement(20 bars of Grade 40) : $d_b = 22 \text{ mm}$ & $f_y = 303.16 \text{ MPa}$

Transverse reinforcement(Grade 40) : $d_b = 6 \text{ mm}$, $f_y = 303.16 \text{ MPa}$, & $s = 127 \text{ mm}$

P (Axial load) = 1780 kN, $M_{yl} = 933 \text{ kN} - \text{m}$

ϕ_y (Yield curvature) = 0.0064 1/m, c_u (Neutral axis depth) = 210 mm

V_c^i (inside of the plastic region) = 16 kN

V_c^o (Out side of the plastic region) = 306 kN

$V_s = 70 \text{ kN}$

$V_p = 139 \text{ kN}$

$\phi_v = 0.85$

$E_f = 124 \text{ GPa}$, $f_{fu} = 1300 \text{ MPa}$, and $\epsilon_{fu} = 0.01$

The jacket thickness inside the plastic-hinge region (t_v^i) and outside the plastic-hinge region (t_v^o) can be determined as;

$$t_v^i = \frac{\frac{V_o}{\phi_v} - (V_c + V_s + V_p)}{\frac{\pi}{2}(0.004E_f D)} = \frac{\frac{350}{0.85} - (16 + 70 + 139)}{\frac{\pi}{2}x(0.004x124020x610)} x10^3 = 0.4 \text{ mm}$$

$$t_v^o = \frac{\frac{V_o}{\phi_v} - (V_c + V_s + V_p)}{\frac{\pi}{2}(0.004E_f D)} = \frac{\frac{350}{0.85} - (306 + 70 + 139)}{\frac{\pi}{2}x(0.004x124020x610)} x10^3 = -0.2 \text{ mm}$$

Outside the plastic hinge region, the nominal shear capacity is greater than the factored ideal shear capacity, so no shear retrofit is necessary in this column region.

Flexural Plastic-Hinge Confinement Requirements

The confinement of the plastic hinge region was designed using a rectangular jacket with twice the jacket thickness required for an equivalent circular jacket with an effective diameter D_e of 625 mm.

Plastic hinge length (L_p)

$$L_p = 0.08L + 0.022f_{sy}d_b = 0.80x4000 + 0.022x303.16 * 22 = 467 \text{ mm}$$

The required curvature ductility equals

$$\mu_\phi = 1 + \frac{8 - 1}{3x(467 / 4000)[1 - 0.5(467 / 4000)]} = 22$$

The required ultimate strain is

$$\varepsilon_{cu} = \Phi_u c_u = \mu_\phi \Phi_y c_u = 22x0.0064x0.210 = 0.0299$$

The jacket thickness required to provide this ultimate concrete strain determined as;

$$t_{c1} = 0.09 \frac{D(\varepsilon_{cu} - 0.004)f_{cc}'}{\phi_f f_{fu} \varepsilon_{fu}} = 0.09 \frac{610(0.0299 - 0.004)x1.5x34.45}{0.9x1309x0.01} 2 = 12.9 \text{ mm}$$

$$t_{c2} = t_{c1} / 2 = \frac{6.3}{2} = 6.4 \text{ mm}$$

Where,

t_{c1} and t_{c2} are the jacket thickness in the primary and secondary confinement regions, respectively.

Lap-splice Clamping Requirements

The available lateral clamping pressure provided by the hoop reinforcement f_h equals 0.165 MPa (0.024 ksi). The required clamping pressure to prevent lap splice debonding can be found as;

$$f_l = \frac{A_s f_{sy}}{\left[\frac{P}{2n} + 2(d_b + cc)\right]L_s} = \frac{284 \times 303.16}{\left[\frac{587\pi}{2 \times 20} + 2(22 + 19)\right]341} = 2.404 \text{ MPa}$$

The carbon jacket thickness can be determined as;

$$t_s = 500 \frac{D(f_l - f_h)}{E_f} = 500 \frac{625(2.404 - 0.165)}{124020} = 5.6 \text{ mm}$$

Summary of Jacket Thickness Specifications

$$L'_v = 1.5D = 938 \text{ mm} \rightarrow t'_v = 0.4 \text{ mm}$$

$$L'_{c1} = 0.125L = 500 \text{ mm} \rightarrow t_{c1} = 12.9 \text{ mm}$$

$$L'_{c2} = 0.125L = 500 \text{ mm} \rightarrow t_{c2} = \frac{t_{c1}}{2} = 6.4 \text{ mm}$$

$$L_s = 341 \text{ mm} \rightarrow t_s = 5.6 \text{ mm}$$

Appendix "M"

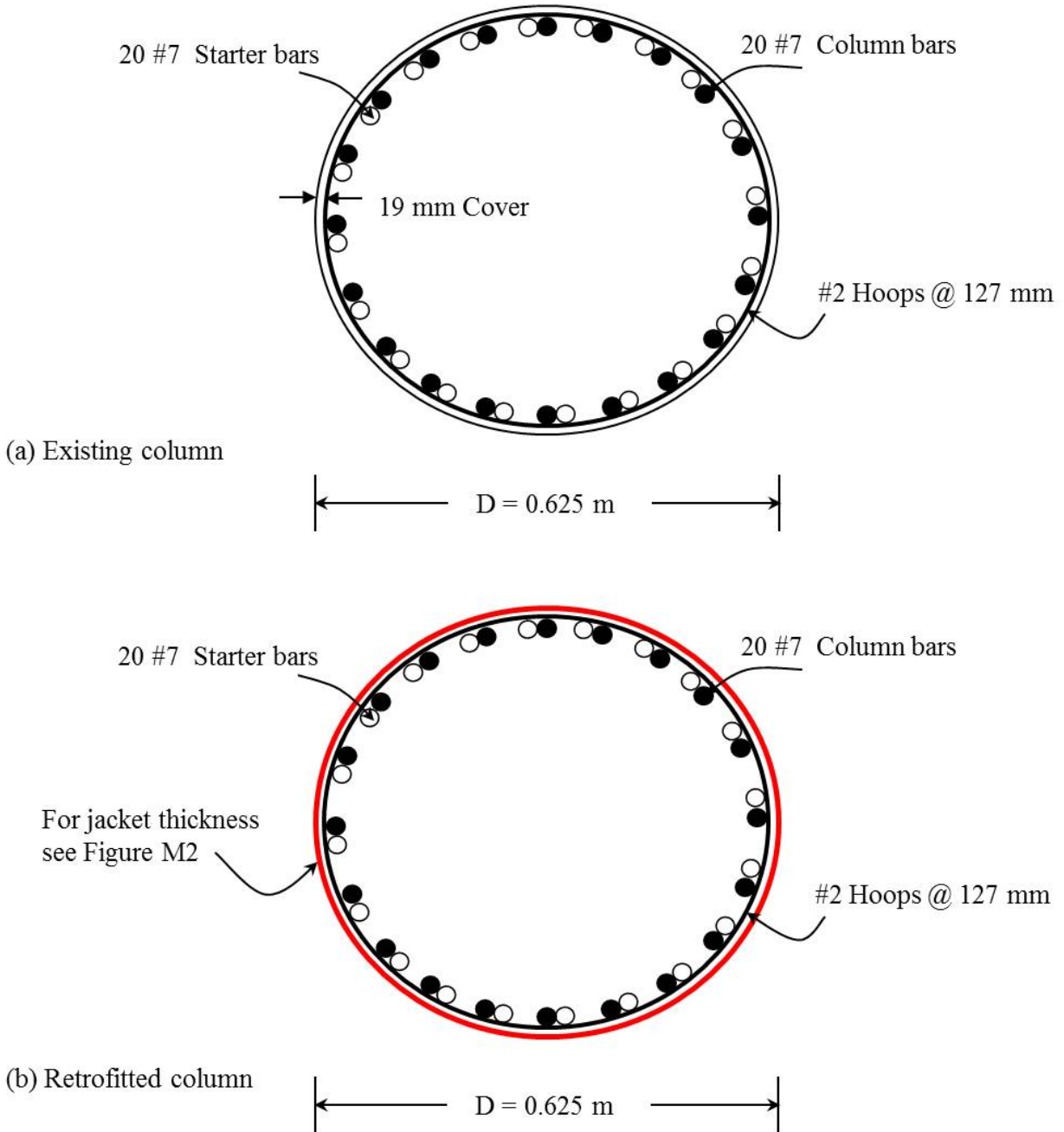
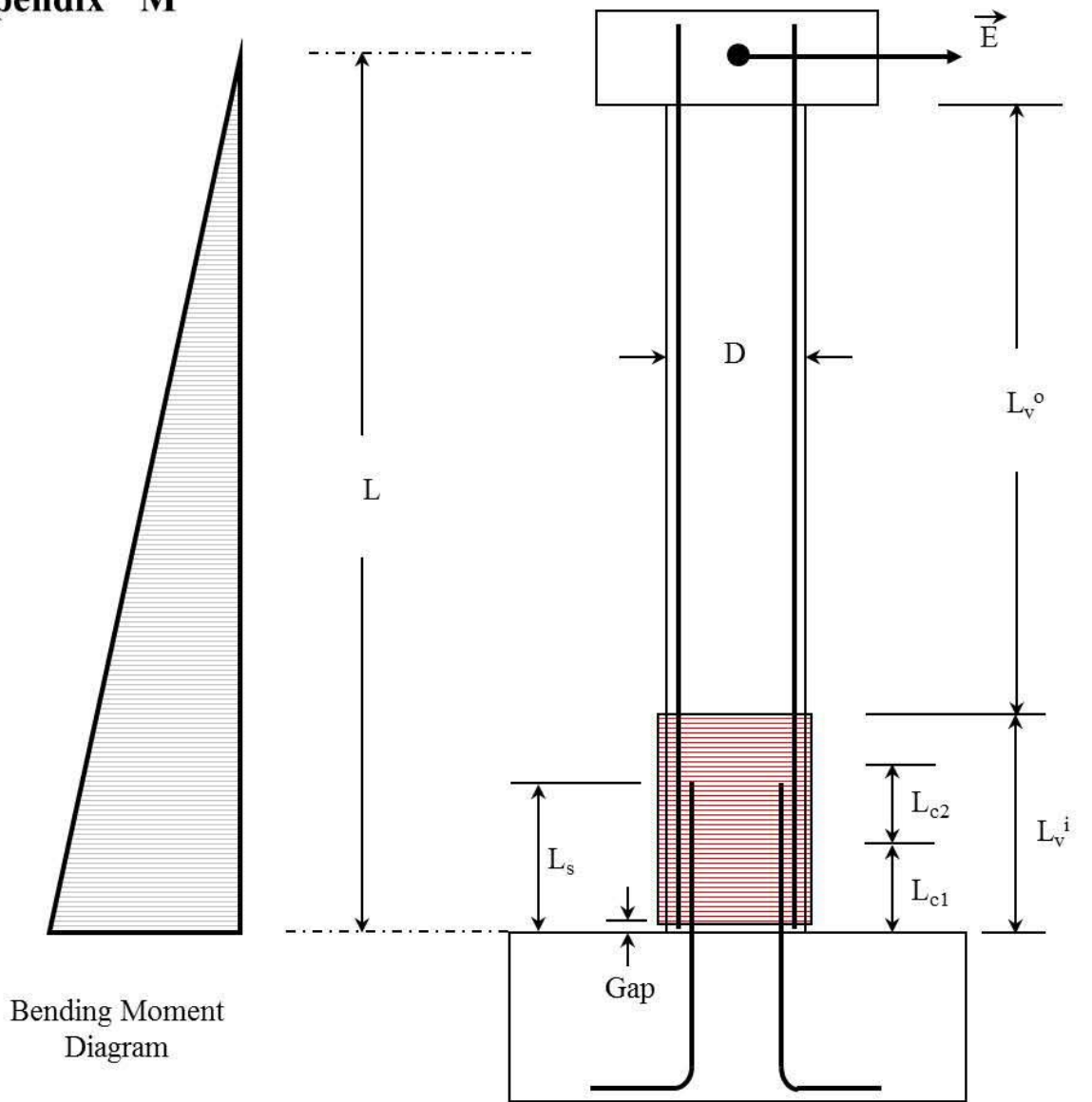


Figure M1. Seismic strengthening of a circular concrete column with inadequate lap splice in the longitudinal steel rebars..

Appendix "M"



$$L_v^i = 1.50 D$$

$$L_s \geq \text{Lap splice length}$$

$$L_{c1} \geq \begin{cases} 0.50D \\ L/8 \end{cases}$$

$$L_{c2} \geq \begin{cases} 0.50D \\ L/8 \end{cases}$$

$$L_v^i = 1.50D = 938 \text{ mm} \rightarrow t_v^i = 0.4 \text{ mm}$$

$$L_{c1} = 0.125L = 500 \text{ mm} \rightarrow t_{c1} = 12.9 \text{ mm}$$

$$L_{c2} = 0.125L = 500 \text{ mm} \rightarrow t_{c2} = \frac{t_{c1}}{2} = 6.4 \text{ mm}$$

$$L_s = 341 \text{ mm} \rightarrow t_s = 5.6 \text{ mm}$$

Figure M2. Seismic strengthening of a circular concrete column with inadequate lap splice in the longitudinal steel rebars..